Biochemical and Pre-clinical Evaluation of 2nd Generation HIV-1 Envelope Vaccine Components

DISSERTATION ZUR ERLANGUNG
DES DOKTORGRADES DER NATURWISSENSCHAFTEN (DR. RER. NAT.)
DER FAKULTÄT FÜR BIOLOGIE UND VORKLINISCHE MEDIZIN
DER UNIVERSITÄT REGENSBURG

Vorgelegt von

Christina Maria Schmalzl

aus

Straubing

im Jahr

2020

Biochemical and Pre-clinical Evaluation of 2nd Generation HIV-1 Envelope Vaccine Components

DISSERTATION ZUR ERLANGUNG
DES DOKTORGRADES DER NATURWISSENSCHAFTEN (DR. RER. NAT.)
DER FAKULTÄT FÜR BIOLOGIE UND VORKLINISCHE MEDIZIN
DER UNIVERSITÄT REGENSBURG

Vorgelegt von
Christina Maria Schmalzl

aus
Straubing

im Jahr
2020

Das Promotionsgesuch wurde eingereicht am:

13.11.2020

Die Arbeit wurde angeleitet von:

Prof. Dr. Ralf Wagner

Christina Schmalzl

Meiner Mama

Table of Contents

Table of Contents

1. Abstract

Evidence from active and passive vaccination trials suggests that both non-neutralizing and neutralizing antibodies (Ab) can confer protection from HIV infection, but the generation of an Envelope-(Env)-based immunogen able to elicit protective humoral responses has not yet been achieved. The major obstacles are high sequence variability, glycan- and structure-mediated shielding of potentially beneficial epitopes, as well as structural flexibility displaying distracting immunodominant sites.

In a mammalian cell-based display approach of gp145 (truncated Env lacking the cytoplasmic tail), the mutants L111A and T278H were detected, which lead to improved binding of broadly neutralizing antibodies (bNAbs). L111A showed enhanced binding to the quaternary-structure-dependent antibody PG9. Yet, L111A is not part of the epitope of PG9, but located in Env's interior, indicating that the effect on PG9-binding seems to be caused by an improved conformation or a higher trimer content. Analysis of the soluble L111A gp140 protein showed a decreased monomer content and a more closed conformation, but no negative effect on the affinities measured by ELISA using a panel of bNAbs directed towards the various vulnerable sites. In DSC analysis, the denaturation midpoint was not affected, but a more homogenous unfolding of L111A was observed. The second amino acid exchange, T278H led to improved binding of the CD4-binding-site-specific bNAb VRC01. As the combination of both mutations (LT) facilitated trimer formation while improving the antigenicity, the antibody profile elicited by the LT variant in comparison to the wildtype, was assessed in a pre-clinical animal study in New Zealand White rabbits. In addition to these uncleaved variants, a conformationally closed Env trimer homolog (SOSIP) alone and in combination with LT (SOSIP-LT) was administered as recombinant protein. Additional experiments showed that stabilization of the protein with chemical cross-linking did not affect the trimers, thus cross-linked protein was used for the last protein boost. All four groups developed overall high Ab titers against the autologous antigen (gp140-wt≈LT>SOSIP≈SOSIP-LT). Sera from animals immunized with the uncleaved gp140 trimer showed the least reactivity with the SOSIP-LT homolog, suggesting structural occlusion of immunodominant epitopes in SOSIP-LT. In contrast, the LT variant induced greatest breadth against a panel of eight gp120s of different clades. Moreover, DNA-prime, protein-boost regimens were tested in three further groups. However, there were only

little differences on the overall antibody profiles as compared to the protein-only-groups, but animals immunized with this LT developed highest breadth against V1V2 scaffolds following two DNA priming immunizations. Depending on the immunogen, linear epitope mapping showed multiple reactivities toward various parts of Env, with dominating responses toward V3. Whereas all animals developed tier 1 neutralizing Abs, moderate autologous tier 2 neutralizing Abs were only observed in the SOSIP groups.

Overall, our data demonstrate that subtle amino acid substitutions can have a major impact on trimer formation, stability and epitope accessibility, which directly translates into improved titer and breadth of binding Abs as well as neutralizing capacity, depending on the selected immunogen.

2. Introduction

2.1. The Human Immunodeficiency Virus Pandemic

The rise of a new pandemic always brings new challenges, as we are currently experiencing firsthand with Covid-19. In the beginning, people don't know about the paths of transmission and how to protect themselves and therefore urge for a vaccine.

For one other pandemic, we still lack this vaccine after nearly 40 years since the isolation and denomination of the causative agent as Human Immunodeficiency Virus (HIV)[1–3]. Without therapy, an infection with this virus leads to the development of the Acquired ImmunoDeficiency Syndrome (AIDS). Worldwide, roughly 75 million people got infected since the start of the pandemic, of whom 32 million died of AIDS-related illnesses[4]. In 2018, 37.9 million people were living with HIV, 1.7 million of them were less than 15 years old and only ~ 79 % of the HIV^+ persons knew about their infection[4].

Phylogenetic analyses of circulating strains showed that HIV-1 can be classified into groups and originated from individual infections of humans with the Simian Immunodeficiency Virus (SIV) from great apes[5]. HIV-1 groups M and N are derived from independent cross-species transmissions of SIV from chimpanzees, while O and P originated from gorillas[6,7]. HIV-2 is the result of transmissions from sooty mangabeys and mainly occurs in West Africa but infected individuals usually do not develop AIDS[6]. HIV-1 group M, which is the predominant agent of the global epidemic, can be differentiated into subtypes A, B, C, D, F, G, H, J, and K, Circulating Recombinant Forms (CRFs), and Unique Recombinant Forms (URFs) (Figure 1). Of these, the clades A, B, and C are the most prevalent ones. Clade A is predominant in Eastern Europe and Eastern Africa while clade B is mostly detected in Western and Central Europe, America and Australia. Clade C accounts for roughly 50 % of the infections worldwide and is the most prevalent clade in Africa and India[8].

Infection with the HI-Virus occurs by sexual contacts across mucosal surfaces, by percutaneous inoculation (especially in the context of intravenous drug-use), childbirth, and breast-feeding[5]. Of all HIV-1 positive individuals, only 24.5 million have access to AntiRetroviral Therapy (ART)[4].Without ART, the proceeding HIV-1 infection leads to the depletion of T-lymphocytes (Figure 2), the diversity of the quasispecies increases, and the

patients suffer from AIDS and eventually die from AIDS-related diseases like e.g. pneumonia, toxoplasmosis, or Kaposi's sarcoma[9,10].

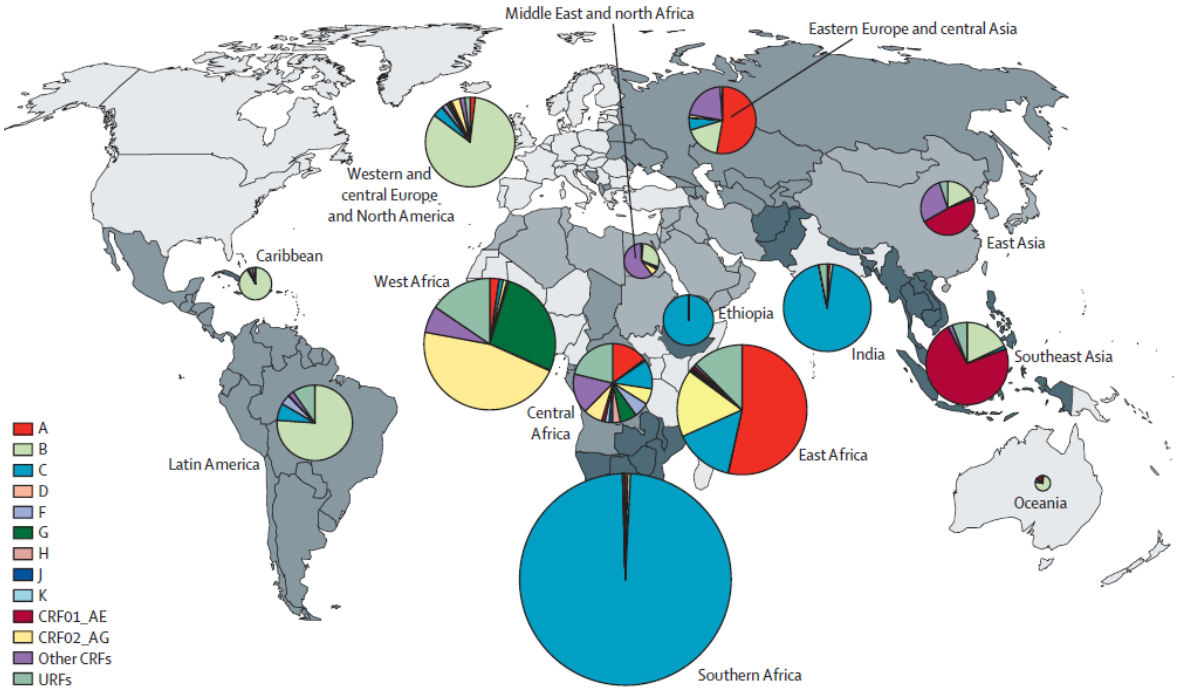

Figure 1: World-wide distribution of HIV-1 subtypes, circulating recombinant forms (CRFs), and unique recombinant forms (URFs) (2010-2015). Countries are grouped into 14 regions (shades of grey) and the pie charts represent the numbers of HIV-positive people living in each region. Reprinted from[11] with permission from Elsevier.

Since 1997, the number of new HIV infections declined by 40 %. Still, in 2018, 1.7 million people still got newly infected with HIV[4]. With the rising numbers of total infections and survival rates, HIV prevalence increases worldwide, while the highest prevalence can be observed in eastern and southern Africa, where 54 % of the world's HIV-infected people are living[12]. Here, but also in other low-income countries, the availability of ART is limited and only 62 % of all people with an HIV-infection knowing their status were virally suppressed in 2018[4]. Up to today, there is no cure available and ART delivers the only change to hinder the progression of the HIV-infection to AIDS. One main obstacle to a cure is the formation of a latent reservoir of infected resting $CD4^+$ T cells[13,14]. The latent reservoir can develop within the first ten days of acute infection and leads to a rebound whenever ART is withdrawn[15]. ART improves the quality of life of HIV-infected individuals, if it is available and if compliance is met, which is not always the case. Due to this, it would be necessary to have a preventive vaccine to decrease the numbers of new HIV infections or even to eradicate the virus.

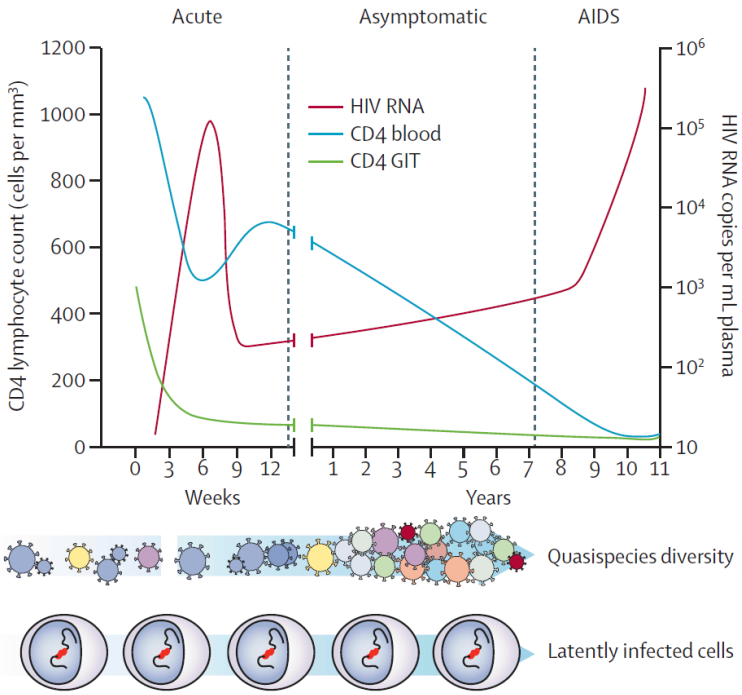

Figure 2: CD4 lymphocyte count and HIV RNA copies during acute infection, asymptomatic phase, and AIDS. In the acute phase, the immune system can cope with the infection. The infection progresses into the asymptomatic phase, where the number of T-lymphocytes is further reduced while HIV RNA copies, the diversity of the quasispecies, and the size of the latent reservoir increase. After some time, the number of T-lymphocytes is too low and constitutional symptoms occur. Adapted from[9] with permission from Elsevier.

2.2. The HI-Virus and its Envelope Glycoprotein

The HI-Virus belongs to the *Retroviridae* family, sub-family *Orthoretrovirinae,* genus *Lentivirus*. The HIV-1 virion is about 100 nm in size[16], surrounded by a lipid bilayer derived from the host cell and there are 14-20 spikes of the Env glycoprotein on its surface[17](Figure 3). The Group specific AntiGens (gag) p17 and p24 form the matrix and the conical capsid, respectively. The viral genome inside the capsid consists of two copies of positive-stranded RNA which is in complex with the nucleocapsid protein p7. Furthermore, there are also the viral enzymes reverse transcriptase, integrase and protease[16]. Of all these components, the HIV-1 Env glycoprotein is the only viral structure present on the surface of the virus particle. Due to this, it is the prime target for humoral immune responses and a key component in HIV-1 vaccine design.

2.2.1. Biosynthesis and Structure of the Envelope Glycoprotein

Env is expressed as full-length gp160 precursor protein which undergoes secondary structure formation and glycosylation in the endoplasmic reticulum[17,18]. The gp160 monomers form trimers via non-covalent interactions, which are cleaved into gp120 and

gp41 subunits by a furin protease in the Golgi apparatus[19,20]. The three gp120 subunits, which are non-covalently linked to three gp41 subunits, are transported to the cell surface and incorporated into budding viral particles[21,22].

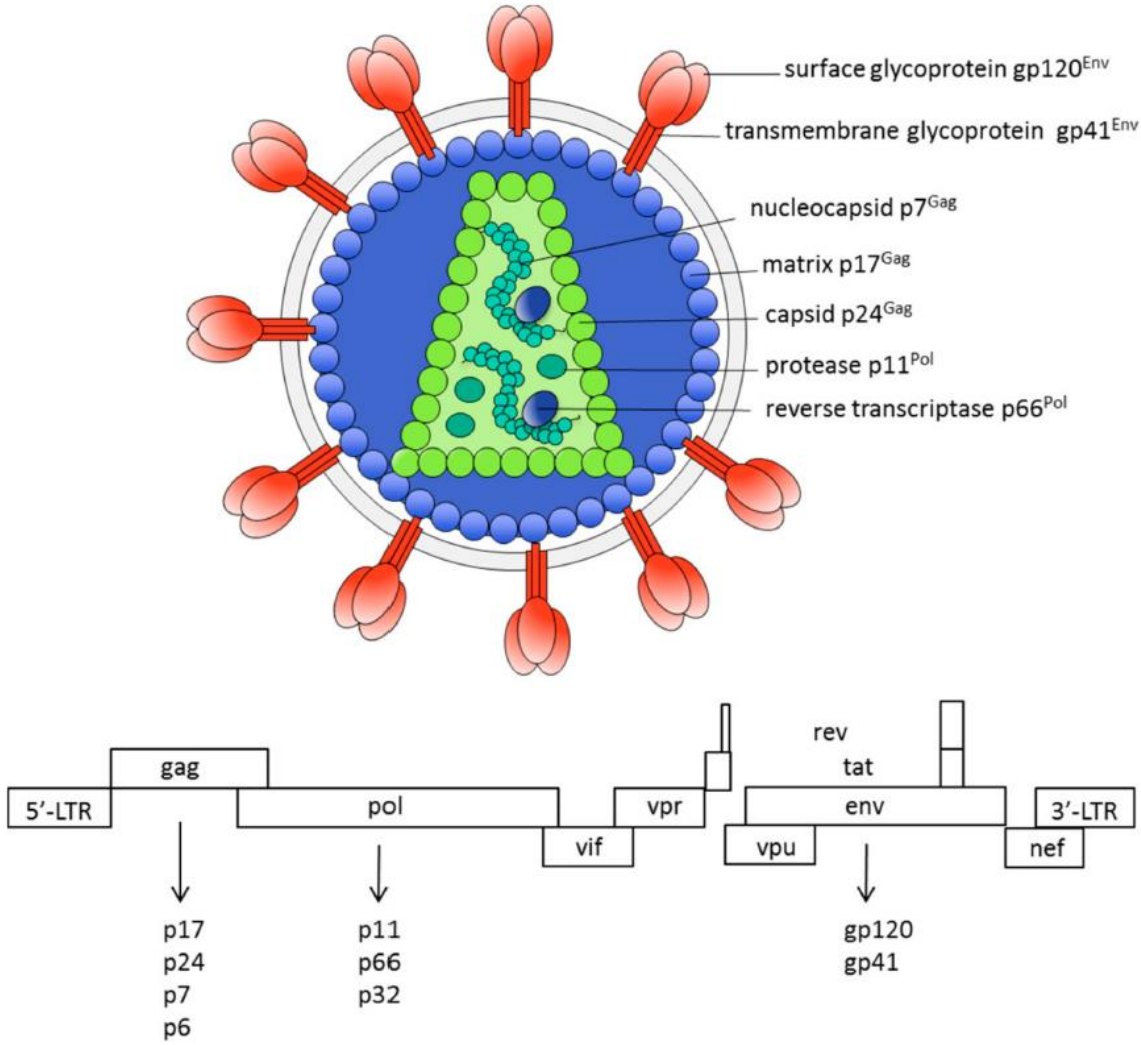

Figure 3: Schematic representation of the mature HIV-1 virion, its genome, and the respective proteins. From[23].

The gp120 subunit consists of 5 variable and 5 constant regions (V1-V5, C1-C5) and is structured into three domains (Figure 4)[24,25]. The inner domain is responsible for the non-covalent interaction of the gp120 and gp41 subunit, the outer domain bears the CD4- and co-receptor binding sites and both domains are connected by the bridging sheet, which consists of four anti-parallel β-sheets[25,26].

Gp41 is more conserved in its amino acid sequence and contains the fusion peptide, the two heptad repeats flanking a conserved disulfide loop, the membrane-proximal external region (MPER), the transmembrane domain, and the cytoplasmatic tail[24].

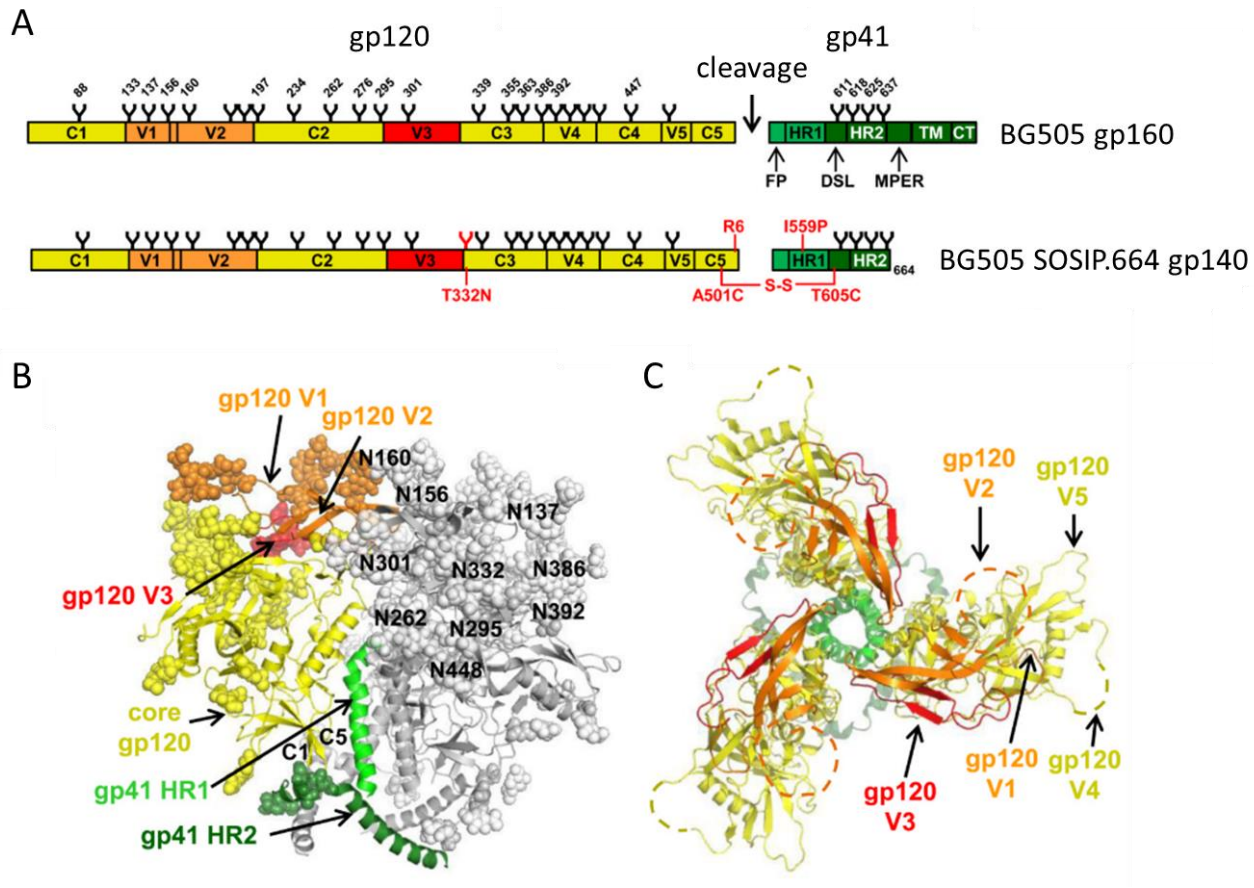

Figure 4: Representation of the Envelope Glycoprotein. A) The full-length gp160 and native-like soluble cleaved SOSIP construct, which is shown on the example of the clade A BG505. SOSIP is the soluble, cleaved form of gp140 trimers and mimics the native-like trimers (explained in 2.2.4). The gp120 subunit consists of Variable loops (V1-5) and Constant regions (C1-5). Gp120 and gp41 are separated by the cleavage site. Gp41 bears the fusion peptide (FP), the heptad repeats 1 and 2 (HR1, HR2), a disulfide loop (DSL), the Membrane-Proximal External Region (MPER), the TransMembrane domain (TM), and the Cytoplasmatic Tail (CT). The schematic trees symbolize glycans. SOSIP.664 is truncated at position 664, N-terminally of the MPER. Further modifications of the SOSIP variant are the improved cleavage site R_6 (instead of the natural cleavage site REKS); A501C and T605C, which lead to the formation of a disulfide bond between gp120 and gp41 while I559P promotes trimerization, and T332N allows binding of antibodies depending on glycan-N332. B) Side-view of the soluble Env trimer. Structures are depicted on one protomer. Protein structures are shown according to their secondary structures and glycans are shown as spheres and numbered according to their asparagine (N) residues. C) Top-view of the soluble Env trimer. Glycans are removed. Dashed lines indicate the variable loops which did not show the required electron density. Adapted from[27] with permission from The American Association for the Advancement of Science.

2.2.2. Function of the Envelope Glycoprotein

Env is essential for the fusion of the virus with the host cell. Upon CD4-binding to the gp120 subunit, a series of conformational changes occur in gp120 and gp41, which enables the virus to bind to its co-receptor CXCR4 or CCR5 and leads to the formation of a gp41 prehairpin intermediate and a six-helix-bundle[28,29,30,31,32] (Figure 5). Ultimately, this coiled-coil gp41 structure brings the cell and viral membrane in close proximity, leading to the

fusion of viral and host cell via the fusion peptide and subsequent unloading of the viral cargo into the cell[33].

The unliganded Env trimer can occur in three conformations (open, intermediate and closed) and based on the preliminary conformation, circulating isolates are classified into tiers: Tier 1A, 1B, 2, and 3[34]. Tier 1A isolates are mainly presented in an open conformation and are most sensitive to neutralization while Tier 1B mainly presents an intermediate state and is less sensitive. Tier 1A and 1B isolates are rare and most circulating isolates are of tier 2. Tier 2 and 3 both show a closed conformation and are more resistant to neutralization[34,35,36].

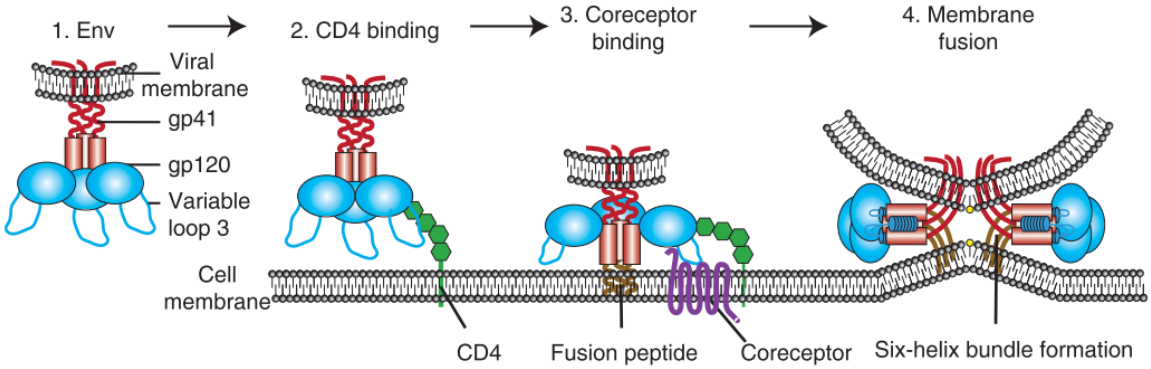

Figure 5: Entry of HIV-1 into its host cell via CD4 binding
Binding of the HI-virus to the target cell is mediated by Env interacting with the CD4-receptor, which enables coreceptor binding and finally the fusion of the membranes. Reprinted from[37] with permission from Cold Spring Harbor Laboratory Press.

2.2.3. Immune Evasion Mechanisms

The main obstacles of HIV vaccine design are the various immune evasion mechanisms presented by the HI-virus which may be addressed by new antigen design strategies.

The reverse transcriptase lacks proof-reading activity and has an estimated error rate ~1×10^{-5} to 3×10^{-5} per base and copy-round[38]. Also, the RNA polymerase II (necessary for the proviral transcription) leads to additional errors and due to all these transcription steps, each produced virus has on average at least one nucleotide exchange[16]. Besides the transcription errors, there is also selection pressure from the immune system leading to changes in the viral epitopes, enabling the virus to escape the humoral and cellular immune responses[16].

As the only viral structure on the surface of the virus particles, Env is exposed to a high selective pressure and therefore many of these escape strategies can be seen, preventing – among others - the induction of effectively neutralizing antibodies (Figure 6).

With roughly 90 N-linked glycans present on the surface of the HIV-1 Env trimer, glycans make up ~ 50 % of the mass of the protein and this extensive glycosylation is leading to a glycan shielding, one mechanism of neutralization escape[39,40,41,42]. The same applies for the conformational masking of conserved epitopes, which avoids binding of antibodies to conserved glycan-free surfaces in the pre-fusion mature closed state and can only be overcome by receptor binding[43,44,45]. Next to this, one protomer has five immunodominant variable loops which do not only tolerate high mutation rates but also possess a high level of flexibility and lead to an escape from strain-specific antibodies[46,47]. A feature of conformational flexibility is displayed by gp120 shedding, which describes the dissociation of gp120 from the gp41 subunits, leading to the presentation of immunodominant epitopes located in the inner part of the trimer and therefore to the induction of non-Neutralizing Antibodies (nNAbs)[48,49,50,51].

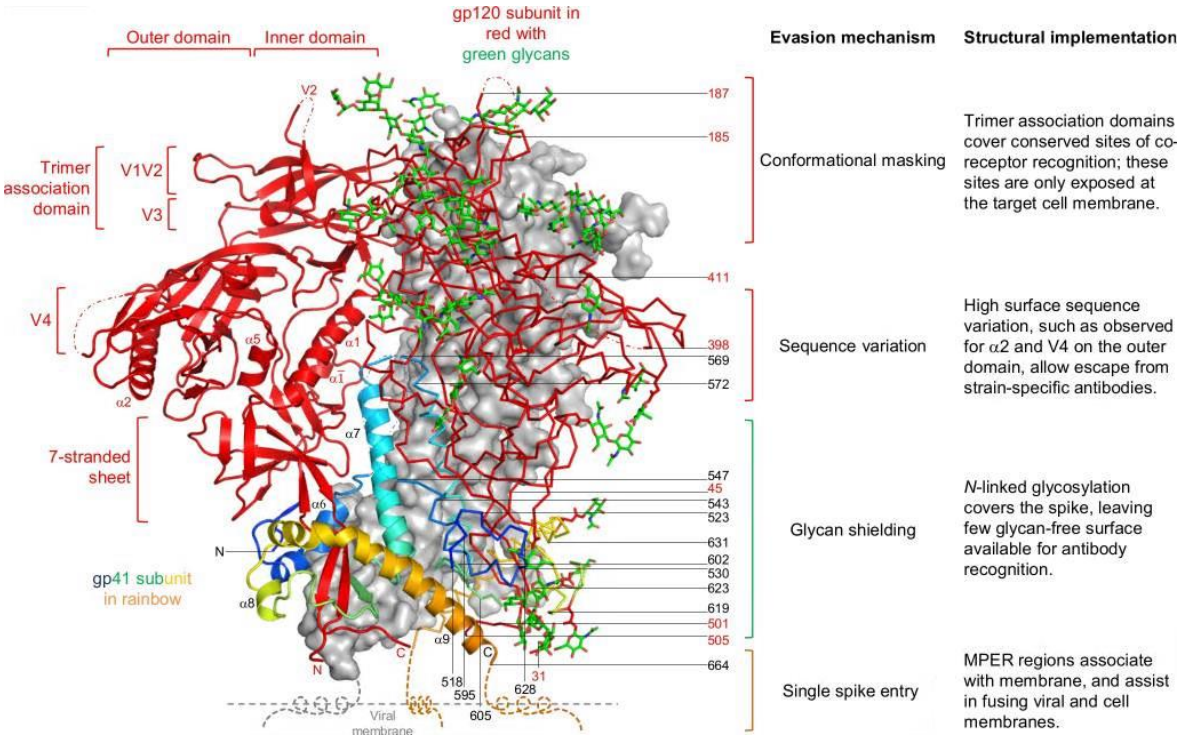

Figure 6: Immune evasion mechanisms of the HIV-1 Env trimer.
Env protomers are shown in either Cα trace with glycans in stick representation, or in ribbon representation with secondary structure elements labelled, or in light grey as surface representation. The MPER is shown as stylized helix bound to the viral membrane for all protomers. Red font is used for gp120 and black for gp41 to label the location of secondary structural elements, termini and residues. From[51] with permission from Springer Nature.

Due to all these obstacles, most antibody responses against HIV are only strain-specific and can be quickly circumvented by escape-mutations or other representatives of the quasi-

species within the patient[52]. Another feature to evade the immune system is the single-spike entry, which allows the entry of HIV-1 into the host cell by the binding of as little as one Env trimer[53], which is why HIV-1 only has a small number of about 7 - 14 trimers per virus particle[54]. This is a rare amount for an enveloped virus, but it is enough for cell-entry and furthermore restricts antibody avidity, which is another positive feature for the virus[55]
In order to overcome these hurdles presented by the virus to escape the immune system, several laboratory adaptations were developed to improve Env as an immunogen and to induce antibodies of improved quality.

2.2.4. Laboratory Adaptations of the Envelope Glycoprotein

The reduction of the conformational flexibility of Env trimers can occur via many ways, e.g. as SOSIP or Native Flexible Linker (NFL) constructs[56,57]. SOSIP constructs are characterized by the introduction of a disulfide bond between gp120 and gp41 (501C and 605C), which allows a native-like conformation and prevents shedding, while they also show increased trimer stabilization (I559P). Moreover, the introduction of epitopes depending on glycosylation at position 332 (T332N mutation) makes it a more valuable target for certain antibodies. Finally, the mutation of the cleavage site to R_6 allows optimal cleavage of the construct (Figure 4A)[56,58,59,60].
The main difference of the NFL to the SOSIP design is the covalent linkage of gp120 and gp41 subunits by a flexible glycine-serine linker that replaces the cleavage sequence, which allows native-like conformation without furin-cleavage[57,61].
Other approaches to keep the Env trimer in a fixed conformation are the mutation of the cleavage site `REKR` to `REKS` (uncleaved) or chemical cross-linking[62,63,64,65]. Uncleaved trimers are highly heterogenous, show a variety of shapes, and do not adopt a native-like conformation, but they are not subjected to gp120 shedding. While the generation of uncleaved trimers or native-like trimers both has to be designed on the DNA level, chemical cross-linking stabilizes recombinant Env protein after purification and hinders the presentation of nNAb epitopes located in the inner part of the trimer[66,67].
Next to the native-like Env trimer approaches, the Env trimers can also be modified by other ways like the removal of glycans, which exposes neutralizing epitopes and therefore increases their antigenicity[68].

2.3. HIV-1 Vaccine Development

2.3.1. Efficacy trials

In 1984, it was postulated that a vaccine against the virus causing AIDS might be available in roughly 2 years[69]. Nearly 40 years later, we still do not have a licensed vaccine, although many vaccine efficacy trials were conducted. (Table 1)[23]. These six vaccine efficacy trials can be classified into three paradigms of vaccine development: The induction of 1) neutralizing antibodies, 2) Cytotoxic T-Lymphocyte (CTL) responses and 3) the combination of different immune responses[70].

The first clinical efficacy trials focused on the induction of neutralizing antibodies. For this, two vaccine trials were performed with a recombinant gp120 vaccine of the bivalent subtype B/B on 5,403 HIV-1 uninfected volunteers (2:1 vaccinee to placebo recipient ratio) in the United States and the Netherlands (VAX004)[71] and the bivalent subtype B/E on 2,546 HIV-1 uninfected volunteers (1:1 vaccinee to placebo recipient ratio) in Thailand (VAX003)[72]. The outcome of these phase III clinical studies demonstrated a lack of efficacy in both trials as the number of HIV infections was constant over time[71,72,73,74].

Due to the failure of the trials based on the gp120 Env glycoprotein and neutralizing antibody responses, the field was focusing on $CD8^+$ T cells, which seem to control viral replication[70]. In order to induce CTL responses, the next two vaccine efficacy trials were based on replication-defective recombinant Adenovirus type 5 (Ad5) vector-based vaccines and HIV-1 clade B gag/pol/nef as antigens[75,76]. Unfortunately, they were showing unexpected outcomes, as both, the Step/HVTN502 (USA, 3000 participants, 1:1 vaccinee to placebo recipient ratio) and the Phambili/HVTN503 (South Africa, 801 participants, 1:1 vaccinee to placebo recipient ratio) led to an increased risk of infection in men who had Ad5-neutralizing antibodies and/or were uncircumcised[70,73,77].

Even though the first two concepts of vaccine design failed, there were new attempts to learn from the past and to systematically explore alternatives: The combination of different immune responses[70]. One of these new trials is HVTN505, which tested a prime-boost regimen on 2,504 participants in the US (1:1 vaccinee to placebo recipient ratio)[78]. For this, DNA encoding clade B HIV *gag*, *pol*, and *nef*, and gp145 *env* from clades A, B and C was used as prime, and the boost was performed with an Ad5-vector-based vaccine candidate

encoding clade B *gag* and *pol*, and *env* from clades A, B, and C. Unfortunately, this trial also failed to induce efficacy[78].

Table 1: Overview of the completed HIV-1 clinical trials (Status as of 2018). *r*: recombinant; MSM: men who have sex with men; bNAbs: broadly neutralizing antibodies; *: prime-boost. From [23].

Study	Regimen	Participants	Aim	Outcome
VAX004 (United States, Netherlands)	*r*gp120 B/B	MSM, high-risk women	bnAbs	No prevention of HIV infection
VAX003 (Thailand)	*r*gp120 B/E	Drug users	bnAbs	No prevention of HIV infection
Step/HVTN502 (USA)	*r*Ad5 HIV-1 gag/pol/nef B	MSM, high-risk women	CD8+ T-cells	Increased infection risk
Phambili/HVTN503 (South Africa)	*r*Ad5 HIV-1 gag/pol/nef B	Heterosexual men, women	CD8+ T-cells	Increased infection risk
HVTN505	* DNA/*r*Ad5	MSM, transgender women	Ab and T-cells	No infection risk, no efficacy
RV144 (Thailand)	* ALVAC-HIV/AIDSVAX B/E gp120 in alum	High risk men and women	Ab and T-cells	31.2% vaccine efficacy

The only trial which showed efficacy was RV144[79]. In Thailand, 16,402 adults (1:1 vaccinee to placebo recipient ratio) received a prime-boost recombinant vaccine consisting of a combination of two vaccines: ALVAC®, a recombinant canarypox vector vaccine, and AIDSVAX B/E, the recombinant Env gp120 subunit vaccine used in VAX003. This trial showed 31.2 % efficacy in preventing HIV infection. An analysis of the antibody and cellular immune correlates of risk showed that the binding of IgG antibodies to the Env V1V2 regions correlated inversely with the rate of HIV infection, while the binding of plasma IgA antibodies to Env correlated directly with infection[80]. A modification of the RV144 has been tested in a Phase 2b/3 study named HVTN702[81]. The enrolment started in 2016 and the vaccine was adapted to clade C, which is most prevalent in South Africa, where the study was conducted. Unfortunately, on the 3rd of February 2020, it was announced that the HVTN702 study was closed due to futility[82].

In summary, the HIV-1 vaccine candidates tested in efficacy trials were all well tolerated but in two of the six trials an increased infection risk was observed and only one trial was able to show some efficacy at all. Currently, a lot of new vaccine approaches are in or entering phase I clinical trials, e.g. based on the idea to induce broadly neutralizing antibodies after sequential immunization with different variants of the Env glycoprotein in

order to induce the maturation of germline antibodies[83]. Next to these, further phase III studies are conducted, like e.g. for a heterologous vaccine regimen using Adenovirus Serotype 26 Mosaic4 HIV which contains antigen of several virus subtypes. The estimated completion date is in 2021 and first results are expected in 2021[84,85].

2.3.2. Adjuvants used to Tailor the Immune Response

There are many approaches to generate an HIV-1 vaccine and a lot of these are based on the administration of soluble protein. The immunogenicity of a protein, however, is lower than for whole attenuated or inactivated viruses, but it can be increased when the protein is administered together with an adjuvant[86]. The choice of the right adjuvant is crucial for the protein's properties, e.g. the Env trimer's integrity and quality. It was shown that acidified alum formulations are not advised and also DNA-based polyanionic CpG oligodeoxynucleotide adjuvants should not be used, as they bind to SOSIP trimers and cover apex epitopes, at least in the case of the quaternary-specific bNAb PGT145[87].
Therefore, new HIV vaccine-adjuvant formulations are needed and already used in many studies to tailor the immune responses and to induce antibodies with greater potency[88] (Table 2).

Table 2: Overview of novel adjuvant formulations used or planned to be used in clinical trials for candidate HIV-1 vaccines (Status as of 2017) *Source abbreviations: GSK: GlaxoSmithKline, IDRI: Infectious Disease Research Institute, **HVTN: HIV Vaccine Trials Network. From[88].

Adjuvant (Source*)	Vaccine	Study
MF59 (GSK): Squalene-in-water emulsions	ALVAC-HIV (vCP2438) and bivalent subtype C gp120/MF59	Pivotal phase 2b/3 trial (HVTN** 702), prime boost regimen in South Africa
	HIV-DNA and bivalent gp120 (all subtype C)	Phase 1/2a trial (HVTN 108), 2 adjuvant arms
	ALVAC-HIV (vCP2438) and bivalent subtype C gp120/MF59	2 adjuvant arm study *(in planning)*
AS01B (GSK): Liposome-based QS-21 + monophosphoryl lipid A	HIV-DNA and bivalent gp120/AS01B (all subtype C)	Phase 1/2a trial (HVTN 108), 2 adjuvant arms
	eOD GT8 60-mer nanoparticle	Germline targeting Env immunogen *(in planning)*
	BG505 SOSIP.664 trimer	Well-ordered native-like soluble Env trimer *(in planning)*
	ALVAC-HIV (vCP2438) and bivalent subtype C gp120/AS01B	2 adjuvant arm study (HVTN 120) *(in planning)*
GLA-SE (IDRI): glucopyranosyl lipid A in stable emulsion	polyvalent gp120	Phase 1 trial (HVTN) *(in planning)*
	CH505 gp120	Phase 1 trial (HVTN), B cell lineage *(in planning)*
GLA-LSQ (IDRI): liposome-based glucopyranosyl lipid A and QS-21	BG505.665 SOSIP trimer	Phase 1 trial (HVTN) *(in planning)*
3M-052 (3M): TLR 7/8 agonists	BG505.665 SOSIP trimer	Phase 1 trial (HVTN) *(in planning)*

One adjuvant, which showed to be well tolerated in humans, is GLA-LSQ[89,90], a Toll-like receptor 4 agonist (Glucopyranosyl Lipid A) adjuvant in a liposomal formulation with QS21, manufactured by IDRI (Infectious Disease Research Institute, Seattle, USA). GLA-LSQ was shown to lead to an increased expansion of T follicular helper cells, followed by a durable and functional antibody response when used for a malaria vaccine and it was able to induce long-lived plasma cells, which, in general, have immunoglobulin-secreting activity and are able to maintain productive antibody levels for years[91]. When tested with SOSIP trimers, the liposomes present in the adjuvant did not detectably associate with the trimers and had no adverse effects on trimer integrity, stability, or conformation, which makes GLA-LSQ an interesting adjuvant for HIV-1 vaccine candidates[87].

2.4. Antibodies and Antibody-based Correlates of Immune Protection

Env can be presented to the immune system in various forms: in its functional form, as disassembled protein or with altered conformation, e.g. as shedded monomeric gp120, gp41 stumps, or aggregated protein[92,93].

In the time-course of an HIV infection, different kinds of antibodies directed against Env can be separated into three groups based on their neutralization capacity[94]: The first class of antibodies are the non-Neutralizing Antibodies (nNAbs), which can already be detected after one week of infection and bind to epitopes on the decayed Env proteins, which are not available on the functional Env trimer[94]. The second class of antibodies are the Neutralizing Antibodies (NAbs), which are highly strain-specific. These antibodies also develop early in infection, but their neutralization capacity is limited as they mainly target epitopes with high sequence variation and therefore viral escape often occurs[94]. The third group are the broadly Neutralizing Antibodies (bNAbs) which are able to neutralize HIV not only in a strain-specific manner, but rather neutralize a broad spectrum of HIV-1 strains, and are therefore interesting for vaccine design[94].

2.4.1. Broadly Neutralizing Antibodies

In contrast to non-neutralizing and strain-specific neutralizing antibodies, bNAbs usually do not develop in HIV-infected individuals suffering from an acute infection, but occur after several years and rounds of stimulation of the immune system with an evolving antigen[95,96]. Approximately 10 – 25 or even 50 % of chronically infected individuals develop bNAbs against a panel of circulating virus strains[97,96,98]. The arms race between the virus and the immune system leads to antibodies with special features, like extensive somatic hypermutation or long Complementarity-Determining Region 3 loops of the Heavy chain (CDRH3), which allows the penetration of the glycan shield[99,98]. When isolated as monoclonal antibodies, bNAbs can neutralize various HIV isolates of different clades and it was shown that they confer protection against simian immunodeficiency virus–HIV chimera (SHIV) after passive immunization of rhesus macaques[100,101].

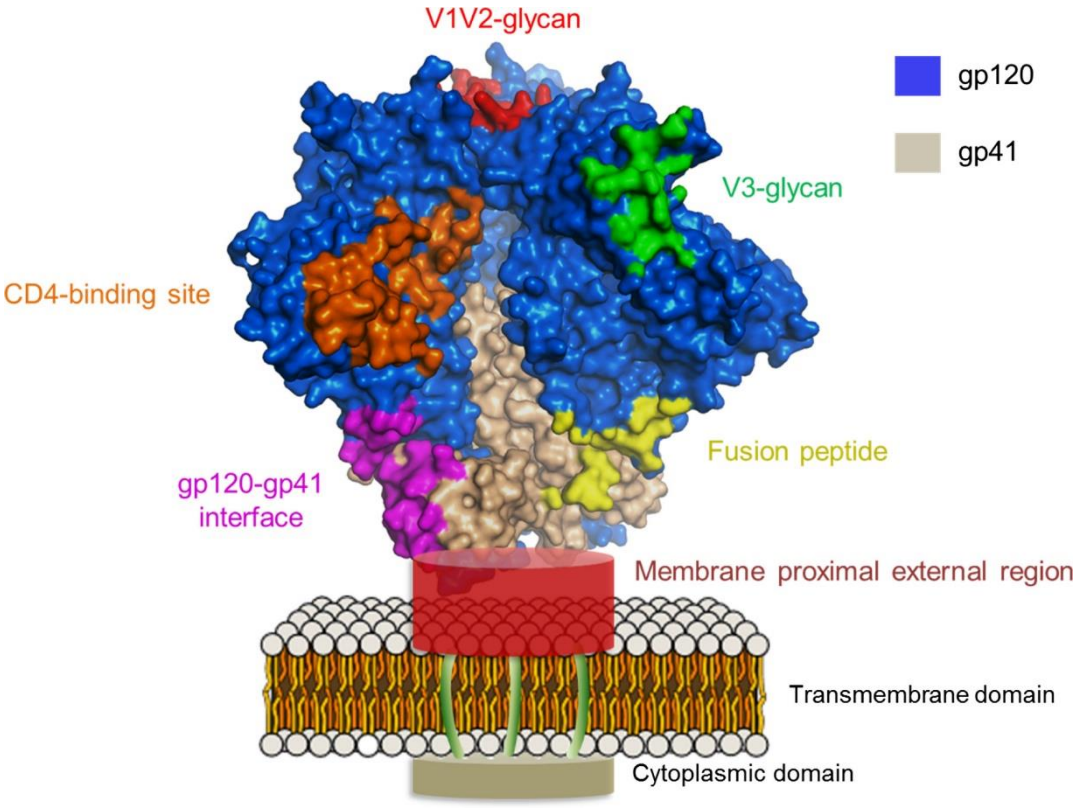

Figure 7: Sites of vulnerability to neutralizing antibodies. The structure of the Env spike is shown for the prefusion trimer (PDB:4TVP). The membrane-proximal external region, the transmembrane, and cytoplasmatic domains only have limited structural information and are presented as red and sand cylinders and green sticks. Figure from[102].

B-cells of HIV-1 infected individuals were originally used for the cloning of these antigen-specific antibodies, and sequence mapping and structural analysis helped to detect

vulnerable sites on Env, like V1V2, the V3-glycan, CD4-binding site (CD4bs), gp120/gp41 interface, and MPER (Figure 7)[98].

Antibodies directed against a quaternary structure-dependent epitope spanning V1V2, e.g. Abs PG9 and PG16[103,104], use their long CDRH3s to penetrate the glycan shield and bind to an epitope composed of V1V2 and N156/N160[105]. In contrast to this, V3-glycan antibodies like PGT121[106] are directed against a high-mannose patch around N332[106,107]. Interestingly, passive administration of PGT121 protected macaques from an SHIV infection upon mucosal challenge[108]. A conserved target which is surrounded by glycans is the CD4bs and respective CD4bs-Abs (e.g. PVG04, HJ16, and VRC01[109,110,111]) are able to neutralize > 90 % of HIV strains[98,112] and also the MPER showed to be an important epitope for MPER Abs like 2F5, 4E10, 10E8 or LN01[113,114,115].

In the last years, state of the art screening technologies with improved Env variants have led to the identification of various new bNAbs with epitopes distributed over the whole Env surface, including the gp41-gp120 interface (PGT151 or 35O22)[115,116].

This multitude of newly identified bNAbs has accelerated the development of more efficient Env antigens aiming at the induction of these kind of antibodies. Although neutralization breadth for tier 2 viruses is still mostly limited to the autologous virus strain after active vaccination with Env immunogens, recent studies suggest that trimeric Env proteins with improved stability and antigenicity (i.e. preserved or improved binding to bNAbs and reduced binding to nNAbs) are able to induce enhanced NAb responses[66,117,118,119,120].

Next to the induction of bNAbs upon active immunization, which, despite high effort, has not yet been achieved[121], also a passive immunization is an option to decrease HIV-1 infection rates as shown by VRC01, which is currently being tested in a Phase 2b study in Sub-Saharan Africa[122,123].

2.4.2. Antibodies Eliciting Fc-mediated Effector Functions

In many Non-Human Primate (NHP) studies and clinical trials performed over the years, several correlates of protection were observed which could help to design a potential HIV-1 vaccine candidate. Besides the bNAbs described in the previous section, there are also

the nNAbs and NAbs, which do not effiently contribute to neutralization but can mediate antiviral effector functions and lead to Fc-fragment-mediated phagocytosis[94,124].

In VAX004 (bivalent, recombinant gp120 vaccine), no efficacy was detected but subsequent analysis showed that vaccinees with high antibody levels had a decreased infection rate in comparison with the placebo group[73] and that this was caused by Antibody-Dependent, Cell-mediated Virus Inhibition (ADCVI), which requires the presence of FcR-bearing effector cells[125]. Of note, ADCVI Abs are also known to reduce viremia during acute HIV-1 infection[125,126].

In the RV144 vaccine efficacy trial, the only trial so far showing partial efficacy (31.2 %[79]), protection correlated with IgG antibodies and related effector functions, e.g. Antibody-Dependent Cellular Cytotoxicity (ADCC), and these protective antibodies were directed against V1V2 and recognized epitopes of multiple clades[127]. The IgG to V2 of CRF01_AE led to a decreased infection risk and this was also observed in other V2 subtypes. Antibodies binding to V3 in CRF01_AE also played an important role, but only if other antibody levels were low, like Env-specific plasma IgA or neutralizing antibodies[128]. As the efficacy was mediated by ADCC of antibodies directed against V1V2 and V3, it may be advantageous to design vaccines which induce these kind of antibodies[129,130,131].

Moreover, polyfunctional antibodies - which can recruit various cells of the immune system[132] - showed to be of interest, just like responses from Env-specific $CD8^+$ T cells, which are relevant for the initial control of infection[23,106].

In sum, the last years of HIV-1 vaccine research showed that effector cell-mediated antiviral antibody responses via FcR-dependent immune functions can comprise important correlates of protection, which should be considered for further vaccine design.

3. Objective

As outlined in the previous section, low-income countries with reduced access to ART would strongly benefit from a preventive HIV vaccine with high efficacy, ideally even after only few boost immunizations. Yet, none of the vaccine efficacy trials achieved the needed efficacy. However, recent studies showed that correlates of immune protection like bNAbs or antibodies eliciting Fc-mediated effector functions can protect the vaccinated individual from an infection with HIV.

Based on this, the aim of the project was to develop antigens with decreased conformational flexibility, in which the presentation of epitopes located in the inner part of the trimers leading to nNAbs[48,49] is avoided, and the possibility of the development of bNAbs is enhanced by the presentation of relevant epitopes. Therefore, conformationally stabilized trimers with increased affinity to bNAbs should be generated as uncleaved as well as native-like stabilized SOSIP-trimers and subsequently analyzed in a pre-clinical animal study.

For this, the first part of this work is the evaluation of the potential of a single amino acid exchange variant (L111A, detected by Veronika Grassmann[133]) in comparison to the wildtype (wt) isoform. This variant should be analyzed via flow cytometry as L111A gp145-variant to evaluate its affinity to selected antibodies. Further, it should be characterized as soluble gp140 construct and the purified gp140 protein should be used for a) analytical size exclusion to evaluate the degree of oligomerization, for b) antibody affinity, and c) thermostability measurements. In order to improve binding of the bNAb VRC01, another amino acid exchange variant detected by Veronika Grassmann (T278H) should be evaluated and the two amino acid exchanges, L111A and T278H, should be combined (LT) and analyzed further as native and cross-linked proteins. After the selection of the best isolate to be tested in a pre-clinical animal study, the variants are planned to be tested in a formulation study to analyse a possible effect of the adjuvant on the immunogens.

The second part of this work is the evaluation of the designed and quality-controlled antigens in an *in vivo* study to assess their immunogenicity. For this, a large-scale method for the endotoxin-free purification of the soluble gp140 proteins has to be set up. Furthermore, the LT variant should be analyzed in comparison to the wt as uncleaved and as native-like, cleaved SOSIP protein. In addition to the protein-only groups, also DNA-

prime/protein boost groups have to be analyzed to detect a possible impact of the DNA-prime on the subsequent immune responses. The readout of the study should be performed via a binding antibody multiplex assay. Here, the serum should be tested for binding to a panel of gp140 and gp120 proteins. As a potent response against V2 had been shown to lead to Fc-mediated effector functions in the RV144 trial, the potential of the variant to induce such responses should be evaluated with scaffolded tags-V1V2 and a gp70 V1V2 breadth panel. In this context, also a linear epitope mapping should be performed. Finally, the neutralizing capacity against tier 1A and tier 2 isolates should be investigated.

4. Materials and Methods

4.1. Gene Optimization

The HIV-1 Env variants used in this work were gene- and codon- optimized employing the online tool "GeneArt GeneOptimizer" (GeneArt/ThermoFisher Scientific, Waltham, USA) using human codon usage [134–136]. The start codon is preceded by a GCCACC-Kozak-sequence.

4.2. Molecular Biology

4.2.1. General Molecular Biology

Cloning of all DNA constructs was performed using common molecular biology protocols[137]. Restriction enzymes were purchased from New England Biolabs (NEB, Ipswich, USA) or Fermentas (Thermo Fisher Scientific, Waltham, USA) and used according to the manufacturer's protocols. Inserts needed for cloning procedures were either obtained by restriction digest from plasmids or via Polymerase Chain Reaction (PCR) using the Phusion High Fidelity Polymerase. The oligonucleotides used for PCR were designed to ensure attachment of restriction sites, sequences for protein tags, and the insertion of nucleotide exchanges, if needed (Supplemental Table 1). The digested or amplified inserts were separated by size via agarose gel electrophoresis and the bands of the correct size were purified using the QIAquick Gel Extraction kit. Cloning into QuickLigation vectors was performed using the one-tube QuickLig protocol restriction-ligation procedure[138] (Supplemental Table 2). The DNA was used to transform chemically competent *Escherichia coli* (*E. coli*) DH10B or DH5α, or DB3.1 if the plasmid contained a control of cell death toxin B (CcdB) cassette[139,140]. For the identification of positive colonies, an analytical PCR was performed with GoTaq Green MasterMix.

Article	**Cat. No.**	**Supplier**
Phusion® High-Fidelity DNA Polymerase	M0530	NEB, Ipswich, USA
GoTaq® Green Master Mix	M712	Promega, Fitchburg, USA

QIAquick Gel Extraction kit	28706	Qiagen, Hilden, Germany

Article	**Genotype**
E. coli DH5α	F- *supE*44 Δ*lacU*169 (*ϕ*80 *lacZ* Δ*M15*) *hsdR*17 *recA*1 *endA*1 *gyrA*96 *thi*-1 *relA*1
E. coli DH10B	F- *mcr*A *Δ(mrr-hsd*RMS-*mcr*BC*) Φ*80*dlacZΔM15 ΔlacX74 endA1 recA1 deoR Δ(ara, leu)7697 araD139 galU galK nupG rpsL λ-*
E. coli DB3.1	F- *gyr*A462 *end*A1 *gln*V44 Δ(*sr1*-*rec*A) *mcr*B *mrr hsd*S20(rB-, mB-) *ara*14 *gal*K2 *lac*Y1 *pro*A2 *rps*L20(Smr) *xyl*5 Δ*leu mtl*1

4.2.2. DNA Vaccine Design

For the DNA immunizations, gp140 genes of 16055 wt gp140, LT gp140, and SOSIP-LT gp140 were cloned into the VRC8400[141] vector via *Sal*I and *Not*I.

For the rabbit study, the DNA was prepared as endotoxin-free plasmid preparation (4.2.3).

4.2.3. Preparation of Plasmid DNA

Transformed *E. coli* were grown in the desired volume of LB-medium over night and the plasmid DNA was isolated using DNA preparation kits from QIAGEN or Thermo Fisher Scientific according to the manufacturers' protocol. Plasmid-DNA concentration and purity was analyzed spectrophotometrically using a NanoDrop ND-1000 photometer (absorbance at 260 and 280 nm).

Article	**Cat. No.**	**Supplier**
GeneJET Plasmid Miniprep Kit	K0503	Thermo Fisher Scientific, Waltham, USA
QIAGEN Plasmid *Plus* Midi Kit	12945	QIAGEN, Hilden, Germany
QIAGEN Plasmid Maxi Kit	12165	QIAGEN, Hilden, Germany
QIAGEN Plasmid Mega Kit	12183	QIAGEN, Hilden, Germany
EndoFree Plasmid Giga Kit	12391	QIAGEN, Hilden, Germany

Media	**Composition**
Lysogeny Broth (LB) medium	1 % (w/v) NaCl, 1 % (w/v) tryptone, 0.5 % (w/v) yeast extract, pH 7.5

4.2.4. Quality Control of Plasmid DNA

The plasmid DNA was subjected to analytical restriction digestion and loaded on a 0.8 % agarose gel. Furthermore, new plasmid-DNA was quality control via Sanger sequencing (SeqLab, Göttingen, Germany).

4.3. Cell Biology

4.3.1. Cultivation of Human Cells

4.3.1.1. Adherent Cell line

The adherent eukaryotic cell line HEK 293T/17 was cultivated in tissue culture flasks at 37°C and 5 % CO_2 in Dulbecco's Modified Eagle's Medium (DMEM) containing 10 % FBS and 1 % Penicillin-Streptomycin ($DMEM_{10}$). The cells were passaged at a ratio of 1:10 whenever they reached a confluency of ~ 80 %. For this, cells were washed with Phosphate Buffered Saline (PBS), trypsinated using Trypsin/EDTA and resuspended in $DMEM_{10}$.

4.3.1.2. Suspension Cell line

The eukaryotic suspension cell line FreeStyle™293-F was cultivated at 37°C, 8 % CO_2 and 90 rpm for 1 L and 5 L or 125 rpm for 125 ml and 250 ml tissue culture flasks in FreeStyle™ 293 Expression Medium containing 0.5 % Penicillin-Streptomycin. The cells were kept at a density between 0.2 and 2.0x10^6 cells/ml. For passaging, the cells were centrifuged at 100 g for 5 min at RT and resuspended in FreeStyle™ 293 Expression Medium.
The eukaryotic suspension cell line Expi293F™ was cultivated at the same conditions, but in Expi293™ Expression Medium without antibiotics. Furthermore, the cells were kept at a density between 0.3 and 3.0x10^6 cells/ml.

Article	**Cat. No.**	**Supplier**
HEK 293T/17	CRL-11268	ATCC, Manassas, USA
FreeStyle™ 293-F Cells	R79007	Gibco™/Thermo Fisher Scientific, Waltham, USA
Expi293F™ Cells	A14527	Gibco™/Thermo Fisher Scientific, Waltham, USA

Dulbecco's Modified Eagle's Medium	11995-065	Gibco™/Thermo Fisher Scientific, Waltham, USA
FreeStyle™ 293 Expression Medium	12338018	Gibco/Thermo Fisher Scientific, Waltham, USA
Expi293™ Expression Medium	A1435101	Gibco™/Thermo Fisher Scientific, Waltham, USA
Fetal Bovine Serum	10270-106	Gibco™/Thermo Fisher Scientific, Waltham, USA
Penicillin-Streptomycin	P06-07100	PAN Biotech, Aidenbach, Germany
Trypsin/EDTA	P10-023500	PAN-Biotech, Aidenbach, Germany
Cell Culture Flask T-25	83.3910.002	SARSTEDT AG & Co, Nümbrecht, Germany
Cell Culture Flask T-75	83.3911.002	SARSTEDT AG & Co, Nümbrecht, Germany
Cell Culture Flask T-175	83.3912.002	SARSTEDT AG & Co, Nümbrecht, Germany
Erlenmeyer Flasks Corning®	CORN431147	Omnilab, München, Germany
Optimum Growth™ 5L flask	931116	Thomson, Oceanside, California, USA

Buffer	**Composition**
Phosphate buffered saline	137 mM NaCl, 2.7 mM KCl, 10 mM Na_2HPO_4, 1.47 mM KH_2PO_4, pH 7.4

4.3.2. Transient Transfection of Adherent Human Cells and Flow Cytometry Analysis

For flow-cytometry analysis, HEK 293T/17 cells were transiently transfected with 96ZM651 wt and L111A gp145 using PolyEthylenImine (PEI)[142,138]. To this end, 4×10^5 cells were seeded into a 96 well flat bottom plate the day before transfection.

Directly before transfection, the medium was exchanged to 30 µl DMEM without supplements. After 10 min of incubation at room temperature (RT), the transfection mix consisting of 12 µl DNA (10 ng/µl), 6 µl PEI (100 ng/µl) and 18 µl DMEM per well without supplements was added to the cells. Duplicates were performed for each condition.

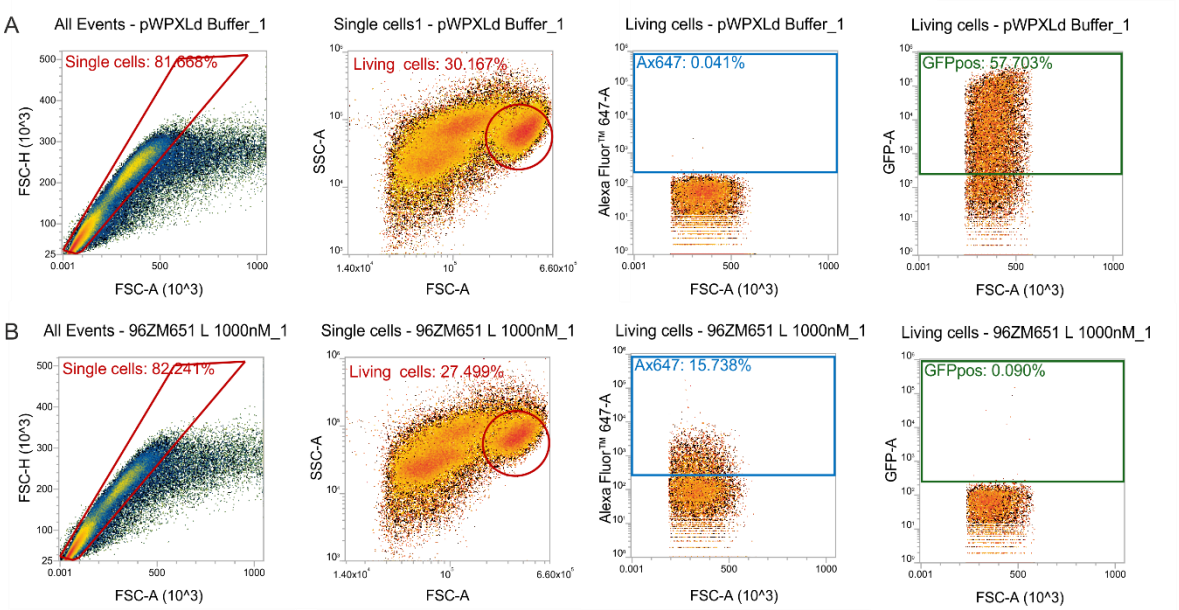

Figure 8: Representative flow cytometry gating strategy. HEK293F cells were transiently transfected with A) pWPXLd-GFP or B) pWPXLd_96ZM651 L111A gp145 and stained with PG9-Alexa647 (1000 mM). Single cells were gated for living cells, which were gated regarding their fluorescence intensities for the respective fluorophore.

Six hours post-transfection, the medium was changed to $DMEM_{10}$. As controls, untransfected cells were used as well as cells transfected with the empty vector pWPXLd. 48 h after transfection, cells were washed twice with PBS and resuspended in FACS buffer (PBS, 1 % (v/v) $FCS_{heat\text{-}inactivated}$, 2mM EDTA). Cells were incubated for 60 min at 4°C with the labelled antibodies (Titration from 1000 mM in a 2.5-fold serial dilution). Cells were washed three times with FACS buffer and analyzed by flow cytometry (Attune Nxt, Thermo Fisher Scientific). For the analysis, the cells were gated for Alexa647 or PE-positive single, living cells (Figure 8).

4.3.3. Transient Transfection of Human Suspension Cells

Transfection of FreeStyle™293-F cells was performed with PEI[142]. For this, 300 µg expression plasmid or 1.5 ml PEI (1 mg/ml) were mixed with 6.5 ml DMEM, each. Higher transfection volumes were scaled up accordingly. After 5 min at RT the two admixtures were combined and incubated for 20 min at RT. Afterwards, the mixture was given to FreeStyle™ 293 Expression Medium containing $1.0x10^6$ cells/ml, which showed a viability of > 90 % before they got harvested at 100 g for 5 min at RT and resuspended in 300 ml FreeStyle™ 293 Expression Medium. As a last step, the mixture was supplemented with 0.5 % Penicillin-Streptomycin. The supernatant was harvested after 5 days. For SOSIP

constructs, the same procedure was performed, except for the use of a mixture of a pcDNA3.1-furin-expression plasmid and the Env-expression plasmid at a ratio of 1:3.

The Expi293F™ cell line was transfected with ExpiFectamine. For this, $80x10^6$ cells were seeded in 40 ml Expi293™ Expression Medium in the morning. When the cell count reached $2.5x10^6$ cells/ml and when the vitality was >95 %, the transfection mix was added to the cells. For the transfection mix 40 µg DNA (1:1 mix of heavy and light chain vector) or 107 µl ExpiFectamine were mixed with 2 ml OptiMem, each. After 5 min on RT, the two admixtures were combined and incubated for 20-30 min, before being added to the cells. After 16-18 h, 200 µl Enhancer I and 2 ml Enhancer II were added as well as 0.5 % Penicillin-Streptomycin. The supernatant was harvested after 5 days.

Article	**Cat. No.**	**Supplier**
Polyethylenimine	23966-2	Polysciences, Warrington, USA
Opti-MEM™ I Reduced-Serum Medium	31985062	Gibco™/Thermo Fisher Scientific, Waltham, USA
ExpiFectamine™ 293 Transfection Kit	A14524	Gibco™/Thermo Fisher Scientific, Waltham, USA

4.4. Protein Biochemistry

4.4.1. Gp140 Env Variants Design

Soluble gp140 variants were either generated as uncleaved or native-like SOSIP[56] variants. For uncleaved variants, the furin cleavage site (REKR) was mutated (REKS)[62,63,64]. For all variants, a C-terminal Flag-His_6 tag sequence ($SG_4SDYKD_4KH_6$) was introduced after position 683 for the C clade variants and 664 for the A clade variants[143,144,145]. The SOSIP variants were designed as already published[56]. In brief, sequence changes were performed to introduce a disulfide bond between gp120 and gp41 (501C and 605C)[58], to increase trimer stabilization (I559P)[59], and to introduce epitopes depending on the glycan 332 (332N). Finally, the furin cleavage site was mutated to R_6[60]. If needed, amino acid exchanges were performed at position 111 (leucine to alanine) and 278 (threonine to histidine). All numbers account for HXB2 numbering.

The constructs were cloned via Quick-ligation into the plasmid pcDNA3.1QL or pQL13 and all constructs were verified by Sanger sequencing[138,146, 147].

Clade	Isolate	GenBank No.
C	96ZM651	AF286224
C	16055	EF117268
A	BG505	DQ208456

4.4.2. Purification of Soluble gp140 Envelope Protein

After 5 days at 37°C and 8 % CO_2, the supernatant of transiently transfected HEK293F suspension cells (4.3.3) was harvested by centrifugation for 20 min at 1000 g, sterile filtered with a Filtropur BT50 to get rid of cell debris and, depending on the volume, concentrated via a Viva-Flow cassette to one-tenth of the initial volume (Figure 9A). The concentrated supernatant was then used for Immobilized Metal ion Affinity Chromatography (IMAC) and loaded on a HisTrap excel column, where the His-tagged protein bound to the Ni-ions, while other protein and cell-culture media were removed. For this, the HisTrap was equilibrated with 10 CV His-EQ before the supernatant was loaded on the column and the protein washed and eluted with 10 CV His-W and 7 CV His-EL, respectively. The HisTrap excel eluate containing aggregate, trimer, dimer and monomer was then concentrated via an Amicon Ultra-15 (100 kDa cutoff) to 1 ml, followed by a buffer exchange to DEAE-A via Illustra™ NAP™-10 columns and a centrifugation step (30 min, 4°C, 14.000 g). Afterwards, the protein was loaded on an Anion Exchange Chromatography column (AEC), HiTrap DEAE-FF, which bound the aggregated protein, while trimer, dimer, and monomer were not influenced (Figure 9B). For this, the column was first equilibrated to DEAE-A (5 CV). The protein was loaded on the column and non-aggregated protein was washed out with DEAE-A and fractionated, while aggregated protein was eluted with DEAE-B. The protein was then concentrated via Amicon-Ultra-4 to a volume of 1 ml and after an additional centrifugation step used for Size Exclusion Chromatography (SEC, Figure 9C). With this, the protein could be separated into fractions containing the different configurations of the protein (trimer = 3n, dimer = 2n, monomer = 1n), which could be observed on Blue-Native (BN)-PolyAcrylamide Gel Electrophoresis (PAGE; 4.4.4) (Figure 9D). The trimeric fractions were

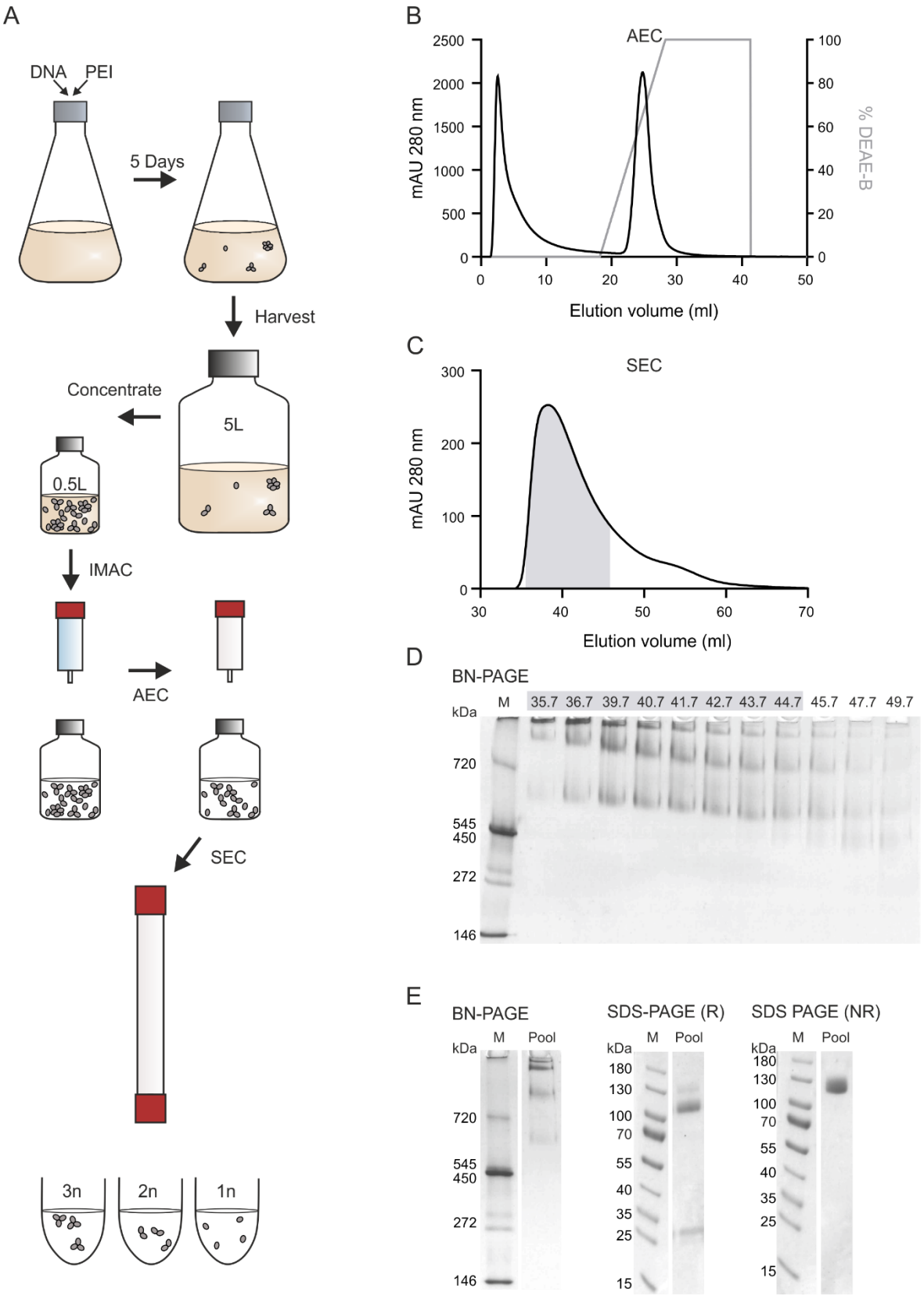

Figure 9: Large-scale purification and quality control

A) HEK293F cells were transiently transfected, the supernatant was harvested after 5 days and concentrated to ~ one-tenth of the initial volume. The His-tagged protein was purified via Immobilized Metal ion Affinity Chromatography (IMAC), followed by Anion Exchange Chromatography (AEC). Finally, a Size Exclusion Chromatography (SEC) was performed, leading to the separation of trimer (3n), dimer, (2n) and monomer (1n). B-E) Purification of gp140 protein on the example of 16055 SOSIP-LT. B) Elution profile observed during

AEC. The first peak resembles the native protein, while the second peak is predominantly aggregated protein, which can only be eluted by a high-salt buffer (DEAE-B). C) SEC elution profile. Fractions of 0.5 ml each were collected and used for D) Blue-Native Polyacrylamide gel electrophoresis (BN-PAGE): Fractions containing the highest trimeric and lowest content of aggregates, dimers or monomer were pooled (Grey shaded areas) and the pool of trimers was loaded E) on a BN-PAGE and Reducing (R) and Non-Reducing (NR) SodiumDodecylSulfate (SDS)-PAGE as final quality control.

pooled, concentrated (Amicon-Ultra-4) and analyzed on BN and SodiumDodecylSulfate (SDS)-PAGE (Figure 9E; 4.4.5).

For lectin affinity chromatography, *Galanthus nivalis* lectin agarose beads were equilibrated with Lectin-W (4 CV), added to the sterile filtered supernatant and rocked over night at 4°C. The beads were centrifuged (500 g, 1 min) and washed with 5 x bead volume (BV) Lectin-W. The elution of the protein was performed for 1 h in a rotating vessel with 1 BV Lectin-EL. Buffer exchange to PBS was performed with Illustra™ NAP™-10 columns. The protein was then concentrated to the desired volume via an Amicon Ultra-0.5 Centrifugal Filter Unit and further analyzed via SEC on a High-Pressure Liquid Chromatography (HPLC) system.

Article	**Cat. No.**	**Supplier**
Filtropur BT50	83.3941.101	SARSTEDT AG & Co, Nümbrecht, Germany
Vivaflow 50 R 30.000 MWCO Hydrosart	VF05H2	Sartorius, Göttingen, USA
HisTrap excel	17-3712-06	GE Healthcare, Chicago, USA
HiTrap DEAE FF	17-5154-01	GE Healthcare, Chicago, USA
Illustra™ NAP™-10 columns	17-0854-02	GE Healthcare, Chicago, USA
Amicon Ultra-15	UFC910024	Merck, Darmstadt, Germany
Amicon Ultra-4	UFC803024	Merck, Darmstadt, Germany
HiPrepTM 16/60 Sephacryl S-300 HR	17-1167-01	GE Healthcare, Chicago, USA
SERVA*Gel*™ N 4 – 16, Vertical Native Gel 4 - 16 %	43253.01	Serva Electrophoresis, Heidelberg, Germany
Galanthus nivalis Lectin, Agarose bound	AL-1243	Biozol, Eching, Germany
Amicon Ultra-0.5 Centrifugal Filter Unit	UFC503096	Merck, Darmstadt, Germany
Yarra™ 3µm SEC 4000	00H-4514-E0	Phenomenex, Torrance, USA

Buffer	Content
His-EQ	20 mM sodium phosphate, 0.5 M NaCl, pH 7.4
His-W	20 mM sodium phosphate, 0.5 M NaCl, 30 mM imidazole, pH 7.4
His-EL	20 mM sodium phosphate, 0.5 M NaCl, 0.5 M imidazole, pH 7.4
DEAE-A	0.1 M NaCl, 0.02 M Tris-HCl, pH 8
DEAE-B	1 M NaCl, 0.02 M Tris-HCl, pH 8
Lectin-W	1 mM EDTA, 1mM EGTA, PBS
Lectin-EL	1M mannopyranoside, 1 mM EDTA, 1mM EGTA, PBS

4.4.3. Chemical Cross-Linking of gp140 Env Trimers

1-Ethyl-3-(3-Dimethylaminopropyl)-Carbodiimide hydrochloride (EDC) and N-HydroxySuccinimide (NHS) cross-linking was performed as previously described[67]. For the cross-linking mix, EDC:NHS was used in a ratio of 100:1 in 2-(N-Morpholino)-ethansulfonic acid monohydrate buffered saline (MES) per mol Env. The optimal CL concentration was determined as 160,000 mol EDC:NHS per mol Env (1 mg/ml). For the cross-linking procedure, one volume of cross-linking mix was given to one volume of Env gp140 in the respective molar amount in PBS. After 30 min at RT, the reaction was stopped by addition of two volumes of 1 M Glycin (pH 7.4) and another incubation step for 10 min at RT. Afterwards, the buffer was exchanged to PBS. The quality control was performed with a reducing 5 % SDS-PAGE analysis and a lectin ELISA.

Article	Cat. No.	Supplier
N-(3-Dimethylaminopropyl)-N'-ethylcarbodiimide hydrochloride	03449-5G	Sigma Aldrich, St. Louis, USA
N-hydroxysuccinimide	24500	Thermo Fisher Scientific, Waltham, USA

Buffer	Content
2-(N-Morpholino)-ethansulfonic acid monohydrat buffered saline	50 mM MES monohydrate, 150 mM NaCl, pH 6.0

4.4.4. Blue-Native PAGE

The purity of the Env proteins was analyzed by Blue-Native Polyacrylamide gel electrophoresis (BN-PAGE). If not stated differently, 2.5 µg Env were mixed with PBS and Sample Buffer (2x) to a total volume of 15 µl and loaded on a precast SERVAGel™ N 4 – 16. Electrophoresis was performed for 20 min at 50 V, followed by 4 h at 100 V. Staining was performed with Coomassie-Staining solution for 10 min, followed by an incubation over night in destain-solution. The Cathode Buffer was supplemented with SERVA Blue G Solution to a total of 0.002 % (w/v).

Article	**Cat. No.**	**Supplier**
SERVAGel™ N 4 – 16	43252	SERVA Electrophoresis, Heidelberg, Germany
SERVA Native Marker	39219	SERVA Electrophoresis, Heidelberg, Germany
Native Cathode Buffer for BN/CN (10x)	42536	SERVA Electrophoresis, Heidelberg, Germany
Native Anode Buffer for BN/CN (10x)	42535	SERVA Electrophoresis, Heidelberg, Germany
Sample Buffer for Blue Native (2x)	42533	SERVA Electrophoresis, Heidelberg, Germany
SERVA Blue G Solution for Blue Native, 1 %	42538.01	SERVA Electrophoresis, Heidelberg, Germany

Buffer	**Content**
Coomassie-Staining solution	0.125 % (w/v) Coomassie Brilliant Blue R-250 50 % (v/v) ethanol, 7 % (v/v) acetic acid
Destain-solution	7 % (v/v) acetic acid

4.4.5. SDS-PAGE

Proteins were analyzed via SodiumDodecylSulfate-(SDS)-PAGE with a 5 % stacking gel and either 5, 10, or 12.5 % separation gel, according to the size of the expected protein bands[148]. For this, protein samples were either mixed with reducing (6x) or non-reducing (5x) Laemmli buffer. After incubation for 5 min at 95°C, the samples were loaded. Electrophoresis was performed at 90 V for 20 min followed by 140 V for 50 min or until the tracking dye reached the bottom of the gel.

Also, precast SERVA*Gel*™ TG PRiME™ 8 - 16 % gels were used when a gradient was needed. Here, electrophoresis was performed at 100 V for 10 min followed by 250 V for 45 min. The same buffers were used as for the self-made SDS-PAGE.

For both types of gels, PageRuler™ Prestained Protein Ladder was used as molecular weight marker and staining was performed with Coomassie-Staining solution for 10 min, followed by an incubation over night in destain-solution.

Article	**Cat. No.**	**Supplier**
SERVAGel™ TG PRiME™ 8 - 16 %	43279	SERVA Electrophoresis, Heidelberg, Germany
PageRuler™ Prestained Protein Ladder	26616	Thermo Fisher Scientific, Waltham, USA
HiMark™ Pre-stained Protein Standard	LC5699	Thermo Fisher Scientific, Waltham, USA

Buffer	**Composition**
SDS running buffer	25 mM Tris, 192 mM glycine, 0.1 % (w/v) SDS
6x Laemmli buffer (R)	375 mM Tris, 6 % (w/v) SDS, 30 % (v/v) β-mercaptoethanol, 30 % (w/v) glycerol (87%), 3 mM EDTA, 0.03 % (w/v) bromophenol blue, pH 6.8
5x Laemmli buffer (NR)	312.5 mM Tris, 5 % (w/v) SDS, 25 % (w/v) glycerol (87 %), 2.5 mM EDTA, 0.025 % (w/v) bromophenol blue, pH 6.8

4.4.6. Silver Staining

The SDS-gel was fixed for one hour in Silver-fixation solution, followed by two incubation steps in 50 % and 30 % ethanol for 10 mins each. After one minute in 0.2 g/L sodium thiosulfate solution, the gel was washed three times (25 sec each step) with H_2O and then the staining was performed for 20 mins in Silver-staining solution. After two more washing steps with H_2O, development was performed with Silver-developing solution until the bands showed the desired intensity. The reaction was stopped with 5 % acetic acid in a 5 min incubation step, followed by two washing steps for 10 min in H_2O. For each step, 25 ml of the respective solution was used.

Buffer	Composition
Silver-fixation solution	50 % (w/w) methanol, 12 % (w/w) acetic acid, 50 µl 37 % formaldehyde solution
Silver-staining solution	0.1 % (w/w) $AgNO_3$, 75 µl 37 % formaldehyde solution
Silver-developing solution	6 % (w/w) Na_2CO_3, 50 µl 37 % formaldehyde solution, 0.2 g/L sodium thiosulfate

4.4.7. Endotoxin Assay

Endotoxin content of the proteins used for the immunization study was evaluated with the QCL-1000™ Endpoint Chromogenic LAL Assay according to the manufacturer's instructions. Next to the proteins, all buffers and solutions needed for endotoxin-free purposes were also tested.

Article	Cat. No.	Supplier
QCL-1000™ Endpoint Chromogenic LAL Assay	50-647U	Lonza, Basel, Switzerland

Immunogen	Endotoxin Units/ immunization dose
16055 wt gp140	0.11
16055 LT gp140	0.05
16055 SOSIP gp140	0.11
16055 SOSIP-LT gp140	0.05
16055 wt_CL gp140	0.05
16055 LT_CL gp140	0.10
16055 SOSIP_CL gp140	0.12
16055 SOSIP-LT_CL gp140	0.05

4.4.8. Negative/Positive Selection – Batch Assay

0.3 g Protein A-sepharose was soaked in 1,500 µl Buffer A for 30 min. After centrifugation for 1 min at 1,000 g, the supernatant was discarded and washed three times with 3 ml PBS for 1 min. 400 µl beads were mixed with 1 ml antibody (~ 1 mg/ml). After 1 h rocking at 4°C, the mixture was centrifuged (1 min, 1,000 g) and the supernatant was used for further evaluation.

Article	Cat. No.	Supplier
Protein A-sepharose	M1320-5	BioVision, Milpitas, USA

4.4.9. Enzyme-Linked ImmunoSorbent Assay (ELISA)

Nunc MaxiSorp™ flat-bottom plates were coated with 1 µg/ml *Galanthus nivalis* lectin in PBS overnight at 4°C (Figure 10). After coating, plates were washed with PBS-T on a HydroFlex microplate washer and subsequently blocked for 2 h at RT using 200 µl ELISA-Blocking-Solution per well. After an additional washing step, 50 µl gp140 Env variants were added at a concentration of 2 µg/ml in PBS and incubated for 1 h at RT. After another washing step, incubation with a dilution series of bNAbs in ELISA-Binding-Buffer followed for 1 h at RT (50 µl per well). Finally, the unbound antibody was washed away, and incubation with 50 µl horseradish peroxidase-coupled polyclonal rabbit anti-human IgG at 1:5000 in ELISA-Binding-Buffer was performed for 30 min at RT, followed by a washing cycle and development with 50 µl 3,3',5,5'-tetramethylbenzidine (TMB) substrate for 2 min. The TMB-substrate was freshly prepared by mixing TMB-A and TMB-B in a ratio of 20:1. The colorimetric reaction was stopped with 25 µl 1 M H_2SO_4 and absorption at 450 nm was analyzed on a Microplate Reader. Curves were fitted using non-linear least squares regression (Fit "One site binding (Hyperbola)", GraphPad Prism 8.1.2).

For the formulation study, 0.12 mg/ml protein were mixed with an equal volume of GLA-LSQ[89,90] (liposomal formulation, 0.05 mg/ml GLA, 0.02 mg/ml QS21) and incubated for 4 h at 25°C before it was used for the ELISA.

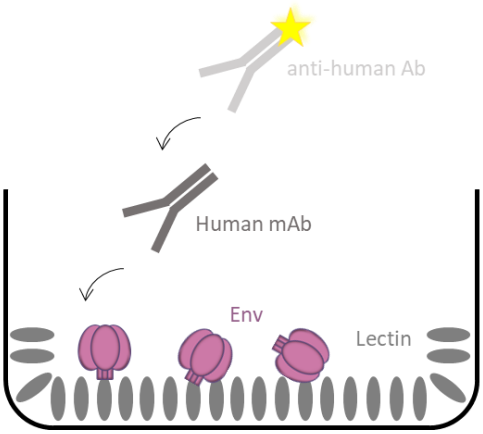

Figure 10: Schematic representation of the sandwich-ELISA format used. Nunc MaxiSorp™ flat-bottom plates were coated with Galanthus nivalis Lectin, which captures Env protein. The primary antibody bound to Env, while an HRP-coupled secondary antibody bound to the primary antibody.

Article	Cat. No.	Supplier
Nunc MaxiSorp™ flat-bottom	44240421	Thermo Fisher Scientific, Waltham, USA
Tween20	3472	Caelo, Hilden, Germany
Galanthus nivalis Lectin	L8275	Sigma Aldrich, St. Louis, USA
Bovine Serum Albumin (BSA)	01400.100	Biomol, Hamburg, Germany
Horseradish peroxidase coupled polyclonal rabbit anti-human IgG	P0214	Dako, Glostrup, Denmark

Buffer	Composition
PBS-T	0.1 % Tween20 in PBS
ELISA-Binding-Buffer	1 % (w/v) BSA in PBS
ELISA-Blocking-Solution	5 % (w/v) skimmed milk powder, 5 % (v/v) Bovine Serum Albumin (BSA) and 0.1 % Tween20 in PBS
TMB A	30 mM tri-potassium citrate-monohydrate adjusted to pH 4.1 with 10 % (w/v) citric acid
TMB B	0.24 % (w/v) 3,3',5,5'-tetramethylbenzidine, 10 % (v/v) acetone, 90 % (v/v) ethanol, 80 mM H_2O_2

Equipment	
HydroFlex microplate washer	Tecan, Männedorf, Switzerland
Microplate reader Model 680	Bio-Rad Laboratories, Hercules, USA
GraphPad Prism, version 8.1.2	GraphPad Software, La Jolla, USA

4.4.10. Antibodies

Antibodies PG9[105], 2G12[113], 447-52D[149] and 5F3[113] (Polymun), 17b[150] (IAVI), HJ16[110] and HGN194[110] (Davide Corti, Lanzavecchia Lab), PGT121[106], PGT145[106] and PGT151[151,152] (Quentin Sattentau) were purchased or kindly provided by cooperation partners. In-house produced antibodies (F105[153], VRC01[154], 35O22[115], and 10E8[155]) were produced based on published sequences. The antibodies were generated via transient transfection of Expi293F™ cells (4.3.1.2). After 5 days, the supernatant was centrifuged to get rid of cell debris and sterile filtered with a 0.2 µm filter. The supernatant was then loaded on a HiTrap rProtein A FF column and the antibody was purified on the Äkta using the program "ProteinA antibody purification" written by Dr. David Peterhoff. For this, the column was washed with PBS and the antibody eluted with the elution buffer (0.1 M glycine pH 3.2, 0.1

M fructose). The fractions containing the antibody were pooled and neutralized with 1 M Tris-HCl pH 9. Dialysis was used to transfer the antibody into the desired buffer. For flow-cytometric analysis, antibodies were labeled with the Alexa Fluor™ 647 Protein Labeling Kit or the Lightning-Link® R-PE labeling kit, as recommended by the manufacturer.

Article	**Cat. No.**	**Supplier**
HiTrap rProtein A FF column	17-5080-01	GE Healthcare, Chicago, USA
Alexa Fluro™ 647 Protein Labeling Kit	A20173	Thermo Fisher Scientific, Waltham, USA
Lightning-Link® R-PE Labeling Kit	703-0015	Innova Biosciences, Cambridge, UK

4.4.11. Differential Scanning Calorimetry

Thermal denaturation of proteins was evaluated with a MicroCal PEAQ DSC (Malvern Panalytical, Kassel, Germany). Protein samples were adjusted to 1 mg/ml with PBS and 250 µl were used for each measurement. Thermal denaturation was performed at a scan rate of 60°C/h, starting from 25°C. PBS was used as a baseline. The evaluation was performed with the MicroCal PEAQ DSC-Software (Malvern Panalytical, Version 1.51). Here, the data was buffer-subtracted, and a baseline-correction was performed.

4.4.12. nano-format of Differential Scanning Fluorimetry (nanoDSF)

NanoDSF measurements were performed at a Prometheus NT.48 (NanoTemper Technologies, Munich, Germany)[156]. For this, 10 µl protein was used at a concentration of 0.05 mg/ml. Protein samples were analyzed in triplicates using a temperature gradient ranging from 20°- 95°C at a scan rate of 60°C/h.

Table 3: Table of antibodies used in this thesis, which target the Envelope glycoprotein. Abbreviations: CDR3H: heavy-chain 3 complementary determining region CDR L: light-chain 3 complementary determining region IAVI: International AIDS Vaccine Initiative VH: heavy chain variable domain. SHM: Somatic HyperMutation. Modified after[157].

Antibody	Class	Recognition properties	Epitope features	Isolation year	Supplier
17b[25,150]	CD4-induced	recognizes open conformation of Env	discontinuous epitope on gp120	1993	IAVI, New York, USA
F105[153,158]	CD4-binding site	recognizes open conformation of Env	discontinuous, or conformational, epitope in gp120	1991	In house production
VRC01[111,112,154]		VH1-2 derived, 5-residue CDR L3, very high SHM	CD4bs	2010	
HJ16[110]		CDR H3 loop-dominated	N276 requirement	2010	Davide Corti, Lanzavecchia Lab
HGN194[110]	V3-directed	neutralizes Tier-1 irrespective of clade	conserved epitope in V3 crown (RRSVRIGPGQTF)	2010	
447-52D[149,159,160,159]		extensively cross-reactive, especially with V3 peptides of clade B viruses	sequence in V3 crown (GPGR)	1992	Polymun Scientific, Klosterneuburg, Austria
PGT121[106,107,162]	N332 glycan patch	25-residue CDR H3 with nonpolar tip	GDIR motif, V1V2 and/or V3 glycans	2011	Quentin Sattentau
2G12[113,163]		domain exchanged structure	glycan only	1994	Polymun Scientific, Klosterneuburg, Austria
PG9[105,164,165]	Apex (V1V2 glycan)	long, protruding CDR H3 with sulfated tyrosine	N156/N160 glycans, V1V2 strand C	2009	
PGT145[106,166,167]		long, protruding CDR H3 with sulfated tyrosine, quaternary specific	N160 glycan, hole at trimer apex	2011	Quentin Sattentau
PGT151[151,152]	gp120-gp41 interface	trimer and cleavage specific, asymmetric 2:1 (Ab:trimer) binding, YYYY motif in CDR H3	Fusion peptide and complex glycans at N611 and N637 on gp41	2014	
35O22[115]		binds cleaved and uncleaved Env	Glycan at N88 requirement	2014	In house production
10E8[115,155,168]	MPER	CDR L3 and CDR H3 mediated	C-terminal helical region	2012	
5F3[113,169]	gp41	targets C-terminal heptad repeat, suggested to interact with fusion proximal peptide region	aa650–657 in gp41: QNQQEKNE, cross-reactivity to subtype C strains	1994	Polymun Scientific, Klosterneuburg, Austria

4.4.13. Formulation Study

Physicochemical analysis of the formulated proteins was performed by IDRI (Seattle, USA). For this, trimeric Env protein was mixed 1:1 (v/v) with GLA-LSQ liposomal formulation[170,171], resulting in a concentration of 0.05 mg/ml GLA and 0.02 mg/ml QS21. The formulated samples were stored at both, 5 and 25°C for 0, 4 and 24 hours and frozen at -80°C until further use.

4.4.13.1. Particle Size Measurement

The measurement of the particle size was performed on a Nano-S (ZEN1600) and Zetasizer Nano-ZS (ZEN3600) Dynamic Light Scattering systems (DLS) according to the standard protocol of IDRI[170,171]. For this, 25 µl admixture were diluted with 475 µl H_2O_{MilliQ} and analyzed in a disposable cuvette. The analysis was performed in triplicates. To determine the particle size *d*, the measured translational diffusion *D* was inserted into the equation $d=K_BT/(3\pi\eta D)$, (K_B: Boltzmann constant, T: temperature, η: fluid viscosity)[172]. To approximate the particle refractive index, standard viscosity and refractive index values for water as the bulk phase were used.

4.4.13.2. SDS-PAGE

For the analysis via SDS-PAGE, 20 µl 4x Lithium Dodecyl Sulfate (LDS) Sample Buffer, 20 µl H_2O_{MilliQ}, and 40 µl admixture were mixed and heated for 5 minutes at 85 - 95 °C[170,171]. The samples were stored at -20°C and reheated for 1 min at 85 - 95°C before analysis. 30 µl of the sample was loaded on a 12-well Tris-Glycine gel, which was subsequently transferred to PVDF membranes. Staining was performed with Colloidal Gold Total Protein Stain.

4.4.13.3. Blue-Native PAGE

For the Blue-Native PAGE, 50 µl admixture were mixed with 25 µl of 4x loading buffer, 10 µl of G-250 sample additive, and 15 µl H_2O_{MilliQ}[170,171]. Until analysis, the samples were stored at -20°C. 35 µl samples were loaded on NativePAGE 4-16 % Bis-Tris 10 well gels. Electrophoresis was performed at 150 V for 100 minutes. After a rinse in H_2O, the gel was fixed and destained.

4.5. Animal Study

4.5.1. Animal System

Female New Zealand White rabbits (6 - 9 months, 3 - 5 kg) were kept in the study facility of R & R Research LLC, Stanwood, WA.

4.5.2. Administration of Immunogens

Whenever protein was used for immunization, 30 µg protein in PBS were thawn at RT and mixed 1:1 by volume with GLA-LSQ[89,90], resulting in 25 µg GLA and 10 µg QS21 per dose and a total injection volume of 0.5 ml. The immunization was administered *i.m.* within 4 hours after admixture into the rear quadriceps muscle. For DNA immunizations, 2 mg DNA in PBS were thawn at RT and administered *i.m.* in two injections of 0.5 ml each into the left and right rear quadriceps muscle.

4.5.3. Collection of Samples

In all groups, blood samples were analyzed at weeks -2, 10, 24, and 26. For this, the blood was collected into 12 ml serum separator tubes.

4.6. Immunological Evaluation

4.6.1. Binding Antibody Multiplex Assay (BAMA)

The serum IgG responses obtained in the immunization study were tested by the CAVD central facility (Tomaras lab, Duke University, Durham, North Carolina, USA) on a gp140 panel (Table 4) as well as on an Env gp120 (Table 5) and V1V2 (Table 6) breadth panel[173].
For the BAMA against the "RepliVax" immunogens (16055 wt, 16055 LT, 16055 SOSIP, 16055 SOSIP-LT) used for the animal study, the assay's set up was changed to neutravidin coupled beads coupled to biotinylated anti-6x His polyclonal or monoclonal antibodies, which were then coupled to the RepliVax antigens.
For the breadth panels, the Luminex-based binding antibody multiplex assay was performed as previously described on a Bio-Plex instrument (Bio-Rad)[80,174,175,176]. Antibody

levels were measured in duplicates as Median Fluorescence Intensity (MFI) and the mean of these two wells was used. Data shown in graphs represent the background-adjusted MFI minus background-adjusted blank (MFI*).

For background measurements, the MFI from wells with beads in buffer without sample was used. Furthermore, for the evaluation of non-specific antibody binding, a blank or reference bead was included. The analysis was either performed as single-point measurement at a dilution of 1:80 or as a 6-fold serial dilution, starting from 1:80. Samples which showed a blank MFI > 5,000 were excluded due to high background. As positive controls, polyclonal IgG from HIV-positive subjects as well as purified rhesus macaque IgG was used, while HIV-1 negative sample, plasma from an SIV negative rhesus macaque, and blank beads were used as negative controls.

Samples at week 10, 24 and 26 were declared positive if they met the following three criteria[177]:

- MFI* values at the screening dilution had to be greater than the maximum of 100 or the 95th percentile of baseline samples (by antigen).
- MFI* values had to be greater than 3 x the baseline background-adjusted MFI minus baseline background-adjusted blank values.
- Background-adjusted MFI values had to be greater than 3 x the baseline background-adjusted MFI values.

Table 4: gp140 panel

Antigen name
16055 wt gp140_FlagHIS
16055 LT gp140_FlagHIS
16055 SOSIP gp140_FlagHIS
16055 SOSIP -LT gp140_FlagHIS
BG505 SOSIP.664 gp140_avi
Con S gp140 CFI

Table 5: gp120 breadth panel

Antigen name	Subtype	Country of origin
51802_D11gp120.avi/293F	A	Kenya
BORI_D11gp120.avi/293F	B	USA
TT31P.2792_D11gp120.avi/293F	B	Trinidad/Tobago
B.6240_D11gp120.avi/293F	B	USA
A244 D11gp120.avi	CRF01_AE	Thailand
254008_D11gp120.avi/293F	CRF01_AE	Thailand
CNE20_D11gp120.avi/293F	CRF07_BC	China (Xinjiang)
BJOX002_D11gp120.avi/293F	CRF07_BC	China (Beijing)

Table 6: V1V2 antigens

Antigen name	Subtype	Country of origin
AE.A244 V1V2 Tags/293F	CRF01_AE	Thailand
C.1086C V1V2 Tags	C	Malawi
gp70-191084_B7 V1V2	A	Uganda
gp70_B.CaseA_V1_V2	B	USA
gp70-RHPA4259.7 V1V2	B	USA
gp70-62357.14 V1V2	B	USA
gp70-700010058 V1V2	B	USA
gp70-TT31P.2F10.2792 V1V2	B	Trinidad/Tobago
gp70-BF1266_431a_V1V2	C	Malawi
gp70-7060101641 V1V2	C	South Africa
gp70-96ZM651.02 V1v2	C	Zambia
gp70-001428.2.42 V1V2	C	India
gp70-CAP210.2.00.E8 V1V2	C	South Africa
gp70-TV1.21 V1V2	C	South Africa
gp70-Ce1086_B2 V1V2	C	Malawi
gp70-CM244.ec1 V1V2	CRF01_AE	Thailand
gp70-C2101.c01_V1V2	CRF01_AE	Thailand
gp70-BJOX002000.03.2 V1V2	CRF07_BC	China

4.6.2. Linear Epitope Mapping

For each animal of the seven groups (n=5), sera from weeks 10 and 26 were analyzed in a peptide library designed by Bette Korber, LANL[178]. For this, 15-mer peptides overlapping by 12 were used. The peptide library covered:

A) Consensus Env (gp160): Clades A, B, C, D, Group M, CRF1, and CRF2

B) Vaccine Strains (gp120): AE.A244, AE.TH023, MN, C.1086, C.TV1, and C.ZM651

For the assay, the samples were diluted 1:50 in BAMA diluent (milk-based blocking buffer). Goat Anti-Hu IgG*Alexa Fluor 647 was used as secondary antibody at a dilution of 1:500. For the scan setting, InnoScan XDR was used.

In order to match positivity criteria (positivity call was made using data processed with "smooth" option in pepStat to reduce false positivity rate[178]), the data had to fulfil the following conditions:

1. Global intensity cut off: Intensity of post sample: > 95th percentile of all baseline sample binding for all peptides
2. Baseline cut off: Intensity for post sample: > 3-fold higher than matched pre-bleed (Log_2Fold >1.58)
3. Per peptide cut off: Intensity for post sample: > 95th percentile of specific activity of all baseline samples

Table 7: Epitopes identified in the Linear Epitope Mapping. Amino acid (AA) range is shown in HXB2 numbering.

Epitope	AA range
C1.1	59 - 73
C1.2	74 - 88
C1.3	83 - 97
V2	157 - 174
V3.1	295 - 312
V3.2	304 - 318
C4	427 - 447
C5.1	475 - 495
C5.2	490 - 504
C5.3	496 - 510
aa532-546	532 - 546
AVERY	580 - 597
gp41ID	592 - 606

4.6.3. TZM-bl Neutralization Assay

The neutralization assay was performed by the CAD central facility (Montefiori Lab, Duke University, Durham, North Carolina, USA) as described previously[179,180]. For this, serum antibodies against HIV-1 pseudoviruses (Tier 1A: MW965.26; Tier 2: 16055-2.3, 25710-2.43, Ce1176_A3, and Ce703010217_B6) and one control isolate (SVA-MLV) were measured as a function of reduction in Tat-regulated luciferase reporter gene expression in TZM-bl cells in order to obtain neutralization ID_{50} titers. The serum dilution at which relative luminescence units (RLUs) were reduced by 50 % relative to the RLUs in virus control wells (cell + virus only) after subtraction of background RLUs (wells with cells only) was defined as neutralization titer. The threshold for a positive response was set to 20 for ID_{50} neutralization titers.

4.6.4. Statistical Analysis

Statistical tests were performed for comparisons of response magnitudes as an unpaired two-samples Wilcoxon test with the software R (Version 3.6.1)[181]. Statistics were only performed if the response rate was ≥ 80 %. Multiple comparison correction was not performed to identify potential differences more easily. Furthermore, non-responders were not shown in the figures for weeks 10, 24, and 26 for better representation of the data.

5. Results

5.1. Influence of Single Amino Acid Substitutions on the HIV-1 Envelope Trimer

In order to find new HIV-Env-based immunogens showing an increased binding to bNAbs, Veronika Grassmann analyzed the interaction between variants of a library of HIV-1 Env mutants and selected bNAbs in a flow cytometry-based cellular display technique in her PhD thesis[133]. This technique allows the presentation of 96ZM651 gp145 Env variants in the natural membrane-bound state on the surface of human cells, including native folding and mammalian glycosylation. In the library, each amino acid in gp120 was exchanged for an alanine once per variant, except for the cysteines, leading to a total of 605 variants to be analyzed. 48 h post transient transfection, the Env-expressing cells were analyzed by flow cytometry. To normalize for varying surface expression levels of the different alanine variants, cells were stained with both, the Alexa647-labelled screening antibody of interest, and the PE-labelled reference antibody 5F3, which binds to a linear epitope in the extracellular domain of gp41 and should hence recognize all gp120 alanine variants alike.

5.1.1. Characterization of L111A

5.1.1.1. L111A gp145 leads to Increased Binding of PG9 in a Flow-Cytometry Based Alanine Scan

Veronika Grassmann found that the alanine scan of all gp120 mutants with the antibody PG9[105] that preferentially binds to Env in its native quaternary structure resulted in 26 positions which exhibited statistically significantly altered PG9 binding levels (Figure 11A). 12 of those were in the inner domain and 14 in the outer domain of Env, with seven mutations located in V1V2 and two in V3. While 25 of those mutations led to a significant loss of PG9 binding, only the variant L111A exhibited increased PG9 binding with a fold change of 2.4 above wildtype binding[133]. In order to validate the finding and further characterize the interaction of the 96ZM651 gp145 wildtype Env protein (hereinafter abbreviated "wt") and its L111A variant (hereinafter abbreviated "L") with PG9, I performed

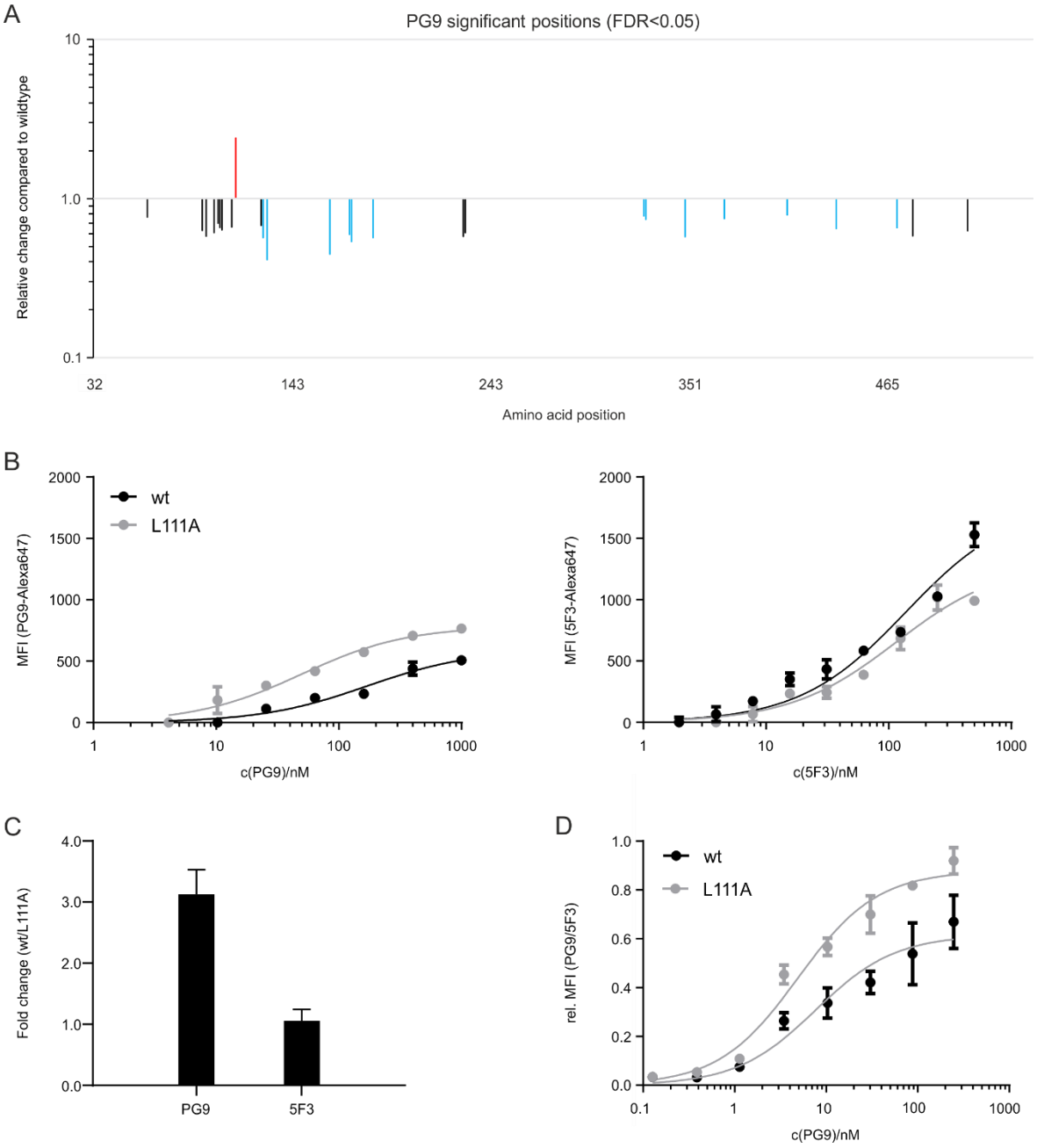

Figure 11: 96ZM651 gp145 alanine scan with PG9 by flow cytometry.
A) 96ZM651 gp145 variants of the alanine screening library were analyzed in six replicates for fold changes compared to the wildtype (wt ≙ 1). Fold changes were normalized with 5F3. For statistical analysis, a two-sided one sample-t test against 1 was performed, False-Discovery-Rate (FDR) adjusted < 5 % for multiple testing. Depicted are positions (in HXB2 numbering) showing a significant fold change. Red: Gain of signal position L111A; Loss of signal positions in outer domain (blue) and elsewhere (black). B Mean fluorescence intensities (MFI) gained after titration of gp145 96ZM651 wt and L111A with PG9-Alexa647 or 5F3-Alexa647. C) Fold change (wt/L111A) of K_D observed after titration with PG9-Alexa647 or 5F3-Alexa647. D) Titration of PG9-Alexa647 normalized with 5F3-PE. A & D: Modified after[133].

separate titrations of the PG9 and 5F3 antibodies (both labelled with Alexa647) and evaluated the signal intensities of the binding to wt and L111A (4.3.1.1, 4.3.2). The binding of PG9-Alexa647 to L111A was increased in comparison to the wildtype, whereas the

titration with 5F3-Alexa647 showed similar signals for both variants (Figure 11B). When I analyzed the ratio of the dissociation constants (K_D) of wt compared to L111A, the K_D was 3.1-fold increased for the wt compared to L111A for PG9, while the ratio of the K_Ds was 1.0 for 5F3 (Figure 11C).

Similar to my results, the titration with PG9-Alexa647 normalized with 5F3-PE performed by Veronika Grassmann had shown an increased signal for L111A (Figure 11D).

In summary, with the flow-cytometry-based alanine scan of 96ZM651, the variant L111A, which showed increased signal intensities for PG9 in comparison to the wt, was detected. As this implicates a difference in the quaternary structure of Env, it is therefore interesting to further analyse this variant biochemically and biophysically.

5.1.1.2. L111A gp140 leads to an Increased Proportion of Trimeric Protein

The flow-cytometry-based approach gave first insights into the characteristics of the variant in comparison to the wildtype, but as the Env protein is hereby expressed as a mixture of monomer, dimer, and trimer on the cellular surface, it was necessary to analyze if the effect of L111A is mediated via an improved conformation and/or changes of the distribution of the different states. For this, soluble gp140 Envelope variants were generated as their purification allows a separation of the different states and therefore an improved biochemical characterization. The variants were designed as a) uncleaved, which stabilizes the protein as it prevents gp120 shedding but does not resemble the native-like conformation as the uncleaved state does not allow for native folding, and as b) SOSIP, which includes more mutations but artificially mimics the native-like trimer conformation (SOSIP) (2.2.4, 4.4.1).

For the evaluation of the soluble protein (gp140), a transient transfection of HEK293F cells and a lectin affinity chromatography of the supernatant was performed, as all Env trimers, dimers and monomers should bind lectin alike (4.3.1.2, 4.3.3, 4.4.2). Afterwards, SEC was performed to obtain the respective elution profiles. Starting with 96ZM651 wt and L111A, a drastic decrease of the monomer in the SEC elution profile for L111A was observed (eluting after 9.0 – 10.0 min) while the trimer peak (7.25 - 8.5 min) was increased for L111A (Figure 12A).

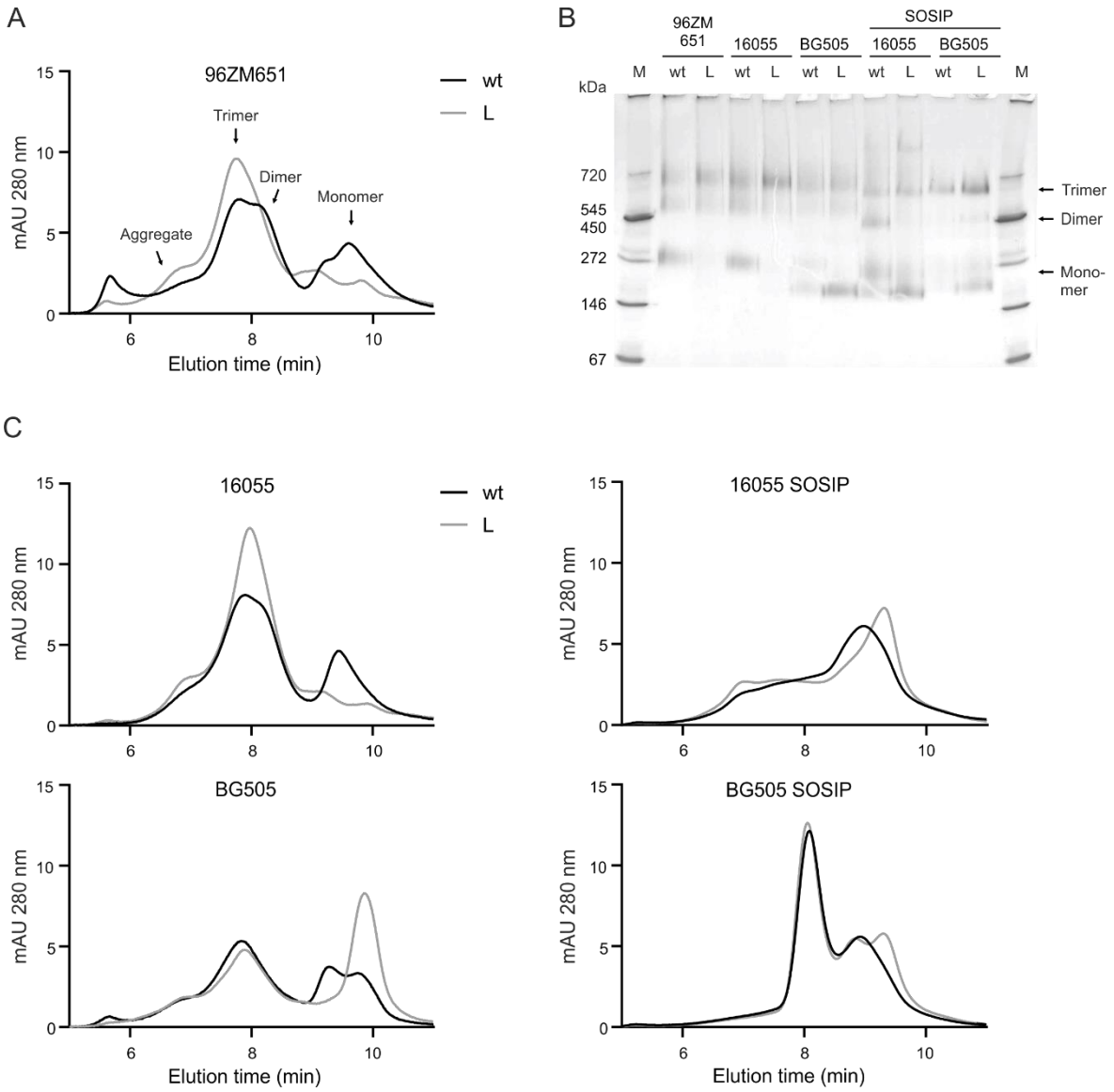

Figure 12: Analysis of lectin-purified wildtype (wt) and L111A (L) gp140 Env proteins.
(A) Size exclusion chromatography of 96ZM651 gp140 wt and L111A after lectin purification. Positions of aggregate, trimer, dimer, and monomer are depicted in the elution profile. B) BN-PAGE analysis of 4 µg lectin eluate of wt and L111A of different isolates after Coomassie staining. Marker (M): Serva Native Marker Liquid Mix for BN/CN. C) SEC elution profile of gp140 wt and L111A of the C clade isolate 16055 and A clade isolate BG505. For the uncleaved variants, which are not subjected to cleavage due to the mutation of the cleavage site, the trimer elutes from minutes ~ 7.25 - 8.5 while the monomer peak elutes from minutes ~ 9.0 - 10.0. The variants were further analyzed as cleavage-competent pre-fusion closed SOSIP variants. Here, the trimer elutes from minutes ~ 7.5 - 8.5 while the monomer elutes from minutes ~ 8.5 - 10.0.

The protein from the Lectin-eluate (before SEC) was analyzed on a BN-PAGE (4.4.4), where trimeric (~680 kDa) and dimeric protein was observed (~500 kDa), with the trimeric band being more prominent for L111A than for wt (Figure 12B). For the monomer band (~270 kDa) a reduction of monomer for L111A was detected. To see if this effect is restricted to 96ZM651 or if it can be transferred to other isolates or even clades, a second C clade isolate (16055) was analyzed, which also showed a decrease in monomer and an increase in trimer

as result of the corresponding L111A mutation (Figure 12B, C). For the A clade isolate BG505, however, neither a reduced monomer peak was detected in the elution profile nor in the BN-PAGE but a more distinct monomer peak for L111A while the wt showed two monomer peaks merging into each other, presumably caused by different states of the monomer or varying glycosylation (Figure 12B). This is also leading to a more prominent monomer fraction for BG505 L111A on the BN-PAGE (Figure 12B).

To see if L111A also leads to a change in the elution profile of native-like, cleavage competent SOSIP variants, wt and L111A variants of 16055 SOSIP as well as BG505 SOSIP were purified, which are by design already trimer-stabilized. Even though trimer-stabilized, 16055 SOSIP per se displays an elution profile with a high monomer and a low trimer content, which is not sufficient to form a dominant trimeric peak. Therefore, for 16055 SOSIP L111A, only a change of the monomer peak (8.5 - 10.0 min) was observed eluting slightly later than the wt, indicating a more closed structure. For BG505 SOSIP L111A, the monomer peak was separated into two peaks (Figure 12B-C). Interestingly, for 16055 SOSIP a decrease in dimer in the BN-PAGE for L111A was seen, too.
In general, the soluble L111A constructs exhibited a markedly reduced monomer peak for the C clade isolates, indicating the favored formation of trimeric protein. Furthermore, some changes for the A clade isolate in comparison to the respective wt were observed, whereas the SOSIP variants showed no relevant difference.

5.1.1.3. Trimeric L111A gp140 Shows a More Closed Conformation

The effect of L111A on the proportion of monomer, dimer, and trimer on the elution profile was especially visible for the C clade isolates, where the monomer content was reduced. This indicates that L111A influences the distribution of monomer, dimer, and trimer but does not give insights about a possible effect on the conformation of the trimers.

In order to further evaluate the effect of L111A, it was sought to determine if the amino acid exchange also leads to an increased or decreased presentation of epitopes for a panel of antibodies and possibly causes changes to the structure of the soluble gp140 Env trimers. To address this question, gp140 trimers of the C clade isolates 96ZM651, 16055, and its more native-like variant 16055 SOSIP were analyzed as well as the A clade isolates BG505

and its more native-like variant BG505 SOSIP. For this, soluble His-tagged gp140 protein from the supernatant of transiently transfected HEK293F cells was purified via nickel-charged immobilized metal ion affinity chromatography and anion exchange columns followed by subsequent size exclusion chromatography (4.4.2, 5.2.4). The purified soluble trimeric proteins (Supplemental Figure 1) were subsequently used in lectin-capture ELISAs (4.4.9). For this, a broad panel of (n)NAbs (Table 3) was titrated (Supplemental Figure 2 - Supplemental Figure 6) against the purified proteins to determine the dissociation constants (K_D) (Figure 13, Supplemental Table 3). For the evaluation of the affinity to non-neutralizing antibodies (nNAbs), 17b and F105 were used, targeting the CD4-induced (CD4i) open conformation and the CD4bs, respectively. The highest difference in binding was observed for 17b, where binding to L111A was at least 10-fold reduced in comparison to wt for the A clade isolate [K_D(L111A): 159 nM – K_D(wt): 13.3 nM] and up to 50-fold for the clade C isolates 96ZM651 [K_D(L111A): 150 nM – K_D(wt): 1.39 nM], 16055 [K_D(L111A): 105 nM – K_D(wt): 2.21 nM], and 16055 SOSIP [K_D(L111A): 58.3 nM – K_D(wt): 0.97 nM]. BG505 SOSIP.664 is by design presented in a native-like closed conformation and therefore does not bind to 17b. Regarding F105, only decreased binding for BG505 L111A [K_D(L111A): 4.51 nM – K_D(wt): 1.16 nM] and 16055 SOSIP L111A [K_D(L111A): 10.1 nM – K_D(wt): 2.47 nM] was observed, while the other isolates showed no difference in binding. Therefore, in summary, the nNAbs showed a decreased binding to variant L111A or were at least equal to the respective wildtype.

Next, a panel of bNAbs targeting different epitopes of the Env trimer was tested to determine their affinity to the wt and L111A variant, as a change in affinity might inform us about a change in the vulnerable sites of the protein. Concerning the CD4bs-specific bNAbs VRC01 and HJ16, only slightly increased binding of VRC01 to 96ZM651 L111A was seen [K_D(L111A): 3.04nM – K_D(wt): 7.52nM] and no difference in binding of HJ16. V3-specific bNAb HGN194 did not lead to a change in binding, indicating that the V3 loop was not subject to structural changes, which is also shown for the other V3-specific bNAbs PGT121 and 447-52D. Also, the affinity to the glycan-specific bNAb 2G12 was largely preserved, apart from binding to 16055 L111A [K_D(L111A): 1.77 nM – K_D(wt): 5.78nM], which was 3-fold increased. Binding to the V1V2-specific bNAb PG9 was only observed for L111A for 96ZM651 [K_D(L111A): 31.1 nM], while the wt showed no binding. The other isolates showed similar binding for both variants. Binding to the bNAb PGT145, directed against V1V2, as

well as interface bNAb 35O22 (gp120/41) was only observed for the SOSIP variants, as only those show a native-like structure as the increased cleavage site leads to an improved conformation (2.2.4), and here there was no difference between wt and L111A. For 10E8, which binds a linear epitope in the MPER[155], binding was also not influenced. Of note, BG505 and its native-like variant BG505 SOSIP do not bind to 10E8 as both are truncated at position 664, which is N-terminally of the epitope of 10E8 and therefore not available.

L111A had been detected because of the increased binding of PG9 to the membrane-bound protein in the flow-cytometry-based assay but for the soluble protein, binding of PG9 is only observable for 96ZM651 L111A. In the flow-cytometry assay, the cells display monomers, dimers, and trimers on their surface and therefore the positive effect of L111A can either be caused by an improved conformation of L111A or by an increased trimeric content. For the soluble proteins, we only used trimeric protein, and as binding to wt was no longer detectable, the positive effect of L111A observed in the flow-cytometry assay can be confirmed in the ELISA format and it strengthens the assumption, that the L111A trimers also show an improved conformation for 96ZM651. However, the other isolates do not show an increased binding of PG9 to their L111A variant, no matter if the uncleaved or the native-like variant was analyzed.

Our results suggest that there is a positive effect of L111A on the trimeric structure, mainly observed by the decreased binding of 17b, which implies a more closed conformation of the trimers, while the binding to other (b)NAbs was largely preserved. Nevertheless, it is not as closed or conformationally improved as the native-like SOSIP trimers, as binding to the quaternary-specific Ab PGT145 (binding to the apex of well-folded trimers) was not observed. Still, further structural analyses are needed to get a complete picture of the effect of L111A on the Env glycoprotein, which does not only seem to influence the trimer content, but also the conformation of the trimers.

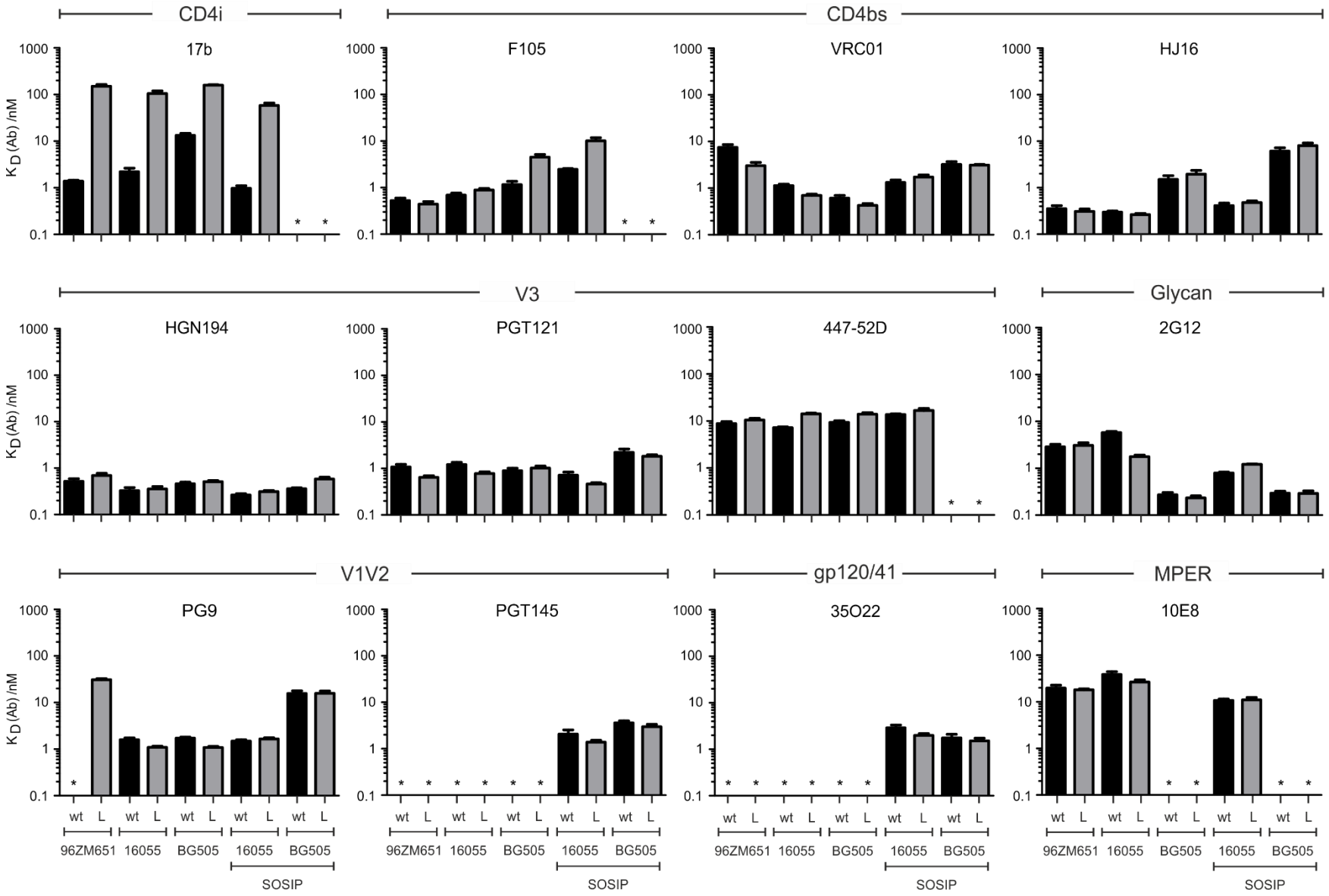
CD4i
CD4bs
17b
F105
VRC01
HJ16
V3
Glycan
HGN194
PGT121
447-52D
2G12
V1V2
gp120/41
MPER
PG9
PGT145
35O22
10E8
K D (Ab) /nM
1000
100
10
1
0.1
wt L
96ZM651
16055
BG505
SOSIP

Figure 13: Binding affinities of soluble wildtype (wt) and L111A (L) variants of different isolates against a panel of (b)NAbs binding to multiple epitopes of the Env glycoprotein.
Wt and L111A were purified as soluble gp140 trimers via nickel-charged immobilized metal ion affinity chromatography columns and subsequent anion exchange and size exclusion chromatography. The fractions containing trimeric protein were pooled and used in a lectin-capture ELISA, where antibodies were titrated in 4-fold dilution. Binding affinities of the respective antibodies (sub header) are represented as bar charts of the dissociation constant (K_D) in nM. Error bars represent the standard error of the mean of triplicates. The tested isolates are 96ZM651, 16055 (both clade C), and BG505 (clade A). 16055 and BG505 were further analyzed as native-like SOSIP variants. Main header represents the epitopes targeted by the antibodies, which are directed against the CD4-induced conformation (CD4i; 17b), the CD4-binding site (CD4bs; F105, VRC01, HJ16), the variable loop 3 (V3; HGN194, PGT121, 447-52D), a glycan patch (2G12), the variable loops 1 and 2 (V1V2; PG9, PGT145), the gp120/41 interface (35O22), and the membrane-proximal external region (MPER). *: no binding detected.

5.1.1.4. Thermostability Measurement Implies a more Homogenous Composition of L111A gp140 Trimers

Next to the biochemical characterization, the effect of L111A on biophysical properties was evaluated, e.g. on thermostability or the unfolding of the soluble gp140 trimers.

For this, a Differential Scanning Calorimetry (DSC) analysis of the purified wt and L111A gp140 trimers of the C clade isolate 96ZM651 was performed (Figure 14A-B). With DSC, the heat capacity of a sample and its reference is measured during unfolding processes induced by a temperature change, which allows to determine factors like the stability of proteins[182,183]. The DSC profiles for both 96ZM651 variants show one distinct peak, with a thermal denaturation midpoint of 60.4°C for wt and 60.8°C for L111A. Similar to this, the onset of the melting temperature is 48.3°C for wt and 47.3°C for L111A (Supplemental Table 4). Interestingly, the width of transition at half height ($Tm_{1/2}$), differs by 2.2°C, which indicates a more cooperative unfolding of L111A, presumably caused by a more homogenous composition of the trimers (Figure 14B).

Next to the DSC, nano-format Differential Scanning Fluorimetry (nanoDSF) measurements were performed, a method to characterize the stability of proteins in a low volume based on the shift of intrinsic tryptophan fluorescence of emission wavelengths at 330 and 350 nm[156,184]. Here, again wt and L111A were analyzed, but not only in the context of 96ZM651 but also with other Envs of clades A and C (Figure 14C).

In general, the nanoDSF measurements resulted in very low signals, especially for the uncleaved variants, but still, L111A showed a more distinct peak for 96ZM651 and BG505.

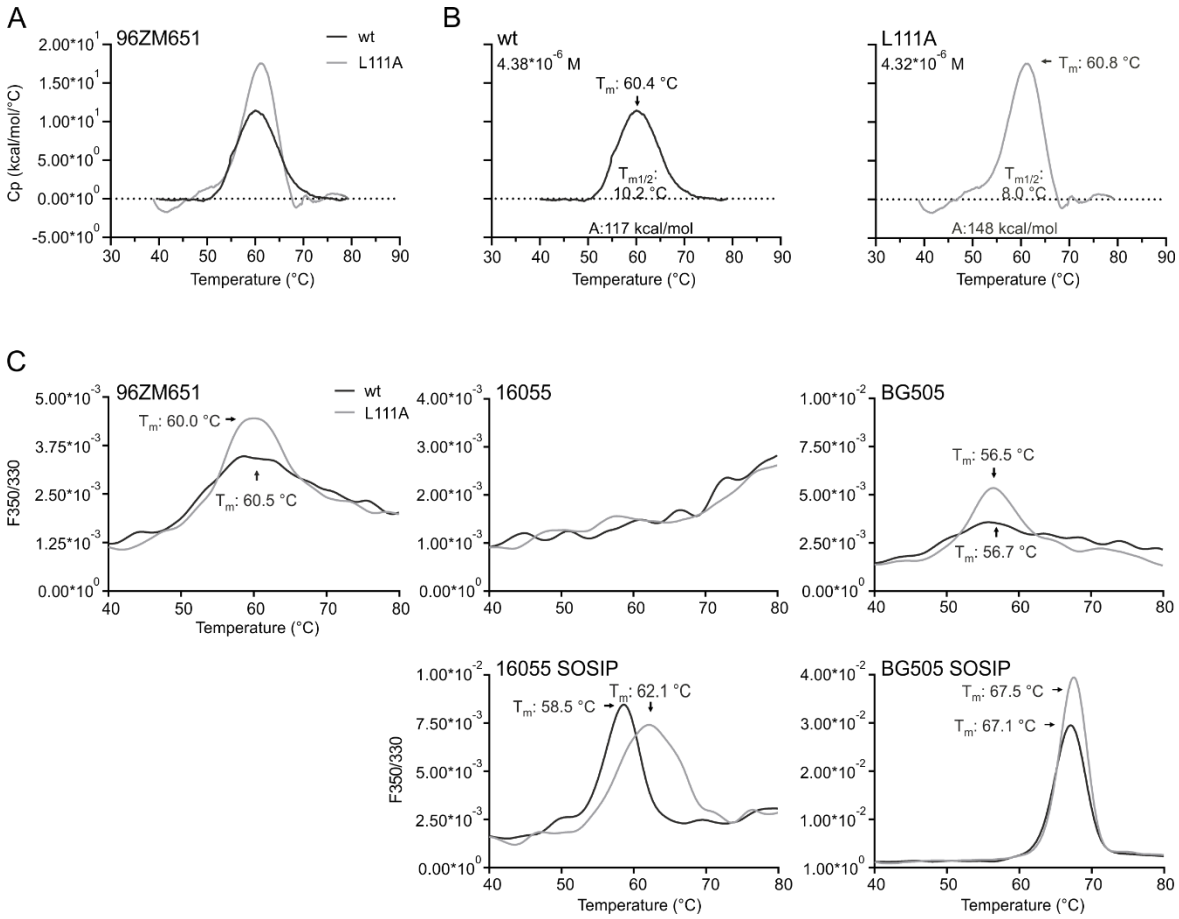

Figure 14: Thermostability analysis of purified gp140 wt and L111A envelope trimers
Thermostability of purified wt and L111A trimers was measured on a A) MicroCal PeaQ DSC via Differential scanning calorimetry or a C) Prometheus NT.48 via nano Differential Scanning Fluorimetry. Depicted are the buffer substracted and baseline-corrected A) overlay of 96ZM651 wt and L111A curves as well as B) single thermograms of wt and L111A with key stability metrics highlighted. C) Purified trimers of uncleaved and native-like wt and L111A variants of isolates of clades C and A. T_m: Melting temperature, $T_{m1/2}$: width of transition at half height, A: peak area.

Unfortunately, 16055 showed no detectable signal at all. The best curve was observed for BG505 SOSIP, but also here, no change in the melting temperature was observed. Unlike this, 16055 SOSIP L111A showed an increased melting temperature of 3.3°C in comparison to the respective wt.

Regarding the thermostability, the results indicate that L111A is not increasing the stability of the protein in regards of an increased denaturation midpoint, but it seems to lead to a more homogenous unfolding, presumably caused by the more homogenous trimeric protein in comparison to the wt.

5.1.2. Characterization of T278H

Veronika Grassmann did not only perform the flow-cytometry based alanine scan with PG9, but also evaluated other antibodies like the CD4bs Ab VRC01. Here, 81 variants with statistically significantly altered binding were detected, but again only one variant exhibited a gain of signal. Amino acid T278A exhibited an increased signal for VRC01 and after permutation of alanine with other amino acids, it was found that a histidine (T278H) at this position leads to the best binding of VRC01[133].

In order the evaluate the impact of the T278H (hereinafter abbreviated "T") mutation on the soluble gp140 protein, I purified trimeric protein of clades A and C harboring the respective mutation and performed analytical size exclusion and lectin-capture ELISAs against the broad panel of antibodies already described in 5.1.1.3.

5.1.2.1. Analytical Size Exclusion Profile of T278H gp140

To evaluate the amino acid substitution T278H, HEK293F cells were transiently transfected with plasmid DNA containing wt and T278H variants of the different clades and isolates and lectin-based affinity chromatography was performed. The eluates were loaded on a SEC-column and further analyzed on a BN-PAGE (Figure 15). The SEC of wt and T278H for the clade C isolate 96ZM651 showed similar profiles for both variants. The trimer elutes between minutes 7.0 and 8.0 and the monomer can be detected between minutes 8.5 and 10.0 for the uncleaved variants (Figure 15A). The overlapping SEC profiles can be verified in the BN-PAGE as the band intensities and pattern of wt and L111A are similar (Figure 15B). This does not only apply to 96ZM651, but can be see with all other isolates tested, no matter if the variants were generated as uncleaved or native-like SOSIP variants (Figure 15C).

In summary, the amino acid substitution T278H does not influence the content of trimer, dimer, or monomer, unlike L111A, but shows the same elution profile as the respective wt variant.

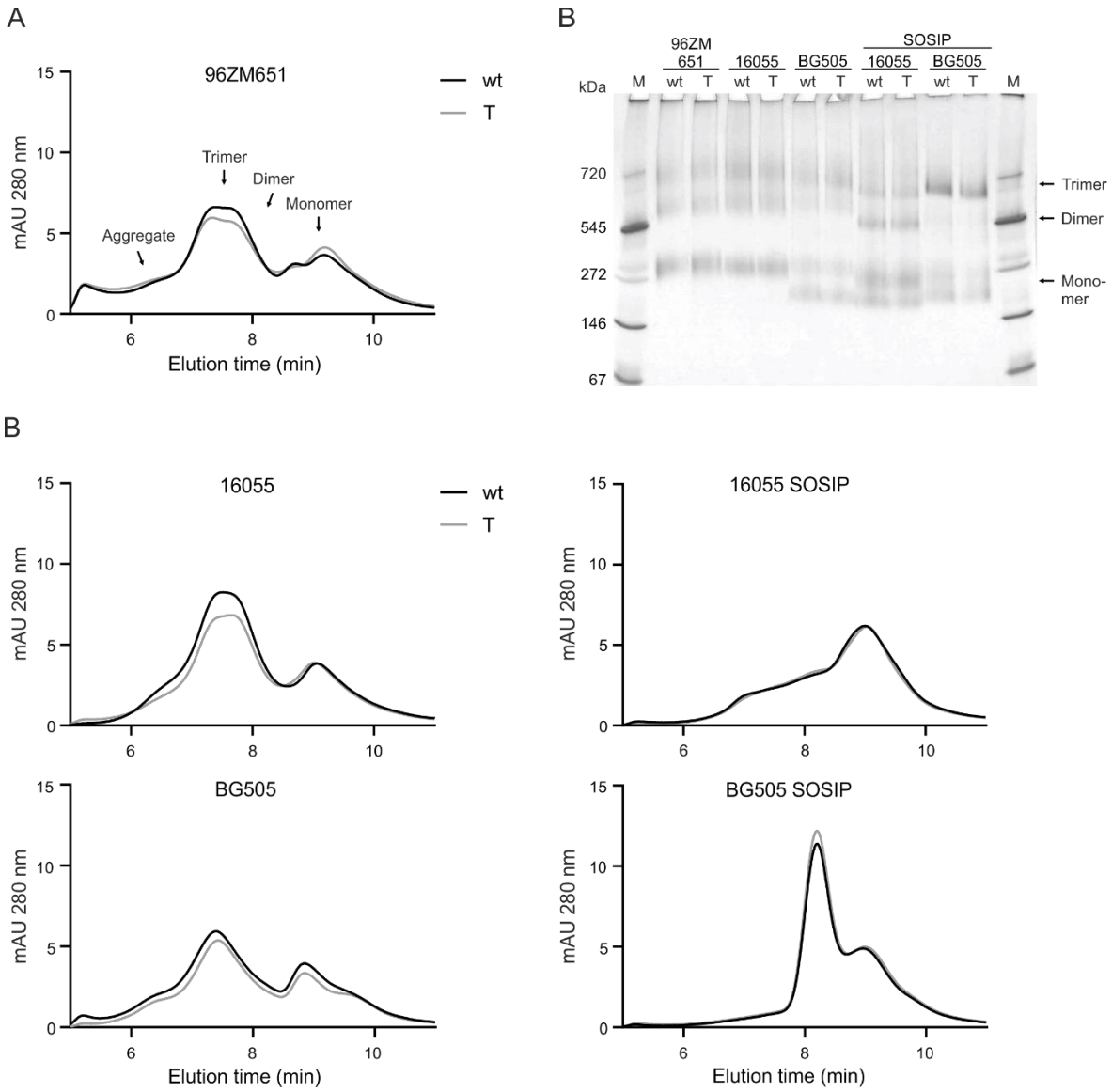

Figure 15: Analysis of lectin-purified wildtype (wt) and T278H (T) gp140 Env proteins.
(A) Size exclusion chromatography of 96ZM651 gp140 wt and L111A after lectin purification. Positions of aggregate, trimer, dimer, and monomer are depicted in the elution profile. B) BN-PAGE analysis of 4 µg lectin eluate of wt and L111A after Coomassie staining. Marker (M): Serva Native Marker Liquid Mix for BN/CN. C) SEC elution profile of the C clade isolate 16055 and A clade isolate BG505. For the uncleaved variants, the trimer elutes from minutes ~ 7.0 - 8.0 while the monomer peak elutes from minutes ~ 8.5 - 10.0. The variants were further analyzed as cleavage-competent pre-fusion closed SOSIP variants. Here, the trimer elutes from minutes 7.5 - 8.5 while the monomer elutes from minutes 8.5 - 10.0.

5.1.2.2. T278H gp140 leads to an Increased Binding of VRC01

Next, it was evaluated if the effect of T278H observed for membrane-bound gp145 can be reproduced and further evaluated in the soluble gp140 protein. For this, transient transfection of HEK293F cells was performed and the His-tagged proteins were purified via nickel-affinity-, anion exchange- and subsequent size exclusion-chromatography (4.4.2). The purified trimers (Supplemental Figure 7) were used for a lectin-capture ELISA in order to evaluate changes in binding affinities of nNAbs and bNAbs.

Overall, the binding affinities to most antibodies were not influenced. However, for some, an increase or decrease in binding affinities compared to the respective wildtype protein was observed (Figure 16, Supplemental Figure 8 - Supplemental Figure 12 , Supplemental Table 5): For VRC01,– as expected – an increased affinity was detected to T278H of 2- to 5-fold for 96ZM651 [K_D(T278H): 1.47 nM, K_D(wt): 7.52 nM], 16055 [K_D(T278H): 0.56 nM, K_D(wt): 1.13 nM] and BG505 SOSIP [K_D(T278H): 0.75 nM, K_D(wt): 3.22 nM], while BG505 [K_D(T278H): 0.37 nM, K_D(wt): 0.61 nM] and 16055 SOSIP [K_D(T278H): 0.70 nM, K_D(wt): 1.32 nM] showed smaller effects. For F105, a decreased binding to 16055 SOSIP T278H [K_D(T278H): 10.1 nM, K_D(wt): 2.47 nM] was observed, which is a positive outcome, as F105 is a nNAb binding to monomeric protein but less well to ordered trimers. Therefore, reduced binding is beneficial as it indicates an improved local structure of the CD4bs. For HJ16, no binding was seen to T278H for 96ZM651, BG505 and BG505 SOSIP while it is 2- and 20-fold decreased for 16055 SOSIP [K_D(T278H): 0.90, K_D(wt): 0.41 nM]and 16055 [K_D(T278H): 6.29 nM, K_D(wt): 0.30 nM], respectively. Of note, T278H leads to a knock-out of glycan N276, which is part of the epitope of HJ16. Therefore, this reduction in binding affinities is caused by the design of the variant.

In summary, the analysis of the affinities confirmed that T278H led to an increased binding of VRC01, while the other antibody epitopes and binding affinities were not negatively influenced apart from HJ16. However, as HJ16 still binds to 16055 and 16055 SOSIP T278H, this C clade shows to be superior to BG505 regarding binding of CD4bs-directed antibodies.

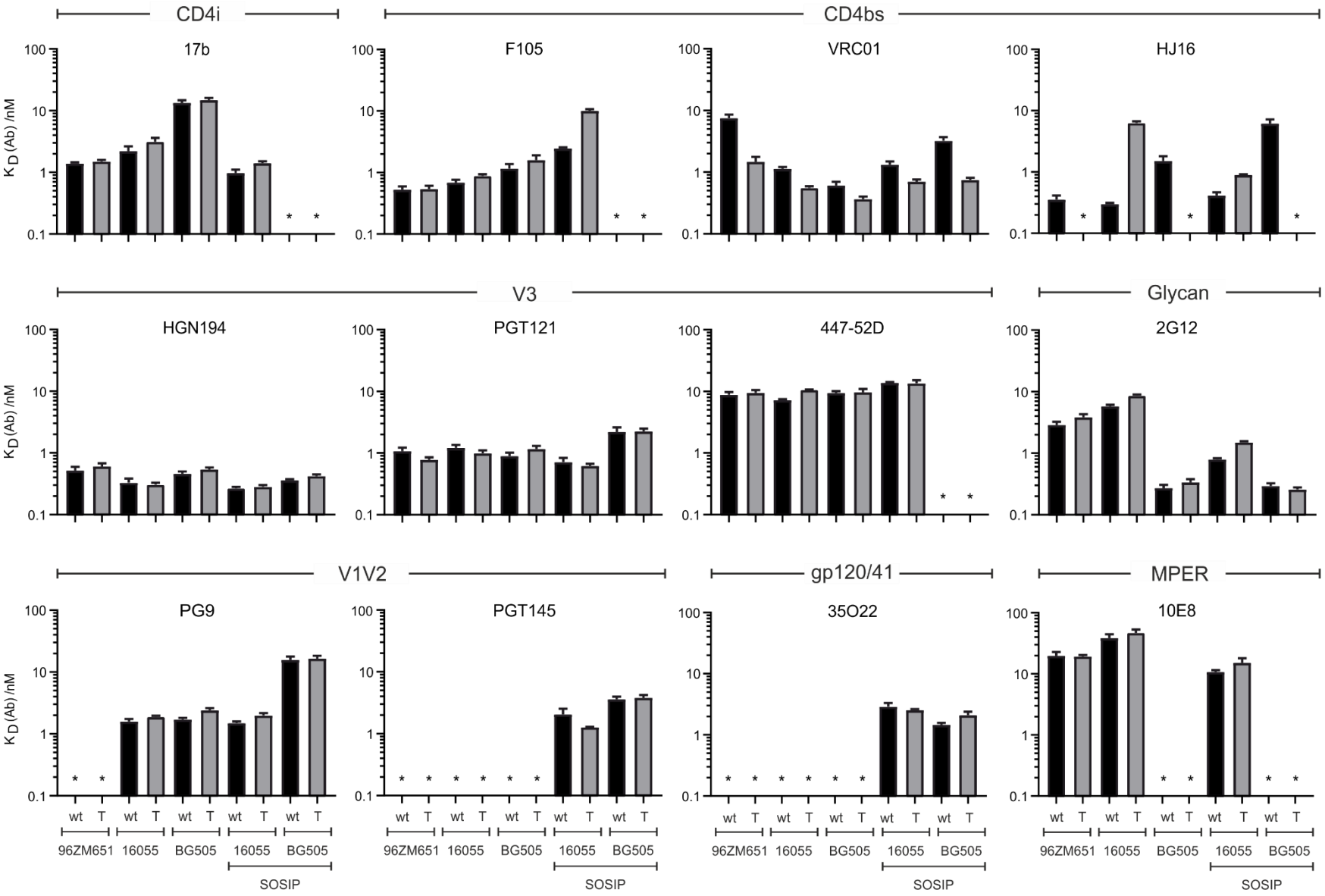
CD4i
CD4bs
17b
F105
VRC01
HJ16
V3
Glycan
HGN194
PGT121
447-52D
2G12
V1V2
gp120/41
MPER
PG9
PGT145
35O22
10E8
K D (Ab) /nM
100
10
1
0.1
wt T wt T wt T wt T wt T
96ZM651 16055 BG505 16055 BG505
SOSIP

Figure 16: Binding affinities of soluble wildtype (wt) and T278H (T) variants of different isolates against a panel of (b)NAbs binding to multiple epitopes of the envelope glycoprotein.
Wt and T278H were purified as soluble gp140 trimers via nickel-charged immobilized metal ion affinity chromatography columns and subsequent anion exchange and size exclusion chromatography. The fractions containing trimeric protein were pooled and used in a lectin-capture ELISA, where antibodies were titrated in 4-fold dilutions. Binding affinities of the respective antibodies (sub header) are represented as bar charts of the dissociation constant in nM. Error bars represent the standard error of the mean of triplicates. The tested isolates are 96ZM651, 16055 (both clade C), and BG505 (clade A). 16055 and BG505 were further analyzed as native-like SOSIP variants. Main header represents the epitopes targeted by the antibodies, which are directed against the CD4-induced conformation (CD4i; 17b), the CD4-binding site (CD4bs; F105, VRC01, HJ16), the variable loop 3 (V3; HGN194, PGT121, 447-52D), a glycan patch (2G12), the variable loops 1 and 2 (V1V2; PG9, PGT145), the gp120/41 interface (35O22), and the membrane-proximal external region (MPER). *: no binding detected.

5.2. Combination of Single Amino Acid Exchanges

The single amino acid substitution L111A can lead to 1) an increased trimer and reduced monomer content and 2) an improved conformation of HIV-1 Env trimers, while T278H leads to an increased binding of VRC01 to the isolates tested. In order to evaluate the potential of both variants, L111A and T278H, on binding affinities of neutralizing antibodies, the two mutations were combined and it was analyzed whether the double mutant L111A/T278H (hereinafter abbreviated "LT") still shows the positive effects observed for the single mutants. For this, LT mutations were introduced into the very gp140 isolates and analyzed as described above for the single mutants.

5.2.1. Biochemical Analysis of the Variants showed Combinability

For analytical size exclusion chromatography, the gp140 proteins were expressed in FreeStyle™ 293-F cells and purified via lectin affinity chromatography. The lectin eluates were further analyzed via analytical SEC and BN-PAGE (Figure 17).

Starting with 96ZM651 LT gp140, a SEC elution profile similar to the L111A single amino acid exchange variant with an increased trimer (7.0 - 8.0) and a reduced monomer peak (8.5 - 10 min) was observed (Figure 17A).
Next, a BN-PAGE was performed and here, again, similar results to the L111A single amino acid exchange variant were seen (Figure 17B). The monomer band of LT (~270 kDa) is no longer detectable for the two clade C isolates and for the clade A isolate BG505 LT gp140, only one distinct monomer band was seen while the wt still displays two bands, presumably caused by different glycosylation patterns.

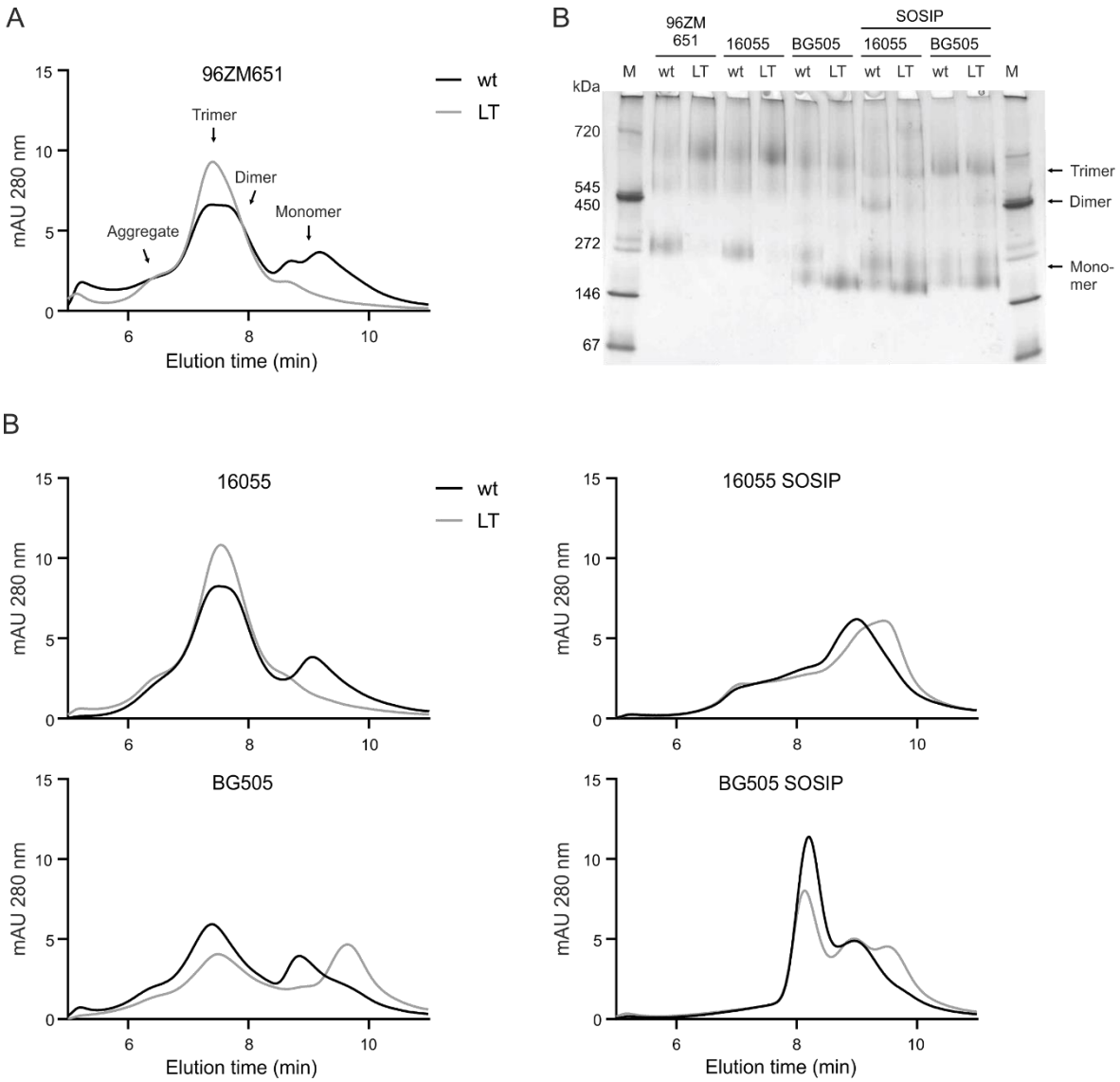

Figure 17: Analysis of lectin purified wildtype (wt) and L111A/T278H (LT) gp140 Env proteins.
A) Size Exclusion Chromatography (SEC) of 96ZM651 gp140 wt and LT after lectin purification. Positions of aggregate, trimer, dimer, and monomer are depicted in the elution profile. B) BN-PAGE analysis of 4 µg lectin eluate of wt and LT. Marker (M): Serva Native Marker Liquid Mix for BN/CN. C) SEC elution profile of the C clade isolate 16055 and A clade isolate BG505. For the uncleaved variants, the trimer elutes from minutes 7.0 - 8.0 while the monomer peak elutes from minutes 8.5-10. The variants were further analyzed as cleavage-competent pre-fusion closed SOSIP variants. Here, the trimer elutes from minutes 7.5 – 8.5 while the monomer elutes from minutes 8.5 - 10.

Besides 96ZM651 LT gp140, the second clade C variant 16055 LT gp140 also showed a reduced peak for monomer in comparison to the respective wildtype and an increase in trimer peak height (7.0 – 8.0 min) (Figure 17C). For BG505 and its respective SOSIP variant, there are two monomer bands, which might resemble different states of glycosylation, but for BG505 LT gp140 it shows a reduction of the first monomer peak which can also be see in the BN-PAGE. Interestingly, this also seemed to be the case for 16055 SOSIP, but here

the mimic of the native-like trimer did not benefit as much as the uncleaved variant and for BG505 SOSIP, no beneficial effect for LT was visible at all.

In summary, LT shows similar elution profiles as the L111A single amino acid exchange and therefore, at least in regard of trimer and monomer content in an analytical size exclusion chromatography profile, the double mutant L111A/T278H is superior to the wt.

Helene Hierl analyzed the purified gp140 LT trimers in an ELISA against a broad panel of antibodies targeting different epitopes[185]. With this, it was shown that the two amino acid substitutions were combinable, as the combination variant LT did not show any negative effects but displayed similar results as the single aa exchange variants. Finally, as the two single amino acid exchanges proved combinable, it was necessary to evaluate which isolate is best suitable for a pre-clinical animal study on New Zealand White rabbits.

5.2.2. Chemical Cross-linking via EDC/NHS Stabilizes the gp140 Trimers

Env trimers can occur in an open, intermediate, or closed conformation, but it is assumed that closed trimers are more likely to elicit bNAbs, whereas open trimers mainly elicit nNAbs, which do not offer protection[34,35,36]. To increase the stability of the purified trimeric protein, in means of keeping them in a closed conformation or at least hinder opening of the trimers, a chemical cross-linking was performed in order to improve the immunogens for the pre-clinical animal study. Eventually, EDC/NHS was applied, as it cross-links carboxyl- and amine-groups without inserting additional atoms[186,187].

In order to detect if the cross-linking negatively affects the LT double mutants of 96ZM651, BG505/BG505 SOSIP and 16055/16055 SOSIP, their antigenicity in comparison to non-cross-linked variants was analyzed. Helene Hierl performed chemical cross-linking of the proteins via EDC/NHS and the subsequent ELISA analyses in her Master's thesis under the supervision of Veronika Grassmann and with my experimental support[133,185]. In general, after cross-linking, the binding of the cross-linked trimers to the bNAbs was similar as to the non-cross-linked variants. For the antibodies used for the detection of the variants L111A and T278H, PG9 and VRC01, the affinity of PG9 was at least wt-like and similar to the not-cross-linked LT variant and the gain of binding for VRC01 was also still preserved[133,185].

Of note, chemical cross-linking is known to lead to an improved stability while the antigenicity *in vitro* is not substantially affected[67] and, based on our results, the cross-linked variants are therefore suitable for testing in a pre-clinical animal study.

5.2.3. Selection of the Antigens for the Immunization study

The analysis of the single gp140 variants L111A and T278H as well as their combination L111A/T278H (LT) showed that the double mutant LT unites the properties of the single variants. Therefore, the double variant was chosen as basis for the immunogens in the pre-clinical animal study. Regarding the isolate to be used in the study, uncleaved as well as native-like SOSIP-variants should be compared and as both, 16055 and BG505 showed good results in regards of antigenicity, we had to choose between these two isolates. After the cross-linking, both variants showed to be suitable. However, the clade C isolate 16055 showed a more favorable elution profile and as clade C is accounting for ~ 50 % of HIV-1 infections world-wide[8], it was decided to perform the pre-clinical animal study with this isolate as uncleaved and native-like, cleaved SOSIP construct, which will be used as non-cross-linked and cross-linked proteins (called "RepliVax"-Immunogens, after the name of the consortium through which the project received funding[188]).

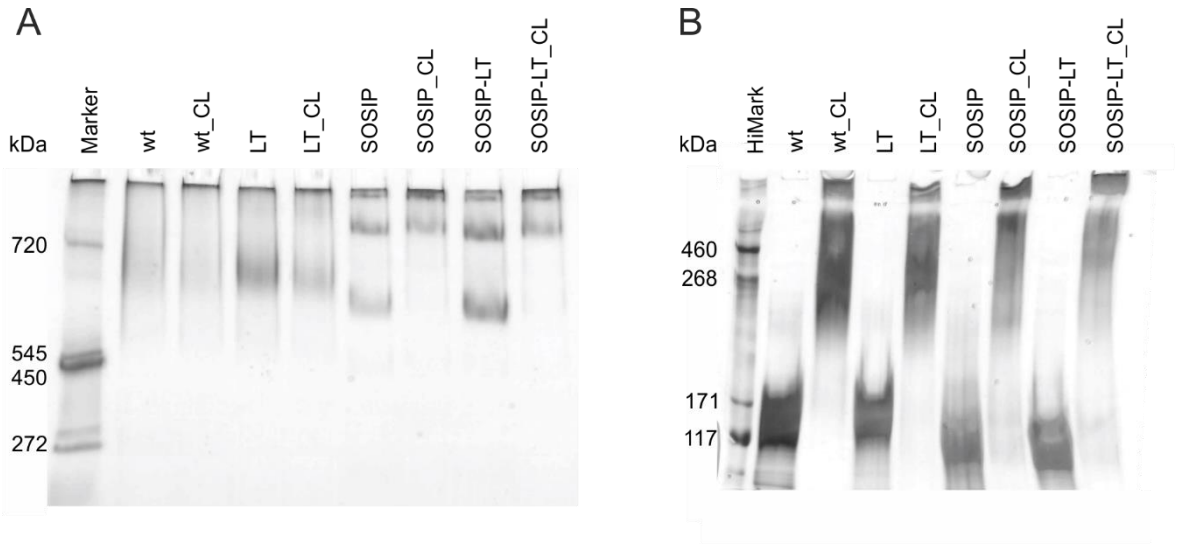

Figure 18: Quality control of the non-crosslinked and Cross-Linked (CL) 16055 variants used for the immunization study. A) BN-PAGE, Marker: SERVA Native Marker, Liquid Mix for BN/CN, 2.5 µg protein were loaded per lane and after electrophoresis the gel was stained with Coomassie-Staining solution. B) 5 % SDS PAGE, 2.1 µg protein were mixed with reducing Laemmli buffer and loaded in each lane. After electrophoresis, the gel was silver stained. Marker: SERVA Native Marker, HiMark: HiMark™ Pre-stained Protein Standard.

5.2.4. Purification of the Antigens for the Immunization Study

The pre-clinical animal-study requires protein of high quality and the quantity has to be sufficiently large to allow for quality controls, formulation studies and the immunization itself to be performed. Previous purification protocols in our working group included a first purification step using a column filled with *Galanthus nivalis* lectin, which was shown to contain unacceptably high levels of endotoxin. As it is essential to produce an endotoxin-free protein for the rabbit study, the use of a lectin containing lipopolysaccharide-impurities is not feasible.

Therefore, the purification protocol was changed and improved and Nickel-charged immobilized metal ion affinity chromatography and anion exchange columns were used followed by subsequent size exclusion chromatography (4.4.2). With this, the endotoxin content of the immunogens showed a range of 0.05 - 0.12 Endotoxin Units (EU) per immunization dose, which was safe to use, given a limit of 5 EU/kg body weight with New Zealand White Rabbits weighing between 3 – 5 kg. Next to the endotoxin, also the low yield required a new purification protocol. As a high amount of protein was needed for the quality control of the protein, the studies performed by the CAVD core facilities, as well as for the immunizations of the rabbits, the protocol had to be scaled up to 5 L cell culture flasks, as e.g. the generation of 16055 SOSIP-LT alone required a total of 25 L of transfected cell culture supernatant (Table 8).

Table 8: Overview of the amount of protein required for the follow up studies, the yield received per liter transfected supernatant and the minimum volume needed to obtain the amount of protein.

	Required	Yield	Volume
	mg	mg/L	L
16055 wt	3.50	0.30	11.67
16055 LT	3.50	0.35	10.00
16055 SOSIP	3.50	0.18	19.44
16055 SOSIP-LT	5.00	0.20	25.00

Finally, the purified protein was quality controlled on a BN-PAGE and SDS-PAGE (Figure 18, Supplemental Figure 13). The proteins were of the expected high trimeric purity except for the SOSIP constructs, where an additional higher and distinct band was detected which was distinct and able to bind to PGT145 in a batch assay while no detectable binding to F105 or

17b occurred, indicating that it is a higher-order assembly of trimeric protein, yet with the correct quaternary structure (Supplemental Figure 14).

5.2.5. Formulation Study

The stimulation of a strong immune response against an immunogen is essential for the success of a vaccine, and adjuvants can make these more potent and prolonged[88]. Proteins used as immunogens are usually highly quality-controlled, also in regards of structure. The structure of a protein is crucial, as its change can affect the functionality of the protein, here especially in means of antibody induction. Since the formulation of the protein with adjuvant and the subsequent administration of the admixture into the study animals is a time-consuming process, it is important to investigate if the formulation of the immunogens with the adjuvant might lead to detrimental effects occurring in this period.
In order to make sure that the adjuvant used does not have such detrimental effects on the quality of the RepliVax immunogens in means of physical damage or the presentation of undesired epitopes, we performed a formulation study together with our cooperation partner IDRI (Infectious Disease Research Institute, Seattle, USA).
For the study, GLA-LSQ was used, which is a Toll-like receptor 4 agonist (Glucopyranosyl Lipid Adjuvant, GLA) in a liposomal formulation containing saponin (QS21). IDRI analyzed the protein with adjuvant ("formulated") and without adjuvant ("untreated") for physicochemical stability for up to 24 hours (0, 4, 24 h) at two different temperatures (5 & 25°C), while I tested detrimental effects of the formulation on the epitopes recognized by our (b)NAb panel after incubation for 4 hours at 25°C by an lectin-capture ELISA.

5.2.5.1. Physicochemical Stability was not Affected

In order to analyze the physicochemical stability of the RepliVax immunogens, the samples were tested for visual appearance as well as particle size and were furthermore loaded on SDS-PAGE and Blue-Native PAGE gels (4.4.13). The parameters tested for visual appearance were color, opacity, and phase, which were all stable for all time points and matched control parameters. A change in the size of the protein is in general a good indicator if the formulation is physically destabilizing the protein. Thus, the particle size was measured with Malvern's DLS Zetasizer, which did not show any significant changes over the course

of the study and showed an average size of 70-71 ± 1 nm (Supplemental Table 6). Of note, the antigen alone samples could not be measured as they were too dilute and polydisperse, therefore the antigen particle size signal is unlikely to contribute to the particle size measurements collected in the presence of adjuvant. Furthermore, no negative effects of the formulation could be observed in the SDS-PAGE, indicating that the protein was not negatively influenced by the adjuvant (Supplemental Figure 15B).

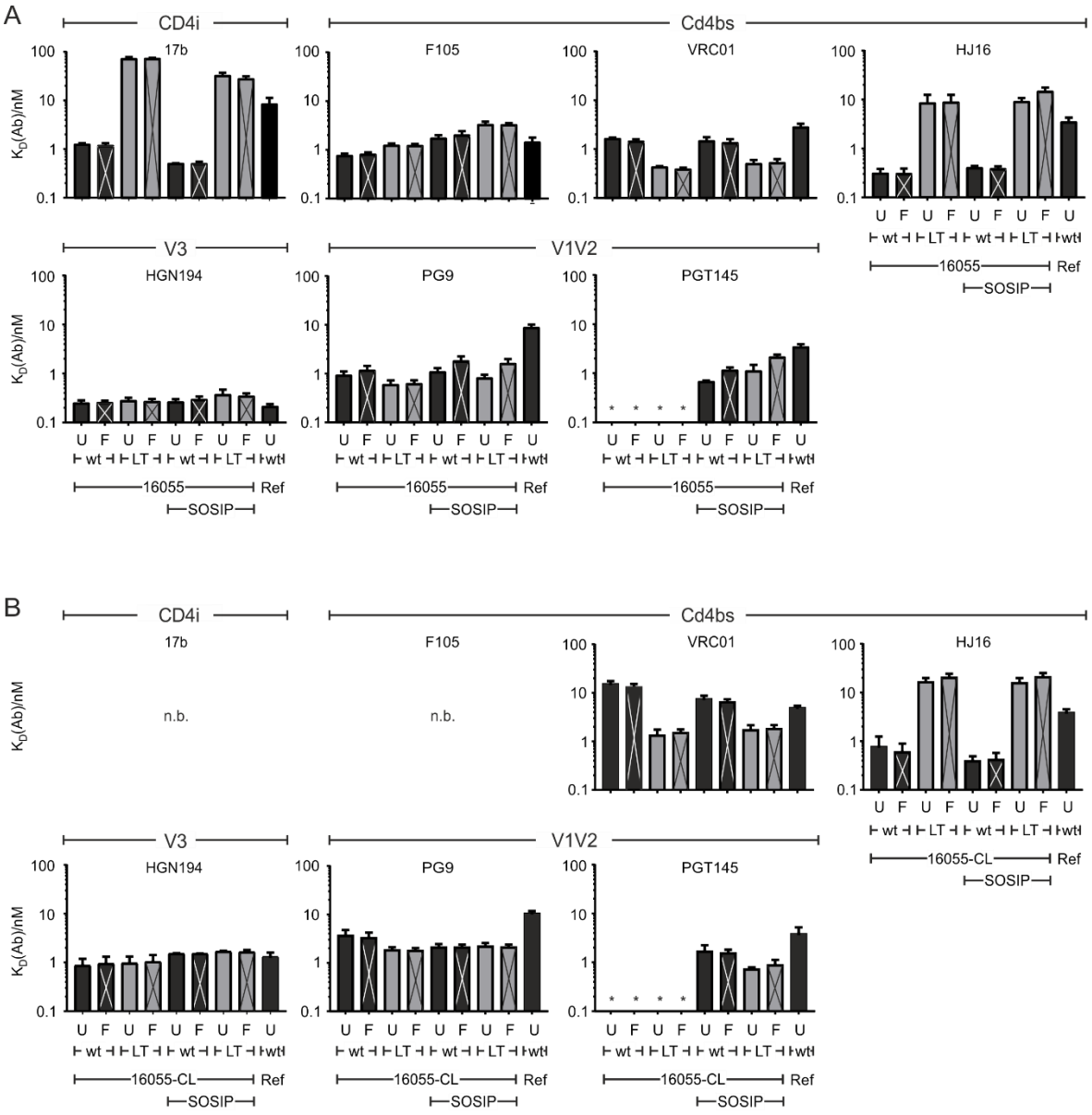

Figure 19: Lectin-capture ELISA of the Untreated (U) and adjuvant-Formulated (F) RepliVax immunogens. In a lectin-capture ELISA, antibodies targeting different epitopes of the purified gp140 RepliVax proteins were titrated in serial dilutions, starting at different concentrations. The bar charts represent the binding affinities (dissociation constant in nM) of the antibodies to the untreated and formulated proteins. Error bars represent the standard error of the mean of triplicates. BG505 SOSIP.664 was used as a reference (Ref). Main header shows the epitope and sub-headers the respective antibodies. Analysis of A) non-cross-linked and B) cross-linked protein. *: no binding detected.

Therefore, all sample groups appeared to be stable at both temperatures over the duration of the study. Only in the BN-PAGE, some change in protein quaternary structure for all of the RepliVax antigens was seen except for 16055 LT, which appeared to be fully stable (Supplemental Figure 15A, Supplemental Figure 16). The same analyses were performed for the cross-linked RepliVax proteins, for which the results were similar, apart from the BN-PAGE, where the cross-linking fixed the negative change in quaternary structure observed for the formulated proteins (Supplemental Table 7, Supplemental Figure 17).
In summary, the admixture of the RepliVax antigens alone and with the adjuvant was physicochemically stable for at least 24 hours and the adjuvant can therefore be used for the immunization study.

5.2.5.2. Antibody Affinity Measurements

Next to the formulation analysis performed by IDRI, I also analyzed the RepliVax immunogens as LSQ-formulated and untreated proteins in a lectin-capture ELISA. For the analysis of the binding affinities, a small panel of representative antibodies was used in a dilution series, targeting the epitopes of CD4i-conformation (17b), the CD4bs (F105, VRC01, HJ16), the variable loop 3 (HGN194), and the variable loops 1/2 (PG9, PGT145). Comparing the K_Ds of the formulated and untreated proteins after 4 h at 25°C, there is no difference in antigenicity detectable between the two conditions (Figure 19A, Supplemental Figure 18, Supplemental Table 8).
However, the calculation of the Area-Under-the-Curve (AUC) of the titration curves showed a decreased AUC for the binding of PGT145, a quaternary-structure-dependent antibody, which was roughly half the value for the formulated as for the untreated protein (Figure 20). This is consistent with the results of IDRI's BN-PAGE for the SOSIP proteins, which indicated a reduction in quaternary structure for the non-crosslinked proteins. Of note, no other antibodies showed a change in AUC values (Supplemental Figure 20A).
The analysis of the cross-linked protein did not show any change in binding affinities between the formulated and the untreated proteins (Figure 19B, Supplemental Figure 19). Furthermore, binding to the non-neutralizing antibodies 17b or F105 was no longer observable, either, which bind to the CD4-induced and open conformation of Envelope glycoprotein, respectively. Therefore, the cross-linking either improved the conformation

of our trimers or destroyed the epitopes for these antibodies, which would still be desired, as the induction of these antibodies is not beneficial. Of note, unlike for the non-cross-linked immunogens, there was no decrease in AUC for any of the antibodies, not even for PGT145 (Figure 20B, Supplemental Figure 20B, Supplemental Table 9).

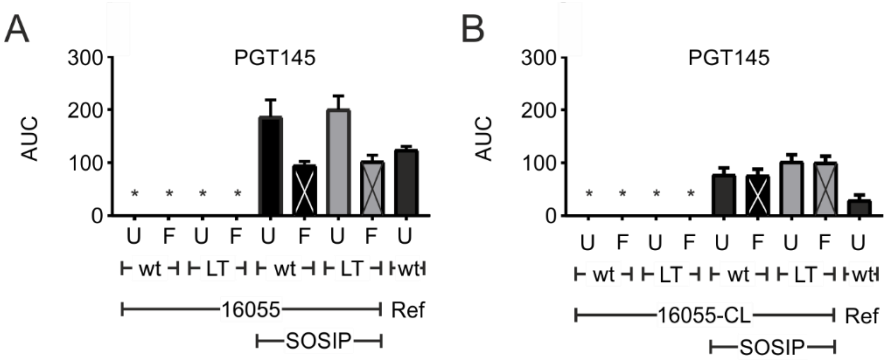

Figure 20: Comparison of Area-Under-the-Curve (AUC) values obtained by lectin-capture ELISA by the titration of the quaternary-dependent antibody PGT145. A) AUC for trimeric formulated (F) and untreated (U) RepliVax protein. B) AUC of cross-linked formulated and untreated RepliVax protein. Ref: BG505 SOSIP.664. *: no binding detected.

In general, there was no detrimental negative effect of the adjuvant, apart from some loss in quaternary structure for the non-cross-linked proteins. Furthermore, the cross-linking led to decreased binding of the non-neutralizing antibodies and could therefore shift the induction of antibodies in a positive direction, especially as a loss in quaternary structure was no longer visible. In summary, none of the desired epitopes was negatively affected by the formulation with the LSQ adjuvant, as the proteins showed to be stable in the formulation. Therefore, the RepliVax immunogens can be used as untreated as well as formulated proteins for the immunization study in New Zealand White rabbits.

5.3. Analysis of Intrinsic Trimer Stabilization in a Pre-clinical Animal Study

In order to determine the impact of our affinity-matured vulnerable sites (PG9, VRC01) and gp140 conformational trimer stabilization on antibody specificity and neutralization breadth, a randomized study in New Zealand White rabbits (called "Pantaleo.662" after the RepliVax-project principal investigator) was performed with the RepliVax immunogens (5.2.3) at the Fred Hutchinson Cancer Research Center (Seattle, Washington, USA) in the animal facility by Greg Mize.

With this rabbit study, protein-only immunizations were used to:

(1) Investigate the impact of LT variants on the elicitation of Env-specific antibody responses in terms of binding antibody immunogenicity and breadth

(2) Compare the uncleaved variants to their native-like SOSIP homologs

(3) Analyze the possible effects of the cross-linking on immunogenicity

Next to this, also a DNA-prime protein-boost strategy was tested to:

(4) Investigate the impact of LT in the context of a vectored delivery, boosted in all cases with the presumably best protein SOSIP-LT

(5) Compare protein-only delivery with DNA/prime-boost delivery of the same antigens

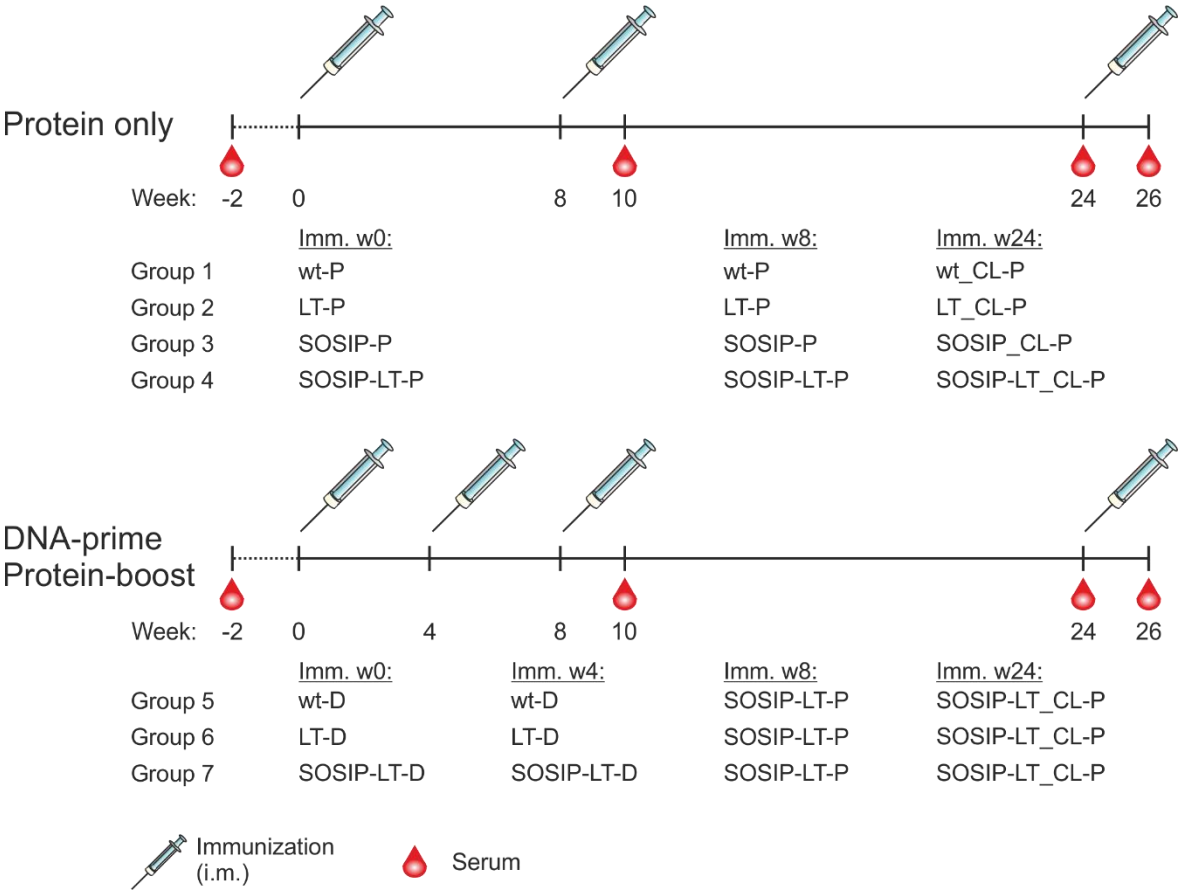

Figure 21: Setup of the immunization study in New Zealand White rabbits.
Groups 1-4 only received protein, while groups 5-7 received a DNA-prime protein-boost. Each group consisted of 5 animals. All animals received a final boost with cross-linked protein (CL). Immunizations and bleeds were performed at the depicted time-points.

In order to address the objectives, 35 New Zealand White rabbits were divided into 7 groups, leading to a total of 5 animals per group. Four groups received a series of protein-only (P) immunizations with different variants (wt-P, LT-P, SOSIP-P, SOSIP-LT-P) in weeks 0, 8, and 24, while three groups (wt-D, LT-D, SOSIP-LT-D) received a gp140 DNA-prime (D) in weeks 0 and 4, followed by a protein boost in weeks 8 and 24 (Figure 21). In week 24, the

protein was always delivered as cross-linked protein, in order to analyze the impact of cross-linked variants on the antibody responses. In the protein-only groups, the autologous cross-linked protein was used, whereas the presumably best protein SOSIP-LT_CL was used for all DNA-primed groups to boost antibody responses. All proteins were formulated with the LSQ adjuvant just before the immunizations. Serum samples were investigated at weeks -2, 10, 24, and 26 for all groups.

5.3.1. Binding Antibody Multiplex Assay Analysis

In order to analyze the antibody responses elicited in the rabbit study, a Binding Antibody Multiplex Assay (BAMA) of the serum IgG responses was performed by the CAVD central facility (Tomaras lab, Duke University, Durham, North Carolina, USA). In contrast to an ELISA, a BAMA allows the simultaneous measurement of serum antibody responses to different antigens at the same time. The results for weeks -2, 10, 24, and 26 were provided for the evaluation of the data sets which contained measurements against gp140, gp120 and V1V2 constructs (4.6.1).

The IgG serum response magnitudes against the gp140 variants were evaluated as a 6-fold dilution series starting at 1:80 for weeks 10 and 26 (Figure 22), while single-point measurements of the sera at a dilution of 1:80 were performed for weeks -2 and 24 (Supplemental Figure 22). Due to this, for weeks 10 and 26 data are presented as titration AUC while the data for week 24 are presented as mean fluorescence intensities.

5.3.1.1. BAMA against a Set of gp140 Antigens

Before the analysis of the IgG serum response magnitude against a set of gp140 antigens (Table 4), the response rates, defined as the number of animals showing a positive response (4.6.1), were evaluated. Regarding the four RepliVax readout antigens, a response rate of 100 % was observed for all time-points (week 10, 24, 26) and groups, and 80 - 100 % for the other two gp140 readout antigens, BG505 SOSIP and Con M gp140 (Supplemental Figure 21).

In general, the titration AUC data for weeks 10 and 26 show overall high responses against the uncleaved 16055 wt and LT readout antigens, while the reactivities to the native-like SOSIP readout variants were lower (Figure 22 A,B).

The first objective was to investigate the impact of LT on the elicitation of Env-specific antibodies. For this, I compared group 2 (LT-P) with group 1 (wt-P) and group 4 (SOSIP-LT-P) with group 3 (SOSIP-P) (Figure 22). At week 10, there was only a statistically significant difference for group 2 (LT-P), which showed a higher titration AUC than group 1 (wt-P) against the readout antigen 16055 SOSIP-LT. In week 26, group 2 (LT-P) was superior to group 1 (wt-P) for the antigens 16055 LT, 16055 SOSIP-LT and BG505 SOSIP. Of note, group 4 (SOSIP-LT-P) was significantly inferior to group 3 (SOSIP-P) in reactivity toward Consensus M.

With the second objective, the uncleaved variants were compared with their native-like SOSIP homologs. For this, group 4 (SOSIP-LT) was compared with 2 (LT), as well as group 3 (SOSIP-P) with 1 (wt-P). The only significant differences between group 4 (SOSIP-LT) and group 2 (LT) could be observed in both weeks 10 and 26 for the readout antigens 16055 wt, BG505 SOSIP, and Con M (also in week 24), with uncleaved LT inducing superior responses. In the comparison of group 3 (SOSIP-P) with group 1 (wt-P), one significant difference was found in week 10, where group 3 (SOSIP-P) was superior to group 1 (wt-P) against the readout antigen 16055 SOSIP-LT. Of note, the significantly higher intensity for group 2 (LT-P) than for group 4 (SOSIP-LT) can also be observed in week 24 for the readout antigens 16055 wt and Con M (Supplemental Figure 22).

The third objective was to evaluate the impact of cross-linking, so the results of week 26 were compared with those of week 10. The only difference between these time-points was observed for group 5 (wt-D) against the readout antigens 16055 LT, 16055 SOSIP, 16055 SOSIP-LT, and BG505 SOSIP. Of note, against the readout antigen BG505 SOSIP, significant changes were observed in three groups (groups 1, 4, and 7). For Consensus M, only group 4 (SOSIP-LT-P) showed a significant increase after the CL-P-boost. In cases where the response was significantly different, week 26 was always superior to week 10.

The fourth objective was the comparison of LT trimers in the context of a vectored delivery, so groups 6 (LT-D) and 7 (SOSIP-LT-D) were compared with group 5 (wt-D). There were no significant differences for these groups at the observed time-points.

The fifth objective was to compare the protein-only groups with DNA-prime/boost groups of the same antigens. Therefore, groups 5 (wt-D), 6 (LT-D), and 7 (SOSIP-LT-D) were compared with groups 1 (wt-P), 2 (LT-P), and 4 (SOSIP-LT-P), respectively. The comparison of group 5 (wt-D) and 1 (wt-P) showed higher signals for group 1 (wt-P) for the readout

antigens 16055 wt and Consensus M at weeks 10 and 26 and for the readout antigens 16055 LT, 16055 SOSIP, 16055 SOSIP-LT, and BG505 SOSIP at week 10.

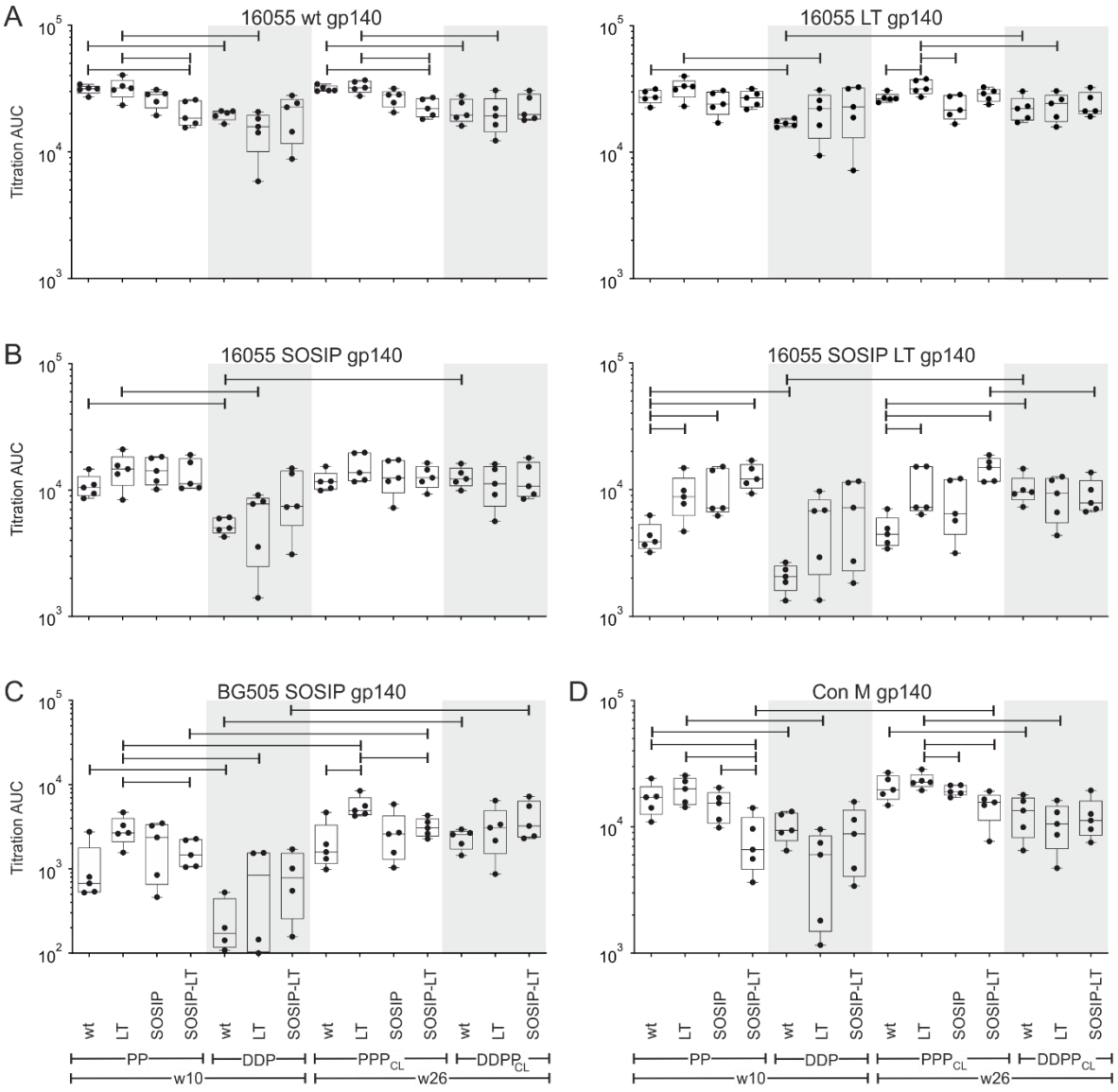

Figure 22: Binding Antibody Multiplex Assay was used to evaluate the binding of serum IgG antibodies to different gp140 readout-antigens. Depicted are the titration AUCs of rabbit serum IgG binding to the four readout 16055 antigens which were initially used as immunogens (wt, LT, SOSIP, SOSIP-LT) and two additional gp140 readout antigens, BG505 SOSIP and Consensus M (Con M). Titration was performed as a 6-fold serial dilution starting at 1:80. Grey areas indicate DNA-primed groups. Black horizontal lines: p-value <0.05. Boxes extend from the 25th to the 75th percentiles while the midline of the box denotes the median. Whiskers are plotted down to the minimum and up to the maximum value. Each individual value is plotted as a point superimposed on the graph. For statistics, an unpaired two-samples Wilcoxon test was performed. Abbreviations: AUC: Area-under-the-curve, P: Protein, D: DNA, CL: Cross-linked, w: week.

Of note, in week 26, group 5 (wt-D) was superior to group 1 (wt-P) against the antigen 16055 SOSIP-LT. For groups 6 (LT-D) and 2 (LT-P), significantly higher signals of the protein-only group can be observed at both time-points for the readout antigens 16055 wt (also in

week 24), 16055 LT, and Consensus M, and at week 10 for 16055 SOSIP and BG505 SOSIP. The comparison of groups 7 (SOSIP-LT-D) and 4 (SOSIP-LT-P) showed higher signals for the DNA-primed group against the readout antigen 16055 wt in week 24 and higher signals for the protein-only group against 16055 SOSIP-LT in week 26.

In summary, the gp140 analysis showed that the uncleaved LT trimers elicited superior or at least equal binding antibody responses than the wt, especially at week 26. Furthermore, when there was a significant difference between the uncleaved and the native-like variants, the uncleaved variants elicited higher responses. Next to this, especially the DNA-primed group 5 (wt-D) benefitted from a protein boost immunization, as this group showed superior signals for several readout-antigens in week 26. For the gp140 panel, there was no impact of the vectored delivery detectable in the DNA-primed groups and the protein-only groups usually elicited higher signals than the DNA-primed groups, even though the protein-boost increased the signals of the DNA-primed groups in week 26.

5.3.1.2. BAMA Analysis of a gp120 Breadth Panel

In the first data set, the binding antibodies against the RepliVax proteins and two further gp140s were analyzed, but with this limited panel, it was not possible to observe whether the induced antibodies broadly react with Env proteins from diverse HIV clades. For this, a gp120 breadth panel was used[173], consisting of readout-antigens from subtypes A, B, and C and the Circulating Recombinant Forms CRF07_BC and CRF01_AE (Table 5), which originate from diverse geographic regions. For the gp120 analysis, each sample was diluted 1:80 and tested against eight gp120 constructs. The data is plotted as background-adjusted MFI minus background-adjusted blank (MFI*).

For the individual gp120 antigens, a response rate of 80 – 100 % was observed for weeks 10 (two weeks after the second prime) and 26 (two weeks after the boost), while response ranges from 0 – 100 % were seen at week 24 (14 weeks after the second prime and immediately before the boost), with 16055 SOSIP-LT showing the least responses (Supplemental Figure 21).

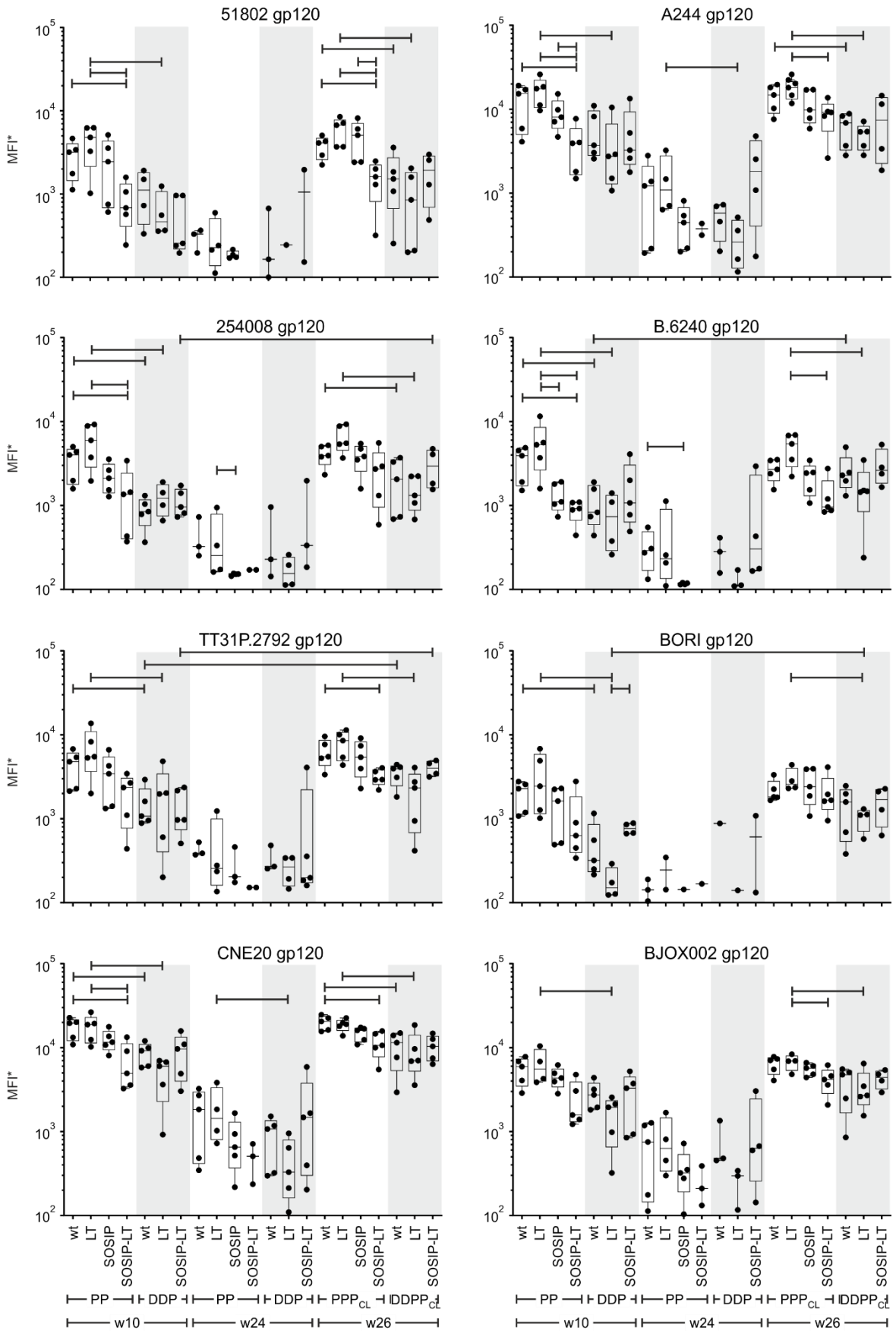

Figure 23: Analysis of the serum IgG reactivities to the gp120 variants of the breadth panel. Figure shows the BAMA analysis of sera from weeks 10, 24, and 26 against each antigen of the gp120 breadth panel at a

dilution of 1:80. Grey areas indicate DNA-primed groups. Black lines: p-value <0.05. Boxes extend from the 25th to the 75th percentiles while the midline of the box denotes the median. Whiskers are plotted down to the minimum and up to the maximum value. Each individual value is plotted as a point superimposed on the graph. Abbreviations: MFI: Mean fluorescence intensities, MFI*: background-adjusted MFI minus background-adjusted blank, P: Protein, D: DNA, CL: Cross-linked, w: week.

Looking at the impact of the LT trimers, only groups 3 and 4 show statistically significant differences for 2/8 antigens, with group 4 (SOSIP-LT-P) being inferior to group 3 (SOSIP-P) against 51802-gp120 in week 26 and against A244-gp120 in week 10 (Figure 23).

While comparing the uncleaved variants with their native-like SOSIP variants, it is seen that group 2 (LT-P) is superior to group 4 (SOSIP-LT-P) against 5/8 antigens in week 10 and 4/8 antigens in week 26. Of note, in week 24, group 3 (SOSIP-P) was inferior to group 1 (wt-P) for one antigen.

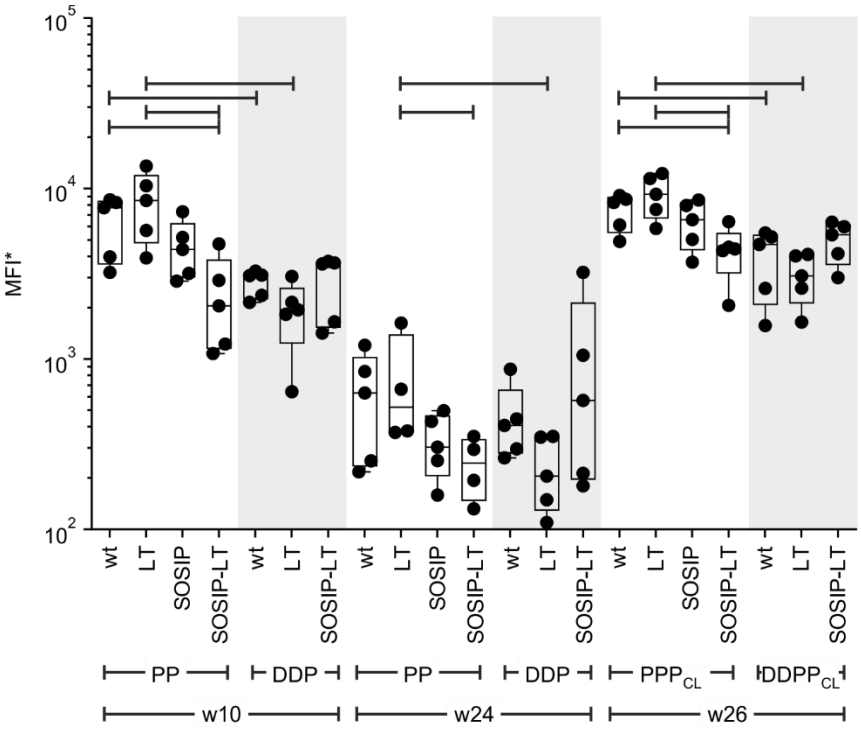

Figure 24: gp120 breadth analysis of the immune responses elicited by the different protein-only and DNA-primed groups. Figure shows the BAMA analysis of sera from weeks 10, 24, and 26. (cf. Figure 23). Each point represents the average MFI* for the 8 gp120 antigens per rabbit. Grey areas highlight DNA-primed groups. Black lines: p-value <0.05. The box extends from the 25th to the 75th percentiles while the midline of the box denotes the median. Whiskers are plotted down to the minimum and up to the maximum value. Each individual value is plotted as a point superimposed on the graph. For statistics, an unpaired two-samples Wilcoxon test was performed. Abbreviations: MFI: Mean fluorescence intensities, MFI*: background-adjusted MFI minus background-adjusted blank, P: Protein, D: DNA, CL: Cross-linked, w: week.

Regarding the effect of the cross-linking, the response magnitude in week 26 appeared to be overall higher than in week 10 but the difference was only statistically significant for groups 5, 6, and 7 for 2/8, 1/8 and 2/8 antigens, respectively.

Interestingly, the impact of the LT variant delivered as DNA-prime was not detectable for any of the antigens or time-points.
However, while comparing the protein-only with the DNA-primed groups, it can be seen that group 1 (wt-P) showed a higher response magnitude than group 5 (wt-D) for 5/8 antigens in weeks 10 and 26. Group 2 (LT-P) was superior to group 6 (LT-D) for all gp120 constructs at weeks 10 and 26, and for 2/8 constructs at week 24.

So far, we only looked at individual constructs but did not consider the breadth of binding. In order to do so, the breadth of the serum responses against the gp120 panel was analyzed. To calculate the breadth score, the responses against the individual gp120 constructs were averaged per animal and plotted as background-adjusted MFI minus background-adjusted blank (Figure 24).
In general, the highest response is always seen for group 2 (LT-P) and the protein-only groups seem to be superior to the DNA-primed groups. In week 24, overall responses were lowest, as the last immunization was performed 14 weeks ago.
Regarding the first objective, groups 2 (LT-P) and 4 (SOSIP-LT-P) did not show significantly higher responses than groups 1 (wt-P) and 3 (SOSIP-P) against the gp120 breadth panel at any time point.
Analysis of the comparison of the uncleaved with the native like SOSIP homologs (objective 2) showed that group 2 (LT-P) was superior to group 4 (SOSIP-LT-P) at all time-points.
There was no statistically significant difference between week 10 and week 26 and, again, there was no impact of LT detectable in the context of the vectored delivery. In general, the protein-only groups were superior to the DNA-primed groups, especially for the groups receiving uncleaved protein.

In summary, the groups immunized with the uncleaved variants always induced greater breadth than the groups immunized with the native-like SOSIP variants, while the lowest breadth was observed for the DNA-primed groups. Of note, animals immunized with LT-P showed the highest breadth against the panel of gp120 readout antigens analyzed.

5.3.1.3. BAMA Analysis of V1V2 Scaffolds

Follow up analysis of the RV144 HIV-1 vaccine efficacy trial detected an inverse correlation of antibodies binding to the variable regions 1 and 2 (V1V2) of the HIV-1 Env glycoprotein and the risk of HIV-1 infection.

In order to identify the capacity of the RepliVax immunogens and immunization scheme to induce antibodies binding to V1V2, a BAMA with scaffolded V1V2 readout antigens was performed by the CAVD immune monitoring core facility. For a first analysis, tags-V1V2-scaffold antigens were used (Table 6), which have an Ig leader at the N-terminus, serving as a mature protein cleavage and secretion signal, and an avi- and His6-tag at the C-terminus that is used for purification[189]. For a second analysis, a panel of 16 gp70-V1V2 scaffold antigens was used (Table 6), which consist of a murine leukemia virus gp70 protein-derived carrier sequence containing a polyhistidine affinity tag and the respective V1V2 domain[190].

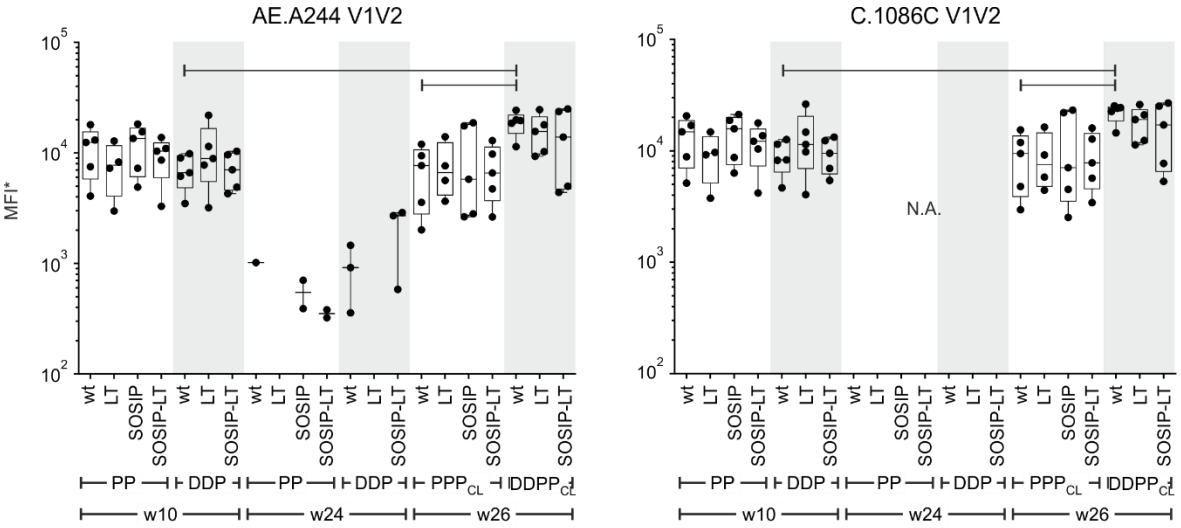

Figure 25: Analysis of Tags-V1V2 scaffold antigen reactivities of the IgG responses elicited by the different protein-only and DNA-primed groups. BAMA analysis of sera from weeks 10, 24 and 26 against two tags-V1V2 scaffold antigens at a dilution of 1:80. Grey areas highlight DNA-primed groups. Black lines: p-value <0.05. Boxes extend from the 25th to the 75th percentiles while the midline of the box denotes the median. Whiskers are plotted down to the minimum and up to the maximum value. Each individual value is plotted as a point superimposed on the graph. For statistics, an unpaired two-samples Wilcoxon test was performed. MFI: Mean fluorescence intensities, MFI*: background-adjusted MFI minus background-adjusted blank, P: Protein, D: DNA, CL: Cross-linked, w: week. N.A: not analyzed.

For the first analysis of the V1V2 tags-scaffolds AE.A244 and C.1086C, a response rate of 80 – 100 % was seen for week 10 and 26 serum samples, while a reduced response rate was seen at week 24 for AE.A244 V1V2 tags. Here, the highest response of 60 % was only

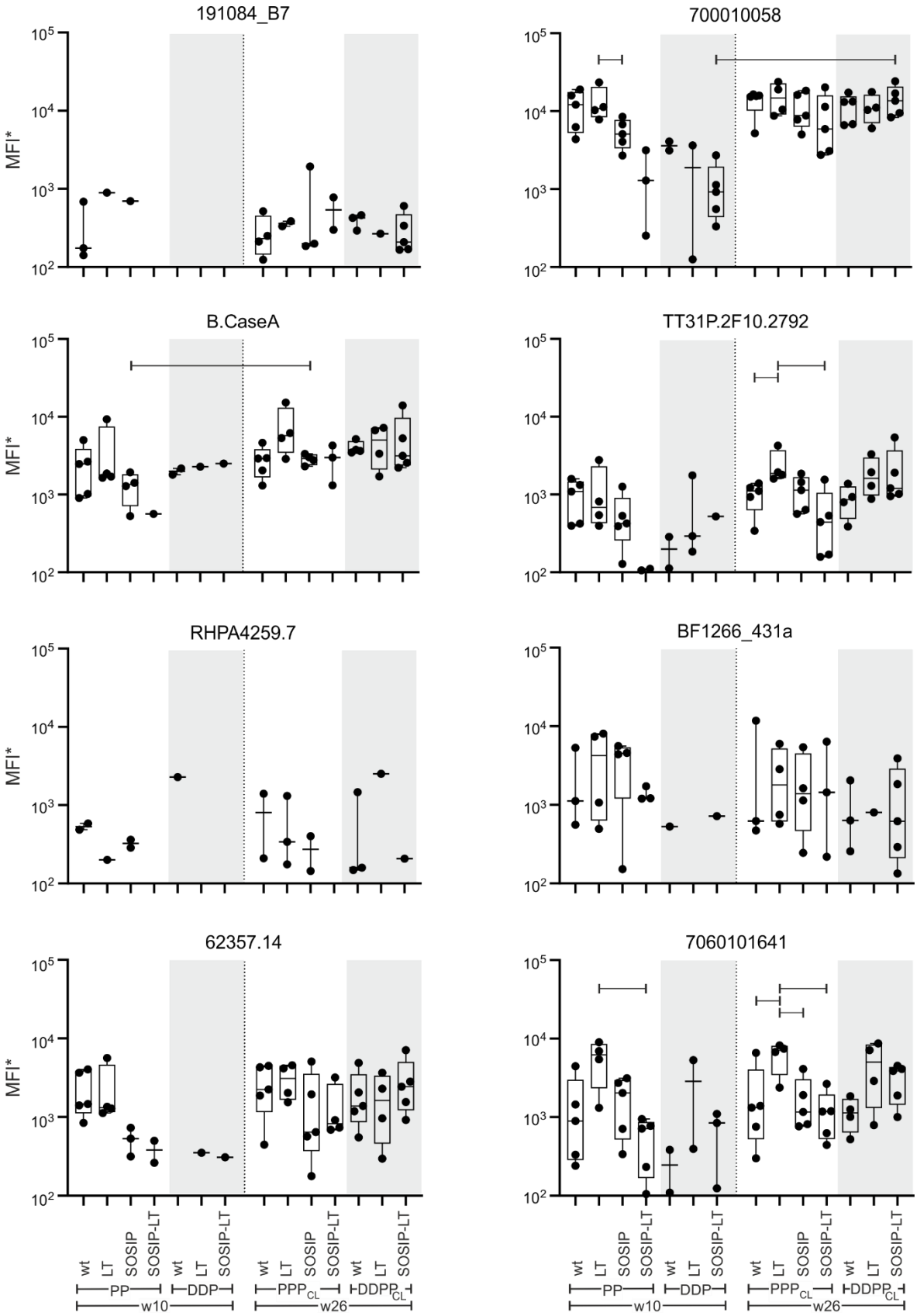

Figure 26: Analysis of the immune responses elicited by the different protein-only and DNA-primed groups against gp70-V1V2 scaffolds antigens of clades A, B, C, CRF01_AE, and CRF07_BC. Continued on next page.

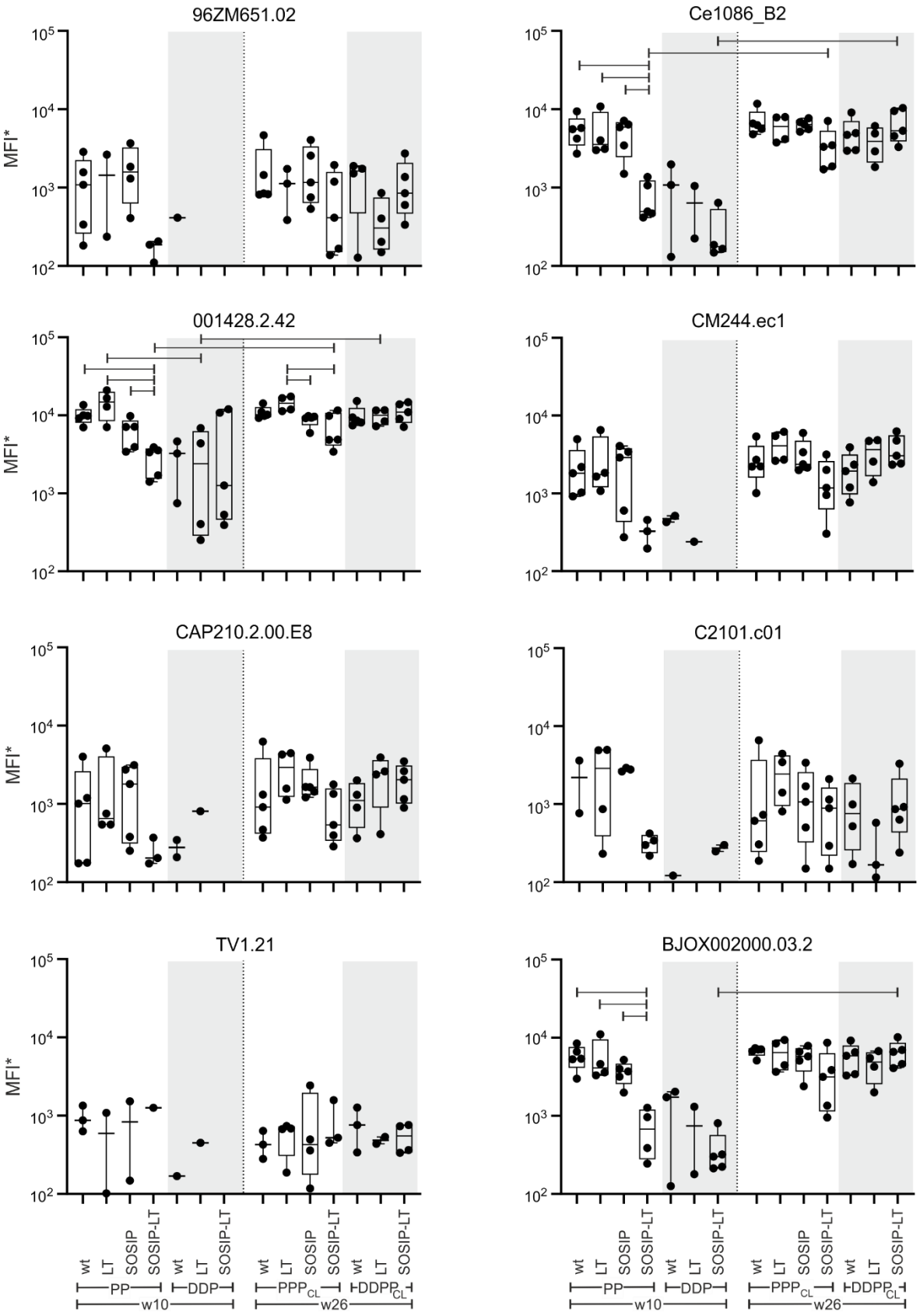

Figure 26: Analysis of the immune responses elicited by the different protein-only and DNA-primed groups against gp70-V1V2 scaffolds antigens of clades A, B, C, CRF01_AE, and CRF07_BC. Figure shows BAMA analysis of sera from weeks 10 and 26 against a panel of 16 gp70-V1V2 scaffold antigens at a dilution of 1:80. Grey areas highlight DNA-primed groups. Black lines: p-value <0.05. Boxes extend from the 25th to the 75th percentiles while the midline of the box denotes the median. Whiskers are plotted down to the minimum

and up to the maximum value. Each individual value is plotted as a point superimposed on the graph. Boxes are only present when response rate is ≥ 80 %. Statistics (unpaired two-samples Wilcoxon test) were only performed if the groups showed a response rate of ≥ 80 %. Abbreviations: MFI: Mean fluorescence intensities, MFI*: background-adjusted MFI minus background-adjusted blank, P: Protein, D: DNA, CL: Cross-linked, w: week.

observed in 2 of the 3 DNA-primed groups, while the protein-only groups showed a maximum response rate of 40 % in the two groups immunized with the native-like SOSIP proteins (Supplemental Figure 21). In regards of MFI*, no statistically significant differences between the immunization groups was detected in week 10 but in week 26 there was a significantly higher response magnitude for the DNA-primed group 5 (wt-D) in comparison to group 1 (wt-P). Next to this, group 5 also had statistically significant higher MFI*s in week 26 than week 10. These observations indicate a positive effect of the DNA-prime on the induction of antibodies able to bind to V1V2, as this was the case for both V1V2 readout constructs (Figure 25).

In order to evaluate if the positive effect of the DNA-prime in regards of antibodies binding to V1V2 can be observed for further V1V2 antigens, a panel of 16 gp70-V1V2 scaffold antigens was tested (Table 6), which also allows a breadth analysis.

For the gp70-V1V1 scaffold antigens, the response rates varied from 0 – 100 %, both in week 10 and 26 (Supplemental Figure 21). In week 10, the response rates obtained in group 1 (wt-P) were ≥ 80 % for 11/16 antigens and 100 % in group 2 (LT-P) for 12/16 antigens.

For groups 3 (SOSIP-P) and 4 (SOSIP-LT-P), the response rate was ≥ 80 % for 11/16 and 5/16 antigens, respectively. At this time point, the DNA-primed groups showed lower response rates than the protein-only groups. Group 5 (wt-D) showed a maximum response rate of 60 % for 3/16 antigens, group 6 (LT-D) ≥ 80 % in only 1/16 antigens, and group 7 (SOSIP-LT-DDP) ≥ 80 % in 4/16 antigens. In summary, at week 10, the response rates were superior in the protein-only groups.

For week 26, groups 1 (wt-P), 2 (LT-P), and 3 (SOSIP-LT-P) displayed slightly higher response rates with ≥ 80 % for 13/16 (Groups 1 and 2) and 14/16 scaffolded V1V2-antigens (Group 3). For group 4 (SOSIP-LT-P) the response rate of ≥ 80 % for 11/16 antigens was greatly increased in comparison to week 10 (5/16). However, the biggest change in response rate was observed for the DNA-primed groups, which showed a response rate of ≥ 80 % for group 5 (wt-D) of 12/16, group 6 (LT-D) of 11/16, and group 7 (SOSIP-LT-D) of 15/16 (SOSIP-

LT-D). Overall, in week 26, DNA-primed groups showed similar response rates as the protein-only groups.

In addition to the response rates, also the MFI* was analyzed, which differed among groups and antigens (Figure 26). The overall impression of the data indicates that the protein-only groups tended to be superior to the DNA-primed groups in week 10, while the MFI*s appeared to be similar in week 26 and - just like for the previous analysis - the SOSIP-immunized groups were inferior to those immunized with the uncleaved proteins. Next to this, statistically significant differences were only observed for the clades B, C and CRF07_BC.

For a deeper analysis according to our pre-formulated objectives, the impact of LT was investigated and group 2 (LT-P) never showed a statistically significant higher MFI* than group 1 (wt-P) at week 10, but for 2 antigens in week 26. In contrast to this, group 4 (SOSIP-LT-P) showed a lower MFI than group 3 (SOSIP-P) in 3/16 antigens in week 10 only.

For a second analysis, the uncleaved variants were compared with their SOSIP homologs. Here, group 2 (LT-P) showed a higher MFI* than group 4 (wt-P) for 4/16 antigens in week 10 and 3/16 antigens in week 26. Group 3 (SOSIP-P) and 4 (SOSIP-LT) did not show statistically significant differences at either time-point.

Next, weeks 10 and 26 were compared and statistically higher MFI*s were found for 5/16 antigens in week 26. Here, the protein-only groups 3 (SOSIP-P) and 4 (SOSIP-LT-P) were superior for 1/16 and 2/16 antigens, respectively. The DNA-primed group 7 (SOSIP-LT-D) showed differences for 3/16 antigens. In general, only clades B, C, and CRF01_BC benefitted from the additional immunization with cross-linked protein, and especially the groups immunized with cross-linked SOSIP-LT showed high responses.

For the fourth analysis, the impact of LT in the vectored context was evaluated. Here, group 5 (wt-D) was compared to groups 6 (LT-D) and 7 (SOSIP-LT-D), but no statistically significant differences were observed at any time-point.

In order to investigate our fifth objective, DNA-primed groups were compared with the autologous protein-only groups to analyze the effect of the DNA-prime on the induction of antibodies binding to V1V2. Here, only group 6 (LT-D) was significantly inferior to group 2 (LT-P), but only for one antigen.

The gp70 V1V2 panel was also analyzed analogously to the gp120 breadth panel to evaluate the potential of the groups to display a certain breadth (Figure 27). Just like before, group

2 (LT-P) tended to show the highest breadth at weeks 10 and 26 and the protein-only groups were superior to the DNA-primed groups, while the immunization with the uncleaved proteins also led to a higher breadth than those immunized with the native-like SOSIP variants.

Evaluating the objectives, no positive effect for group 2 (LT-P) was seen in comparison to group 1 (wt-P), and the SOSIP-LT-P immunized group 4 even showed a statistically significantly reduced breadth compared to group 3 (SOSIP-P) in week 10. Of note, the uncleaved LT trimers led to a significantly higher breadth than the native-like SOSIP-LT trimers. The greatest difference was observed when we compared weeks 10 and 26. Here, groups 4 (SOSIP-LT-P), 5 (Wt-D), 6 (LT-D), and 7 (SOSIP-LT-P) showed a statistically significant higher breadth than in week 10. Although no differences were observed between the DNA-primed groups at any time-point, group 5 (wt-D) showed a significantly reduced breadth compared to the respective protein-only group 1 (wt-P).

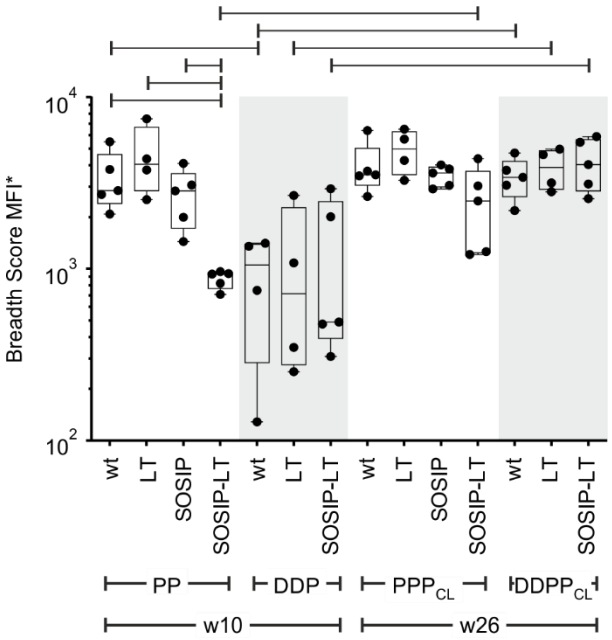

Figure 27: V1V2 breadth analysis of the immune responses elicited by the different protein-only and DNA-primed groups. The diagram shows the BAMA analysis of sera from weeks 10 and 26 against a breadth panel consisting of 16 HIV-1 Env V1V2 gp70-scaffolded antigens (cf. Figure 26). One point represents the average MFI* toward all V1V2 antigens per rabbit. Grey areas indicate DNA-primed groups. Horizontal black lines: p-value <0.05. The box extends from the 25th to the 75th percentiles while the midline of the box denotes the median. Whiskers are plotted down to the minimum and up to the maximum value. Each individual value is plotted as a point superimposed on the graph. For statistics, an unpaired two-samples Wilcoxon test was performed. MFI: Mean fluorescence intensities, MFI*: background-adjusted MFI minus background-adjusted blank, P: Protein, D: DNA, CL: Cross-linked, w: week.

In summary, the V1V2 scaffold analysis showed that LT leads to higher response magnitudes and breadth than the wt. However, this only applies for the groups immunized with uncleaved protein, as groups immunized with the native-like SOSIP proteins showed lower magnitudes and breadth. Just like for gp140 and gp120, the SOSIP variants in general led to lower magnitudes and breadth against V1V2 than the uncleaved variants. Overall, the positive effect of the DNA-prime on V1V2 binding at week 26 observed for the V1V2 tags proteins was not evident for the gp70 scaffold antigens.

5.3.2. Linear Epitope Mapping

The binding antibody multiplex assay helped us to analyze binding of the antibodies in the sera to specific antigens in general, but so far, there is no information about the specific epitopes of these antibodies. To further analyze the epitope specificity of the antibodies induced in our rabbit study, a linear epitope mapping was performed by Shaunna (Xiaoying) Shen/ Georgia Tomaras (DHVI) of the CAVD central core facility. For this, a peptide library designed by Bette Korber (LANL) was used, consisting of 15-mer peptides overlapping by 12 amino acids (4.6.2). For the analysis, the log_2-fold difference of the mean intensities of post-immunization samples and the matched pre-immunization sample which met positivity criteria was used. The 15-mer peptides targeted the regions C1, V2, V3, C4, and C5 of gp120 and aa532-546, AVERY (aa581-585, N-terminal heptad repeat HR downstream sequence[191]), and the gp41ImmunoDominant (ID[192]) region of gp41.

First, the binding of serum antibodies per group were analyzed against gp160 consensus Envs of clades A, B, C, D, Group M, CRF01 (AE), and CRF02 (AG).

Overall, the signals obtained for the seven groups at week 10 and week 26 varied for the different consensus sequences in regards of signal intensity as well as the overall availability of a signal meeting the positivity criteria (Supplemental Figure 23).

For the consensus sequences, the number of positive responses was higher for the protein-only groups than for the DNA-primed groups in week 10, with the groups that had been immunized with uncleaved proteins, i.e. Group 1 (wt-P) and 2 (LT-P), showing more positive responses than the two native-like SOSIP variants (Supplemental Figure 23). In week 26, a higher number of positive responses was detected for the uncleaved protein immunizations in groups 1 (wt-P) and 2 (LT-P), followed by the DNA-primed groups 5 (wt-

D), 6 (LT-D), and 7 (SOSIP-LT-D) and the native-like proteins in the groups 3 (SOSIP-P) and 4 (SOSIP-LT-P).

The magnitude of binding to the tested epitopes was variable over groups and antigens (Figure 28). The region C1 showed higher binding magnitudes for the protein-only groups, where especially group 2 (LT-P) exhibited high binding magnitudes to C1.3 in all tested consensus sequences. In general, all groups showed binding to C1.2 apart from group 6 (LT-D), which did not show any positive signal for C1.1 and C1.2.

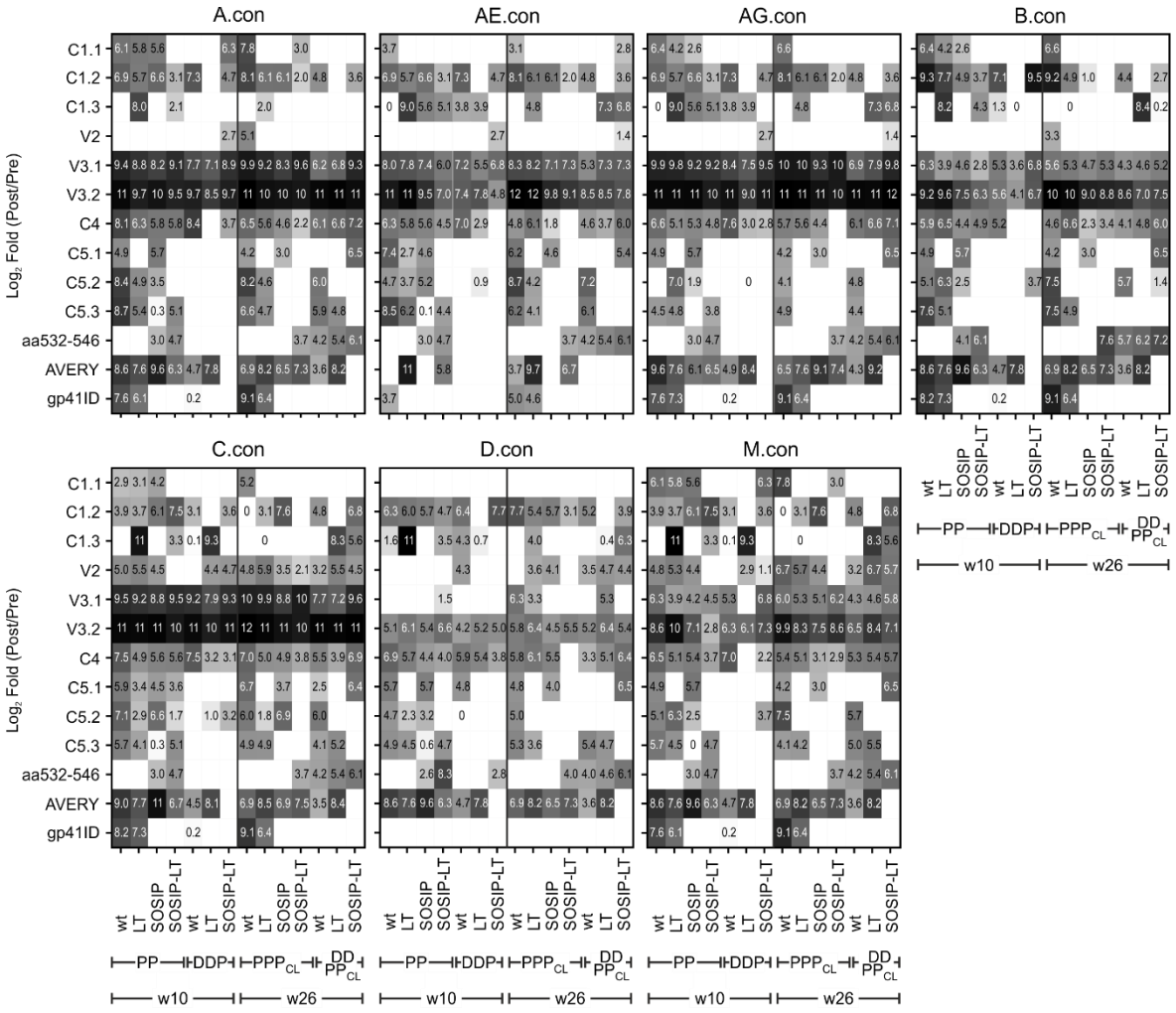

Figure 28: Greyscale-map of the linear epitope mapping against Consensus gp160 Env.
Depicted are the magnitudes of binding calculated as $\log_2$ fold change of the mean intensity of the post-immunization samples and the matched pre-immunization sample ($\log_2$ Fold (Post/Pre)) which met positivity criteria against 15-mer peptides of consensus gp160s of clades A, B, C, E, group M, CRF01 (AE), and CRF02 (AG). The linear epitope mapping was done for serum samples of weeks 10 and 26. CX: Constant region X, VX: Variable region X, aa532-546: Amino acid region 532-546, AVERY and gp41ID: immunodominant regions of gp41, w: week.

Only minimal V2 binding was observed for the consensus sequences A, B, C and the CRFs AE and AG. Here, especially group 7 (SOSIP-LT-P) showed binding to the epitope. Of note, the consensus variants C and M displayed overall good binding to V2 for most groups.

The overall highest and most consistent binding was observed to the variable loop 3 (V3.1, V3.2). Only for consensus D and M readout peptides, a less strong binding of the serum samples of the different groups was observed.

The responses against C4 were detectable for most groups and sequences. For C5, the protein-only groups showed more and increased binding in week 10, while the DNA-groups showed increased binding in week 26.

For the gp41 peptides, especially AVERY showed good reactivity with serum IgG from the immunized rabbits, and for the DNA-primed groups, reactivity with the peptide aa532-546 was boosted by the last immunization.

Secondly, the binding of serum antibodies against peptide panels resembling gp120 Envs of the strains AE.A244, AE.TH023, B.MN, C.TV1, C.1086, and C.ZM651 were analyzed as above (Figure 29). For the gp120 sequences, the number of overall positive responses was reduced compared to the consensus sequences but the overall ranking of positive responses was equal (week 10: uncleaved > native-like SOSIP > DNA-primed, week 26: uncleaved > DNA-primed > native-like SOSIP) (Supplemental Figure 23).

Binding magnitudes to C1.1 were overall low, and responses were mainly obtained for week 10. C1.2 showed the highest binding magnitude of the three C1 peptides.

Interestingly, binding to V2 was only observed for DNA-primed groups and especially in group 7 (SOSIP-LT-D), but just like for the consensus variants, the binding magnitude was rather low.

Binding to V3 again displayed the highest magnitudes for all groups and antigens, binding to C4 was detectable for most groups and antigens, and binding to C5 was mostly observed for the protein-only groups.

In summary, serum antibodies induced by the different immunization schemes targeted multiple linear epitopes in Env, including the C1, V2, V3, C4, and C5 regions of gp120, as well as AVERY, gp41ID, and an epitope within aa 532-546 in gp41, but the linear epitope binding response was dominated by V3.

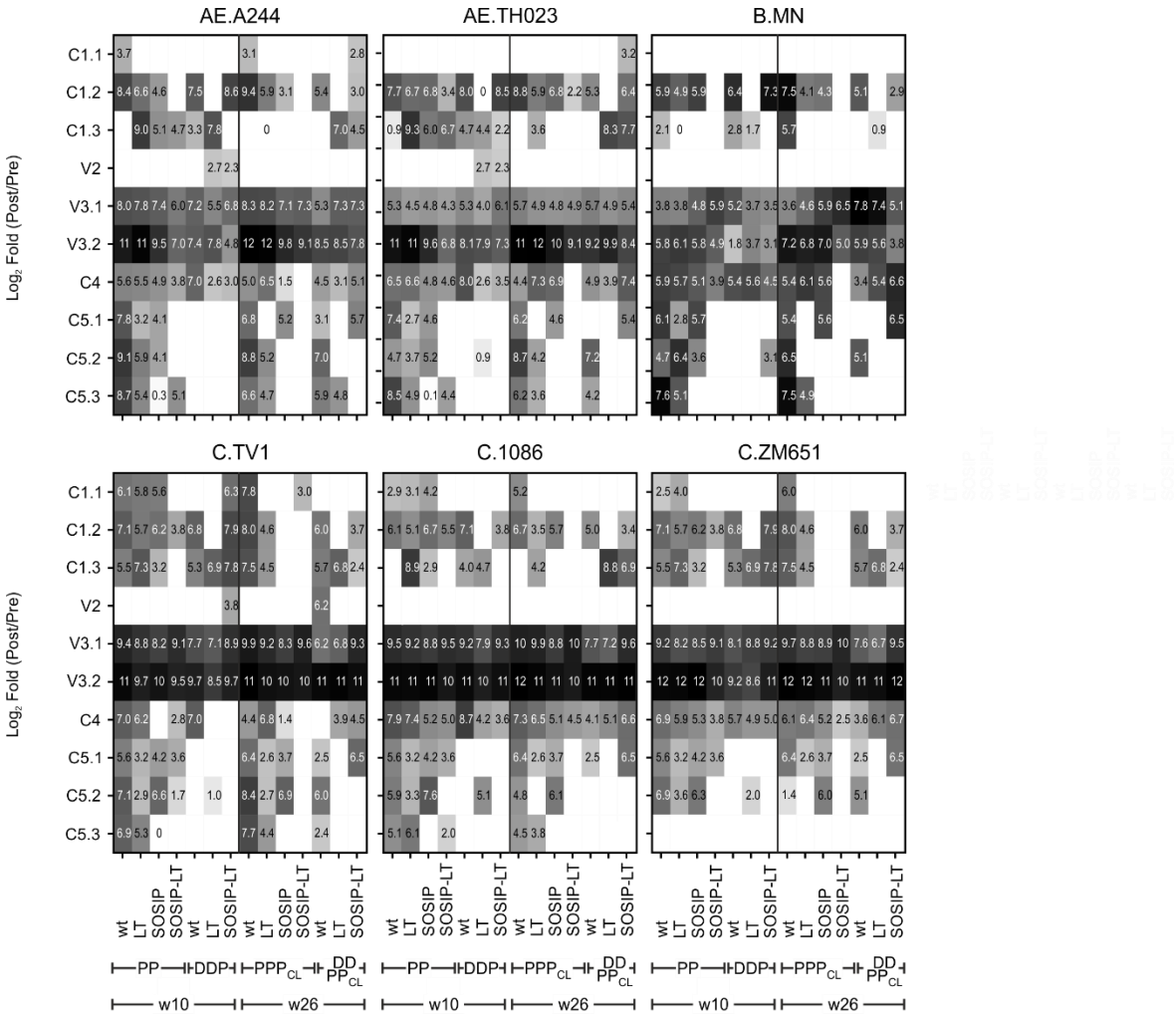

Figure 29: Greyscale-map of the linear epitope mapping against selected gp120 Env isolates.
Depicted are the magnitudes of binding calculated as Log_2 fold intensity of the mean of post-immunization samples and the matched pre-immunization sample (Log2 Fold (Post/Pre) which met positivity criteria against 15-mer peptides of Env gp120 (AE.A244, AE.TH023, B.MN, C.TV1, C.1086, C.ZM651). The linear epitope is shown for the Log_2 Fold (Post/Pre) of weeks 10 and 26. CX: Constant region X, VX: Variable region X, w: week.

The binding to the other epitopes was variable and did not show a clear association with a certain immunization scheme, except for the response rates, which were highest for the protein-only immunizations in week 10, while the cross-linking was most beneficial for the DNA-primed groups. Regarding the epitope region V2 as analyzed in this assay, it is interesting to note that the region is immediately upstream of the V2 hotspot detected in the RV144 trial. Therefore, it is an interesting region and especially the results for the clade-matched consensus C are promising, although the magnitude of binding was rather low.

5.3.3. Neutralization Assay

In order to investigate the neutralizing capacity of the antibodies induced in the rabbit study, a neutralization assay was performed against viruses of different tiers (4.6.3). For this, six isolates were tested, consisting of one tier 1A virus (MW965.26), four tier 2 viruses (16055-2.3, 25710-2.43, Ce1176_A3, and Ce703010217_B6), and one control isolate (SVA-MLV). The serum dilutions at which the HIV-1 infectivity was inhibited by 50 % were determined (ID_{50}).

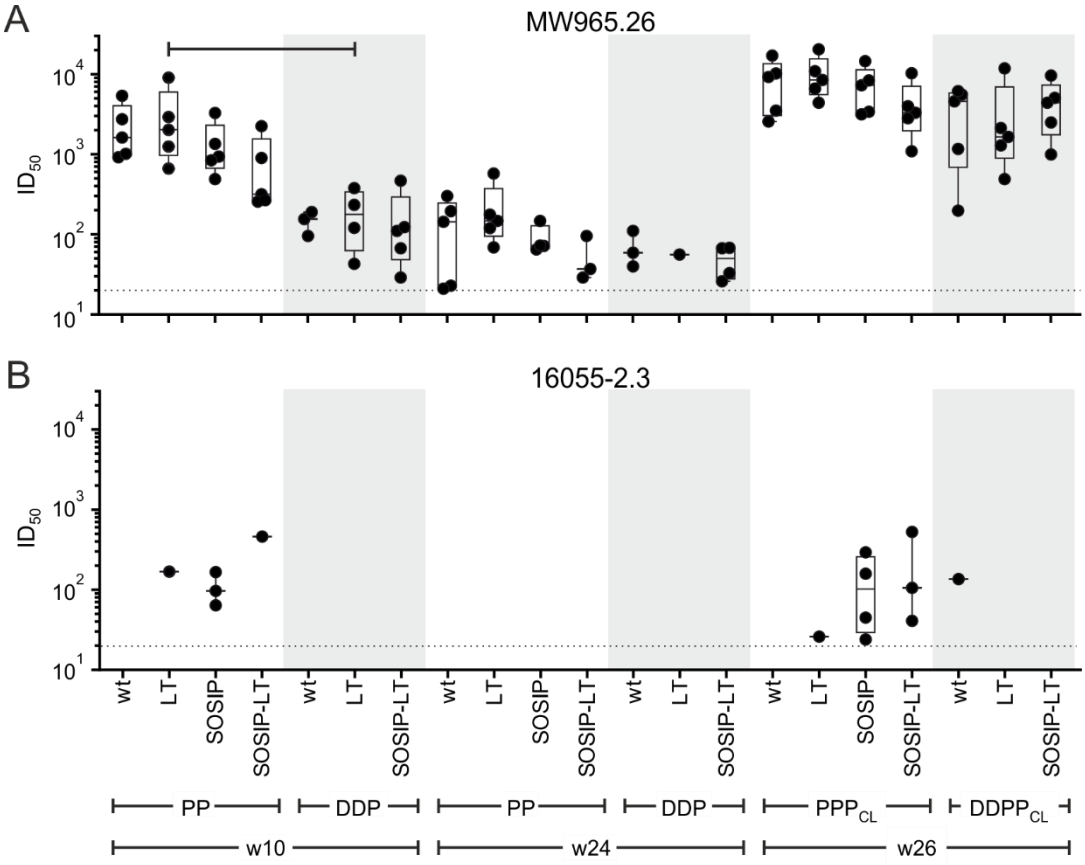

Figure 30: Neutralizing antibody responses of sera from the different immunization groups.
The response magnitude of the sera from the different immunization groups and schemes is expressed as ID_{50} titer for each rabbit for the clade C isolates (A) MW965.26 and (B) 16055-2.3 at weeks 10, 24 and 26. Grey areas highlight DNA-primed groups. Boxes extend from the 25th to the 75th percentiles while the midline of the box denotes the median. Whiskers are plotted down to the minimum and up to the maximum value. Each individual value is plotted as a point superimposed on the graph. Boxes are only present when response rate is ≥ 80 %. Statistics (unpaired two-samples Wilcoxon test) were only performed if the groups showed a response rate of ≥ 80 %. Non-responders are not shown. Horizontal black lines: p-value <0.05. P: Protein, D: DNA, CL: Cross-link.

In general, there were more and higher responses against the tier 1A isolate than the respective tier 2 isolates (Figure 30, Supplemental Table 10), as expected.

In week 10, all seven groups showed responses to tier 1A virus MW965.26. Here, the responses rates for the protein-only and DNA-primed groups were 100 % and 60 - 100 %, respectively (Supplemental Table 10). In week 24 (14 weeks after the 2nd immunization) there were lower response rates of 60 - 100 % for the protein-only groups and 20-80 % for the DNA-primed groups. In contrast to this, in week 26 (2 weeks after the final protein-boost) the response rate was 100 % for all groups against the tier 1A virus with overall high ID_{50}.

Regarding the objectives, there was no statistically significant difference of the LT trimers in groups 2 (LT-P) and 4 (SOSIP-LT-P) in comparison to the trimers used in groups 1 (wt-P) and group 3 (SOSIP-P) (Figure 30A). However, group 2 (LT-P) always showed the highest ID_{50} of all groups. Furthermore, immunization with the uncleaved variants led to higher ID_{50} values than when using the SOSIP variants, but the effects were not statistically significant, which also applies for the overall higher ID_{50} values in week 26 in comparison to week 10. At this time-point, the DNA primed groups seemed to be inferior to the protein-only groups, and the protein-only group 2 (LT-P) showed statistically higher ID_{50} values than the respective DNA-primed group 6 (LT-D).

Responses rates against the tier 2 virus 16055_2.3 - which is the autologous isolate of the RepliVax immunogens - were limited (20 – 80 %) and only occurred for the protein-only groups 2, 3 and 4 in week 10 and groups 2, 3, 4, and 5 in week 26 for some animals (Supplemental Table 10). For the tier 2 isolate, no statistically significant differences were observed, but it is notable that neutralization was primarily observed for the protein-only groups 2, 3, and 4 and the highest ID_{50} value was detected for group 4 (SOSIP-LT-P) in week 10 and 26 (Figure 30B). For the other tier 2 viruses, no neutralization was detectable apart for 25710-2.43, where one animal of group 2 (LT-P) showed an ID_{50} of 32, while there were no responses against Ce1176_A3, and Ce703010217_B6 (Supplemental Table 10) in any sample.

Taken together, the response rate was best against the tier 1A isolate MW965.26 in week 26, followed by week 10, where all protein-only groups showed 100 % response. For group 1 (wt-P) and group 2 (LT-P) the tier 1A neutralizing antibodies were more durable, as neutralization was still observed in week 24 in all animals. Group 2 (LT-P) showed the highest ID_{50} titers, but the differences to the other groups were not statistically significant in weeks 24 and 26. Regarding the tier 2 isolate, the highest response rate was observed

for SOSIP-P and SOSIP-LT-P, but also here, the difference in ID_{50} titers to the other groups was not statistically significant.

6. Discussion

The generation of a safe, efficient, and globally accessible HIV-1 vaccine has not yet been successful. Even though ART has turned the infection that once caused a deadly disease into a chronic one, and even though pre-exposure prophylaxis leads to a reduced infection risk[193], a vaccine is still desired and necessary, especially for low-income countries.

The first vaccines against viruses were based on live-attenuated or inactivated microorganisms and work well for diseases like measles or rabies. However, for HIV-1, the possibility that the virus might revert to its original form due to its high mutation rate is too much of a safety concern, just like the incomplete inactivation of HIV-1, to follow these classical approaches[193].

Therefore, other approaches need to be used for HIV-1, but difficulties in vaccine design caused by HIV's various immune escape mechanisms hindered success, so far. The detection of broadly Neutralizing Antibodies (bNAbs) in chronically infected patients and their use in animal studies and clinical trials set hope on this specific type of antibodies, just like the Fc-mediated effector functions found after analysis of the RV144[108,122,123,127].

An immunogen targeting such immune responses might be suitable for further vaccine approaches. For this, an improved conformation leading to decreased binding of nNAbs, while showing an improved trimer content with more accessible epitopes for bNAbs might possibly lead to the induction of such responses. This, together with further stabilization approaches, is a promising strategy for vaccine design, as these features could lead to a neutralizing immune response, which is in the best case even cross-neutralizing for other HIV clades.

6.1. Amino Acid Substitutions Can Influence Structure and Antigenicity

To find a more stable Env variant, which leads to a decreased presentation of nNAbs while keeping a closed conformation and showing increased binding of bNAbs, Veronika Grassmann screened 96ZM651 gp145 Env variants, where each amino acid had been exchanged to alanine once per variant. She analyzed the binding signal of various bNAbs like PG9 and VRC01. In the screening with the bNAb PG9 that preferentially binds to Env

exhibting the native quaternary structure, i.e. forming trimers, variant L111A was detected, which showed an increased signal when leucine was replaced by alanine. This mutant was further characterized in this thesis. In addition, the screening with the CD4bs-directed antibody VRC01 led to the identification of T278A, and subsequent analyses found an even increased binding for T278H[133].

6.1.1. L111A shows an Improved Trimeric Content and Conformation

L111A gp145 is the only variant which showed an increased signal for PG9 in comparison to the wt in the flow cytometry assay and this was observed for the assay with two antibodies in a double staining at once as well as for the assay with one antibody at a time, therefore the antibodies did not influence each other and can both be used for the assay (Figure 11).

PG9 is known to be quaternary-structure-specific[103] and therefore its increased binding to L111A might either be caused by a) an improved conformation of the epitope leading to a higher affinity of PG9 to the protein or b) by a change in the distribution of trimer, dimer, and monomer present on the surface of the cells toward the trimer or c) a mixture of both conditions.

Position L111 is located inside layer 2 of the inner domain of gp120[194] and therefore not part of the PG9 epitope, which consists of N156, N160 and the variable loops 1 and 2[165,195]. Therefore, aa 111 cannot serve as a direct interaction partner of PG9. However, due to the increased binding of PG9, it presumably leads to an improved conformation. L111A gp120 has already previously been described in the HIV-1 isolates YU2 (clade B)[194,196] and BG505 (clade A)[197], where it was reported to strongly decrease dimer formation based on its role on layer1-layer 2 interactions which stabilize the gp120 association[196], but so far, no effect on the trimeric protein was published.

The further characterization of the variant was performed with soluble L111A gp140 protein not only of the clade C isolate 96ZM651, but with other isolates of clades A, and C as well. For the C clades, an overall decreased monomer content of lectin eluates for the uncleaved variants was seen or at least a more distinct separation of trimer and monomer. However, the analysis of the two SOSIP variants showed no positive effect, presumably as

these variants already show an improved conformation by design[56]. For the analysis of the trimeric proteins in an ELISA against a broad panel of antibodies, a reduced binding of 17b was seen, an antibody recognizing the CD4-induced state of Env. The decreased binding indicates a more closed conformation of L111A, as the epitope presented in the open conformation is no longer accessible. This more closed conformation did not lead to an increased denaturation midpoint, as shown by DSC and nanoDSF, but L111A showed a reduced width of transition at half signal height, which indicates a more homogenous unfolding compared to the wt.

In conclusion, L111A did not only show a higher trimeric content but also a more closed and more homogenous conformation, which both lead to an increased binding of PG9. However, L111A alone does not lead to a native-like structure, as binding of PGT145 – an antibody binding to the apex of well-folded trimers – was only see for the SOSIP variants, which resemble a more native-like conformation. Due to their native-like conformation, the SOSIP variants are additionally to the uncleaved variants interesting candidates, as they resemble another type conformation and are therefore possibly leading to another immune response.

These findings present L111A as an interesting candidate for an *in vivo* study, as its increased trimerization and conformation might lead to an improved antibody response in contrast to the respective wildtype variant.

6.1.2. T278H leads to a Removal of Glycan 276 and Allows Increased Binding of VRC01

T278A gp145 was originally detected in a flow-cytometry-based scan, as it led to increased binding of bNAb VRC01. Subsequent permutation analysis of position T278 showed an even stronger effect of T278H. The transfer of this variant into the soluble form of 96ZM651 and other isolates of clades A and C did not lead to changes in the trimer, dimer, and monomer content of the variant (Figure 15). Analysis of the VRC01 binding affinities showed a reduced K_D of T278H in comparison to the wt for all isolates, while the binding to other antibodies was not influenced apart from HJ16, which is known to rely on glycan N276 that gets removed by the amino acid exchange of T278H, which is part of a glycosylation sequon (Figure 16)[198]. However, both 16055 T278H variants (uncleaved and native-like) did show

binding to HJ16, albeit it was reduced, which indicates a superior effect of 16055 over the other isolates. The increased binding of VRC01 to T278H is, on the one hand, caused by the removal of glycan 276. as this amino acid exchange destroys the glycosylation motif N-X-T/S[199]. On the other hand, the histidine variant T278H was superior to T278A that both lead to the loss of the glycan. Therefore, the improved binding of VRC01 is not solely caused by the removal of the glycan but presumably also by the positive charge of the amino acid and the resulting interaction with VRC01[133]. Due to the removal of this glycan, the glycan shield is disrupted and the CD4bs seems to be more accessible for VRC01. Furthermore, it is known that the removal of this glycan leads to VRC01 germline binding[200], which would be beneficial for the possible induction of bNAbs like VRC01, as it helps to direct antibody maturation. This makes T278H an ideal candidate for an HIV-1 vaccine to be tested in a pre-clinical animal study.

6.1.3. Combination of Single Amino Acid Exchanges and Additional Cross-linking is Feasible

In order to generate an improved vaccine candidate, the two single amino exchanges were combined in one variant (LT) and its characterization led to similar results as for the single variants, as shown by Helene Hierl[185] and by my further analyses (Figure 17). Also, the chemical cross-linking with EDC/NHS showed good results. EDC is a heterobifunctional reagent, which cross-links amines to carboxyl groups, and as a zero length linker, it leaves no residual atoms between the two components, while NHS is only used to stabilize the reaction[187]. Chemical cross-linking was already used for antigen stabilization in vaccines like polio[201]. As the procedure might influence the structure as well as the antigenicity and therefore also the immunogenicity of the proteins, the cross-linked products must be evaluated, and experiments performed in our group showed that the trimers can be used without negative consequences after EDC/NHS cross-linking.

The LT-variant was tested as uncleaved and native-like SOSIP construct in various isolates[185]. The strongest positive effect of the mutations was observed for the A clade isolate BG505 and the C clade isolate 16055, as well as their native-like SOSIP versions. However, as C clades are most prominent in Africa, the continent with the highest number

of new and total infections, and as this region would benefit the most from an effective HIV-1 vaccine, we decided to further work with the C clade isolate 16055.

6.1.4. Mixing Compatibility Study

Before the animal study could be started, it was necessary to establish a large-scale, endotoxin-free protein production process. The generated and quality-controlled trimers were subsequently tested in an adjuvant-formulation-study in order to detect possible detrimental effects of the adjuvant GLA-LSQ on the protein.

The data show that the liposomal formulation did not lead to a change in visual appearance, particle size and properties in SDS-PAGE analysis for the protein at the analyzed time-points and temperatures. However, the non-cross-linked protein showed some change in its quaternary structure observed by BN-PAGE, but this was not the case for 16055 LT (Supplemental Figure 15). It is interesting that it is variant LT, which shows this phenotype. The decreased sensitivity to dissociation might be caused by the more homogenous composition of the uncleaved LT trimers caused by the positive effect of L111A compared to the uncleaved wt. As shown in the BN-PAGE for 16055 LT (Supplemental Figure 15), not all RepliVax immunogens are affected by the dissociation and it may be that only a specific type of trimer is targeted. So, LT seems to preferentially assemble into the more closed or even less flexible trimer types and might therefore be less susceptible to dissociation.

Further analyses of binding affinities of a panel of antibodies to the RepliVax proteins did not show any change in affinities between the untreated and formulated proteins apart from the quaternary-structure-specific bNAb PGT145, which showed decreased binding to the formulated protein (Figure 19A).

For the cross-linked protein, neither a negative effect of the adjuvant-formulation on the quaternary structure nor any other disadvantageous effects were observed, and therefore it shows an ideal physicochemical stability. Furthermore, the binding of bNAbs to the untreated and the formulated proteins was equal, also for PGT145 (Figure 19B). Of note, the cross-linking led to decreased binding of the non-neutralizing antibodies and might therefore shift the induction of antibodies in a positive direction, especially as dissociation of the quaternary structure was no longer visible (Figure 19B, Figure 20). This led to the assumption that cross-linked proteins are the best among the analyzed variants and would

therefore be suitable as a final boost in the animal study, in order to increase the responses primed in the beginning of the study.

Liposomes are beneficial for antigen delivery, but they make up poor adjuvants. However, if they contain special lipids like e.g. TLR4-ligands, they can activate innate immune responses that lead to enhanced antigen presentation and adaptive immune responses[202]. GLA-LSQ is such a liposomal adjuvant with QS21 and a TLR4 agonist[89]. While the TLR4 agonist functions as intrinsic adjuvant, the saponin QS21 is known to show immunostimulatory traits such as stimulation of antibody-based humoral immune responses (Th2) as well as cellular immunity (Th1), and it leads to the production of antigen-specific CTLs[203,204]. GLA-LSQ was recently used for the formulation of a vaccine candidate, which aims at prevention of pregnancy-associated Malaria. The vaccine formulated with GLA-LSQ had a good safety profile, was well tolerated and induced functionally active antibodies[90]. These findings and previously published data show that our protein can be delivered together with the adjuvant and should also be suitable for further studies, if needed.

6.1.5. Conclusion

It is known that the passive immunization with bNAbs protects vaccinated individuals from infection with HIV[205]. Therefore, following the approach of reverse vaccinology[206], the use of an antigen engineered to exhibit increased affinity for bNAbs might lead to the induction of such antibodies, which offers the possibility to use these antigens as immunogens.
The increased structural stability of L111A, displayed in the higher trimeric content as well as the improved conformation of the protein shown for membrane-bound as well as soluble protein might lead to an increased presentation of bNAb epitopes, which then might induce bNAbs (Figure 31). Next to this, the addition of a further amino acid exchange leading to increased binding of CD4bs-directed bNAbs, like VRC01, should further improve the immunogen and therefore, soluble trimeric gp140 protein harboring L111A in combination with the second amino acid exchange T278H which leads to an increased binding of CD4bs Ab VRC01 are promising candidates for testing in a pre-clinical animal model and their evaluation as native-like SOSIP variants will give further information about the responses to protein of different conformations. Additionally, the cross-linked proteins

which exhibit increased stability compared to the non-cross-linked proteins might further increase the responses.

In the immunization study in New Zealand White rabbits, serum responses can be analyzed regarding binding antibodies as well as neutralization breadth. Here, it is possible to test the trimeric proteins, which show a more closed conformation, as well as DNA vaccines, which will presumably lead to differences between the LT and wt immunized groups, as the groups immunized with membrane-bound LT gp145 might benefit from the intrinsically higher trimeric content compared to the wt gp145.

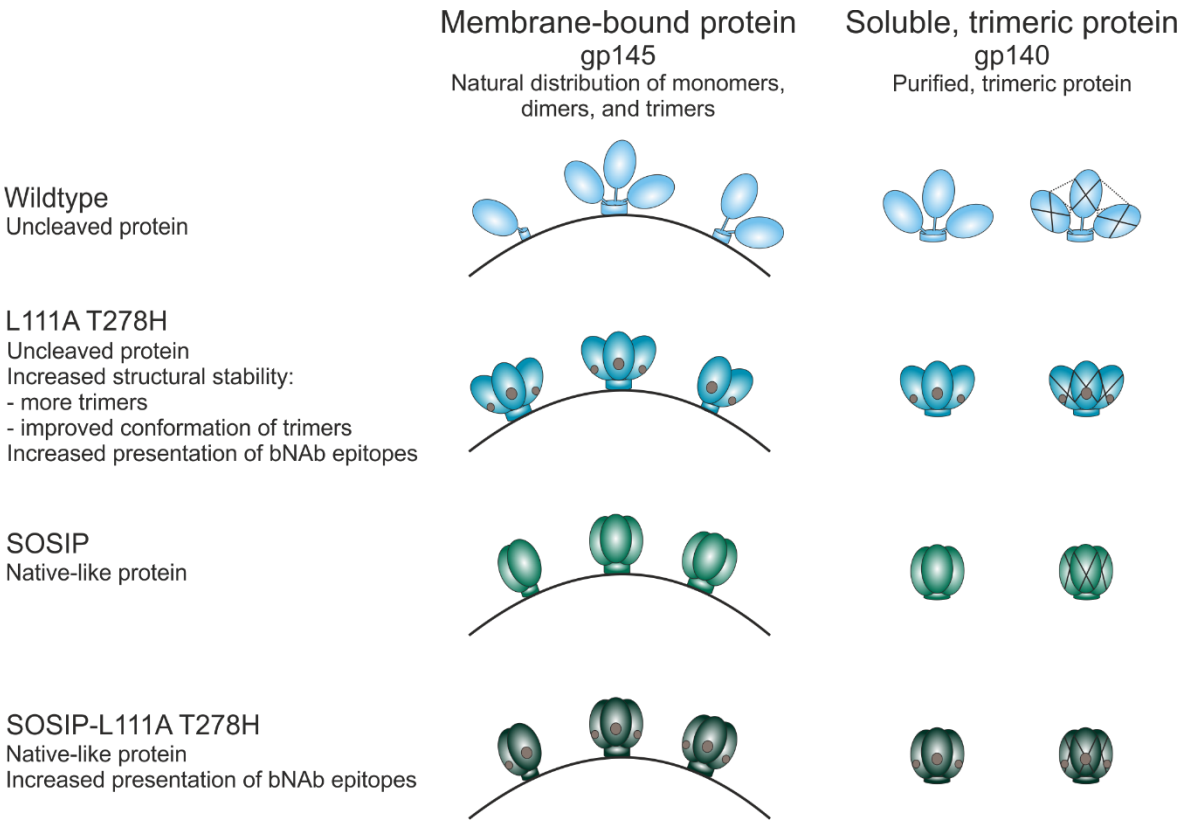

Figure 31: Schematic representation of the different Env variants used. Env-schemes represent the expected shape and composition of Env proteins as membrane-bound gp145 and purified gp140 protein. Grey dots indicate amino acid exchange T278H which leads to increased binding of CD4bs Ab VRC01. Black lines between and on the protomers indicate cross-linked protein.

6.2. Pre-clinical Animal Study

The Pantaleo.662 study is a randomized study performed in New Zealand White rabbits to determine the possible impact of affinity-matured vulnerable epitopes (VRC01, PG9) and gp140 conformational trimer stabilization (L111A) on antibody specificity and neutralization breadth. In the animal study (Figure 21) the effect of the LT variant on the elicited immune responses was analyzed in comparison to the wildtype (LT vs. wt) and in the context of native-like closed trimers (SOSIP-LT vs. SOSIP; 2.2.4). For the final boost, the autologous, chemically cross-linked protein was used, which decreases the presentation of non-neutralizing antibody epitopes usually hidden in the inner part of the Env trimer. Furthermore, in a subset of groups, a DNA-prime was used to improve the helper T cell responses, thus possibly leading to functionally superior antibody responses. As the translation into protein occurs *in vivo* in this case, the effect of increased trimer yield should lead to visible changes in the antibody profile. Furthermore, the use of variants of different quality (wt<LT<SOSIP-LT) should lead to different immune responses detectable in regards of binding antibodies, breadth, and neutralization.

6.2.1. Binding Antibody Multiplex Assay

With a BAMA it is possible to quantitatively measure binding to conformational as well as linear epitopes. This method allowed to determine the specifities of the antibodies induced by the different immunization regimens in a high through-put format, as the different antigens could be measured simultaneously.

6.2.1.1. Antibody Binding to gp140 Antigens

The gp140 immunogens used for the immunization study showed overall high response rates for all gp140 readout antigens and are therefore able to induce antibodies which can bind other gp140 proteins as well. This was not only observed for the autologous gp140 proteins, but also for the heterologous gp140 readout proteins BG505-SOSIP and Consensus M. A criterion for an ideal HIV-1 vaccine is that is has to be able to induce a broad immune response and antibodies binding to multiple clades[207] and therefore, it is

beneficial to see that the antibodies elicited by our RepliVax immunogens also bind to other clades than only clade C.

The overall highest signal intensities for all groups were observed against the uncleaved readout antigens 16055 wt and 16055 LT, followed by the native-like 16055 SOSIP and 16055 SOSIP-LT. The native-like SOSIP proteins show a more closed conformation than the uncleaved proteins, which expose epitopes that are covered in a trimer with correctly folded gp120 subunits[56,208]. The decreased antibody binding observed for the native-like readout antigens is most likely caused by their conformation, as a lot of epitopes are covered. Therefore, of all the polyclonal serum IgGs, only those that bind available epitopes are detected, while their binding is not limited against the uncleaved readout antigens. This indicates that all groups developed antibodies of varying quality, as IgG from sera from all groups were able to bind to both, uncleaved and native-like proteins. Especially the analysis of the readout antigen 16055 SOSIP-LT, which is presumably the best in class immunogen when it comes to conformation, showed that the groups immunized with the native-like SOSIP immunogens developed more quaternary-specific antibodies binding to the readout antigen, than the group immunized with the uncleaved wt protein (Figure 22). Of note, group 2 (LT-P) samples showed significantly higher binding to SOSIP-LT than group 1 samples (wt-P), which indicates that the antibodies induced by this variant were more like those induced by the native-like SOSIP variants than the uncleaved wt.

By trend, the DNA-primed groups seem to be inferior to the protein-only groups and especially the additional boost with the cross-linked native-like 16055 SOSIP-LT led to increased signals for group 5 (wt-D) in week 26 as compared to week 10 (Figure 22). This effect is caused by the additional boost with another protein, but it can either be caused by the increased conformation of the protein or by the cross-linking. A previous study performed with 97CN54 gp140 showed that the peak IgG titers were reached after two priming immunizations and that a third dose did not lead to an additional increase of the magnitude of IgG antibody titers, however, it might increase the durability of the antibody response[209]. As our study was terminated two weeks after the third protein immunization, it is not possible to make conclusions about the durability of the antibody responses after this time-point, but the peak magnitude for the protein-only groups was often similar in weeks 10 and 26, which both received at least two protein immunizations. Only the DNA-groups seemed to benefit from the second protein boost in week 26, and especially the

group immunized with the wt-DNA-prime often showed significant differences. The DNA-primed groups had received protein only once at week 10, while the protein-only groups already had received protein twice, which might explain the observation, that the difference in magnitude was rather low and barely significant between weeks 10 and 26 for the protein-only groups, which is consistent with the published findings for 97CN54 gp140.

Just like 16055, 97CN54 is a clade C isolate and so far it was often used as HIV-1 Envelope protein in an uncleaved state, even in clinical studies, and has a good safety profile[209,210,211]. However, due to the uncleaved state, the conformation only shows aberrant trimers, which even partially disintegrate into gp120 ectodomains[65,211] and especially the aberrant trimers most presumably display the fate of our uncleaved trimers.

6.2.1.2. Antibody Binding to gp120 Antigens

In order to elucidate if the antibodies induced upon immunization can react against a broader panel of readout antigens, the gp120 breadth panel was evaluated. The response rates in weeks 10 and 26 were overall high with 80-100 % of the animals responding to all gp120 antigens, which is remarkable as it indicates a potential of the RepliVax immunogens to induce cross-clade binding antibodies. The gp120 panel antigens represent multiple clades and geographic regions and were initially selected to determine breadth of antibody responses based on findings of the RV144 study, as the antigens show binding to both non- and broadly-neutralizing antibodies[173].

Group 2 (LT-P) showed significantly higher intensities than its DNA-primed counterpart in weeks 10 and 26 and it showed the highest breadth in the gp120 panel. As described before, our LT variant showed a more closed conformation than the wt and as it contains the L mutation it presumably also leads to a more homogenous composition of trimers. Although the protein used for the immunization study were purified, recombinant trimers, there is always a fraction of other conformations present in the preparations, as the purification does not allow a total separation of the isoforms. However, the LT variant showed less of these impurities than the wt and is therefore by design an improved immunogen, which is further strengthened by the findings obtained with the gp120 panel, where LT showed the best breadth in week 10 and 26.

DNA primed groups showed a higher response magnitude in week 26 than in week 10, which again is most likely caused by the second protein boost. As all DNA-primed groups were boosted with the same immunogen, differences in the response magnitudes within the DNA-primed groups are caused by the initial priming of the groups. However, as there is hardly any difference observable between the DNA-primed groups, the idea that the prime with LT-D induces different responses than the prime with wt-D is either not evident within this assay, or the boosts with one identical protein for all the groups did only boost specific types of antibodies, which lead to the insignificant differences within the groups. In order to answer this question, additional DNA-primed groups boosted with the autologous proteins would have been needed, but the limitations of the study did not allow for further groups.

The data for week 24, however, gives hints about the longevity of the antibody response. For the protein-only groups, the highest breadth and MFI* was seen for the groups immunized with the uncleaved protein, followed by those immunized with the native-like protein. The glycosylation pattern of native-like SOSIP proteins is different to uncleaved proteins, as the latter show a higher degree of processing, possibly leading to a more open and irregular conformation of the protein[212]. These differences in glycosylation might also lead to different types of antibodies and as the SOSIP immunogens showed the lowest breadth and signal, the glycosylation pattern might - among other factors - influence the durability of the antibody response.

Unfortunately, the hypothesis, that the DNA-prime leads to functionally superior antibody responses due to the T helper cell responses did not appear to be true, as the DNA-primed groups usually were inferior to the protein-only groups.

6.2.1.3. V1V2 Reactivities

It was shown that in the RV144 trial, IgG antibodies binding to V1V2 led to a decreased infection risk, as they mediated Fc-related effector functions like ADCC. Based on these findings, the potential of the immunogens and immunization regimens to induce antibodies displaying potency and breadth against scaffolded V1V2 antigens was analyzed.

At first tags-V1V2 antigens were used, which showed overall high responses in weeks 10 and 26. In week 26, the DNA primed group 5 (wt-D) was statistically superior to the protein-

only group 1 (wt-P) and to group 5 (wt-D) in week 10 (Figure 25). This indicates that the DNA-primed group leads to a superior binding to V1V2 for the tags-V1V2 antigens.

Of note, overall high binding in week 26 might be influenced by the design of the RepliVax immunogens, which are His-tagged. This might lead to the induction of anti-His-antibodies, which are able to bind to the HIS-tagged V1V2 scaffolds[127].

Due to the essential role of V1V2 in the RV144 study, a breadth panel of gp70-scaffolded V1V2s was further evaluated, but the effect observed for the tags-V1V2 could neither be reproduced for the single antigens (Figure 23, Figure 24), nor in a breadth analysis (Figure 25). However, in the breadth analysis, the protein-only groups again showed by trend higher breadth for the uncleaved variants, with group 2 (LT-P) showing the highest breadth, followed by the SOSIP-groups and the DNA-primed groups. Of note, the least breadth was observed for group 4 (SOSIP-LT-P), which was statistically inferior to all other protein-only groups. Yet, the last immunization with SOSIP-LT_CL was able to shift the breadth to a level equal to the other variants. This finding is quite interesting, as the boost with a third protein immunization led to increased breadth in this case. In contrast, an additional protein boost did not lead to better results in our previous experiments, and therefore it is likely that this effect is caused by the increased stabilization of the protein by the cross-linking. It is known that the cross-linking leads to a reduced binding of non-neutralizing antibodies, which was also confirmed by our ELISA experiments. This fact is also published for other cross-linkers and there, the cross-linking also led to increased binding to V1V2 regions[66].

In the RV144 study, the readout antigen used for analysis of the correlate of risk contained the V1V2 of a subtype B, while most infections were caused by a subtype AE HIV-strain[127], which shows that these V1V2 antibodies were cross-reactive and protective via effector functions[127,189]. This is consistent with our findings, as binding to V1V2 gp70 scaffolds of various clades was detected with the RepliVax immunogens, too.

6.2.2. Linear Epitope Mapping

Linear epitope mapping showed that vaccinated rabbits developed antibodies targeting multiple linear epitopes in Env, including C1, V2, V3, C4, C5 regions of gp120, as well as gp41 ID, and an epitope located at aa 532-546 in gp41, with dominating responses toward V3. The variable loop 3 is highly variable in its sequence but its length is rather constant

with 34-35 amino acids. Its deletion leads to the loss of viral infectivity[213]. In the RV144 study, V3-specific antibodies were elicited in ~ 90 % of the vacinees at the peak point, which were cross reactive, and like V2, they led to antibody-mediated protection[214].

The V2 loop is more variable than V3 and shows a higher variety in its length as it is not important for infectivity but for Env formation and stabilization[127,213]. The findings of the RV144 study showed that V2-binding antibodies can mediate ADCC[127]. A DNA prime-protein boost immunization scheme tested in a phase I clinical trial showed strong Fc-mediated effector functions like ADCC[215]. Fc-mediated functions are not as dependent on the well-folded and functional trimer as bNAbs[216], therefore all our groups could elicit antibodies leading to these effects, especially those receiving the DNA-prime/protein-boost. In the RV144 study, of all the vacinees developing $CD4^+$ T cell responses against Env, 60 % recognized V2 peptides and further analyses showed that these T cells were polyfunctional effector memory T cells[214]. These findings indicate the importance of a strong T helper cell response leading to an improved interaction and induction of B cells.

Furthermore, it is known that proteins produced *in vivo* are leading to T cell responses after presentation via MHC, which lead to antigen-specific T cells[217]. This T cell help can lead to increased or more specific antibody responses[217]. Following this, the DNA-prime used for our study might indeed have led to an increased T cell response inducing improved antibodies as binding to V2 was mainly seen for the DNA-primed groups, which would need to be further evaluated upon their ability to perform Fc-mediated protection.

Next to this, it would be interesting to map not only the binding to linear epitopes but to evaluate the binding to e.g. N-linked glycans, which might lead to improved results for the native-like SOSIP constructs[218].

6.2.3. Neutralization Assay

In order to complete the *in vivo* results of the RepliVax immunogens and immunization schemes, the Montefiori laboratory performed a TZM-bl assay to determine neutralization activity of sera obtained in the Pantaleo.662 Env rabbit study.

For a first analysis, the neutralization assay with the tier 1A pseudovirus MW965.26 showed overall strong neutralization responses in week 26, but in week 10, there are differences observable between the protein-only and the DNA-primed groups, with the latter showing

a lower response magnitude (Figure 30A). Due to their more open conformation, tier 1A viruses are more sensitive to neutralization and therefore many previously tested and published immunogens were able to elicit antibodies capable of neutralizing such strains[219]. So, the neutralization of tier 2 viruses is of higher interest. However, in our second assay, neutralization against the autologous tier 2 isolate was mainly observed for the SOSIP-proteins in the protein-only group (Figure 30B), and here only for the autologous tier 2, while the other three tier 2 viruses tested were only neutralized in a single case and at a low serum dilution (Supplemental Table 10).

Presumably, the native-like and more closed SOSIP trimers induce less antibodies directed against the open conformation of the pseudoviruses. Hence, the neutralization of the tier 1A virus was by trend reduced in weeks 10 and week 26, while the moderate tier 2 neutralization was primarily observed for these native-like proteins. Therefore, the uncleaved and native-like proteins seem to induce different subsets of antibodies, while no difference of the LT-trimers was detectable. However, this cannot be transferred to the DNA-primed groups that show the least neutralization against tier 1A and do not show neutralization against tier 2, which speaks against this immunization scheme. Of note, it is known that Env stability correlates with autologous neutralization activity, as shown for cross-linked trimeric protein compared to non-cross-linked protein[119] which leads to the assumption that the boost with the cross-linked protein in week 24 might be the reason for the higher response rate and magnitude in week 26. The neutralization assay also showed that the antibody responses induced by the protein-only groups are more durable than in the DNA-primed groups, with the uncleaved protein inducing by trend antibodies with greater longevity.

6.2.4. Conclusion

In summary, all the tested immunogens and immunization schemes can induce potent responses against gp140, gp120, and V1V2. The protein-only immunization showed high responses in the groups immunized with the uncleaved protein, and especially the LT trimers elicited antibodies showing a high breadth which might be caused by their improved trimeric structure and more homogenous composition. Although it was expected that the native-like SOSIP variants show additive or synergistic effects, this was not

detected for the protein-only groups, as the uncleaved variants were often superior. However, this might be characteristic of the readout antigens, as most of them do not show a native-like conformation. It was observed that the immunogens elicit antibodies of a different quality in regards of their ability to bind to native-like trimers, and the antibodies increased for groups immunized with the SOSIP variants. Consistent with these findings, the neutralization to the tier 2 virus 16055 was mainly observed for the protein only groups, especially for the SOSIP variants. This is presumably a consequence of the improved quality of the elicited antibodies able to bind to native-like protein. Next to this, the positive effect of the cross-linking is indicated. However, to make a firm conclusion, a group immunized with non-cross-linked protein would be necessary to assess whether the effect is caused by the additional protein boost or by the cross-linking itself.

DNA-immunization can stimulate the innate and adaptive immunity and is furthermore leading to improved antibodies as it also leads to helper T cell responses. Next to this, the *in vivo* production of the proteins leads to a native structure and enables post-translational modifications, which is beneficial for the immunogen. An impact of the LT trimers in a vectored delivery was not detected, as all DNA-primed groups generally induced similar antibody responses. Maybe the boosting with the autologous cross-linked protein would have been beneficial, but as it was expected that these immunogens are too weak to boost the initial responses, it was decided to employ the best in class antigen, which might have led to a bias in the boosting of individual responses. Even though the DNA-priming did not lead to generally superior effects compared to the protein-only groups, it was able to induce antibodies against gp140 and gp120, and it led to antibodies binding to regions which are associated with antibodies that are involved in Fc- mediated responses relevant for a decreased infection risk.

Overall, the favorable impact of specific affinity-matured vulnerable bNAb epitopes and conformational trimer stabilization on antibody specifity and neutralization breadth was shown. Therefore, it is possible to direct the immune response into a desired direction with specific antigens by employing a rational design approach.

7. Perspective

Due to its remarkable effect on the trimer formation, L111A must be further analyzed to evaluate its effect on gp140 trimers in more detail. For this, negative stain electron microscopy (NS-EM) comparing the wt and L111A should be performed.

Next to this, it would be interesting to evaluate the effect of the adjuvant on 16055 wt and 16055 LT, as the formulation study showed less disintegration of LT compared to the wt. For this, NS-EM of the proteins incubated with and without adjuvant should be performed to further determine the effect of the adjuvant on the proteins and the positive effect of LT, as this variant was least affected by the adjuvant.

The BAMA, linear epitope mapping, and neutralization assay showed interesting results and helped to classify the RepliVax immunogens. However, in the history of HIV clinical trials, especially the effector functions showed to be relevant. Therefore, it would be interesting to perform an ADCC assay to determine the potential of the immunogens to elicit function Fc responses. Next to this, a subclass profiling of the IgG responses would be interesting, as especially the IgG3 against V1V2 was shown to correlate with a reduced infection rate[220].

The linear epitope mapping gave first hints about the epitopes targeted by the antibodies induced by the different immunizations, but the system shows limitations, as structural epitopes are not targeted and the role of glycans was not evaluated, which would be especially interesting for the native-like SOSIP immunogens. Therefore, a mapping for discontinuous or conformational epitopes would be helpful, as it can address epitopes within loops, beta sheets or helical structures[221]. Furthermore, also a glycan mapping can be performed[222].

In the course of the study, also peripheral blood mononuclear cells were isolated and therefore a B-cell sorting could be performed[223]. With this, monoclonal antibodies could be cloned and further analyzed, also in regards of the difference between the antibodies induced by the different immunogens.

As LT leads to an increased breadth, it could be considered to use this variant in a sequential immunization scheme, as different versions of Env might guide B cell development[224]. As the removal of glycan N276 leads to binding of germline VRC01, the uncleaved variants

could be used for early immunizations while the closed SOSIP variants could be used to direct antibodies towards quaternary structures.

Next to this, also the delivery format can be changed to induce more potent responses, like e.g. osmotic pumps, which would allow a continuous presentation of the immunogen over a long time. However, here the effect of the adjuvant and body temperature on the proteins must be evaluated for a longer period. Finally, also a delivery via virus-like particles, which often showed to be immunologically beneficial[225], should be taken into consideration together with a protein boost.

8. Appendix

Supplemental Table 1: Primers used for cloning and sequencing

Primer	Sequence
pC-CMV-For	GTAGGCGTGTACGGTGGGAGG
THB ZM96 seq-1-fwd	ATCCCCATCCACTACTGCG
THB ZM96 seq-2-fwd	*AGCACCAACGACAGCACC*
Seq-VRC8400-For	GACAGACTAACAGACTGTTCCTTTCC
Seq-16055-For-1	GGTCAACACCACCAACGCC
pcDNA3.1seq r3191 BGHpA rev	CCCCCAGAATAGAATGACACC
RevZM96gp140TagQL	ATATTCGTCTCCTCGAGCTATCAGTGGTGATGGTGGTGGTGCTTGTC GTCGTCGTCCTTGTAGTCGCTGCCGCCTCCGCCGCTCTTGATGTACC ACAGCCACTTGG
QL-zm96-gp145-HA-rev	ATATTCGTCTCCTCGAGCTAGGCGTAGTCGGGCACATCGTAGGGGTA GTAGCCCTGCCGCAC
zm96 for QL	ATAATACGTCTCGCTAGCATGGGAGTGCGGGAGATCC
pWPXLD seq for 2	ATCTCGACGGTATCGGTTAAC
BG505 SOSIP Seq1	GGACAAGAAGTTCAACGG
pQL13_seq_for	CTGAGCACCCAGTCCGCCCTGAGC
pWPXLd rev seq	GGGAATTCGTCTCCTCGAGCCTGC
Furin-seq-for2	CTGCGGTGGCCAACAACG
16055-Env-Sal-fwd	CGTCGTCGAC GCCACCATGAGAGTGCGGGGCATC
16055-Env-Not-rev	GTCTAGAGCGGCCGCCTATTAGCTGTATCCCTGCCGC

Supplemental Table 2: Vectors used for cloning

Name	Bacterial resistance	Description
pWPXLd	Amp^R	Lentiviral vector (Addgene, Cat. No. 12258)
pcDNA3.1(+)QL	Amp^R	Derivative of pcDNA3.1(+) (Invitrogen/Thermo Fisher Scientific, Cat. No. V790-20), contains a *ccdB* cloning cassette
pQL13	Amp^R	Lentiviral vector including a CcdB cloning cassette and eGFP
VRC8400	Kan^R	Mammalian expression vector

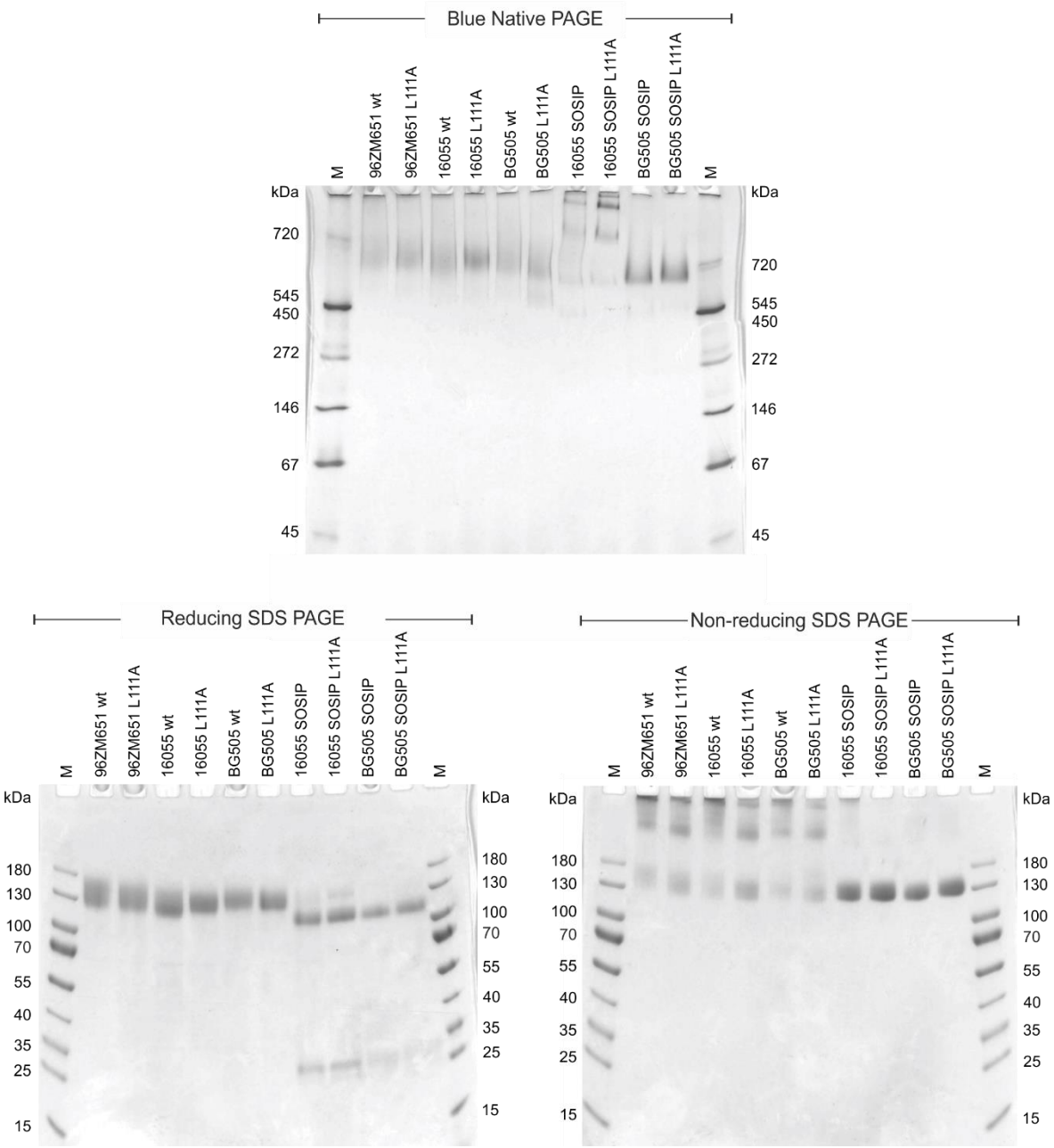

Supplemental Figure 1: Purified trimeric wt and L111A gp140 proteins of different isolates analyzed by Blue Native (4 – 16 %) and SDS PAGE (8 – 16 %). All gels were loaded with 2.5 µg trimeric protein per lane and the SDS-PAGEs were performed under reducing and non-reducing conditions. Staining was performed with Coomassie staining solution.

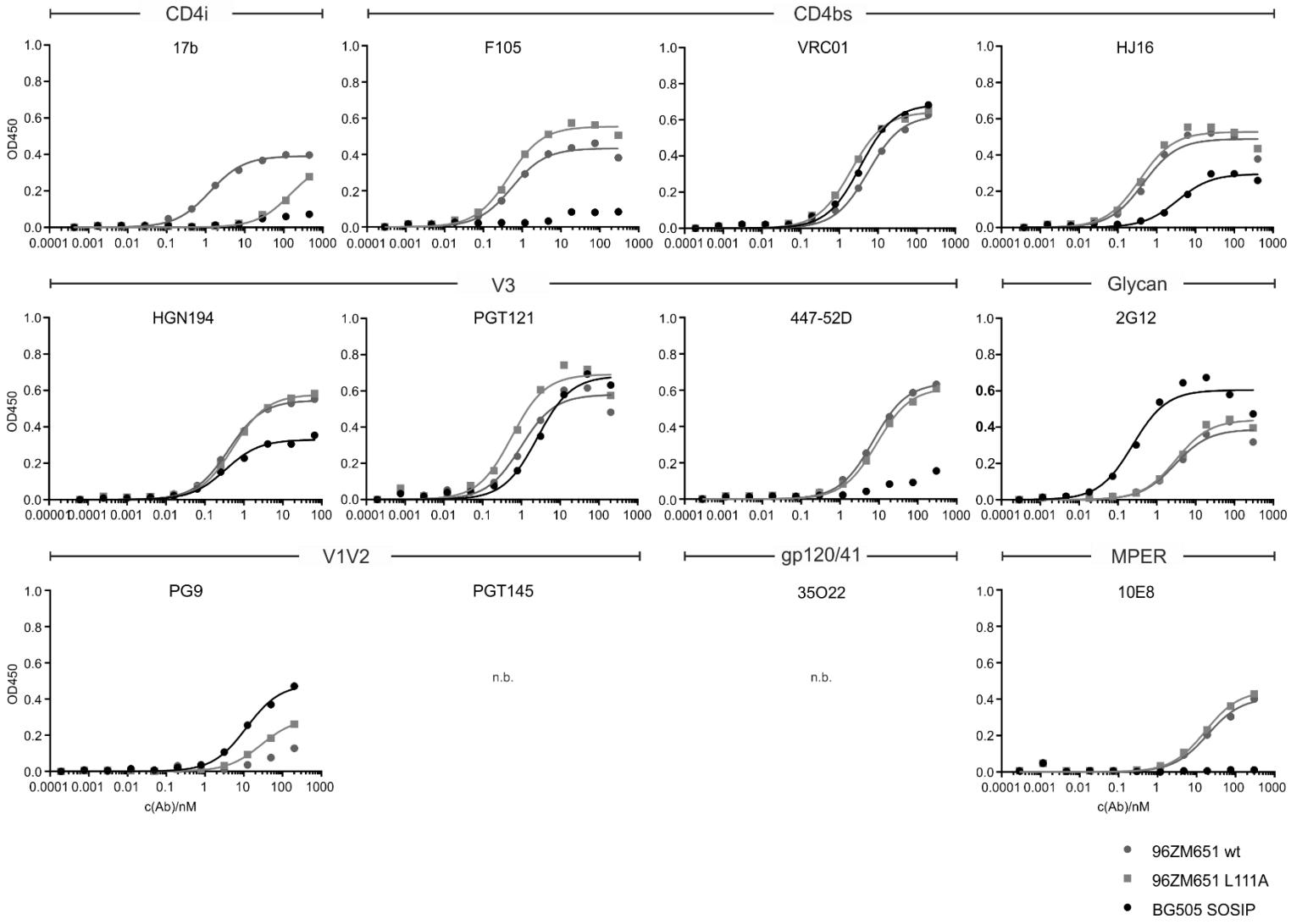

Supplemental Figure 2: ELISA titration curves of 96ZM651 gp140 wt and L111A.
Wt and L111A were purified as soluble gp140 trimers via nickel-charged immobilized metal ion affinity chromatography columns and subsequent anion exchange and size exclusion chromatography. The fractions containing trimeric protein were pooled and used in a lectin-capture ELISA, where antibodies were titrated in 4-fold dilution. BG505 SOSIP is shown as reference. Main header represents the epitopes targeted by the antibodies, which are directed against the CD4-induced conformation (CD4i; 17b), the CD4-binding site (CD4bs; F105, VRC01, HJ16), the variable loop 3 (V3; HGN194, PGT121, 447-52D), a glycan patch (2G12), the variable loops 1 and 2 (V1V2; PG9, PGT145), the gp120/41 interface (35O22), and the membrane-proximal external region (MPER). N.b.: no relevant binding.

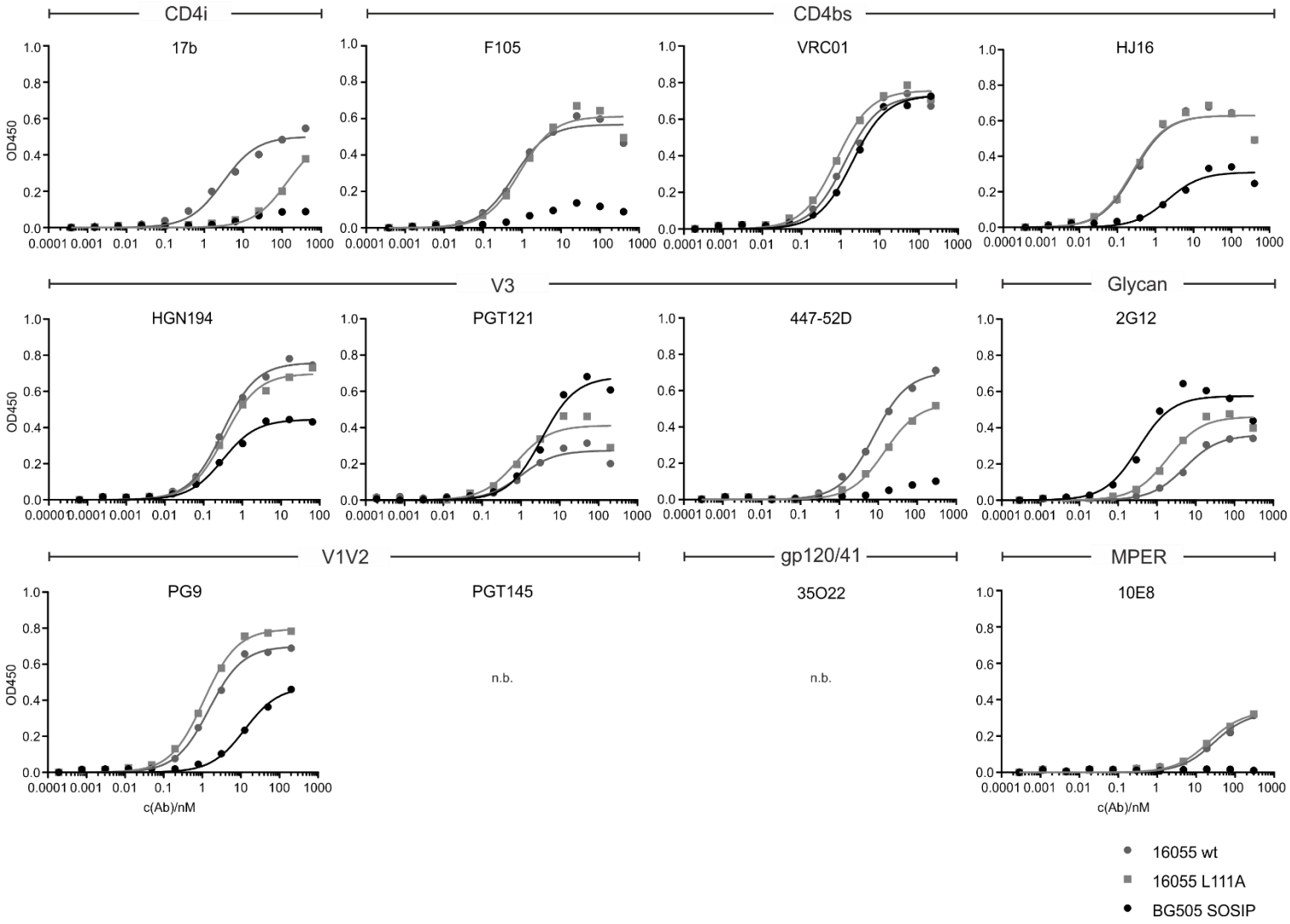

Supplemental Figure 3: ELISA titration curves of 16055 gp140 wt and L111A. Wt and L111A were purified as soluble gp140 trimers via nickel-charged immobilized metal ion affinity chromatography columns and subsequent anion exchange and size exclusion chromatography. The fractions containing trimeric protein were pooled and used in a lectin-capture ELISA, where antibodies were titrated in 4-fold dilution. BG505 SOSIP is shown as reference. Main header represents the epitopes targeted by the antibodies, which are directed against the CD4-induced conformation (CD4i; 17b), the CD4-binding site (CD4bs; F105, VRC01, HJ16), the variable loop 3 (V3; HGN194, PGT121, 447-52D), a glycan patch (2G12), the variable loops 1 and 2 (V1V2; PG9, PGT145), the gp120/41 interface (35O22), and the membrane-proximal external region (MPER). n.b.: no relevant binding.

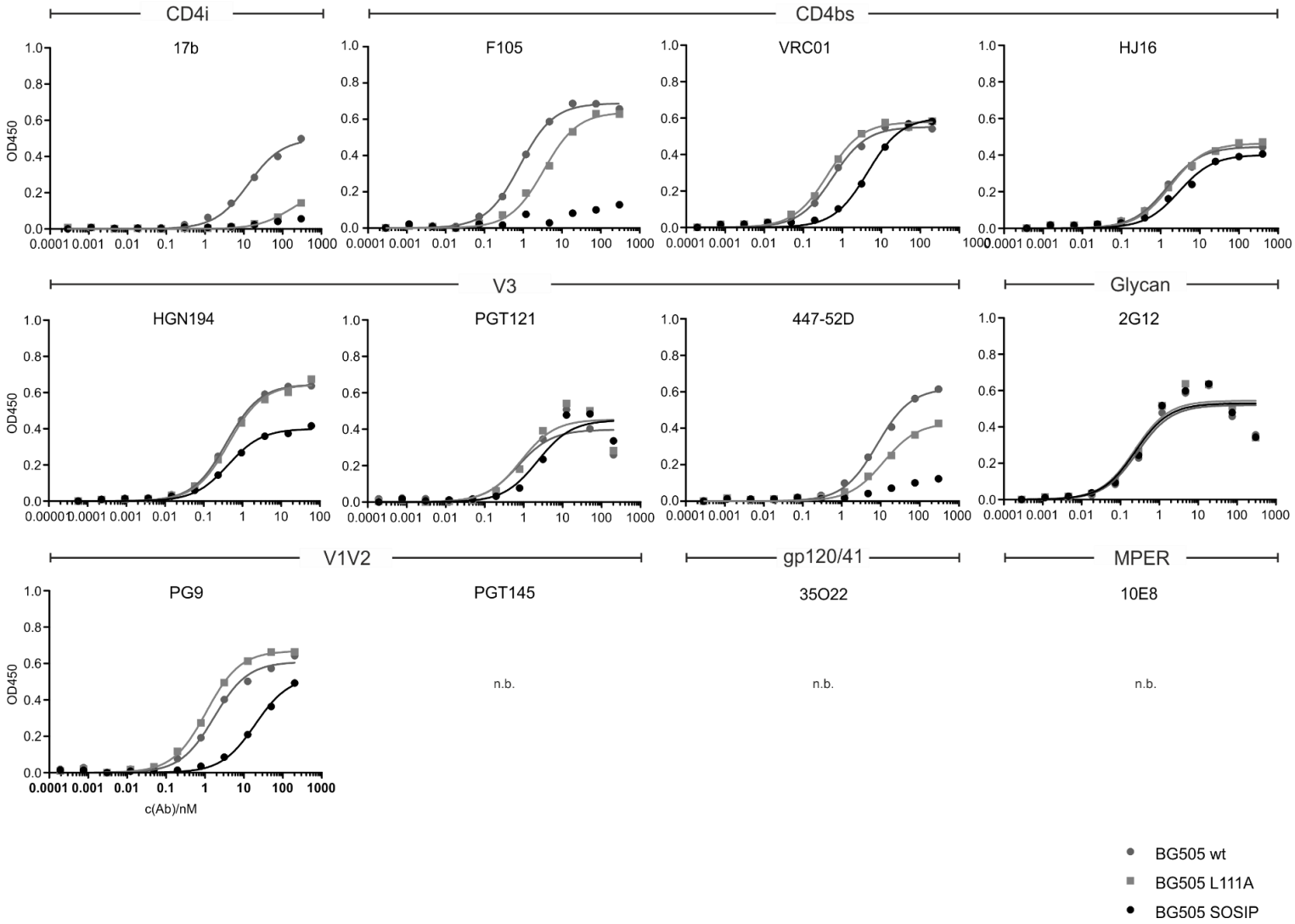

Supplemental Figure 4: ELISA titration curves of BG505 gp140 wt and L111A.
Wt and L111A were purified as soluble gp140 trimers via nickel-charged immobilized metal ion affinity chromatography columns and subsequent anion exchange and size exclusion chromatography. The fractions containing trimeric protein were pooled and used in a lectin-capture ELISA, where antibodies were titrated in 4-fold dilution. BG505 SOSIP is shown as reference. Main header represents the epitopes targeted by the antibodies, which are directed against the CD4-induced conformation (CD4i; 17b), the CD4-binding site (CD4bs; F105, VRC01, HJ16), the variable loop 3 (V3; HGN194, PGT121, 447-52D), a glycan patch (2G12), the variable loops 1 and 2 (V1V2; PG9, PGT145), the gp120/41 interface (35O22), and the membrane-proximal external region (MPER). N.b.: no relevant binding.

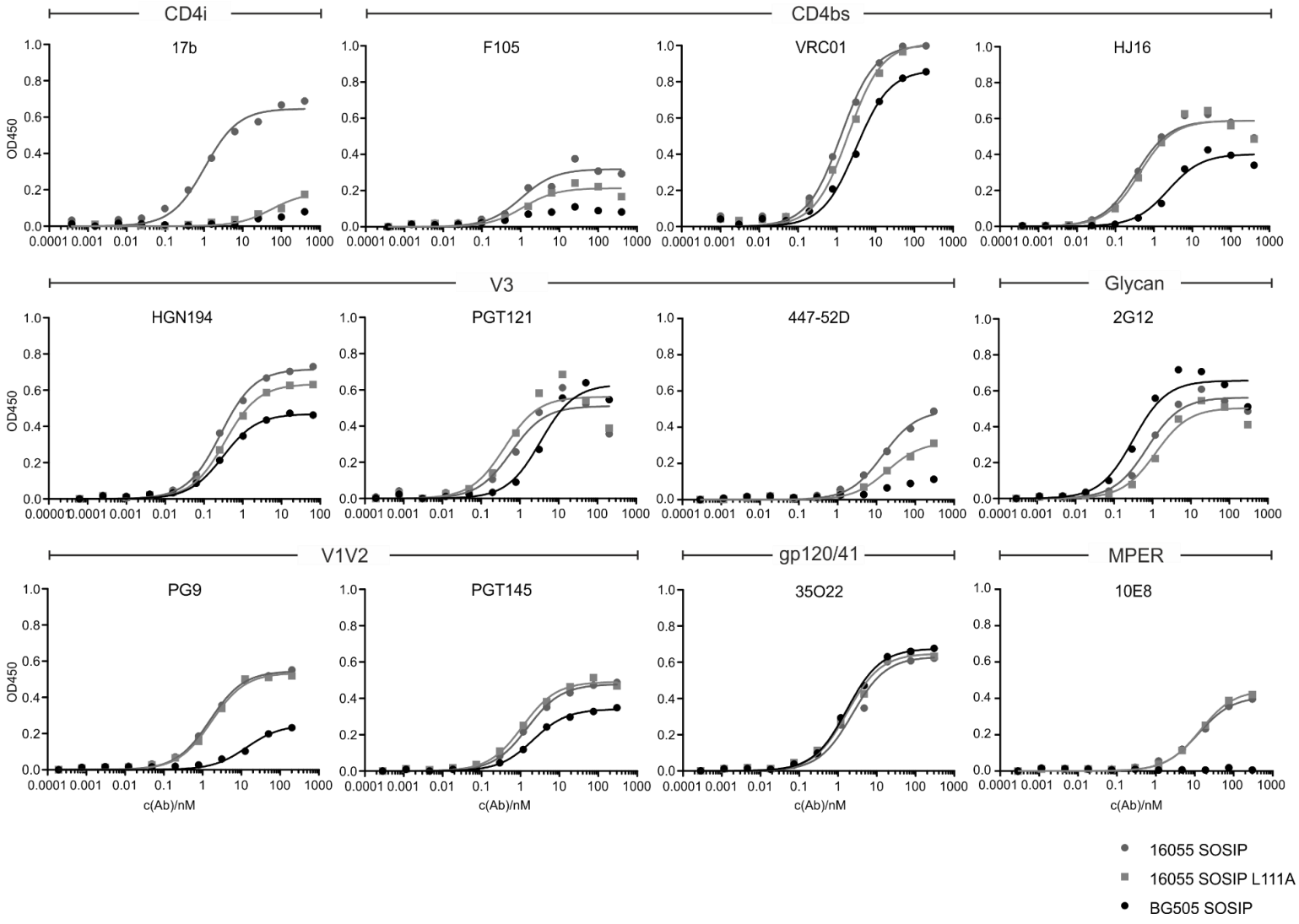

Supplemental Figure 5: ELISA titration curves of 16055 SOSIP gp140 wt and L111A. Wt and L111A were purified as soluble gp140 trimers via nickel-charged immobilized metal ion affinity chromatography columns and subsequent anion exchange and size exclusion chromatography. The fractions containing trimeric protein were pooled and used in a lectin-capture ELISA, where antibodies were titrated in 4-fold dilution. BG505 SOSIP is shown as reference. Main header represents the epitopes targeted by the antibodies, which are directed against the CD4-induced conformation (CD4i; 17b), the CD4-binding site (CD4bs; F105, VRC01, HJ16), the variable loop 3 (V3; HGN194, PGT121, 447-52D), a glycan patch (2G12), the variable loops 1 and 2 (V1V2; PG9, PGT145), the gp120/41 interface (35O22), and the membrane-proximal external region (MPER).

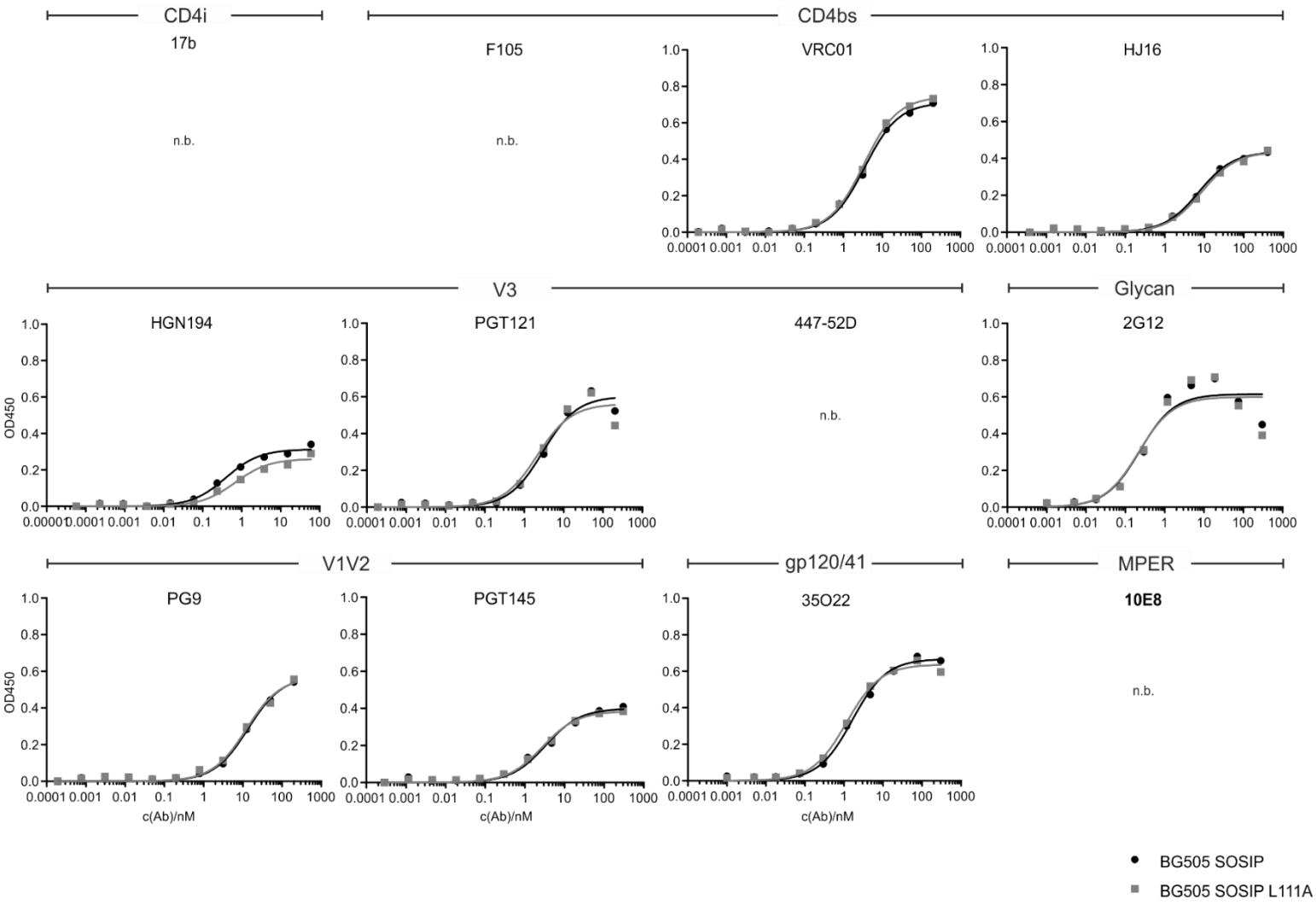

Supplemental Figure 6: ELISA titration curves of BG505 SOSIP gp140 wt and L111A. Wt and L111A were purified as soluble gp140 trimers via nickel-charged immobilized metal ion affinity chromatography columns and subsequent anion exchange and size exclusion chromatography. The fractions containing trimeric protein were pooled and used in a lectin-capture ELISA, where antibodies were titrated in 4-fold dilution. BG505 SOSIP is shown as reference. Main header represents the epitopes targeted by the antibodies, which are directed against the CD4-induced conformation (CD4i; 17b), the CD4-binding site (CD4bs; F105, VRC01, HJ16), the variable loop 3 (V3; HGN194, PGT121, 447-52D), a glycan patch (2G12), the variable loops 1 and 2 (V1V2; PG9, PGT145), the gp120/41 interface (35O22), and the membrane-proximal external region (MPER). N.b.: no relevant binding.

Supplemental Table 3: Heatmap of the Dissociation constant (K_D) of the ELISA data for wt and L111A.
Mean was taken from triplicates. SEM: Standard error of the mean.

	CD4i		CD4bs					
	17b		**F105**		**VRC01**		**HJ16**	
	Mean	SEM	Mean	SEM	Mean	SEM	Mean	SEM
96ZM651 wt	1.39	0.06	0.52	0.07	7.52	1.06	0.35	0.06
96ZM651 L111A	150.30	13.63	0.44	0.06	3.04	0.53	0.31	0.04
16055 wt	2.21	0.42	0.69	0.08	1.13	0.08	0.30	0.01
16055 L111A	105.21	14.92	0.89	0.07	0.70	0.04	0.26	0.02
BG505 wt	13.34	1.43	1.16	0.21	0.61	0.09	1.51	0.29
BG505 L111A	158.80	4.10	4.51	0.62	0.43	0.04	1.96	0.39
16055 SOSIP	0.97	0.13	2.47	0.10	1.32	0.18	0.41	0.05
16055 SOSIP L111A	58.29	7.45	10.12	1.70	1.73	0.20	0.48	0.04
BG505 SOSIP	n.b.		n.b.		3.22	0.49	6.15	1.06
BG505 SOSIP L111A	n.b.		n.b.		3.12	0.12	8.05	1.13

	V3						Glycan	
	HGN194		**PGT121**		**447-52D**		**2G12**	
	Mean	SEM	Mean	SEM	Mean	SEM	Mean	SEM
96ZM651 wt	0.52	0.08	1.08	0.15	8.78	0.99	2.88	0.37
96ZM651 L111A	0.69	0.08	0.65	0.06	10.49	0.98	3.09	0.41
16055 wt	0.33	0.05	1.21	0.14	7.22	0.25	5.78	0.34
16055 L111A	0.36	0.05	0.78	0.07	14.23	0.53	1.77	0.15
BG505 wt	0.46	0.04	0.89	0.12	9.40	0.70	0.27	0.03
BG505 L111A	0.51	0.03	1.02	0.11	13.94	1.13	0.23	0.03
16055 SOSIP	0.26	0.02	0.71	0.12	13.79	0.41	0.79	0.04
16055 SOSIP L111A	0.31	0.02	0.46	0.03	16.81	1.68	1.22	0.03
BG505 SOSIP	0.36	0.01	2.21	0.40	n.b.		0.29	0.03
BG505 SOSIP L111A	0.58	0.05	1.82	0.16	n.b.		0.29	0.04

	V1V2				gp120/41		MPER	
	PG9		**PGT145**		**35O22**		**10E8**	
	Mean	SEM	Mean	SEM	Mean	SEM	Mean	SEM
96ZM651 wt	n.b.		n.b.		n.b.		19.74	3.16
96ZM651 L111A	31.08	1.76	n.b.		n.b.		18.13	0.91
16055 wt	1.59	0.15	n.b.		n.b.		38.65	5.88
16055 L111A	1.09	0.07	n.b.		n.b.		26.57	3.14
BG505 wt	1.71	0.10	n.b.		n.b.		n.b.	
BG505 L111A	1.08	0.06	n.b.		n.b.		n.b.	
16055 SOSIP	1.49	0.10	2.06	0.48	2.89	0.44	10.76	0.76
16055 SOSIP L111A	1.65	0.10	1.39	0.13	1.98	0.19	11.03	1.46
BG505 SOSIP	15.71	2.07	3.63	0.37	1.76	0.34	n.b.	
BG505 SOSIP L111A	15.84	1.86	2.98	0.36	1.52	0.21	n.b.	

0.01 5 150nM

Supplemental Table 4: Biophysical properties of purified 96ZM651 wt and L111A trimers as measured by differential scanning calorimetry.

	96ZM651 wt	**96ZM651 L111A**
M	$4.32*10^{-6}$	$4.38*10^{-6}$
Tm (°C)	60.4	60.8
T_{onset} (°C)	48.3	47.3
$Tm_{1/2}$ (°C)	10.2	7.98
Total area (kcal/mol)	117	148
ΔH_{cal} (Kcal/mol)	121	150
ΔH_{VH} (Kcal/mol)	86.1	107
Reduced Chi-Sqr. $(kcal/mol/°C)^2$	0.153	1.06

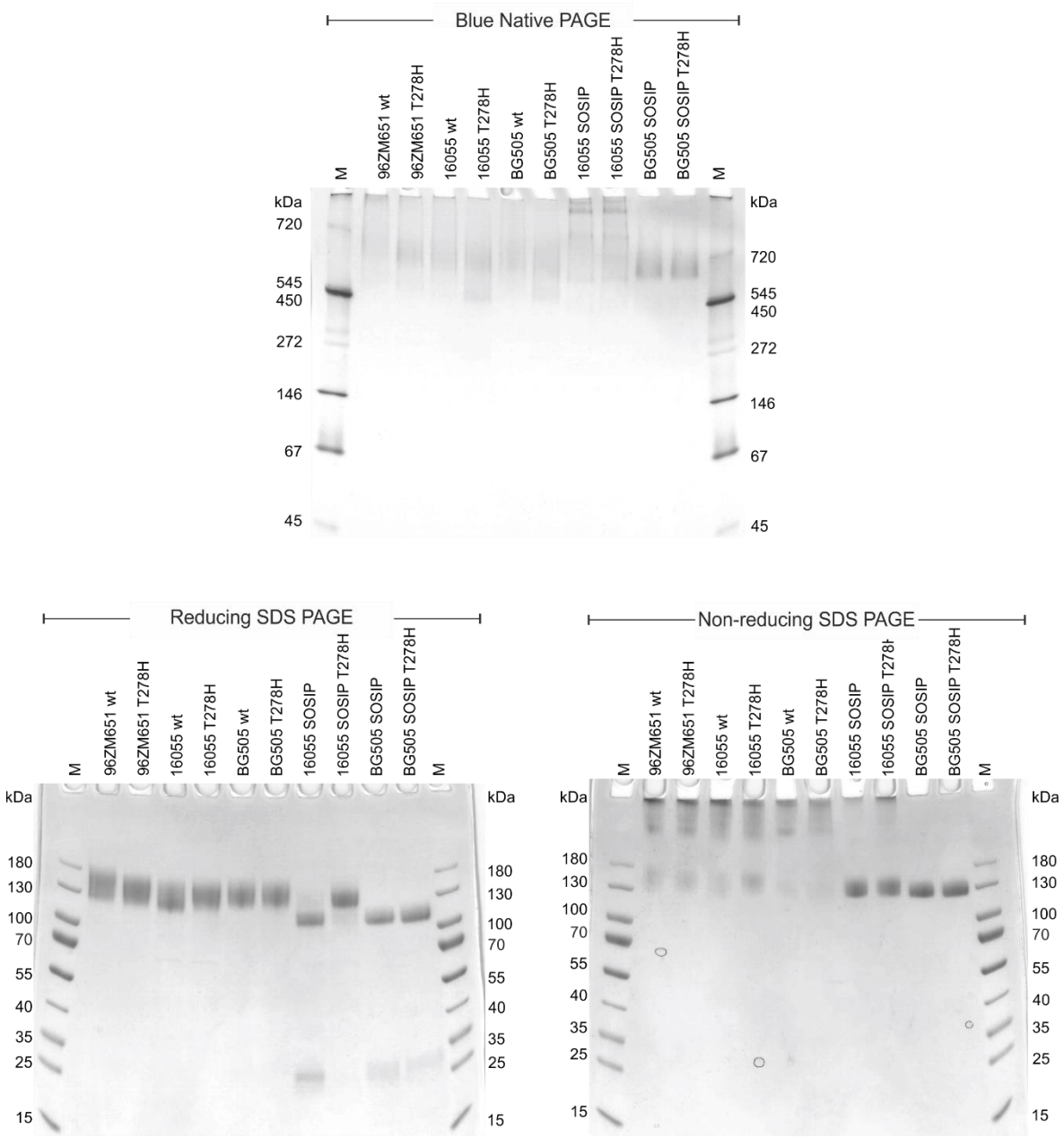

Supplemental Figure 7: Trimeric wt and T278H gp140 proteins of different isolates analyzed by Blue Native (4 – 16 %) and SDS PAGE (8 – 16 %). All gels were loaded with 2.5 µg trimeric protein and the SDS PAGEs were performed under reducing and non-reducing conditions. Staining was performed with Coomassie staining solution.

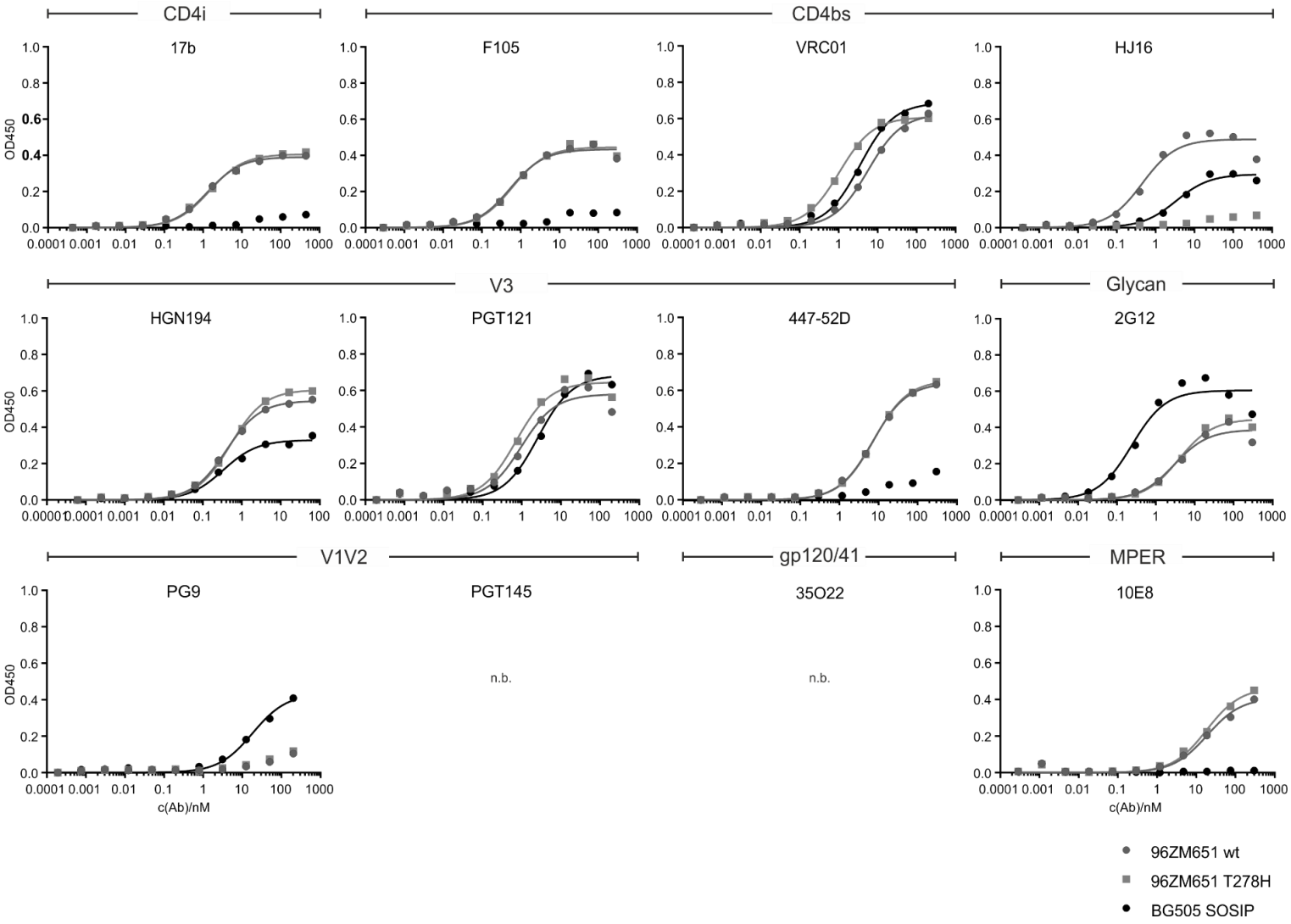

Supplemental Figure 8: ELISA titration curves of 96ZM651 gp140 wt and T278H.
Wt and T278H were purified as soluble gp140 trimers via nickel-charged immobilized metal ion affinity chromatography columns and subsequent anion exchange and size exclusion chromatography. The fractions containing trimeric protein were pooled and used in a lectin-capture ELISA, where antibodies were titrated in 4-fold dilution. BG505 SOSIP is shown as reference. Main header represents the epitopes targeted by the antibodies, which are directed against the CD4-induced conformation (CD4i; 17b), the CD4-binding site (CD4bs; F105, VRC01, HJ16), the variable loop 3 (V3; HGN194, PGT121, 447-52D), a glycan patch (2G12), the variable loops 1 and 2 (V1V2; PG9, PGT145), the gp120/41 interface (35O22), and the membrane-proximal external region (MPER). N.b.: no relevant binding.

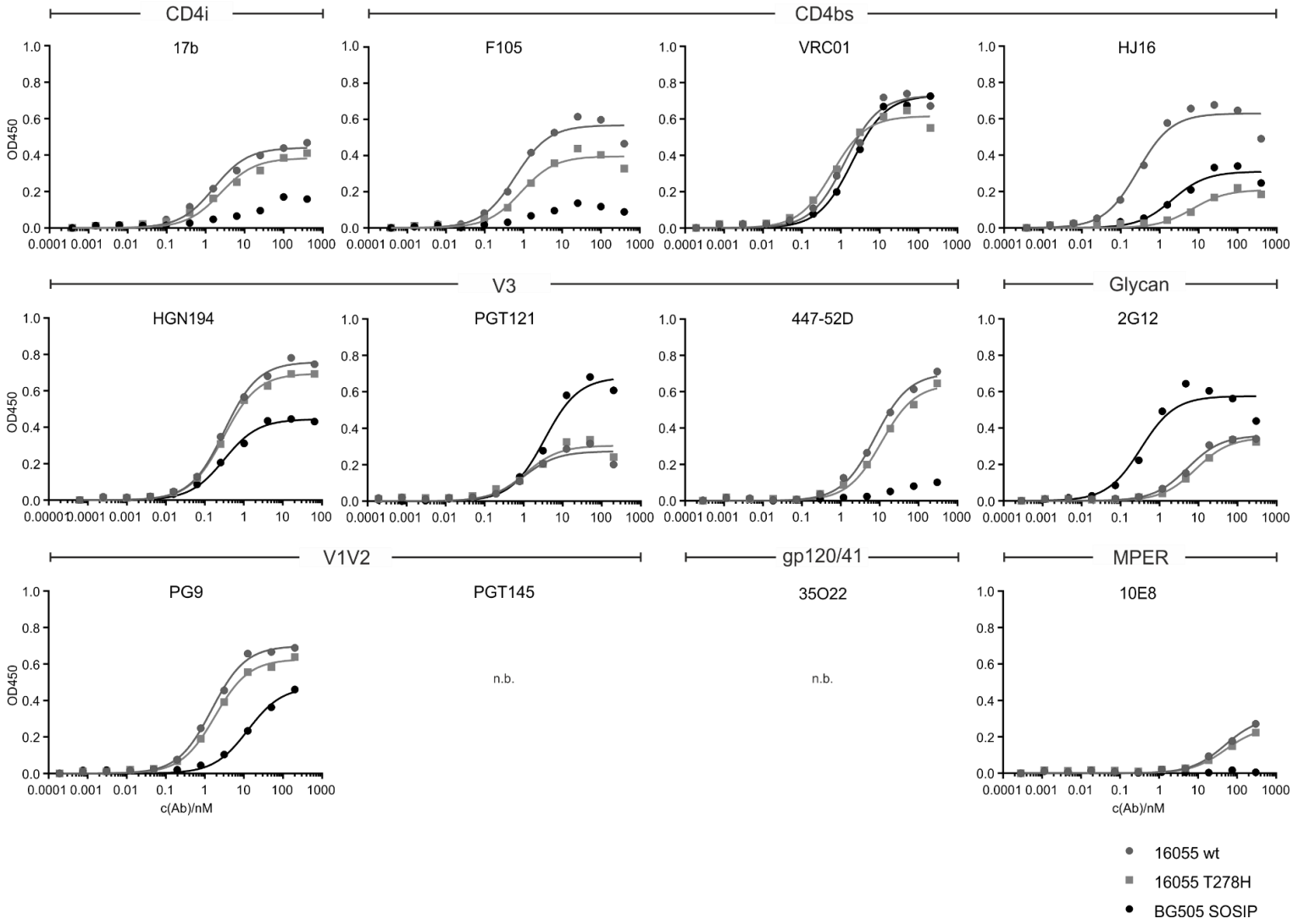

Supplemental Figure 9: ELISA titration curves of 16055 gp140 wt and T278H.
Wt and T278H were purified as soluble gp140 trimers via nickel-charged immobilized metal ion affinity chromatography columns and subsequent anion exchange and size exclusion chromatography. The fractions containing trimeric protein were pooled and used in a lectin-capture ELISA, where antibodies were titrated in 4-fold dilution. BG505 SOSIP is shown as reference. Main header represents the epitopes targeted by the antibodies, which are directed against the CD4-induced conformation (CD4i; 17b), the CD4-binding site (CD4bs; F105, VRC01, HJ16), the variable loop 3 (V3; HGN194, PGT121, 447-52D), a glycan patch (2G12), the variable loops 1 and 2 (V1V2; PG9, PGT145), the gp120/41 interface (35O22), and the membrane-proximal external region (MPER). N.b.: no relevant binding.

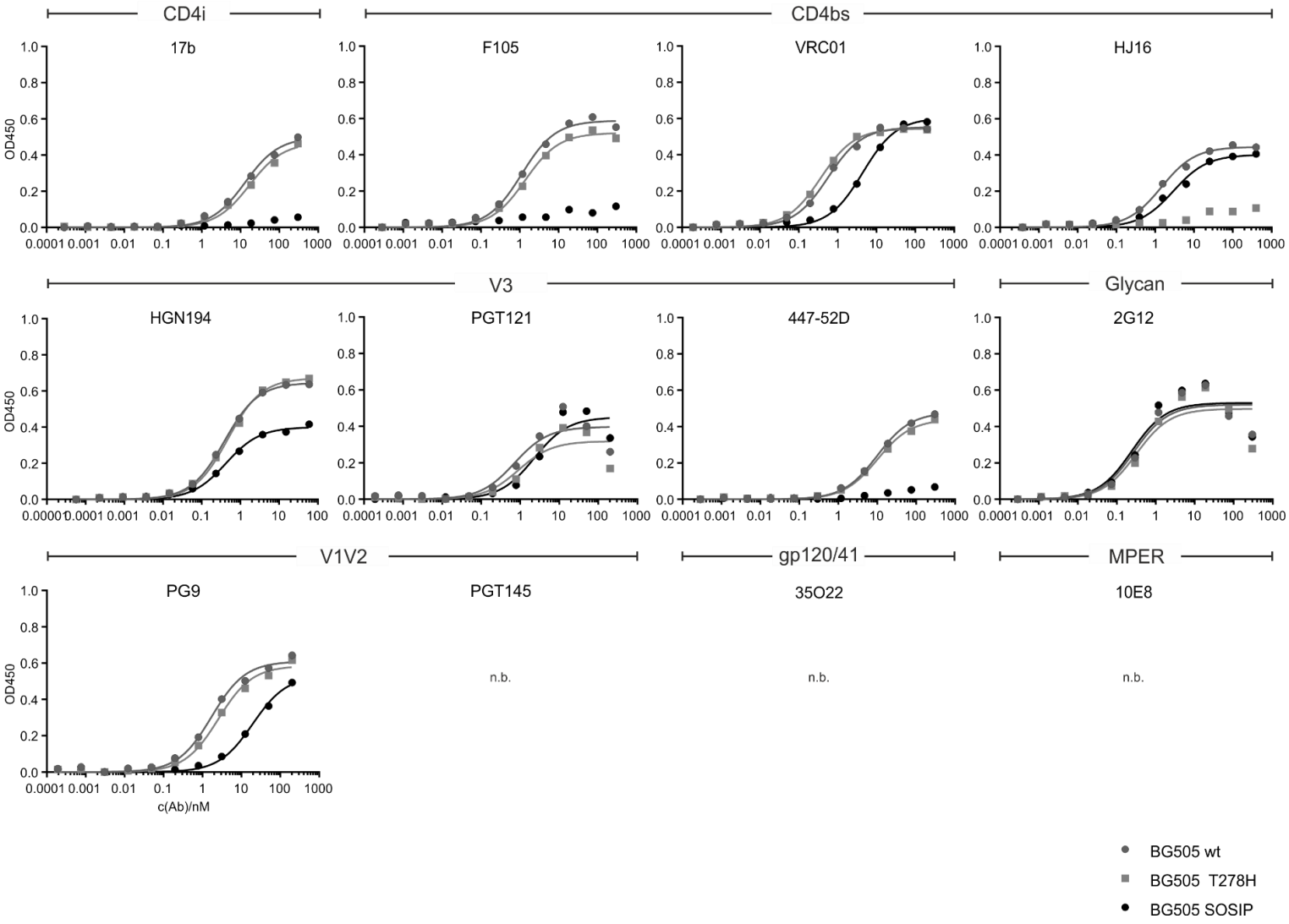

Supplemental Figure 10: ELISA titration curves of BG505 gp140 wt and T278H. Wt and T278H were purified as soluble gp140 trimers via nickel-charged immobilized metal ion affinity chromatography columns and subsequent anion exchange and size exclusion chromatography. The fractions containing trimeric protein were pooled and used in a lectin-capture ELISA, where antibodies were titrated in 4-fold dilution. BG505 SOSIP is shown as reference. Main header represents the epitopes targeted by the antibodies, which are directed against the CD4-induced conformation (CD4i; 17b), the CD4-binding site (CD4bs; F105, VRC01, HJ16), the variable loop 3 (V3; HGN194, PGT121, 447-52D), a glycan patch (2G12), the variable loops 1 and 2 (V1V2; PG9, PGT145), the gp120/41 interface (35O22), and the membrane-proximal external region (MPER). N.b.: no relevant binding.

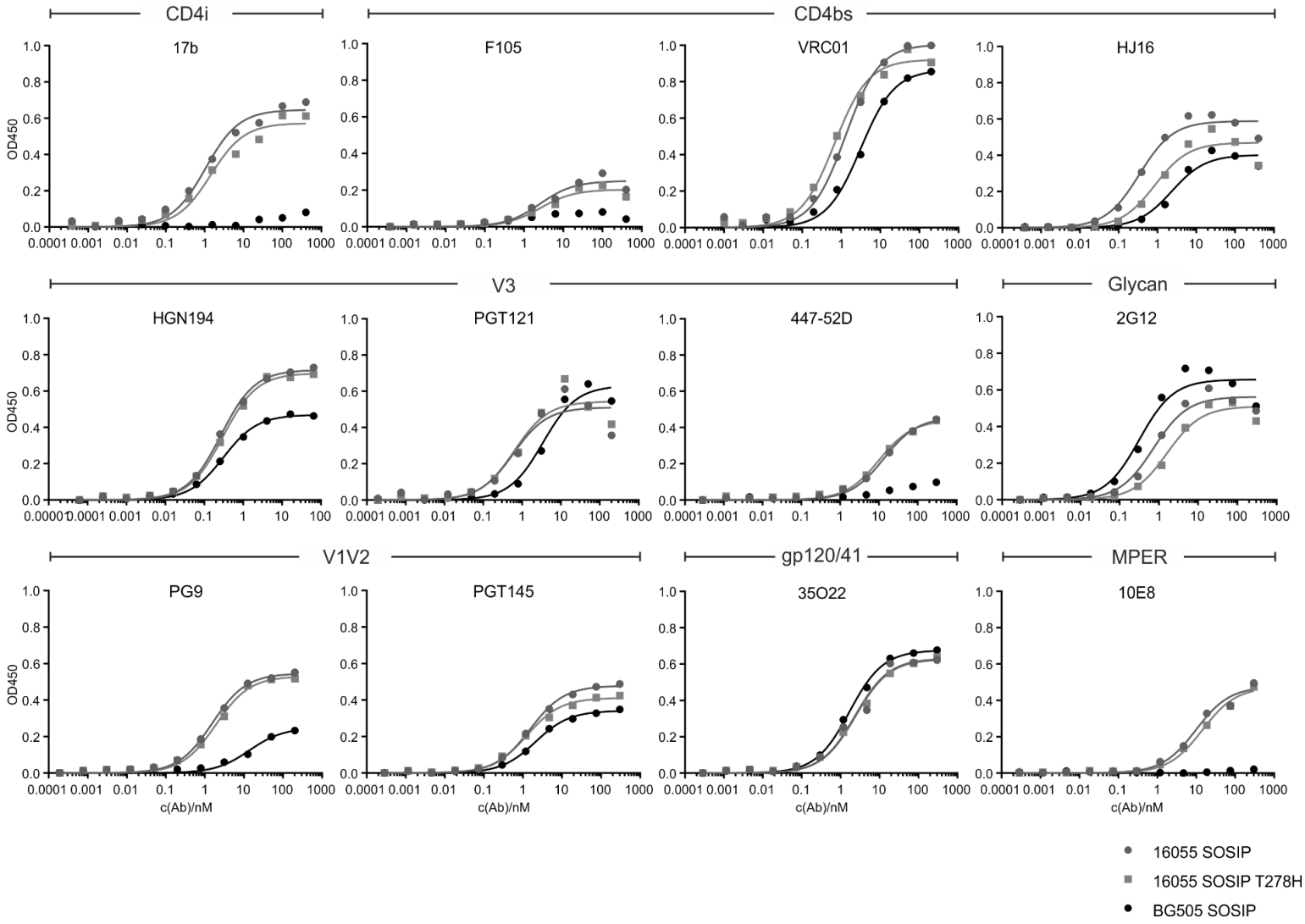

Supplemental Figure 11: ELISA titration curves of 16055 SOSIP gp140 wt and T278H.

Wt and T278H were purified as soluble gp140 trimers via nickel-charged immobilized metal ion affinity chromatography columns and subsequent anion exchange and size exclusion chromatography. The fractions containing trimeric protein were pooled and used in a lectin-capture ELISA, where antibodies were titrated in 4-fold dilution. BG505 SOSIP is shown as reference. Main header represents the epitopes targeted by the antibodies, which are directed against the CD4-induced conformation (CD4i; 17b), the CD4-binding site (CD4bs; F105, VRC01, HJ16), the variable loop 3 (V3; HGN194, PGT121, 447-52D), a glycan patch (2G12), the variable loops 1 and 2 (V1V2; PG9, PGT145), the gp120/41 interface (35O22), and the membrane-proximal external region (MPER). N.b.: no relevant binding.

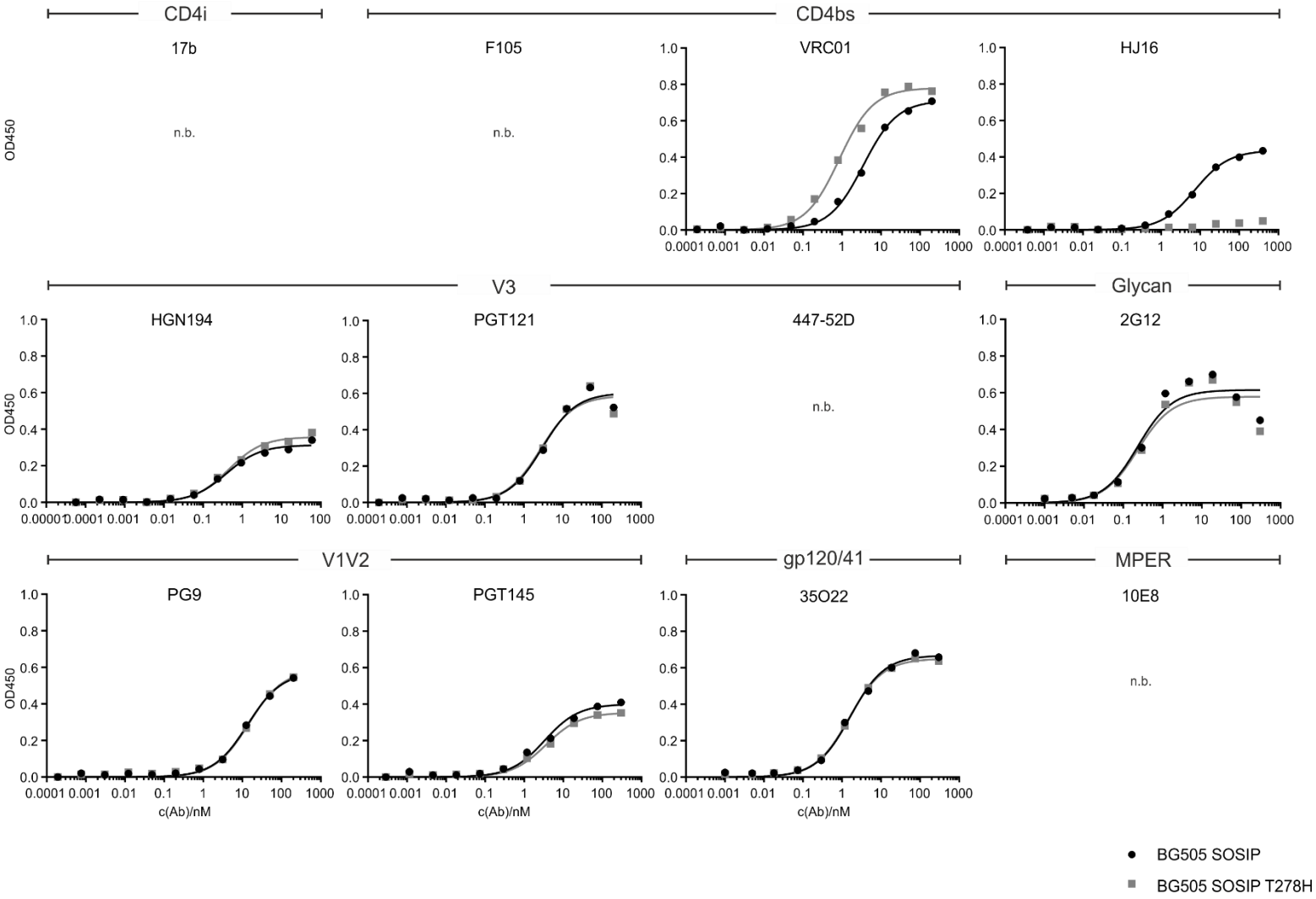

Supplemental Figure 12: ELISA titration curves of BG505 SOSIP gp140 wt and T278H.

Wt and T278H were purified as soluble gp140 trimers via nickel-charged immobilized metal ion affinity chromatography columns and subsequent anion exchange and size exclusion chromatography. The fractions containing trimeric protein were pooled and used in a lectin-capture ELISA, where antibodies were titrated in 4-fold dilution. BG505 SOSIP is shown as reference. Main header represents the epitopes targeted by the antibodies, which are directed against the CD4-induced conformation (CD4i; 17b), the CD4-binding site (CD4bs; F105, VRC01, HJ16), the variable loop 3 (V3; HGN194, PGT121, 447-52D), a glycan patch (2G12), the variable loops 1 and 2 (V1V2; PG9, PGT145), the gp120/41 interface (35O22), and the membrane-proximal external region (MPER). N.b.: no relevant binding.

Supplemental Table 5: Heatmap of the Dissociation constant (K_D) of the ELISA data for wt and T278H.
Mean was taken from triplicates. SEM: Standard error of the mean.

	CD4i		CD4bs					
	17b		**F105**		**VRC01**		**HJ16**	
	Mean	SEM	Mean	SEM	Mean	SEM	Mean	SEM
96ZM651 wt	1.39	0.06	0.52	0.07	7.52	1.06	0.35	0.06
96ZM651 T278H	1.50	0.09	0.54	0.07	1.47	0.30	n.b.	
16055 wt	2.21	0.42	0.69	0.08	1.13	0.08	0.30	0.01
16055 T278H	3.14	0.47	0.88	0.06	0.56	0.03	6.29	0.42
BG505 wt	13.34	1.43	1.16	0.21	0.61	0.09	1.51	0.29
BG505 T278H	14.86	1.19	1.59	0.32	0.37	0.03	n.b.	
16055 SOSIP	0.97	0.13	2.47	0.10	1.32	0.18	0.41	0.05
16055 SOSIP T278H	1.41	0.10	10.05	0.63	0.70	0.06	0.90	0.02
BG505 SOSIP	n.b.		n.b.		3.22	0.49	6.15	1.06
BG505 SOSIP T278H	n.b.		n.b.		0.75	0.07	n.b.	

	V3						Glycan	
	HGN194		**PGT121**		**447-52D**		**2G12**	
	Mean	SEM	Mean	SEM	Mean	SEM	Mean	SEM
96ZM651 wt	0.52	0.08	1.08	0.15	8.78	0.99	2.88	0.37
96ZM651 T278H	0.60	0.07	0.78	0.08	9.45	1.06	3.84	0.47
16055 wt	0.33	0.05	1.21	0.14	7.22	0.25	5.78	0.34
16055 T278H	0.31	0.02	0.99	0.11	10.54	0.22	8.58	0.39
BG505 wt	0.46	0.04	0.89	0.12	9.40	0.70	0.27	0.03
BG505 T278H	0.54	0.04	1.16	0.14	9.69	1.27	0.34	0.04
16055 SOSIP	0.26	0.02	0.71	0.12	13.79	0.41	0.79	0.04
16055 SOSIP T278H	0.28	0.02	0.62	0.05	13.50	1.70	1.50	0.06
BG505 SOSIP	0.36	0.01	2.21	0.40	n.b.		0.29	0.03
BG505 SOSIP T278H	0.42	0.03	2.24	0.25	n.b.		0.26	0.02

	V1V2				gp120/41		MPER	
	PG9		**PGT145**		**35O22**		**10E8**	
	Mean	SEM	Mean	SEM	Mean	SEM	Mean	SEM
96ZM651 wt	n.b.		n.b.		n.b.		19.74	3.16
96ZM651 T278H	n.b.		n.b.		n.b.		19.30	1.09
16055 wt	1.59	0.15	n.b.		n.b.		38.65	5.88
16055 T278H	1.87	0.10	n.b.		n.b.		46.97	6.36
BG505 wt	1.71	0.10	n.b.		n.b.		n.b.	
BG505 T278H	2.40	0.20	n.b.		n.b.		n.b.	
16055 SOSIP	1.49	0.10	2.06	0.48	2.89	0.44	10.76	0.76
16055 SOSIP T278H	1.99	0.18	1.28	0.02	2.54	0.10	15.20	2.79
BG505 SOSIP	15.71	2.07	3.63	0.37	1.46	0.12	n.b.	
BG505 SOSIP T278H	16.52	1.83	3.84	0.42	2.10	0.29	n.b.	

0.01 5 50nM

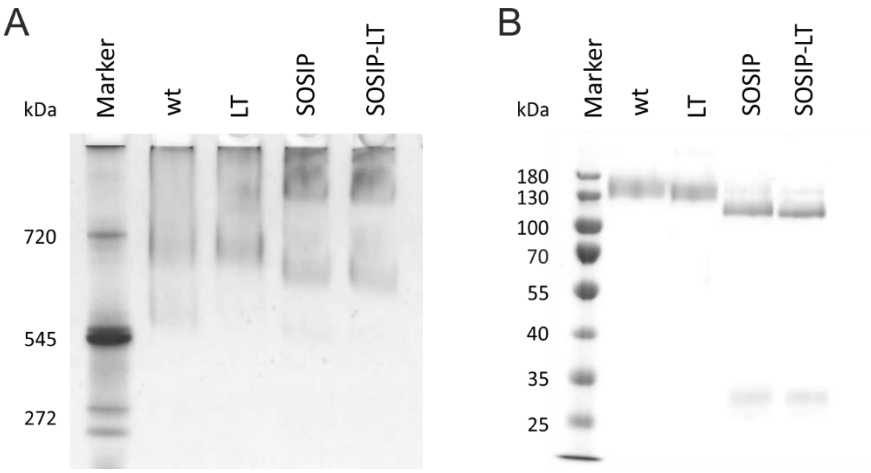

Supplemental Figure 13: Quality control of the RepliVax proteins
A) 2.5 µg protein per lane were loaded on BN-PAGE. Marker: SERVA Native Marker, Liquid Mix for BN/CN. B) 1.2 µg protein per lane were loaded on a 10 % SDS PAGE. Both gels were stained with Coomassie-Staining solution. Marker: PageRuler™ Prestained Protein Ladder.

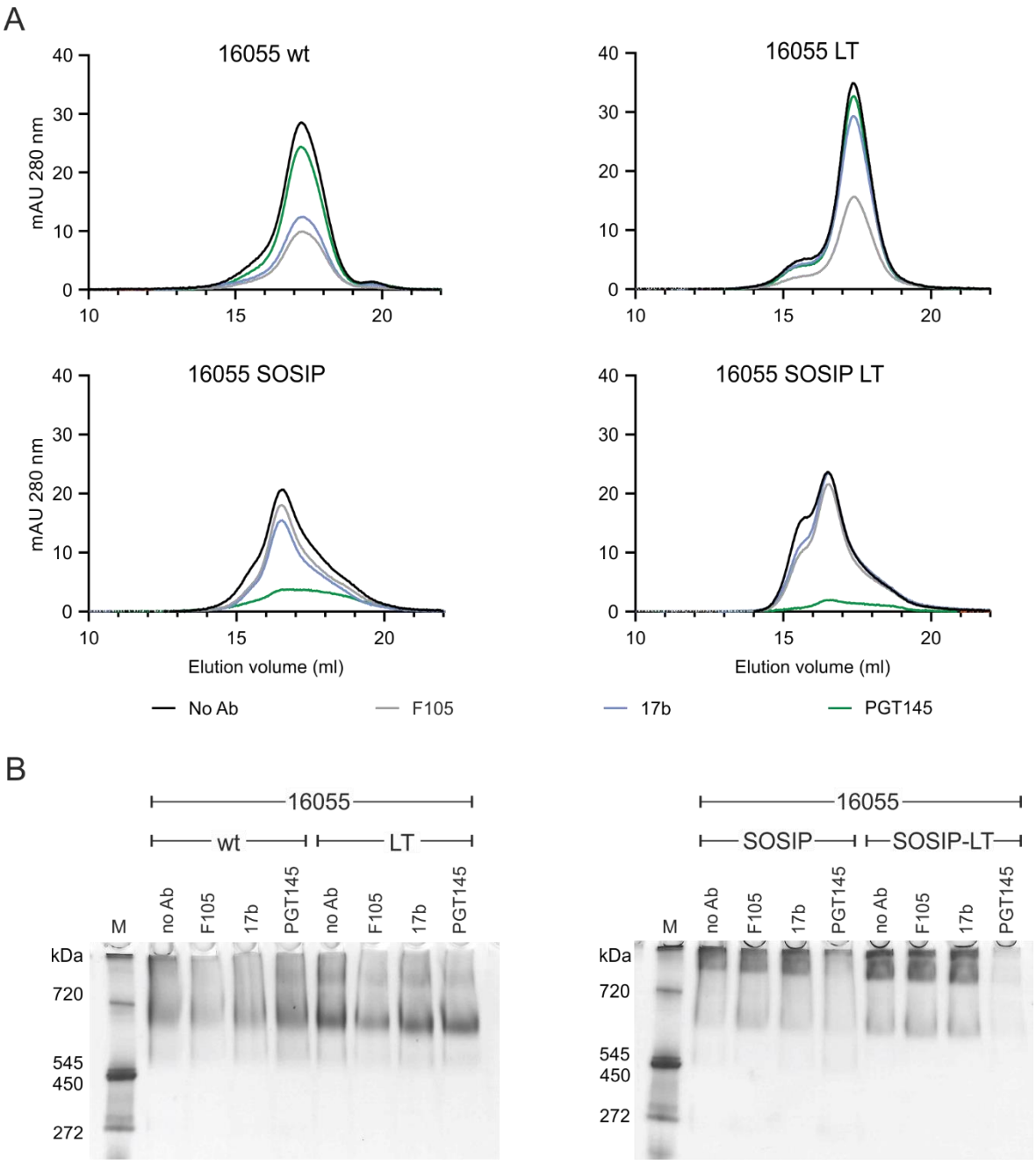

Supplemental Figure 14: Analysis of supernatants after negative (F105, 17b) and positive (PGT145) selection. A) HPLC elution profiles of supernatant after negative/positive selection with the respective antibody. B) BN-PAGE: 3.33 µg protein were loaded as reference in "no Ab" while 10 µl supernatant after negative/positive selection with the respective antibody were loaded in the other lanes. After electrophoresis, the gels were stained with Coomassie staining solution.

Supplemental Table 6: Particle Size Averages of Antigen-Adjuvant Admixtures for the RepliVax Proteins.
*Some measurement data were excluded due to instrumental error in selecting a measurement position.
PDI: polydispersity index.

Protein	Storage Temperature	Time (h)	Particle Size Average (nm)	PDI
16055 wt + GLA-LSQ		0	71 ± 1	0.264 ± 0.014
	5 °C	4	70 ± 1	0.260 ± 0.007
		24	70 ± 2	0.270 ± 0.021
	25 °C	4	70 ± 1	0.253 ± 0.006
		24	69 ± 2	0.267 ± 0.016
16055 LT + GLA-LSQ		0*	70 ± 1	0.276 ± 0.024
	5 °C	4	70 ± 1	0.258 ± 0.004
		24	70 ± 1	0.291 ± 0.024
	25 °C	4	71 ± 1	0.268 ± 0.005
		24	69 ± 1	0.272 ± 0.015
16055 SOSIP + GLA-LSQ		0	72 ± 1	0.263 ± 0.008
	5 °C	4	72 ± 1	0.270 ± 0.020
		24	71 ± 1	0.264 ± 0.010
	25 °C	4	71 ± 1	0.270 ± 0.015
		24	70 ± 1	0.257 ± 0.008
16055 SOSIP-LT + GLA-LSQ		0*	72 ± 1	0.264 ± 0.005
	5 °C	4*	71 ± 1	0.286 ± 0.023
		24	71 ± 1	0.288 ± 0.031
	25 °C	4	71 ± 1	0.303 ± 0.020
		24	71 ± 1	0.292 ± 0.027
GLA-LSQ		0	71 ± 1	0.261 ± 0.005
	5 °C	4	70 ± 2	0.309 ± 0.032
		24	70 ± 2	0.288 ± 0.028
	25 °C	4	71 ± 2	0.311 ± 0.022
		24	71 ± 1	0.328 ± 0.024

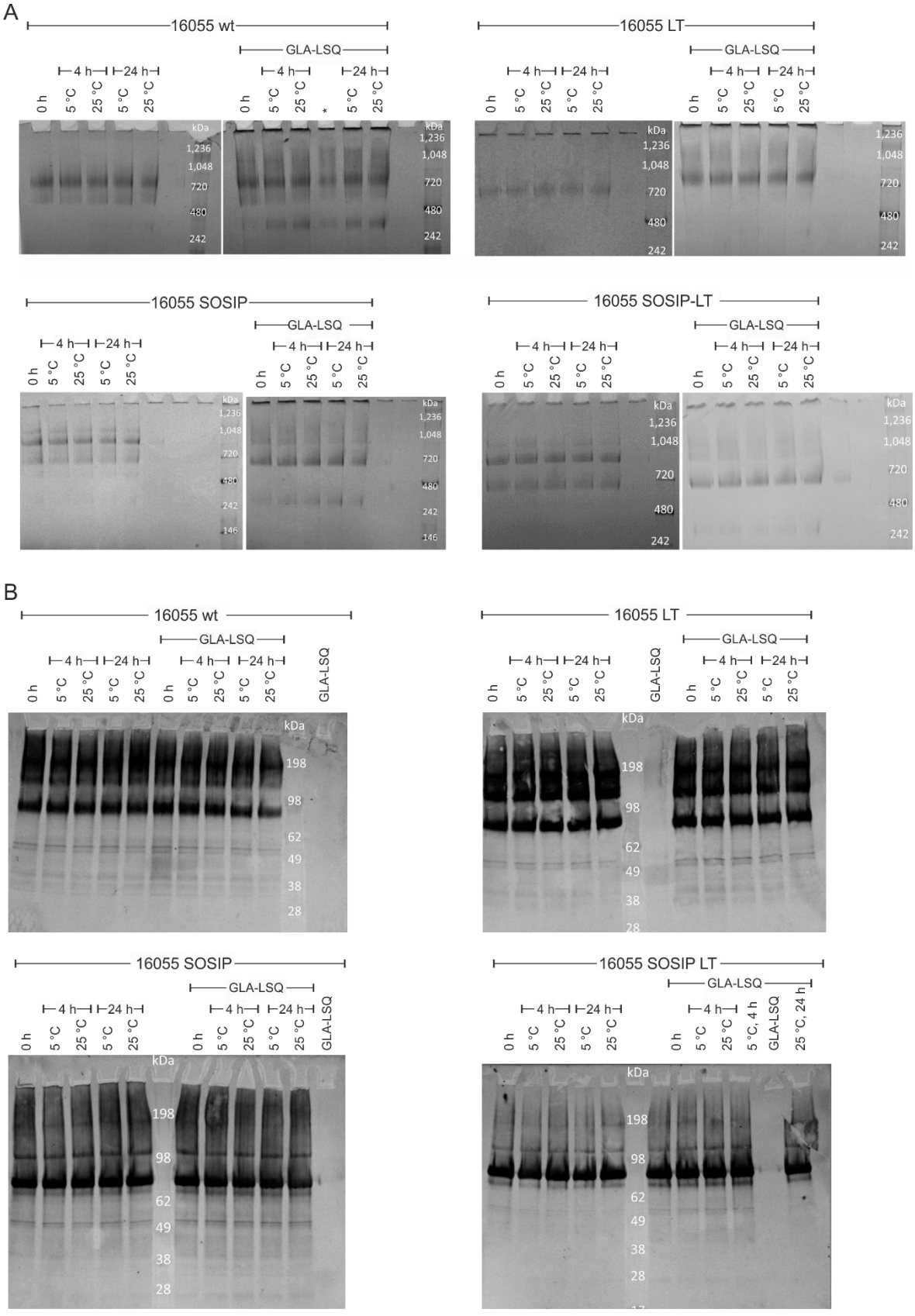

Supplemental Figure 15: Antigen-adjuvant admixture samples of the RepliVax proteins analyzed by IDRI after 0, 4, and 24 h at 5 or 25°C with and without GLA-LSQ.

A) 35 µl sample were loaded per well on a 4-16 % Bis-Tris BN-PAGE and B) 30 µl sample were loaded per well on a 4-20 % Tris glycine gel. After a transfer to a PVDF membrane, the gels were stained with Colloidal Gold Total protein stain. GLA-LSQ was used as adjuvant control. Modified after the IDRI report[170].

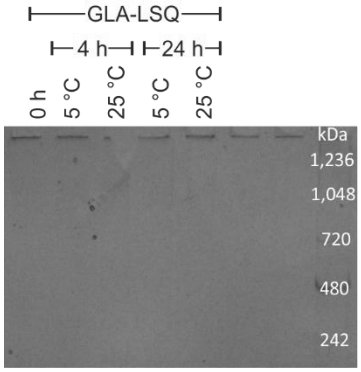

Supplemental Figure 16: Adjuvant control for the antigen-adjuvant admixture samples after 0, 4, and 24 h at 5 or 25°C. The samples were loaded on a 4-16 % Bis-Tris BN-PAGE. Modified after the IDRI report[170].

Supplemental Table 7: Particle size averages of antigen-adjuvant admixtures for cross-linked RepliVax proteins.

Protein	Storage Temperature	Time (h)	Particle Size Average (nm)	PDI
16055 wt_CL + GLA-LSQ		0	73 ± 2	0.288 ± 0.014
	5 °C	4	76 ± 3	0.327 ± 0.007
		24	74 ± 2	0.309 ± 0.021
	25 °C	4	74 ± 2	0.284 ± 0.006
		24	71 ± 2	0.248 ± 0.016
16055 LT_CL + GLA-LSQ		0	74 ± 2	0.283 ± 0.024
	5 °C	4	73 ± 3	0.318 ± 0.004
		24	76 ± 3	0.338 ± 0.024
	25 °C	4	74 ± 2	0.295 ± 0.005
		24	73 ± 5	0.321 ± 0.015
16055 SOSIP_CL + GLA-LSQ		0	72 ± 1	0.267 ± 0.008
	5 °C	4	72 ± 3	0.275 ± 0.020
		24	74 ± 3	0.309 ± 0.010
	25 °C	4	72 ± 1	0.301 ± 0.015
		24	67 ± 2	0.244 ± 0.008
16055 SOSIP-LT_CL + GLA-LSQ		0	75 ± 3	0.312 ± 0.005
	5 °C	4	73 ± 2	0.264 ± 0.023
		24	76 ± 2	0.300 ± 0.031
	25 °C	4	74 ± 2	0.303 ± 0.020
		24	76 ± 4	0.332 ± 0.027
GLA-LSQ		0	70 ± 1	0.247 ± 0.005
	5 °C	4	71 ± 3	0.250 ± 0.032
		24	72 ± 2	0.267 ± 0.028
	25 °C	4	72 ± 1	0.263 ± 0.022
		24	68 ± 2	0.227 ± 0.024

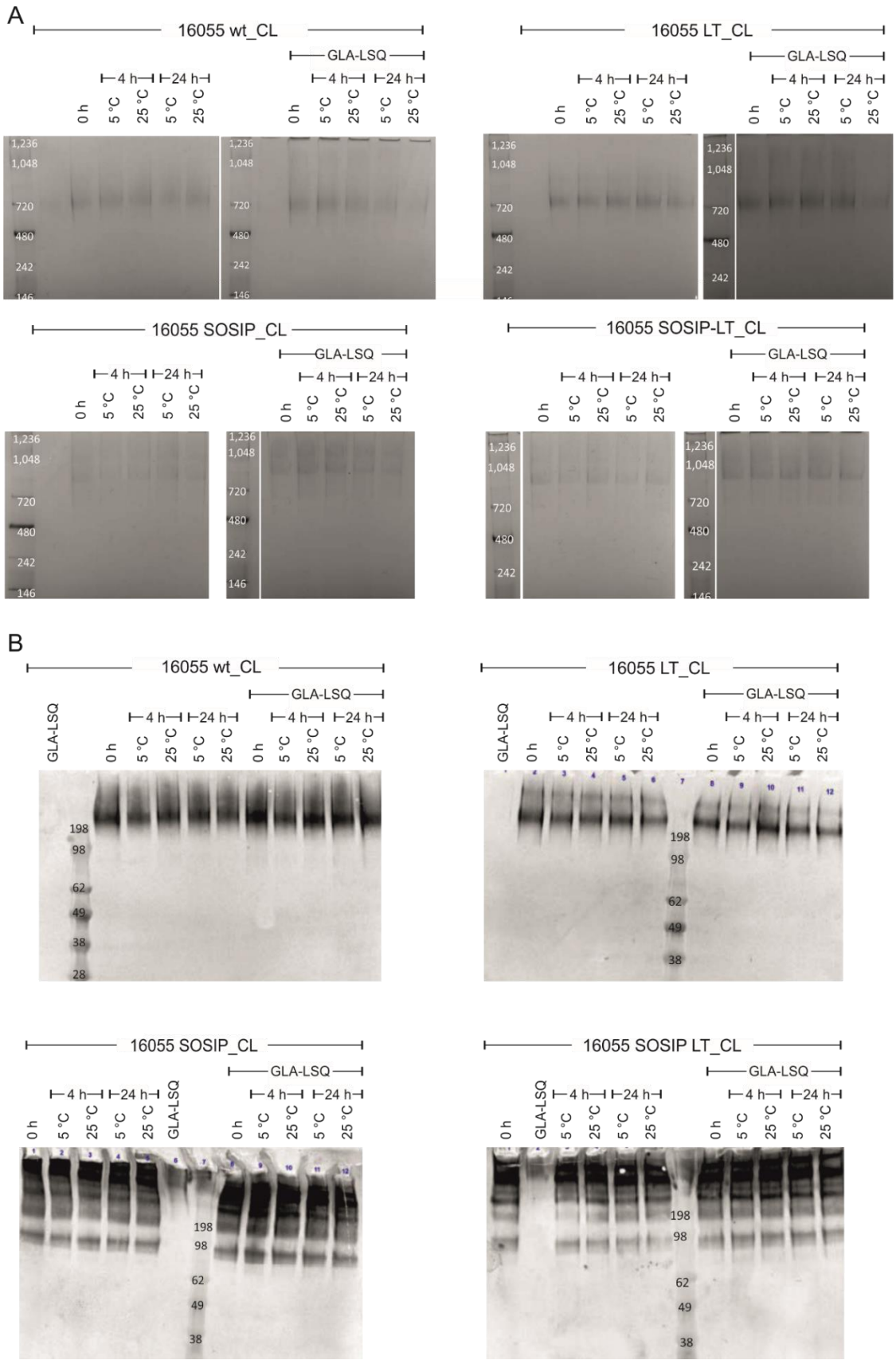

Supplemental Figure 17: Antigen-adjuvant admixture samples of the cross-linked RepliVax proteins analyzed by IDRI after 0, 4, and 24 h at 5 or 25°C with and without GLA-LSQ.

A) 35 µl sample were loaded per well on a 4-16 % Bis-Tris BN-PAGE and B) 30 µl sample were loaded per well on a 4-20 % Tris glycine gel. After a transfer to a PVDF membrane, the gels were stained with Colloidal Gold Total protein stain. GLA-LSQ was used as adjuvant control. Modified after the IDRI report[171].

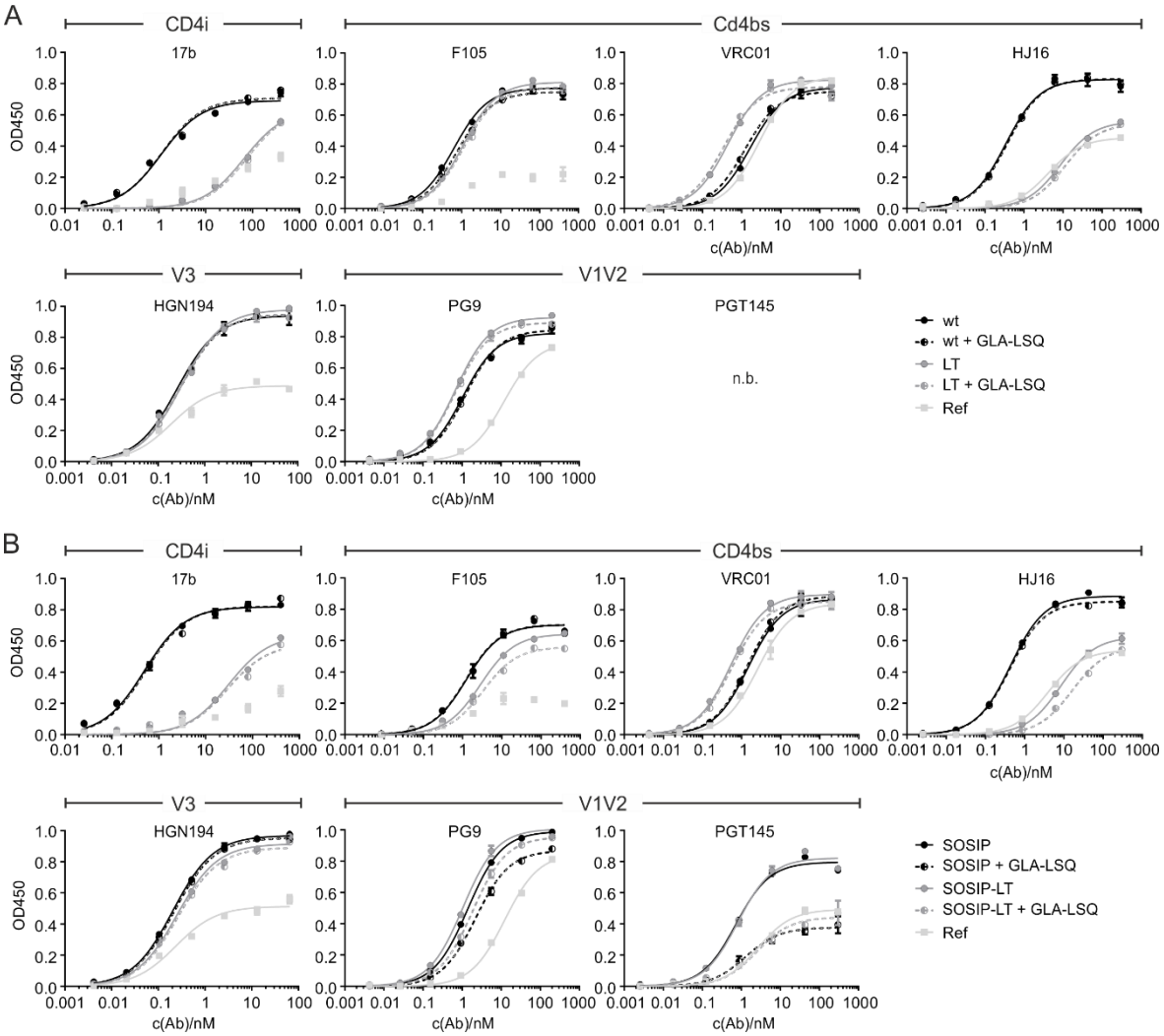

Supplemental Figure 18: Titration curves of the Lectin-capture ELISA of the RepliVax antigens formulated with and without GLA-LSQ. The RepliVax proteins were purified as soluble gp140 trimers. In a lectin-capture ELISA, antibodies targeting different epitopes were titrated in a dilution series. BG505 SOSIP was used as reference (Ref). Main header shows the epitope and sub-headers the respective antibodies. A-B) Titration curves of A) 16055 wt and LT, and B) 16055 SOSIP and 16055 SOSIP-LT.

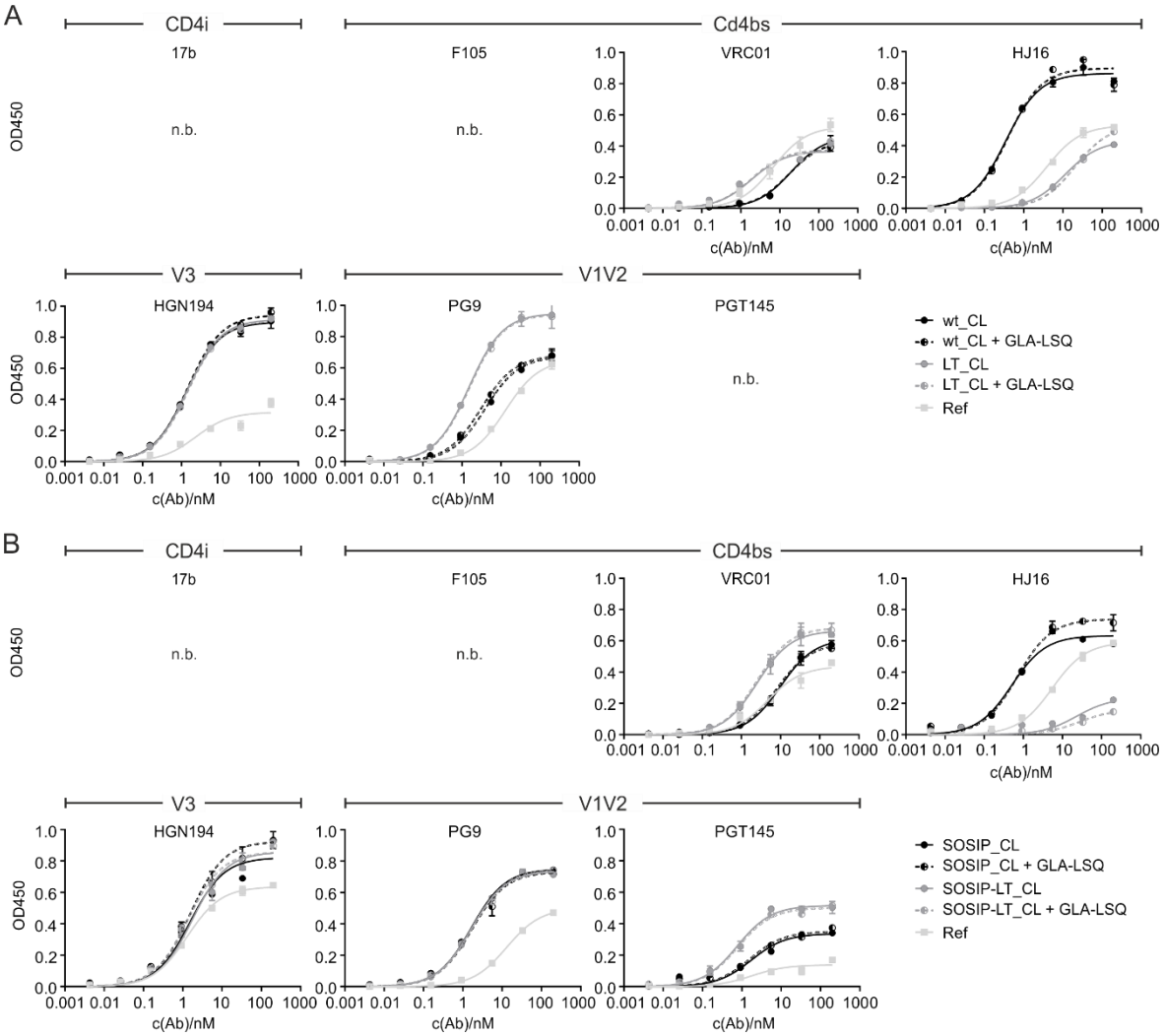

Supplemental Figure 19: Titration curves of the Lectin-capture ELISA of the cross-linked RepliVax antigens formulated with and without GLA-LSQ. The RepliVax proteins were purified as soluble gp140 trimers and cross-linked via EDC/NHS. In a lectin-capture ELISA, antibodies targeting different epitopes were titrated in a 6-fold dilution series, starting at different concentrations (HGN194: 60 nM; PG9 and VRC01: 200nM; 17b, F105, PGT145: 300 nM; HJ16 400 nM). BG505 SOSIP was used as reference (Ref). Main header shows the epitope and sub-headers the respective antibodies. A-B) Titration curves of A) 16055 wt_CL and LT_CL, and B) 16055 SOSIP_CL and 16055 SOSIP-LT_CL.

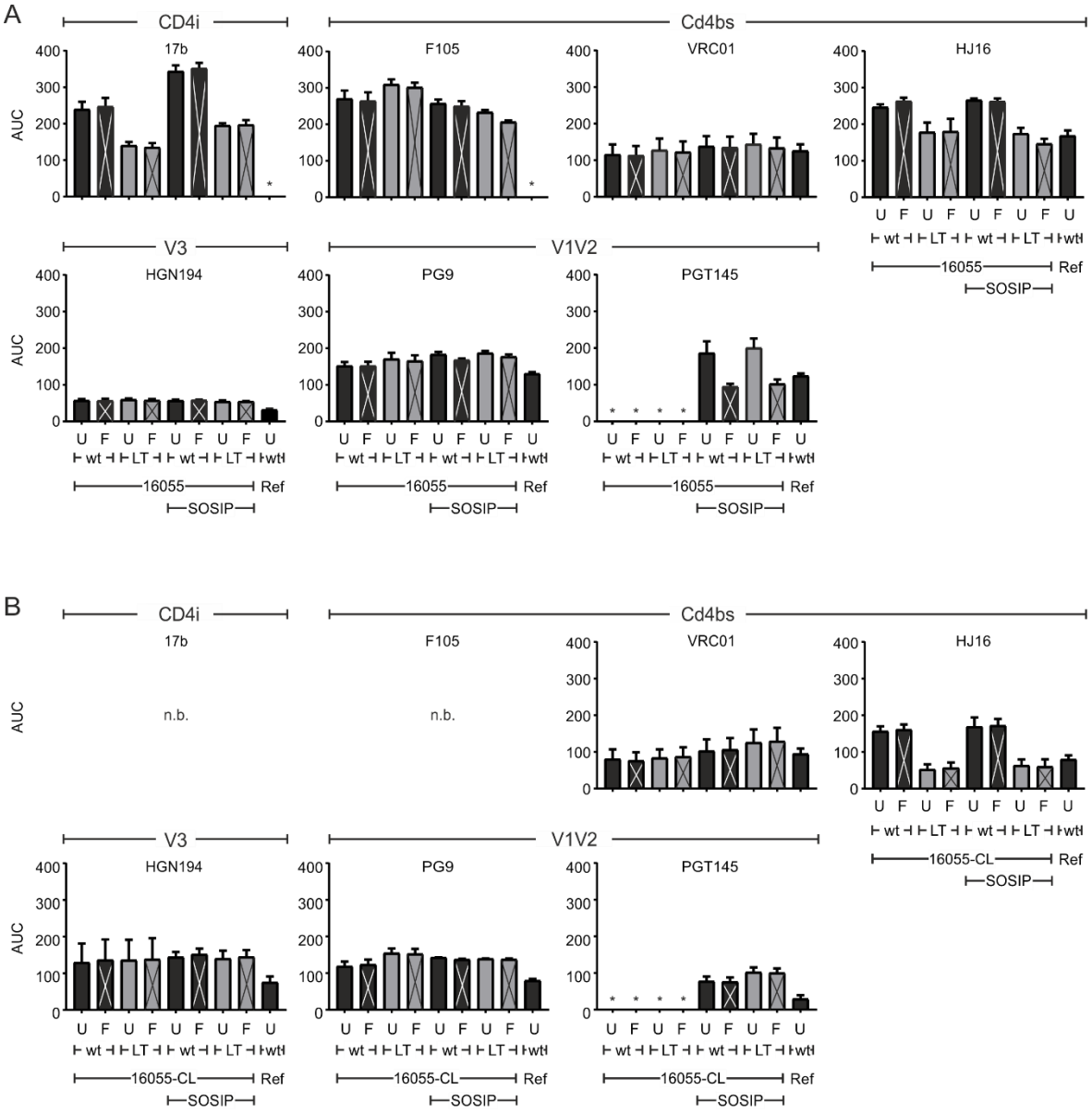

Supplemental Figure 20: Area-Under-the-Curve (AUC) values of the titration curves of the Lectin-capture ELISAs of the untreated (U) and adjuvant-formulated (F) RepliVax immunogens.
In a lectin-capture ELISA, antibodies targeting different epitopes of the purified gp140 RepliVax proteins were titrated in serial dilutions, starting at different concentrations. The bar charts represent the area-under-the-curve (AUC) values of the antibody titration curves. Error bars represent the standard error of the mean of triplicates. BG505 SOSIP was used as reference (Ref). Main header shows the epitope and sub-headers the respective antibodies. Analysis of A) non cross-linked and B) cross-linked RepliVax protein.

Supplemental Table 8: Heatmap of the Dissociation constants (K_D) of the RepliVax proteins used for formulation study. Mean was taken from triplicates. U: Untreated protein, F: Formulated protein. SEM: Standard error of the mean.

	CD4i		CD4bs					
	17b		**F105**		**VRC01**		**HJ16**	
	Mean	SEM	Mean	SEM	Mean	SEM	Mean	SEM
16055 wt U	1.26	0.07	0.76	0.07	1.65	0.07	0.31	0.07
16055 wt F	1.19	0.14	0.81	0.07	1.45	0.13	0.31	0.08
16055 LT U	72.11	5.27	1.24	0.10	0.43	0.02	8.56	3.87
16055 LT F	72.74	2.18	1.23	0.10	0.39	0.03	8.87	3.54
16055 SOSIP U	0.51	0.01	1.73	0.26	1.48	0.28	0.40	0.03
16055 SOSIP F	0.50	0.05	2.01	0.40	1.35	0.25	0.38	0.05
16055 SOSIP-LT U	32.44	4.75	3.30	0.46	0.51	0.09	9.08	1.62
16055 SOSIP-LT F	27.91	3.37	3.27	0.27	0.53	0.10	14.69	2.87
BG505 SOSIP	n.b.		n.b.		2.83	0.47	3.49	0.77

	V1V2				V3	
	PG9		**PGT145**		**HGN194**	
	Mean	SEM	Mean	SEM	Mean	SEM
16055 wt U	0.92	0.18	n.b.		0.25	0.03
16055 wt F	1.17	0.27	n.b.		0.25	0.03
16055 LT U	0.60	0.13	n.b.		0.28	0.04
16055 LT F	0.62	0.11	n.b.		0.27	0.03
16055 SOSIP U	1.08	0.21	0.68	0.03	0.26	0.03
16055 SOSIP F	1.82	0.43	1.16	0.15	0.29	0.05
16055 SOSIP-LT U	0.81	0.13	1.12	0.36	0.37	0.10
16055 SOSIP-LT F	1.61	0.37	2.14	0.25	0.34	0.05
BG505 SOSIP	8.78	1.36	3.44	0.46	0.21	0.02

0.01 5 100nM

Supplemental Table 9: Heatmap of the Dissociation constants (K_D) of the cross-linked RepliVax proteins used for formulation study. Mean was taken from triplicates. U: Untreated protein, F: Formulated protein. SEM: Standard error of the mean.

	CD4i		CD4bs					
	17b		**F105**		**VRC01**		**HJ16**	
	Mean	SEM	Mean	SEM	Mean	SEM	Mean	SEM
16055 wt_CL U	n.b.		n.b.		15.34	2.10	0.78	0.46
16055 wt_CL F	n.b.		n.b.		13.21	1.94	0.61	0.28
16055 LT_CL U	n.b.		n.b.		1.34	0.41	16.59	3.22
16055 LT_CL F	n.b.		n.b.		1.53	0.24	20.49	3.72
16055 SOSIP_CL U	n.b.		n.b.		7.55	1.19	0.40	0.10
16055 SOSIP_CL F	n.b.		n.b.		6.56	0.78	0.42	0.15
16055 SOSIP-LT_CL U	n.b.		n.b.		1.74	0.41	15.85	3.91
16055 SOSIP-LT_CL F	n.b.		n.b.		1.84	0.32	21.09	4.02
BG505 SOSIP	n.b.		n.b.		4.95	0.43	3.90	0.63

	V1V2				V3	
	PG9		**PGT145**		**HGN194**	
	Mean	SEM	Mean	SEM	Mean	SEM
16055 wt_CL U	3.68	1.07	n.b.		0.87	0.32
16055 wt_CL F	3.31	0.91	n.b.		0.95	0.36
16055 LT_CL U	1.85	0.24	n.b.		0.97	0.35
16055 LT_CL F	1.80	0.21	n.b.		1.04	0.38
16055 SOSIP_CL U	2.12	0.32	1.69	0.55	1.52	0.03
16055 SOSIP_CL F	2.12	0.26	1.56	0.25	1.53	0.01
16055 SOSIP-LT_CL U	2.22	0.34	0.73	0.06	1.68	0.05
16055 SOSIP-LT_CL F	2.13	0.26	0.89	0.23	1.65	0.15
BG505 SOSIP	10.54	1.18	3.84	1.36	1.31	0.28

0.01 5 50nM

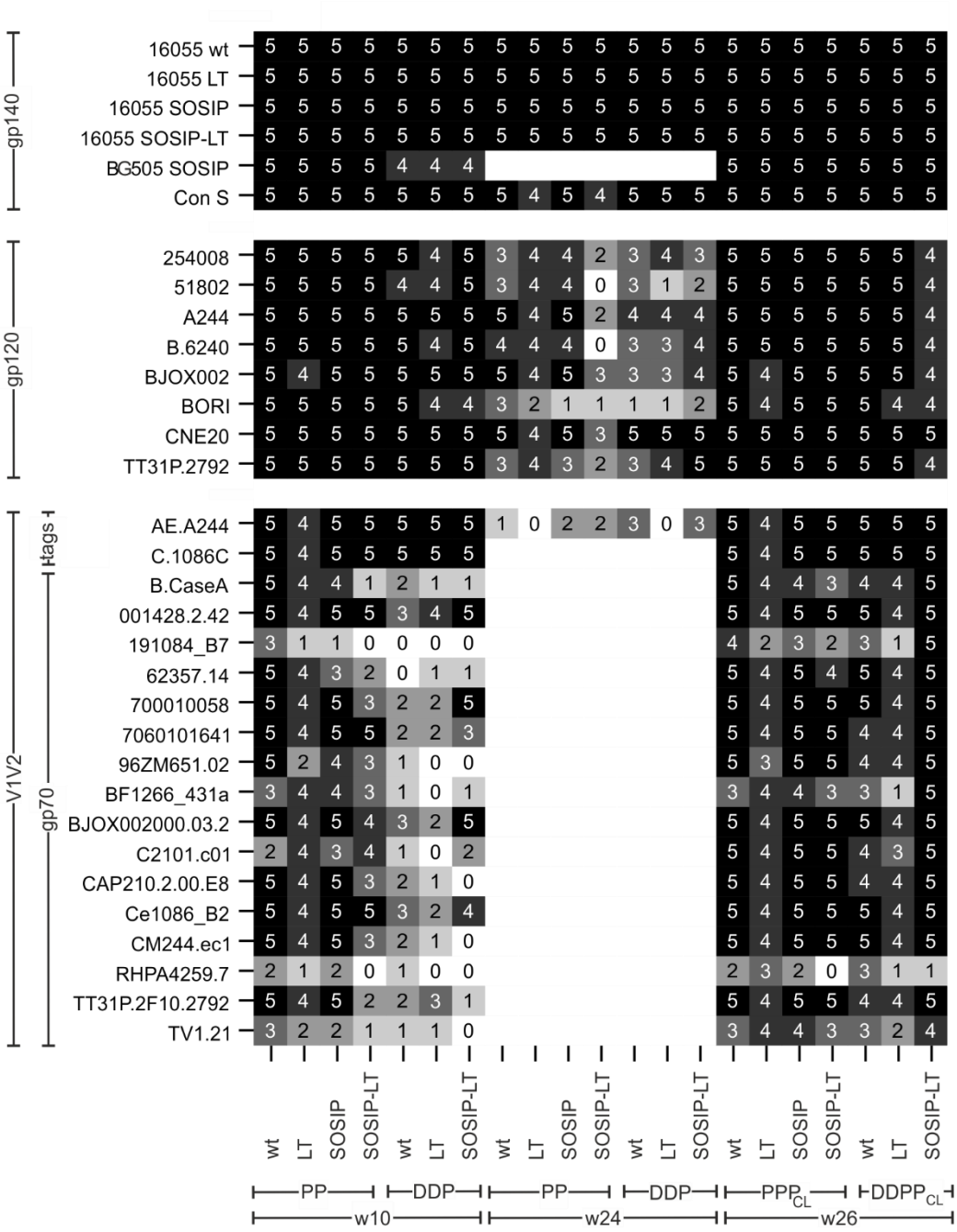

Supplemental Figure 21: Response rates of the different groups to the antigens tested. On the left-hand side, antigens tested as gp140, gp120 and V1V2-scaffold-antigens are listed. At the bottom, the immunization groups are shown for the different time points at weeks 10, 24, and 26: Protein (P), DNA (D) and Cross-linked (CL) indicate the immunizations, which occurred before the given analysis time-point. As each group consists of 5 animals, a response of 5 is the maximum. Blank areas indicate that groups were not tested against the antigen listed at this time-point.

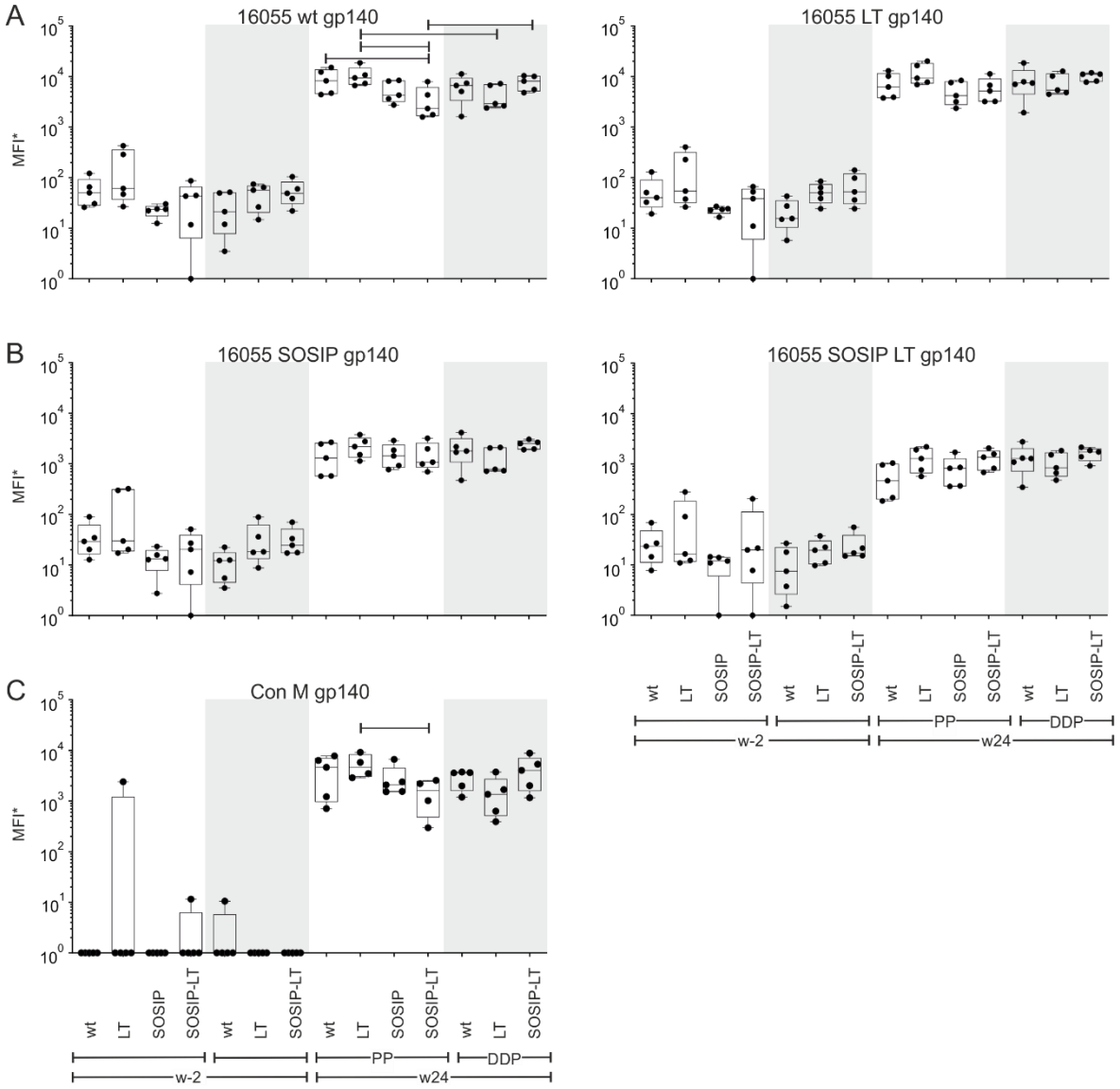

Supplemental Figure 22: Binding Antibodies Multiplex Assay was used to evaluate the binding of serum antibodies against different gp140 proteins in weeks -2 and 24. Depicted are the four immunogens (wt, LT, SOSIP, SOSIP-LT) and one additional protein Consensus M. Values for week -2 are all counted as non-responders as they did not fulfil positivity criteria. The single-point measurements were performed at a dilution of 1:80. Grey areas highlight DNA-primed groups. Black lines: p-value <0.05. Boxes extend from the 25th to the 75th percentiles while the midline of the box denotes the median. Whiskers are plotted down to the minimum and up to the maximum value. Each individual value is plotted as a point superimposed on the graph. MFI: Mean fluorescence intensities, MFI*: background-adjusted MFI minus background-adjusted blank, P: Protein, D: DNA, CL: Cross-linked, w: week.

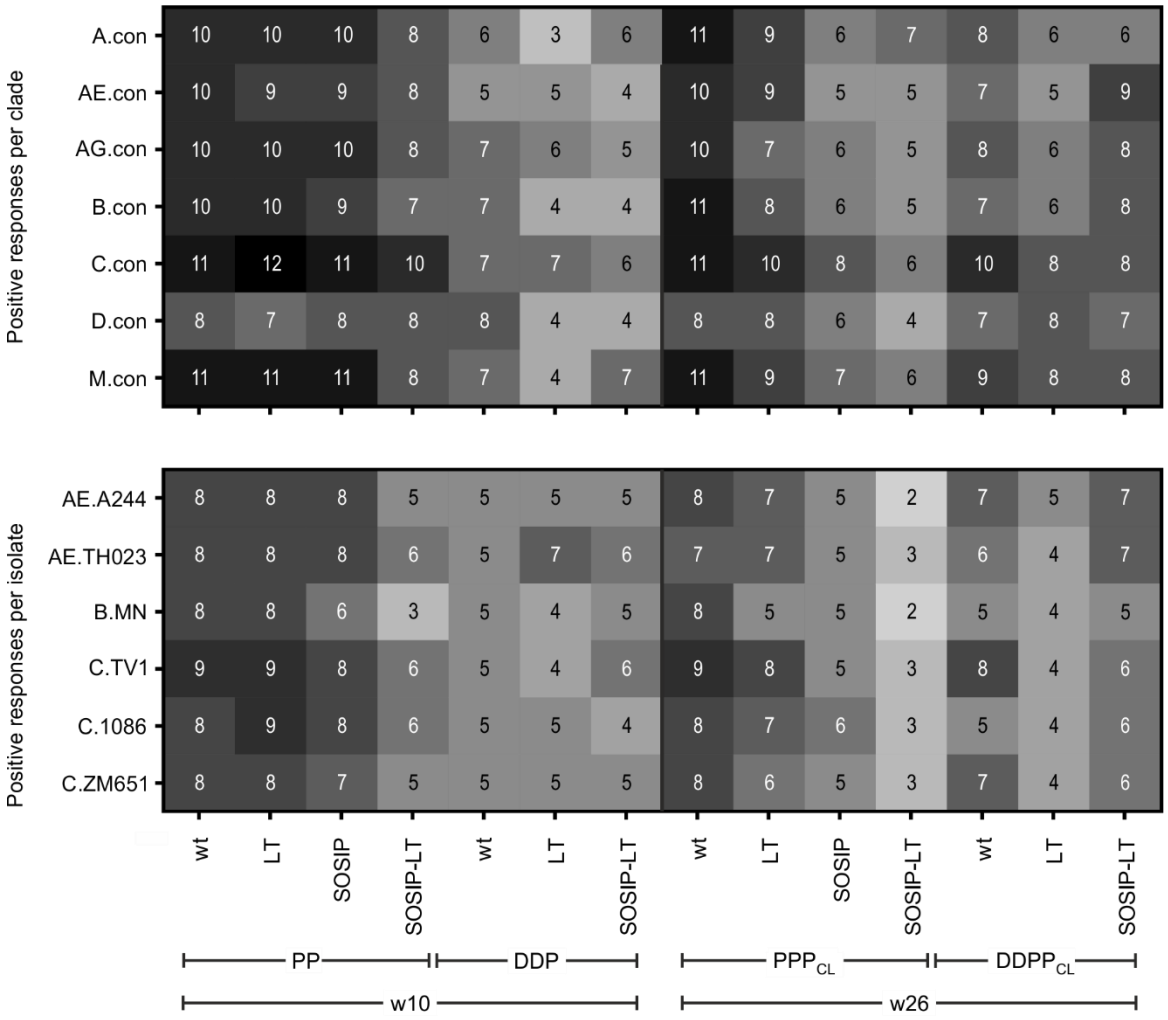

Supplemental Figure 23: Heat-map depicting the number of epitopes fulfilling positivity criteria in the linear epitope mapping. Depicted are the clades/isolates (left) and groups (below). Upper panel: Consensus gp160 sequences, lower panel: gp120 sequences. P: Protein, D: DNA, CL: Cross-linked, w: week.

Supplemental Table 10: Neutralization assay response rates of groups per virus isolate. All tested isolates were of clade C. Tier 1: MW965.26; Tier 2: 16055-2.3, 25710-2.43, Ce1176_A3, Ce Ce703010217_B6; *: Control. n.t.: not tested.

Response rates		SVA-MLV*	MW965.26	16055-2.3	25710-2.43	Ce1176_A3	Ce703010217_B6
Week	Condition						
10	wt-PP	0/5	5/5	0/5	0/5	0/5	0/5
	LT-PP	0/5	5/5	1/5	1/5	0/5	0/5
	SOSIP-PP	0/5	5/5	3/5	0/5	0/5	0/5
	SOSIP-LT-PP	0/5	5/5	1/5	0/5	0/5	0/5
	wt-DDP	0/5	3/5	0/5	0/5	0/5	0/5
	LT-DDP	0/5	4/5	0/5	0/5	0/5	0/5
	SOSIP-LT-DDP	0/5	5/5	0/5	0/5	0/5	0/5
24	wt-PP	0/5	5/5	0/5	n.t.	n.t.	n.t.
	LT-PP	0/5	5/5	0/5	n.t.	n.t.	n.t.
	SOSIP-PP	0/5	4/5	0/5	n.t.	n.t.	n.t.
	SOSIP-LT-PP	0/5	3/5	0/5	n.t.	n.t.	n.t.
	wt-DDP	0/5	3/5	0/5	n.t.	n.t.	n.t.
	LT-DDP	0/5	1/5	0/5	n.t.	n.t.	n.t.
	SOSIP-LT-DDP	0/5	4/5	0/5	n.t.	n.t.	n.t.
26	wt-PPP_{CL}	0/5	5/5	0/5	0/5	0/5	0/5
	LT-PPP_{CL}	0/5	5/5	1/5	0/5	0/5	0/5
	SOSIP-PPP_{CL}	0/5	5/5	4/5	0/5	0/5	0/5
	SOSIP-LT-PPP_{CL}	0/5	5/5	3/5	0/5	0/5	0/5
	wt-$DDPP_{CL}$	0/5	5/5	1/5	0/5	0/5	0/5
	LT-$DDPP_{CL}$	0/5	5/5	0/5	0/5	0/5	0/5
	SOSIP-LT-$DDPP_{CL}$	0/5	5/5	0/5	0/5	0/5	0/5

Abbreviations

Ab	Antibody
Ad5	Adenovirus Type 5
ADCC	Antibody-Dependent Cellular Cytotoxicity
ADCVI	Ab-Dependent, Cell-mediated Virus Inhibition
AEC	Anion Exchange Chromatography
AIDS	Acquired ImmunoDeficiency Syndrome
ART	AntiRetroviral Therapy
AUC	Area Under the Curve
BN	Blue Native
bNAb	broadly Neutralizing Antibody
BSA	Bovine Serum Albumin
C1-C5	Constant regions of HIV-1 Envelope
CcdB	Control of cell death toxin B
CCR5	C-C Chemokine Receptor type 5
CD4	Cluster of Differentiation 4
CD4i	CD4-induced conformation
CD8	Cluster of Differentiation 8
CDRH3	Complementarity Determining Region 3 of the antibody Heavy chain
CRF	Circulating Recombinant Form
CT	Cytoplasmic Tail of HIV-1 Envelope
CTL	Cytotoxic T-Lymphocyte
CV	Column Volume
CXCR4	Chemokine Receptor Type 4
DLS	Dynamic Light Scattering
DSL	DiSulfide Loop
DMEM	Dulbecco's Modified Eagle's Medium
DNA	DeoxyriboNucleicAacid
DSC	Differential Scanning Calorimetry
DSF	Differential Scanning Fluorimetry
E. coli	*Escherichia Coli*
EDC	1-Ethyl-3-(3-Dimethylamino-propyl)-Carbodiimide hydro-chloride
EDTA	EthyleneDiamineTetraacetic Acid
EGTA	Ethylene Glycol-bis(β-aminoethyl ether)-N,N,N',N'-Tetraacetic Acid
Env	Envelope protein
eOD	engineered Outer Domain
ER	Endoplasmatic Reticulum
EU	Endotoxin Unit
FACS	Fluorescence-Activated Cell Sorting
Fc	Fragment crystallizable
FCS	Fetal Calf Serum
FDR	False Discovery Rate
FP	Fusion Peptide
Gag	HIV-1 Group-Specific Antigen
GFP	Green Fluorescent Protein
GLA	Glucopyranosyl Lipid A
gp	glycoprotein
GSK	GlaxoSmithKline
GT X	Envelope Variant with X Germline-Targeting Mutations
h	hour
HEK	Human Embryonic Kidney
HIV	Human Immunodeficiency Virus
HPLC	High Pressure Liquid Chromatography
HR1/2	Heptad Repeats/Helical Regions 1 and 2 of HIV-1 Envelope
HVTN	HIV Vaccine Trials Network
IDRI	Infectious Disease Research Institute
IgG	Immunoglobulin G
IMAC	Immobilized Metal ion Affinity Chromatography
K_D	Dissociation constant

LB	Lysogeny Broth
M	Molar
mAb	monoclonal Antibody
MES	2-(N-Morpholino)EthaneSulfonic acid
MFI	Mean Fluorescence Intensity
min	minute
MPER	Membrane-Proximal External Region of HIV-1 Envelope
mRNA	messenger Ribonucleic Acid
nNAb	non-Neutralizing Antibody
NAb	neutralizing Antibody
nef	Accessory regulatory HIV protein
NFL	Native Flexible Linker
NHP	Non-Human Primate
NHS	N-HydroxySuccinimide
NIH	National Institute of Health
nM	nano Molar
nm	nano meter
OD 450	Optical density at 450 nm
PAGE	PolyAcrylamide Gel Electrophoresis
PBS	Phosphate Buffered Saline
PCR	Polymerase Chain Reaction
PDI	PolyDispersity index
PE	PhycoErythrin
PEI	PolyEthylenImine
pol	HIV-1 Enzyme
QL	Quick Ligation
R_6	RRRRRR
rpm	revolutions per minute
RT	Room Temperature
sCD4	soluble CD4
SDS	Sodium Dodecyl Sulfate
SEC	Size Exclusion Chromatography
sec	second
SEM	Standard Error of the Mean
SHIV	Simian-Human Immuno-deficiency Virus (chimeric)
SHM	Somatic HyperMutation
SIV	Simian Immunodeficiency Virus
SOSIP	SOS: Disulfide Bridge between gp120 and gp41, IP: I559P mutation in gp41
TD	Trimer-Derived (HIV-1 Envelope trimer stabilizing mutations
TLR	Toll-Like Receptor
TM	TransMembrane domain
T_m	melting Temperature
UNAIDS	The Joint United Nations Program on HIV/AIDS
URF	Unique Recombinant Form
v/v	volume per volume
V1-V5	Variable regions of HIV-1 Envelope
VRC	Vaccine Research Center
w/v	weight per volume
WHO	World Health Organization
wt	wildtype

9. Bibliography

1. Barré-Sinoussi, F. *et al.* Isolation of a T-Lymphotropic Retrovirus from a Patient at Risk for Acquired Immune Deficiency Syndrome (AIDS). *Science (80-.).* **220**, 868–871 (1983).
2. Gallo, R. C. *et al.* Frequent Detection and Isolation of Cytopathic Retroviruses (HTLV-III) from Patients with AIDS and at Risk for AIDS. *Science (80-.).* **224**, 500–503 (1984).
3. Coffin, J. *et al.* What to call the AIDS virus? *Nature* **321**, 10 (1986).
4. FACT SHEET – WORLD AIDS DAY 2019. *UNAIDS* (2019).
5. Shaw, G. M. & Hunter, E. HIV transmission. *Cold Spring Harb. Perspect. Med.* **2**, 1–23 (2012).
6. Sharp, P. M. & Hahn, B. H. Origins of HIV and the AIDS Pandemic. *Cold Spring Harb. Perspect. Med.* **1**, 1–22 (2011).
7. Mirela, D. *et al.* Origin of the HIV-1 group O epidemic in western lowland gorillas. *PNAS* **112**, 1343–1352 (2015).
8. Buonaguro, L., Tornesello, M. L. & Buonaguro, F. M. Human immunodeficiency virus type 1 subtype distribution in the worldwide epidemic: pathogenetic and therapeutic implications. *J. Virol.* **81**, 10209–10219 (2007).
9. Maartens, G., Celum, C. & Lewin, S. R. HIV infection: Epidemiology, pathogenesis, treatment, and prevention. *Lancet* **384**, 258–271 (2014).
10. Mocroft, A. *et al.* The incidence of AIDS-defining illnesses in 4883 patients with human immunodeficiency virus infection. *Arch. Intern. Med.* **158**, 491–497 (1998).
11. Hemelaar, J. *et al.* Global and regional molecular epidemiology of HIV-1, 1990–2015: a systematic review, global survey, and trend analysis. *Lancet Infect. Dis.* **19**, 143–155 (2019).
12. UNAIDS DATA 2019. in 1–474 (2019).
13. Davey, R. T. *et al.* HIV-1 and T cell dynamics after interruption of highly active antiretroviral therapy (HAART) in patients with a history of sustained viral suppression. *Proc. Natl. Acad. Sci. U. S. A.* **96**, 15109–15114 (1999).
14. Chun, T.-W. *et al.* In vivo fate of HIV-1-infected T cells: Quantitative analysis of the transition to stable latency TAE-WOOK. *Nature* **1**, 1284–1290 (1995).
15. Chun, T. W. *et al.* Early establishment of a pool of latently infected, resting CD4+ T cells during primary HIV-1 infection. *Proc. Natl. Acad. Sci. U. S. A.* **95**, 8869–8873 (1998).
16. Susanne Modrow, Dietrich Falke, Uwe Truyen, H. S. *Molekulare Virologie*. (Spektrum Akademischer Verlag, 2010).
17. Wyatt, R. & Sodroski, J. The HIV-1 envelope glycoproteins: fusogens, antigens, and immunogens. *Science* **280**, 1884–8 (1998).
18. Doms, R. W., Lamb, R. A., Rose, J. K. & Helenius, A. Folding and Assembly of Viral Membrane Proteins. *Virology* **193**, 545–562 (1993).
19. Moulard, M. & Decroly, E. Maturation of HIV envelope glycoprotein precursors by cellular endoproteases. *Biochim. Biophys. Acta - Rev. Biomembr.* **1469**, 121–132 (2000).
20. Earl, P. L., Moss, B. & Doms, R. W. Folding, interaction with GRP78-BiP, assembly, and transport of the human immunodeficiency virus type 1 envelope protein. *J. Virol.* **65**, 2047–2055 (1991).
21. Colman, P. M. & Lawrence, M. C. The structural biology of type I viral membrane fusion. *Nat. Rev. Mol. Cell Biol.* **4**, 309–319 (2003).
22. Lobritz, M. A., Ratcliff, A. N. & Arts, E. J. HIV-1 entry, inhibitors, and resistance. *Viruses* **2**, 1069–1105 (2010).
23. Trovato, M., D'Apice, L., Prisco, A. & De Berardinis, P. HIV vaccination: A roadmap among advancements and concerns. *Int. J. Mol. Sci.* **19**, 1–14 (2018).
24. Ward, A. B. & Wilson, I. A. Insights into the trimeric HIV-1 envelope glycoprotein structure. *Trends Biochem. Sci.* **40**, 101–107 (2015).
25. Kwong, P. D. *et al.* Structure of an HIV gp120 envelope glycoprotein in complex with the CD4 receptor and a neutralizing human antibody. *Nature* **393**, 648–659 (1998).
26. Da, L. T., Quan, J. M. & Wu, Y. D. Understanding of the bridging sheet formation of HIV-1 glycoprotein gp120. *J. Phys. Chem. B* **113**, 14536–14543 (2009).
27. Julien, J.-P. P. *et al.* Crystal structure of a soluble cleaved HIV-1 envelope trimer. *Science (80-.).* **342**, 1477–1483 (2013).
28. Dalgleish, A. G. *et al.* The CD4 (T4) antigen is an essential component of the receptor for the AIDS

retrovirus. *Nature* **312**, 763–767 (1984).
29. Berger, E. A., Murphy, P. M. & Farber, J. M. CHEMOKINE RECEPTORS AS HIV-1 CORECEPTORS: Roles in Viral Entry, Tropism, and Disease. *Annu. Rev. Immunol.* **17**, 657–700 (1999).
30. Chan, D. C., Fass, D., Berger, J. M. & Kim, P. S. Core structure of gp41 from the HIV envelope glycoprotein. *Cell* **89**, 263–273 (1997).
31. Wilen, C. B., Tilton, J. C. & Doms, R. W. HIV: Cell Binding and Entry. *Cold Spring Harb. Perspect. Med.* **2**, a006866 (2012).
32. Chen, B. Molecular Mechanism of HIV-1 Entry. *Trends Microbiol.* **27**, 878–891 (2019).
33. Blumenthal, R., Durell, S. & Viard, M. HIV entry and envelope glycoprotein-mediated fusion. *J. Biol. Chem.* **287**, 40841–40849 (2012).
34. Montefiori, D. C., Roederer, M., Morris, L. & Seaman, M. S. Neutralization tiers of HIV-1. *Curr. Opin. HIV AIDS* **13**, 128–136 (2018).
35. Munro, J. B. *et al.* Conformational dynamics of single HIV-1 envelope trimers on the surface of native virions. *Science (80-.).* **346**, 759–763 (2014).
36. Cai, Y. *et al.* Antigenicity-defined conformations of an extremely neutralization-resistant HIV-1 envelope spike. *PNAS* **114**, 4477–4482 (2017).
37. Wilen, C. B., Tilton, J. C. & Doms, R. W. HIV: Cell binding and entry. *Cold Spring Harb. Perspect. Med.* **2**, 1–14 (2012).
38. Achuthan, V., Keith, B. J., Connolly, B. A. & DeStefano, J. J. Human Immunodeficiency Virus Reverse Transcriptase Displays Dramatically Higher Fidelity under Physiological Magnesium Conditions In Vitro. *J. Virol.* **88**, 8514–8527 (2014).
39. Bonomelli, C. *et al.* The glycan shield of HIV is predominantly oligomannose independently of production system or viral clade. *PLoS One* **6**, e23521 (2011).
40. Leonard, C. K. *et al.* Assignment of intrachain disulfide bonds and characterization of potential glycosylation sites of the type 1 recombinant human immunodeficiency virus envelope glycoprotein (gp120) expressed in Chinese hamster ovary cells. *J. Biol. Chem.* **265**, 10373–10382 (1990).
41. Cao, L. *et al.* Global site-specific N-glycosylation analysis of HIV envelope glycoprotein. *Nat. Commun.* **8**, 1–13 (2017).
42. Wei, X. *et al.* Antibody neutralization and escape by HIV-1. *Nature* **422**, 307–312 (2003).
43. Kwong, P. D. *et al.* HIV-1 evades antibody-mediated neutralization through conformational masking of receptor-binding sites. *Nature* **420**, 678–682 (2002).
44. Lewis, G., Finzi, A., DeVico, A. & Pazgier, M. Conformational Masking and Receptor-Dependent Unmasking of Highly Conserved Env Epitopes Recognized by Non-Neutralizing Antibodies That Mediate Potent ADCC against HIV-1. *Viruses* **7**, 5115–5132 (2015).
45. Myszka, D. G. *et al.* Energetics of the HIV gp120-CD4 binding reaction. *Proc. Natl. Acad. Sci. U. S. A.* **97**, 9026–9031 (2000).
46. Rong, R. *et al.* Role of V1V2 and other human immunodeficiency virus type 1 envelope domains in resistance to autologous neutralization during clade C infection. *J. Virol.* **81**, 1350–1359 (2007).
47. Sagar, M., Wu, X., Lee, S. & Overbaugh, J. Human immunodeficiency virus type 1 V1-V2 envelope loop sequences expand and add glycosylation sites over the course of infection, and these modifications affect antibody neutralization sensitivity. *J. Virol.* **80**, 9586–9598 (2006).
48. Pancera, M. *et al.* Structure and immune recognition of trimeric pre-fusion HIV-1 Env. *Nature* **514**, 455–61 (2014).
49. Moore PL *et al.* Nature of nonfunctional envelope proteins on the surface of human immunodeficiency virus type 1. *J. Virol.* **80**, 2515–2528 (2006).
50. Poignard, P., Fouts, T., Naniche, D., Moore, J. P. & Sattentau, Q. J. Neutralizing antibodies to human immunodeficiency virus type-1 gp120 induce envelope glycoprotein subunit dissociation. *J. Exp. Med.* **183**, 473–484 (1996).
51. Pancera, M. *et al.* Structure and immune recognition of trimeric pre-fusion HIV-1 Env. *Nature* **514**, 455–461 (2014).
52. Overbaugh, J. *et al.* The Antibody Response against HIV-1 The Antibody Response against HIV-1. *Cold Spring Harb. Perspect. Med.* **1**, 1–17 (2012).
53. Yang, X., Kurteva, S., Ren, X., Lee, S. & Sodroski, J. Stoichiometry of Envelope Glycoprotein Trimers in the Entry of Human Immunodeficiency Virus Type 1. *J. Virol.* **79**, 12132–12147 (2005).
54. Chertova, E. *et al.* Envelope glycoprotein incorporation, not shedding of surface envelope glycoprotein (gp120/SU), Is the primary determinant of SU content of purified human immunodeficiency virus type 1 and simian immunodeficiency virus. *J. Virol.* **76**, 5315–25 (2002).

55. Klein, J. S. & Bjorkman, P. J. Few and far between: How HIV may be evading antibody avidity. *PLoS Pathog.* **6**, 1–6 (2010).
56. Sanders, R. W. *et al.* A Next-Generation Cleaved, Soluble HIV-1 Env Trimer, BG505 SOSIP.664 gp140, Expresses Multiple Epitopes for Broadly Neutralizing but Not Non-Neutralizing Antibodies. *PLoS Pathog.* **9**, (2013).
57. Sharma, S. K. *et al.* Cleavage-Independent HIV-1 Env Trimers Engineered as Soluble Native Spike Mimetics for Vaccine Design. *Cell Rep.* **11**, 539–550 (2015).
58. Binley, J. M. *et al.* A recombinant human immunodeficiency virus type 1 envelope glycoprotein complex stabilized by an intermolecular disulfide bond between the gp120 and gp41 subunits is an antigenic mimic of the trimeric virion-associated structure. *J. Virol.* **74**, 627–43 (2000).
59. Sanders, R. W. *et al.* Stabilization of the Soluble, Cleaved, Trimeric Form of the Envelope Glycoprotein Complex of Human Immunodeficiency Virus Type 1. **76**, 8875–8889 (2002).
60. Binley, J. M. *et al.* Enhancing the Proteolytic Maturation of Human Immunodeficiency Virus Type 1 Envelope Glycoproteins. **76**, 2606–2616 (2002).
61. Guenaga, J. *et al.* Structure-Guided Redesign Increases the Propensity of HIV Env To Generate Highly Stable Soluble Trimers. *J. Virol.* **90**, 2806–2817 (2016).
62. Earl, P. L., Doms, R. W. & B., M. Oligomeric Structure of the Human Immunodeficiency Virus Type 1 Envelope Protein. *Proc. Natl. Acad. Sci.* **87**, 648–652 (1990).
63. Srivastava, I. K. *et al.* Purification and Characterization of Oligomeric Envelope Glycoprotein from a Primary R5 Subtype B Human Immunodeficiency Virus. *J. Virol.* **76**, 2835–2847 (2002).
64. Stacey, G. & Davis, J. *Medicines from Animal Cell Culture (Hardcover)*. *John Wiley & Sons* (2007).
65. Ringe, R. P. *et al.* Cleavage strongly influences whether soluble HIV-1 envelope glycoprotein trimers adopt a native-like conformation. *Proc. Natl. Acad. Sci. U. S. A.* **110**, 18256–18261 (2013).
66. Schiffner, T. *et al.* Immune Focusing and Enhanced Neutralization Induced by HIV-1 gp140 Chemical Cross-Linking. *J. Virol.* **87**, 10163–10172 (2013).
67. Schiffner, T. *et al.* Chemical Cross-Linking Stabilizes Native-Like HIV-1 Envelope Glycoprotein Trimer Antigens. *J. Virol.* **90**, 813–828 (2016).
68. Reitter, J. N., Means, R. E. & Desrosiers, R. C. A role for carbohydrates in immune evasion in AIDS. *Nat. Med.* **4**, 679–684 (1998).
69. Office_of_Technology_Assessment. Review of the Public Health Service ' s Response to AIDS. (1985).
70. Esparza, J. A brief history of the global effort to develop a preventive HIV vaccine. *Vaccine* **31**, 3502–3518 (2013).
71. Flynn, N. M. *et al.* Placebo-Controlled Phase 3 Trial of a Recombinant Glycoprotein 120 Vaccine to Prevent HIV-1 Infection. *J. Infect. Dis.* **191**, 654–665 (2005).
72. Pitisuttithum, P. *et al.* Randomized, Double-Blind, Placebo-Controlled Efficacy Trial of a Bivalent Recombinant Glycoprotein 120 HIV-1 Vaccine among Injection Drug Users in Bangkok, Thailand. *J. Infect. Dis.* **194**, 1661–1671 (2006).
73. Gilbert, P. B. *et al.* Correlation between Immunologic Responses to a Recombinant Glycoprotein 120 Vaccine and Incidence of HIV-1 Infection in a Phase 3 HIV-1 Preventive Vaccine Trial. *J. Infect. Dis.* **191**, 666–677 (2005).
74. Harro, C. D. *et al.* Recruitment and baseline epidemiologic profile of participants in the first phase 3 HIV vaccine efficacy trial. *J. Acquir. Immune Defic. Syndr.* **37**, 1385–1392 (2004).
75. Buchbinder, S. P. *et al.* Efficacy assessment of a cell-mediated immunity HIV-1 vaccine (the Step Study): a double-blind, randomised, placebo-controlled, test-of-concept trial. *Lancet* **372**, 1881–1893 (2008).
76. Gray, G. E. *et al.* Safety and efficacy of the HVTN 503/Phambili Study of a clade-B-based HIV-1 vaccine in South Africa: A double-blind, randomised, placebo-controlled test-of-concept phase 2b study. *Lancet Infect. Dis.* **11**, 507–515 (2011).
77. Duerr, A. *et al.* Extended follow-up confirms early vaccine-enhanced risk of HIV acquisition and demonstrates waning effect over time among participants in a randomized trial of recombinant adenovirus HIV vaccine (Step Study). *J. Infect. Dis.* **206**, 258–266 (2012).
78. Hammer, S. M. *et al.* Efficacy trial of a DNA/rAd5 HIV-1 preventive vaccine. *N. Engl. J. Med.* **369**, 2083–2092 (2013).
79. Rerks-Ngarm, S. *et al.* Vaccination with ALVAC and AIDSVAX to Prevent HIV-1 Infection in Thailand. *N. Engl. J. Med.* **361**, 2209–2220 (2009).
80. Haynes, B. F. *et al.* Immune-Correlates Analysis of an HIV-1 Vaccine Efficacy Trial. *N. Engl. J. Med.*

366, 1275–1286 (2012).
81. Bekker, L. G. *et al.* Subtype C ALVAC-HIV and bivalent subtype C gp120/MF59 HIV-1 vaccine in low-risk, HIV-uninfected, South African adults: a phase 1/2 trial. *Lancet HIV* **5**, e366–e378 (2018).
82. NIAID Website. Available at: https://www.niaid.nih.gov/news-events/experimental-hiv-vaccine-regimen-ineffective-preventing-hiv. (Accessed: 30th May 2020)
83. HIV vaccines go to trial. *Nat. Med.* **25**, 703 (2019).
84. Clinical Trials Website. Available at: https://clinicaltrials.gov/ct2/show/results/NCT03964415?recrs=adf&cond=%5EHIV+vaccine&phase=2&draw=2&rank=3. (Accessed: 24th October 2020)
85. HIV and more Website. Available at: https://www.hivandmore.de/kongresse/ias2019/schutzimpfung.shtml. (Accessed: 24th October 2020)
86. Eppstein, D. A., Byars, N. E. & Allison, A. C. New adjuvants for vaccines containing purified protein antigens. *Adv. Drug Deliv. Rev.* **4**, 233–253 (1989).
87. Ozorowski, G. *et al.* Effects of Adjuvants on HIV-1 Envelope Glycoprotein SOSIP Trimers In Vitro. *J. Virol.* **92**, 1–19 (2018).
88. McElrath, M. J. Adjuvants: Tailoring humoral immune responses. *Curr. Opin. HIV AIDS* **12**, 278–284 (2017).
89. Noe, A. R. *et al.* A full-length Plasmodium falciparum recombinant circumsporozoite protein expressed by Pseudomonas fluorescens platform as a Malaria vaccine candidate. *PLoS One* **9**, (2014).
90. Mordmüller, B. *et al.* First-in-human, Randomized, Double-blind Clinical Trial of Differentially Adjuvanted PAMVAC, A Vaccine Candidate to Prevent Pregnancy-associated Malaria. *Clin. Infect. Dis.* **69**, 1509–1516 (2019).
91. Radtke, A. J. *et al.* Adjuvant and carrier protein-dependent T-cell priming promotes a robust antibody response against the Plasmodium falciparum Pfs25 vaccine candidate. *Sci. Rep.* **7**, 1–12 (2017).
92. Poignard, P. *et al.* Heterogeneity of Envelope Molecules Expressed on Primary Human Immunodeficiency Virus Type 1 Particles as Probed by the Binding of Neutralizing and Nonneutralizing Antibodies. *J. Virol.* **77**, 353–365 (2003).
93. Moore, P. L. *et al.* Nature of nonfunctional envelope proteins on the surface of human immunodeficiency virus type 1. *J. Virol.* **80**, 2515–2528 (2006).
94. Burton, D. R. & Mascola, J. R. Antibody responses to envelope glycoproteins in HIV-1 infection. *Nat. Immunol.* **16**, 571–576 (2015).
95. Breden, F. *et al.* Comparison of antibody repertoires produced by HIV-1 infection, other chronic and acute infections, and systemic autoimmune disease. *PLoS One* **6**, (2011).
96. Moore, P. L., Williamson, C. & Morris, L. Virological features associated with the development of broadly neutralizing antibodies to HIV-1. *Trends Microbiol.* **23**, 204–211 (2015).
97. Hraber, P. *et al.* Prevalence of broadly neutralizing antibody responses during chronic HIV-1 infection. *AIDS* **28**, 163–9 (2014).
98. Wang, Q. & Zhang, L. Broadly neutralizing antibodies and vaccine design against HIV-1 infection. *Front. Med.* **14**, 30–42 (2020).
99. Scheid, J. F. *et al.* Broad diversity of neutralizing antibodies isolated from memory B cells in HIV-infected individuals. *Nature* **458**, 636–640 (2009).
100. Ng, C. T. *et al.* Passive neutralizing antibody controls SHIV viremia and enhances B cell responses in infant macaques. *Nat. Med.* **16**, 1117–1119 (2010).
101. Watkins, J. D. *et al.* An Anti-HIV-1 V3 Loop Antibody Fully Protects Cross-Clade and Elicits T-Cell Immunity in Macaques Mucosally Challenged with an R5 Clade C SHIV. *PLoS One* **6**, e18207 (2011).
102. Bonsignori, M. *et al.* Antibody-virus co-evolution in HIV infection: paths for HIV vaccine development. *Immunol. Rev.* **275**, 145–160 (2017).
103. Pancera, M. *et al.* Crystal structure of PG16 and chimeric dissection with somatically related PG9: structure-function analysis of two quaternary-specific antibodies that effectively neutralize HIV-1. *J. Virol.* **84**, 8098–8110 (2010).
104. Davenport, T. M. *et al.* Binding interactions between soluble HIV envelope glycoproteins and quaternary-structure-specific monoclonal antibodies PG9 and PG16. *J. Virol.* **85**, 7095–107 (2011).
105. Walker, L. M. *et al.* Broad and potent neutralizing antibodies from an African donor reveal a new HIV-1 vaccine target. *Science* **326**, 285–9 (2009).

106. Walker, L. M. *et al.* Broad neutralization coverage of HIV by multiple highly potent antibodies. *Nature* **477**, 466–470 (2011).
107. Mouquet, H. *et al.* Complex-type N-glycan recognition by potent broadly neutralizing HIV antibodies. *Proc. Natl. Acad. Sci. U. S. A.* **109**, (2012).
108. Moldt, B. *et al.* Highly potent HIV-specific antibody neutralization in vitro translates into effective protection against mucosal SHIV challenge in vivo. *Proc. Natl. Acad. Sci. U. S. A.* **109**, 18921–18925 (2012).
109. Falkowska, E. *et al.* PGV04, an HIV-1 gp120 CD4 binding site antibody, is broad and potent in neutralization but does not induce conformational changes characteristic of CD4. *J. Virol.* **86**, 4394–4403 (2012).
110. Corti, D. *et al.* Analysis of memory B cell responses and isolation of novel monoclonal antibodies with neutralizing breadth from HIV-1-infected individuals. *PLoS One* **5**, (2010).
111. Zhou, T. *et al.* Structural basis for broad and potent neutralization of HIV-1 by antibody VRC01. *Science* **329**, 811–7 (2010).
112. Wu, X. *et al.* Rational Design of Envelope Identifies Broadly Neutralizing Human Monoclonal Antibodies to HIV-1. *Science (80-.).* **329**, 856–861 (2010).
113. BUCHACHER, A. *et al.* Generation of Human Monoclonal Antibodies against HIV-1 Proteins; Electrofusion and Epstein-Barr Virus Transformation for Peripheral Blood Lymphocyte Immortalization. *AIDS Res. Hum. Retroviruses* **10**, 359–369 (1994).
114. Frey, G. *et al.* Distinct conformational states of HIV-1 gp41 are recognized by neutralizing and non-neutralizing antibodies. *Nat. Struct. Mol. Biol.* **17**, 1486–1491 (2010).
115. Huang, J. *et al.* Broad and potent HIV-1 neutralization by a human antibody that binds the gp41-gp120 interface. *Nature* **515**, 138–42 (2014).
116. Blattner, C. *et al.* Structural Delineation of a Quaternary, Cleavage-Dependent Epitope at the gp41-gp120 Interface on Intact HIV-1 Env Trimers. *Immunity* **40**, 669–680 (2014).
117. Sanders, R. W. *et al.* HIV-1 VACCINES. HIV-1 neutralizing antibodies induced by native-like envelope trimers. *Science* **349**, aac4223 (2015).
118. Briney, B. *et al.* Tailored Immunogens Direct Affinity Maturation toward HIV Neutralizing Antibodies Article Tailored Immunogens Direct Affinity Maturation toward HIV Neutralizing Antibodies. *Cell* **166**, 1459-1464.e11 (2016).
119. Feng, Y. *et al.* Thermostability of Well-Ordered HIV Spikes Correlates with the Elicitation of Autologous Tier 2 Neutralizing Antibodies. *PLoS Pathog.* **12**, 1–26 (2016).
120. Kovacs, J. M. *et al.* HIV-1 envelope trimer elicits more potent neutralizing antibody responses than monomeric gp120. *Proc. Natl. Acad. Sci.* **109**, 12111–12116 (2012).
121. Escolano, A., Dosenovic, P. & Nussenzweig, M. C. Progress toward active or passive HIV-1 vaccination. *J. Exp. Med.* **214**, 3–16 (2017).
122. Morris, L. & Mkhize, N. N. Prospects for passive immunity to prevent HIV infection. *PLoS Med.* **14**, 1–5 (2017).
123. Clinical Trials Website. Available at: https://clinicaltrials.gov/ct2/show/NCT02568215. (Accessed: 30th May 2020)
124. Weiss, R. A. *et al.* Neutralization of human T-Lymphotropic virus type III by sera of AIDS and AIDS-risk patients. *Nature* **316**, 69–72 (1985).
125. Forthal, D. N., Gilbert, P. B., Landucci, G. & Phan, T. Recombinant gp120 Vaccine-Induced Antibodies Inhibit Clinical Strains of HIV-1 in the Presence of Fc Receptor-Bearing Effector Cells and Correlate Inversely with HIV Infection Rate. *J. Immunol.* **178**, 6596–6603 (2007).
126. Forthal, D. N., Landucci, G. & Daar, E. S. Antibody from Patients with Acute Human Immunodeficiency Virus (HIV) Infection Inhibits Primary Strains of HIV Type 1 in the Presence of Natural-Killer Effector Cells. *J. Virol.* **75**, 6953–6961 (2001).
127. Zolla-Pazner, S. *et al.* Vaccine-induced IgG antibodies to V1V2 regions of multiple HIV-1 subtypes correlate with decreased risk of HIV-1 infection. *PLoS One* **9**, (2014).
128. Gottardo, R. *et al.* Plasma IgG to Linear Epitopes in the V2 and V3 Regions of HIV-1 gp120 Correlate with a Reduced Risk of Infection in the RV144 Vaccine Efficacy Trial. *PLoS One* **8**, 1–16 (2013).
129. Corey, L. *et al.* Immune correlates of vaccine protection against HIV-1 acquisition. *Sci. Transl. Med.* **7**, 1–10 (2015).
130. Karasavvas, N. *et al.* The Thai Phase III HIV Type 1 Vaccine trial (RV144) regimen induces antibodies that target conserved regions within the V2 loop of gp120. *AIDS Res. Hum. Retroviruses* **28**, 1444–57 (2012).

131. Excler, J. L. & Michael, N. L. Lessons from HIV-1 vaccine efficacy trials. *Curr. Opin. HIV AIDS* **11**, 607–613 (2016).
132. Ackerman, M. E. *et al.* Polyfunctional HIV-Specific Antibody Responses Are Associated with Spontaneous HIV Control. *PLoS Pathog.* **12**, 1–14 (2016).
133. Grassmann, V. Development and application of high- throughput screening methods to generate novel HIV-1 envelope immunogens. (2017).
134. Graf, M. *et al.* Concerted Action of Multiple cis-Acting Sequences Is Required for Rev Dependence of Late Human Immunodeficiency Virus Type 1 Gene Expression. *J. Virol.* **74**, 10822–10826 (2000).
135. Raab, D., Graf, M., Notka, F., Schödl, T. & Wagner, R. The GeneOptimizer Algorithm: Using a sliding window approach to cope with the vast sequence space in multiparameter DNA sequence optimization. *Syst. Synth. Biol.* **4**, 215–225 (2010).
136. Fath, S. *et al.* Multiparameter RNA and codon optimization: A standardized tool to assess and enhance autologous mammalian gene expression. *PLoS One* **6**, (2011).
137. Lessard, J. C. *Molecular cloning*. *Methods in Enzymology* **529**, (2013).
138. Bruun, T.-H., Mühlbauer, K., Benen, T., Kliche, A. & Wagner, R. A mammalian cell based FACS-panning platform for the selection of HIV-1 envelopes for vaccine development. *PLoS One* **9**, e109196 (2014).
139. Hanahan, D. Studies on transformation of Escherichia coli with plasmids. *J. Mol. Biol.* **166**, 557–580 (1983).
140. Bernard, P., Gabant, P., Bahassi, E. M. & Couturier, M. Positive-selection vectors using the F plasmid ccdB killer gene. *Gene* **148**, 71–74 (1994).
141. Barouch, D. H. *et al.* A Human T-Cell Leukemia Virus Type 1 Regulatory Element Enhances the Immunogenicity of Human Immunodeficiency Virus Type 1 DNA Vaccines in Mice and Nonhuman Primates. *Prog. Econ. Res. Vol. 14* **79**, 8828–8834 (2005).
142. Boussif, O. *et al.* A versatile vector for gene and oligonucleotide transfer into cells in culture and in vivo: polyethylenimine. *Proc. Natl. Acad. Sci. U. S. A.* **92**, 7297–7301 (1995).
143. Klasse, P. J. *et al.* Influences on Trimerization and Aggregation of Soluble, Cleaved HIV-1 SOSIP Envelope Glycoprotein. *J. Virol.* **87**, 9873–9885 (2013).
144. Hopp, T. P. *et al.* A short polypeptide marker sequence useful for recombinant protein identification and purification. *Bio/Technology* **6**, 1204–1210 (1988).
145. Hochuli, E., Bannwarth, W., Dobeli, H., Gentzi, R. & Stuber, D. Genetic approach to facilitate purification of recombinant proteins with a novel metal chelate adsorbent. *Bio/Technology* **6**, 1321–1325 (1988).
146. Bruun, T.-H. Development of mammalian cell display and panning techniques for the selection of HIV-1 vaccine candidates. *DIssertation* (2012).
147. Sanger, F. & Coulson, A. R. A rapid method for determining sequences in DNA by primed synthesis with DNA polymerase. *J. Mol. Biol.* **94**, 441–448 (1975).
148. Laemmli, U. K. Cleavage of structural proteins during the assembly of the head of bacteriophage T4. *Nature* **227**, 680–685 (1970).
149. Gorny, M. K. *et al.* Neutralization of diverse human immunodeficiency virus type 1 variants by an anti-V3 human monoclonal antibody. *J. Virol.* **66**, 7538–42 (1992).
150. Thali, M. *et al.* Characterization of conserved human immunodeficiency virus type 1 gp120 neutralization epitopes exposed upon gp120-CD4 binding. *J. Virol.* **67**, 3978–88 (1993).
151. Falkowska, E. *et al.* Broadly neutralizing HIV antibodies define a glycan-dependent epitope on the pre-fusion conformation of the gp41 protein on cleaved Envelope trimers. **40**, 657–668 (2014).
152. Blattner, C. *et al.* Structural Delineation of a Quaternary , Cleavage-Dependent Epitope at the gp41-gp120 Interface on Intact HIV-1 Env Trimers. *Immunity* **40**, 669–680 (2014).
153. Posner, M. R. *et al.* An IgG human monoclonal antibody that reacts with HIV-1/GP120, inhibits virus binding to cells, and neutralizes infection. *J. Immunol.* **146**, (1991).
154. Wu, X. *et al.* Rational Design of Envelope Identifies. *Science (80-.).* **329**, 856–861 (2010).
155. Huang, J. *et al.* Broad and potent neutralization of HIV-1 by a gp41-specific human antibody. *Nature.* **491**, 406–412 (2012).
156. Magnusson, A. O. *et al.* nanoDSF as screening tool for enzyme libraries and biotechnology development. *FEBS J.* **286**, 184–204 (2019).
157. Pancera, M., Changela, A. & Kwong, P. D. How HIV-1 entry mechanism and broadly neutralizing antibodies guide structure-based vaccine design. *Curr. Opin. HIV AIDS* **12**, 229–240 (2017).
158. Chen, L. *et al.* Structural basis of immune evasion at the site of CD4 attachment on HIV-1 gp120.

Science **326**, 1123–7 (2009).
159. Gorny, M. K., Xu, J. Y., Karwowska, S., Buchbinder, A. & Zolla-Pazner, S. Repertoire of neutralizing human monoclonal antibodies specific for the V3 domain of HIV-1 gp120. *J. Immunol.* **150**, 635–643 (1993).
160. Dutta, M., Liu, J., Roux, K. H. & Taylor, K. A. Visualization of Retroviral Envelope Spikes in Complex with the V3 Loop Antibody 447-52D on Intact Viruses by Cryo-Electron Tomography. *J. Virol.* **88**, 12265–12275 (2014).
161. Gorny, M. K. *et al.* Human Monoclonal Antibodies to the V3 Loop of HIV-1 with Intra- and Interclade Cross-Reactivity. *J. Immunol.* **159**, 5114–5122 (1997).
162. Julien, J. P. *et al.* Broadly Neutralizing Antibody PGT121 Allosterically Modulates CD4 Binding via Recognition of the HIV-1 gp120 V3 Base and Multiple Surrounding Glycans. *PLoS Pathog.* **9**, (2013).
163. Murin, C. D. *et al.* Structure of 2G12 Fab2 in Complex with Soluble and Fully Glycosylated HIV-1 Env by Negative-Stain Single-Particle Electron Microscopy. *J. Virol.* **88**, 10177–10188 (2014).
164. McLellan, J. S. *et al.* Structure of HIV-1 gp120 V1/V2 domain with broadly neutralizing antibody PG9. *Nature* **480**, 336–43 (2011).
165. Julien, J.-P. *et al.* Asymmetric recognition of the HIV-1 trimer by broadly neutralizing antibody PG9. *Proc. Natl. Acad. Sci. U. S. A.* **110**, 4351–6 (2013).
166. Walker, L. M. *et al.* Broad neutralization coverage of HIV by multiple highly potent antibodies. *Nature* **477**, 466–470 (2011).
167. Lee, J. H. *et al.* A Broadly Neutralizing Antibody Targets the Dynamic HIV Envelope Trimer Apex via a Long, Rigidified, and Anionic β-Hairpin Structure. *Immunity* **46**, 690–702 (2017).
168. Irimia, A. *et al.* Lipid interactions and angle of approach to the HIV-1 viral membrane of broadly neutralizing antibody 10E8: Insights for vaccine and therapeutic design. *PLoS Pathog.* **13**, 1–20 (2017).
169. Fiebig, U., Schmolke, M., Eschricht, M., Kurth, R. & Denner, J. Mode of interaction between the HIV-1-neutralizing monoclonal antibody 2F5 and its epitope. *Aids* **23**, 887–895 (2009).
170. IDRI. *Mixing Compatibility Study: RepliVax antigens and GLA-LSQ (IDRI-LS130)*. (2017).
171. IDRI. *Mixing Compatibility Study: RepliVax cross-linked antigens and GLA-LSQ (IDRI-LS130)*. (2018).
172. Adlington, K. *et al.* Molecular Design of Squalene/Squalane Countertypes via the Controlled Oligomerization of Isoprene and Evaluation of Vaccine Adjuvant Applications. *Biomacromolecules* **17**, 165–172 (2016).
173. Yates, N. L. *et al.* HIV-1 Envelope Glycoproteins from Diverse Clades Differentiate Antibody Responses and Durability among Vaccinees. **92**, 1–20 (2018).
174. Tomaras, G. D. *et al.* Initial B-Cell Responses to Transmitted Human Immunodeficiency Virus Type 1: Virion-Binding Immunoglobulin M (IgM) and IgG Antibodies Followed by Plasma Anti-gp41 Antibodies with Ineffective Control of Initial Viremia. *J. Virol.* **82**, 12449–12463 (2008).
175. Yates, N. L. *et al.* HIV-1 gp41 envelope IgA is frequently elicited after transmission but has an initial short response half-life. *Mucosal Immunol.* **6**, 692–703 (2013).
176. Tomaras, G. D. *et al.* Vaccine-induced plasma IgA specific for the C1 region of the HIV-1 envelope blocks binding and effector function of IgG. *Proc. Natl. Acad. Sci.* **110**, 9019–9024 (2013).
177. Mayer, B., Eddy, C., Tomaras, G. & Yates, N. PT Report for Pantaleo 662.01 BAMA. (2018).
178. Shen, S. (Xiaoying) & Tomaras, G. Pantaleo 662.01 Linear Epitope Mapping Peptide Microarray. in (2018).
179. Montefiori, D. C. Measuring HIV Neutralization in a Luciferase Reporter Gene Assay. in *HIV Protocols* (eds. Prasad, V. R. & Kalpana, G. V) 395–405 (Humana Press, 2009).
180. Sarzotti-Kelsoe, M. *et al.* Optimization and validation of the TZM-bl assay for standardized assessments of neutralizing antibodies against HIV-1. *J. Immunol. Methods* **409**, 131–146 (2014).
181. RCoreTeam. R: A language and environment for statistical computing. *R Found. Stat. Comput. Vienna, Austria* (2018).
182. Jackson, W. M. & Brandts, J. F. Thermodynamics of Protein Denaturation. A Calorimetric Study of the Reversible Denaturation of Chymotrypsinogen and Conclusions Regarding the Accuracy of the Two-State Approximation. *Biochemistry* **9**, 2294–2301 (1970).
183. Johnson, C. M. Differential scanning calorimetry as a tool for protein folding and stability. *Arch. Biochem. Biophys.* **531**, 100–109 (2013).
184. Wedde, S., Kleusch, C., Bakonyi, D. & Gröger, H. High-Throughput Feasible Screening Tool for Determining Enzyme Stabilities against Organic Solvents Directly from Crude Extracts. *ChemBioChem* **18**, 2399–2403 (2017).

185. Hierl, H. Chemical Crosslinking of HIV-1 Immunogens to Improve Stability and Antigenicity. (2017).
186. Thermo Scientific, C. T. H. Crosslinking Technology. *Thermo Sci.* 1–56 (2012).
187. Grabarek, Z. & Gergely, J. Zero-length crosslinking procedure with the use of active esters. *Anal. Biochem.* **185**, 131–135 (1990).
188. Pantaleo: RepliVax Vaccine Platform. Available at: https://www.cavd.org/ReplicatingVectors/Pages/PantaleoRepliVax.aspx. (Accessed: 24th September 2020)
189. Liao, H. *et al.* Vaccine Induction of Antibodies Against a Structurally Heterogeneous Site of Immune Pressure within HIV-1 Envelope Protein Variable Regions 1 and 2. *Immunity* **38**, 176–186 (2013).
190. Pinter, A., Honnen, W. J., Kayman, S. C., Trochev, O. & Wu, Z. Potent neutralization of primary HIV-1 isolates by antibodies directed against epitopes present in the V1/V2 domain of HIV-1 gp120. *Vaccine* **16**, 1803–1811 (1998).
191. He, Y. *et al.* Identification of a Critical Motif for the Human Immunodeficiency Virus Type 1 (HIV-1) gp41 Core Structure: Implications for Designing Novel Anti-HIV Fusion Inhibitors. *J. Virol.* **82**, 6349–6358 (2008).
192. Gohain, N. *et al.* Molecular basis for epitope recognition by non-neutralizing anti-gp41 antibody F240. *Sci. Rep.* **6**, 1–15 (2016).
193. Phanuphak, N. & Gulick, R. M. HIV treatment and prevention 2019: Current standards of care. *Curr. Opin. HIV AIDS* **15**, 4–12 (2020).
194. Finzi, A. *et al.* Topological Layers in the HIV-1 gp120 Inner Domain Regulate gp41 Interaction and CD4-Triggered Conformational Transitions. *Mol. Cell* **37**, 656–667 (2010).
195. Andrabi, R. *et al.* Identification of Common Features in Prototype Broadly Neutralizing Antibodies to HIV Envelope V2 Apex to Facilitate Vaccine Design. *Immunity* **43**, 959–973 (2015).
196. Finzi, A. *et al.* Conformational characterization of aberrant disulfide-linked HIV-1 gp120 dimers secreted from overexpressing cells. *J. Virol. Methods* **168**, 155–61 (2010).
197. Hoffenberg, S. *et al.* Identification of an HIV-1 clade A envelope that exhibits broad antigenicity and neutralization sensitivity and elicits antibodies targeting three distinct epitopes. *J. Virol.* **87**, 5372–83 (2013).
198. Balla-Jhagjhoorsingh, S. S. *et al.* The N276 Glycosylation Site Is Required for HIV-1 Neutralization by the CD4 Binding Site Specific HJ16 Monoclonal Antibody. *PLoS One* **8**, 8–13 (2013).
199. Balzarini, J. *et al.* Marked depletion of glycosylation sites in HIV-1 gp120 under selection pressure by the mannose-specific plant lectins of Hippeastrum hybrid and Galanthus nivalis. *Mol. Pharmacol.* **67**, 1556–1565 (2005).
200. Jardine, J. *et al.* Rational HIV immunogen design to target specific germline B cell receptors. **340**, 711–716 (2013).
201. Wilton, T., Dunn, G., Eastwood, D., Minor, P. D. & Martin, J. Effect of Formaldehyde Inactivation on Poliovirus. *J. Virol.* **88**, 11955–11964 (2014).
202. Kanzler, H., Barrat, F. J., Hessel, E. M. & Coffman, R. L. Therapeutic targeting of innate immunity with Toll-like receptor agonists and antagonists. *Nat. Med.* **13**, 552–559 (2007).
203. Ragupathi, G., Gardner, J. R., Livingston, P. O. & Gin, D. Y. Natural and synthetic saponin adjuvant QS-21 for vaccines against cancer. *Expert Rev Vaccines* **10**, 463–470 (2011).
204. Fernández-Tejada, A., Tan, D. S. & Gin, D. Y. Development of Improved Vaccine Adjuvants Based on the Saponin Natural Product QS-21 through Chemical Synthesis. *Acc. Chem. Res.* **49**, 1741–1756 (2016).
205. Kumar, R., Qureshi, H., Deshpande, S. & Bhattacharya, J. Broadly neutralizing antibodies in HIV-1 treatment and prevention. *Ther. Adv. Vaccines Immunother.* **6**, 61–68 (2018).
206. Burton, D. R. Antibodies, viruses and vaccines. *Nat. Rev. Immunol.* **2**, 706–713 (2002).
207. Verrier, F. *et al.* A Human Immunodeficiency Virus Prime-Boost Immunization Regimen in Humans Induces Antibodies That Show Interclade Cross-Reactivity and Neutralize Several X4-, R5-, and Dualtropic Clade B and C Primary Isolates. *J. Virol.* **74**, 10025–10033 (2000).
208. Sattentau, Q. Envelope Glycoprotein Trimers as HIV-1 Vaccine Immunogens. *Vaccines* **1**, 497–512 (2013).
209. Joseph, S. *et al.* A comparative phase I study of combination, homologous subtype-C DNA, MVA, and Env gp140 protein/adjuvant HIV vaccines in two immunization regimes. *Front. Immunol.* **8**, 1–14 (2017).
210. Su, L. *et al.* Characterization of a Virtually Full-Length Human Immunodeficiency Virus Type 1 Genome of a Prevalent Intersubtype (C/B') Recombinant Strain in China. *J. Virol.* **74**, 11367–11376

(2000).
211. Kratochvil, S. *et al.* A phase 1 human immunodeficiency virus vaccine trial for cross-profiling the kinetics of serum and mucosal antibody responses to CN54gp140 modulated by two homologous prime-boost vaccine regimens. *Front. Immunol.* **8**, 1–17 (2017).
212. Pritchard, L. K. *et al.* Structural Constraints Determine the Glycosylation of HIV-1 Envelope Trimers. *Cell Rep.* **11**, 1604–1613 (2015).
213. Zolla-Pazner, S. & Cardozo, T. Sequence-Variable Regions Provide a Paradigm for Vaccine Design. *Nat Rev Immunol* **10**, 527–535 (2010).
214. Corey, L. *et al.* Immune Correlates of Vaccine Protection Against HIV-1 Acquisition: A Review. *Sci Transl Med* **7**, 1–9 (2015).
215. Costa, M. R. *et al.* Fc Receptor-Mediated Activities of Env-Specific Human Monoclonal Antibodies Generated from Volunteers Receiving the DNA Prime-Protein Boost HIV Vaccine DP6-001. *J. Virol.* **90**, 10362–10378 (2016).
216. Su, B. *et al.* Update on Fc-Mediated Antibody Functions Against HIV-1 Beyond Neutralization. *Front. Immunol.* **10**, (2019).
217. Liu, S., Wang, S. & Lu, S. Using DNA Immunization to Elicit Monoclonal Antibodies in Mice, Rabbits, and Humans. *Hum. Gene Ther.* **29**, 997–1003 (2018).
218. Nadai, Y. *et al.* Envelope-Specific Recognition Patterns of HIV Vaccine-Induced IgG Antibodies Are Linked to Immunogen Structure and Sequence. *Front. Immunol.* **10**, 717 (2019).
219. Seaman, M. S. *et al.* Tiered Categorization of a Diverse Panel of HIV-1 Env Pseudoviruses for Assessment of Neutralizing Antibodies. *J. Virol.* **84**, 1439–1452 (2010).
220. Yates, N. L. *et al.* Vaccine-induced Env V1-V2 IgG3 correlates with lower HIV-1 infection risk and declines soon after vaccination. *Sci. Transl. Med.* **6**, (2014).
221. Pepscan Website. Available at: https://www.pepscan.com/epitope-mapping/clips-conformational-and-discontinuous-epitope-mapping/?gclid=EAIaIQobChMIz73b07P27AIVSed3Ch0kKgxPEAAYAiADEgJXl_D_BwE. (Accessed: 9th November 2020)
222. Lavine, C. L. *et al.* High-Mannose Glycan-Dependent Epitopes Are Frequently Targeted in Broad Neutralizing Antibody Responses during Human Immunodeficiency Virus Type 1 Infection. *J. Virol.* **86**, 2153–2164 (2012).
223. Lei, L. *et al.* Antigen-Specific Single B Cell Sorting and Monoclonal Antibody Cloning in Guinea Pigs. *Front. Microbiol.* **10**, 1–19 (2019).
224. Peterhoff, D. & Wagner, R. Guiding the long way to broad HIV neutralization. *Curr. Opin. HIV AIDS* **12**, 257–264 (2017).
225. Asbach, B. & Wagner, R. Particle-based delivery of the HIV envelope protein. *Curr. Opin. HIV AIDS* **12**, 265–271 (2017).

Danksagung

Im Laufe der Zeit erhielt ich die Unterstützung und Hilfe vieler Personen, bei denen ich mich hiermit gerne auch schriftlich bedanken möchte.

Zu Beginn möchte ich meinem Doktorvater Prof. Dr. Ralf Wagner danken, dass ich meine Doktorarbeit in dieser großartigen Arbeitsgruppe anfertigen konnte. All die Jahre wurde ich von Dir intensiv betreut, fand bei meinen Anliegen immer ein offenes Ohr und konnte mich auf Deine hilfreiche Unterstützung verlassen. Sowohl die fachlichen als auch die persönlichen Gespräche habe ich sehr geschätzt und dabei auch sehr viel gelernt.

Meinen Mentoren Prof. Dr. Rainer Merkl und Prof. Dr. Hendrik Streeck möchte ich für die Ratschläge und Ideen danken, die meine Arbeit weiter voranbrachten und Prof. Dr. Barbara Schmidt für die Übernahme des Zweitgutachtens.

Während meiner Doktorarbeit erhielt ich auch im Labor Unterstützung. Dr. David Peterhoff möchte ich hierbei für die enorme Hilfe beim Aufsetzen der Proteinreinigung, bei diversen Messungen, sowie der Hilfe bei sämtlichen Fragen und Problemen danken. Gerade das erste halbe Jahr hätte ich ohne Dich nicht annähernd so gut gemeistert. Des Weiteren möchte ich Dr. Benedikt Asbach ganz herzlich danken, für all die Hilfe und Unterstützung, sei es bei Fragen zur Statistik oder den zahlreichen Anregungen zu meiner Arbeit. Ich habe die Zusammenarbeit mit Dir immer sehr genossen und die Zeit im Schreibraum war mit Dir nicht nur lehrreich, sondern auch sehr angenehm und amüsant.

Ich danke auch meinen lieben Kolleginnen und Kollegen, die meinen Arbeitsalltag bereichert haben. Durch den Zusammenhalt und die wunderbare Arbeitsatmosphäre wurde die Zeit unvergesslich und trotz stressiger Phasen bin ich wegen Euch allen immer gerne ins Labor gekommen. Wenn Kolleginnen und Kollegen so schnell zu Freunden werden, ist das ein ganz wunderbares Geschenk. Zudem möchte ich Melina Daniilidis vom Bayerischen NMR-Zentrum in Garching für die Hilfe am MicroCal PEAQ-DSC danken, sowie 2bind für die Unterstützung bei den nanoDSF Messungen.

Zu guter Letzt möchte ich meiner Familie - allen voran meiner Mama - von ganzen Herzen danken: Während meines ganzen Lebens habt ihr mich immer begleitet und mich unterstützt, seid mein Ansprechpartner bei allen Situationen und mein sicherer Hafen. So auch während der finalen Phase meiner Doktorarbeit, für die ich mich auch bei Dir, lieber Christoph, herzlich bedanke.